



Non-conventional GluN3A signaling modulates memory ontogeny, formation and consolidation

Doctoral thesis presented by

Óscar Elía Zudaire

Thesis Director:

Isabel Pérez-Otaño, PhD

- 2023-

PhD Program in Neuroscience

Instituto de Neurociencias de Alicante (UMH-CSIC)

Universidad Miguel Hernández de Elche





Yo, D. Óscar Elía Zudaire con DNI/Pasaporte nº 72704180F, declaro que los siguientes artículos que forman parte de mi tesis doctoral titulada “**Non-conventional GluN3A signaling modulates memory ontogeny, formation and consolidation**” no han sido utilizados en ninguna otra tesis:

- Conde-Dusman, M. J., Dey, P. N., **Elía-Zudaire, Ó.**, Rabaneda, L. G., García-Lira, C., Grand, T., Briz, V., Velasco, E. R., Andero, R., Niñerola, S., Barco, A., Paoletti, P., Wesseling, J. F., Gardoni, F., Tavalin, S. J., & Perez-Otaño, I. (2021). Control of protein synthesis and memory by GluN3A-NMDA receptors through inhibition of GIT1/mTORC1 assembly. *ELife*, 10, e71575.
- Verhaeghe, R., **Elía-Zudaire, Ó.**, Escamilla, S., Sáez-Valero, J. & Pérez-Otaño, I (2023). No evidence for cognitive decline or neurodegeneration in strain-matched GluN3A knockout mice. *Alzheimer's & Dementia* (accepted for publication).

Fdo. D. Óscar Elía Zudaire

En San Juan de Alicante, a 1 de junio de 2023



Sant Joan d'Alacant, 1st of June 2023

Dr. Isabel Pérez-Otaño, director of the doctoral thesis entitled “**Non-conventional GluN3A signaling modulates memory ontogeny, formation and consolidation**”

CERTIFIES:

That Óscar Elía Zudaire has carried out under my supervision the work entitled “**Non-conventional GluN3A signaling modulates memory ontogeny, formation and consolidation**” in accordance with the terms and conditions defined in his Research Plan and in accordance with the Code of Good Practice of the University Miguel Hernández of Elche, satisfactorily fulfilling the objectives foreseen for its public defense as a doctoral thesis.

I sign for appropriate purposes, at Sant Joan d'Alacant, 1st of June 2023.

Thesis Director

Dra. Dña. Isabel Pérez-Otaño



Sant Joan d'Alacant, 1st of June 2023

Ms. Elvira de la Peña García, Coordinator of the Neurosciences PhD programme at the Institute of Neurosciences in Alicante, a joint center of the Miguel Hernández University (UMH) and the Spanish National Research Council (CSIC),

INFORMS:

That D. Óscar Elía Zudaire has carried out under the supervision of our PhD Programme the work entitled “**Non-conventional GluN3A signaling modulates memory ontogeny, formation and consolidation**” in accordance with the terms and conditions defined in its Research Plan and in accordance with the Code of Good Practice of the University Miguel Hernández de Elche, fulfilling the objectives satisfactorily for its public defense as a doctoral thesis.

Which I sign for the appropriate purposes, in Sant Joan d'Alacant, 1st of June 2023.

Dr. Elvira de la Peña García

Coordinator of the PhD Programme in Neurosciences

Email: elvirap@umh.es
www.in.umh.es

Tel: +34 965 919533
Fax: +34 965 919549

Av Ramón y Cajal s/n
CAMPUS DE SANT JOAN
03550 SANT JOAN D'ALACANT- ESPAÑA



Sant Joan d'Alacant, 1st of June 2023

To whom it may concern,

The present PhD thesis has been funded by the following research agencies:

D. Óscar Elía Zudaire is recipient of an ACIF contract (ACIF/218/216) granted by “Conselleria de Innovación, Universidades, Ciencia y Sociedad Digital, Generalitat Valenciana”.

Yours sincerely,

Óscar Elía Zudaire

Table of contents

Abstract/Resumen	10
Introduction and Objectives	16
1. The study of memory	16
1.1 Sensory memory	16
1.2 Short-term memory.....	17
1.3 Long-term memory	18
1.3.1 Declarative or explicit memory.....	18
1.3.2 Non-declarative or implicit memory.....	19
2. Features of memory	21
2.1 Persistence of memory	21
2.2 Transience of memory	22
2.3 Memory ontogeny	24
3. Substrates of memory.....	27
3.1 Long-term potentiation (LTP)	27
3.2 NMDARs	27
3.2.1 Properties and expression pattern of GluN3A-NMDARs ..	28
3.2.2 GluN3A links to CNS disorders.....	31
3.3 The mTOR pathway and protein synthesis.....	33
4. Objectives.....	36
Materials and methods.....	38
1. Experimental animals.....	38
1.1 Generation of cell type-specific GluN3A-lacking mice	41
2. Behavioral tests	41
2.1 Spatial learning: Morris water maze.....	41
2.2 Y-maze spontaneous alternation task	43
2.3 Fear conditioning.....	44
2.4 Contextual fear discrimination	45
3. Protein quantification by Western blotting	47

4. Protein synthesis measurements.....	50
5. In vivo electrophysiological recordings	51
6. Histology.....	53
Results	56
1. Testing cognition-related behaviors on constitutive <i>Grin3a</i> ^{-/-} mice.....	56
1.1 <i>Grin3a</i> ^{-/-} mice perform as wild-type littermates under standard testing conditions	56
1.2 <i>Grin3a</i> ^{-/-} mice perform better on demanding memory tasks.....	58
1.3 Associative memory is enhanced in <i>Grin3a</i> ^{-/-} mice	60
1.4 <i>Grin3a</i> ^{-/-} mice enhanced memory is mTOR dependent.....	62
2. Generation and characterization of cognition phenotypes in population specific GluN3A-lacking mice	64
2.1. <i>Grin3a</i> ^{ff} × <i>Camk2a</i> -Cre ^{ERT2}	64
2.2. <i>Grin3a</i> ^{ff} × <i>Sst</i> -Ires-Cre	66
2.3 Validation of enhanced associative memory using a second, context specific, fear conditioning paradigm	68
2.4 GluN3A gates memory through limiting mTORC1-dependent protein synthesis in excitatory synapses	72
3. GluN3A deletion is not associated with common side effects of translation manipulations.....	74
3.1. Behavioral flexibility.....	75
3.2 Memory precision.....	78
4. Removal of GluN3A-NMDARs enhances LTP in vivo.....	80
5. Testing GluN3A effect on memory ontogeny.....	82
5.1 The emergence of memory is not altered in mice lacking GluN3A ..	82
5.2 Challenging paradigms unveil increased fear responses in postnatal <i>Grin3a</i> ^{-/-} mice	84
5.3 Removing GluN3A accelerates the emergence of the persistence of memory	85

5.4 Selective ablation of GluN3A from principal excitatory neurons is sufficient to accelerate fear ontogeny	86
5.4.1 Early postnatal ablation of GluN3A from excitatory neurons	86
5.4.2 Postnatal GluN3A expression in excitatory neurons controls the ontogeny of memory persistence.....	87
6. Unveiling the mechanisms underlying accelerated memory ontogeny.....	88
6.1. GluN3A ablation promotes protein synthesis in postnatal mice.....	89
6.2 Blocking enhanced mTORC1-signaling occludes GluN3A effects on fear memory ontogeny	90
6.3 Neurogenesis levels remain unchanged in <i>Grin3a</i> ^{-/-} mice	91
7. GluN3A-related memory enhancement is lifelong	93
Discussion.....	98
Conclusions/Conclusiones	110
References	113
Annex: Scientific publications	128
1. Control of protein synthesis and memory by GluN3A-NMDA receptors through inhibition of GIT1/mTORC1 assembly	
2. No evidence for cognitive decline or neurodegeneration in strain-matched GluN3A knockout mice	

Abstract/Resumen



During early brain development, an excess production of synapses occurs, resulting in the establishment of weak functional connections between neurons. Subsequently, neuronal activity refines the initial circuitry by strengthening and maintaining specific connections while suppressing (pruning) others. This process ultimately leads to the formation of more precise and long-lasting connections. Compelling evidence suggests that even subtle imbalances in synapse maturation and pruning can contribute to various severe brain disorders, including autism, schizophrenia, bipolar disorder, and neurodegenerative conditions that manifest in adulthood. GluN3A subunit-containing NMDA receptors (GluN3A-NMDARs) have emerged as crucial regulators of this synaptic refinement. GluN3A-NMDARs are typically expressed before and during critical periods of postnatal development. They play a role in preventing premature synapse maturation and stabilization until sensory experience occurs, subsequently targeting less utilized or non-active synapses for pruning.

Previous research from our lab have revealed that GluN3A-NMDARs exhibit selective inhibition of a specific subset of activity- and NMDAR-regulated signaling pathways. Among these pathways, the mTOR pathway, particularly the multiprotein complex mTORC1, stands out due to its crucial involvement in stimulating dendritic protein synthesis in response to synaptic signals.

Building on this work, here we investigated whether GluN3A-NMDARs impact cognition-related behaviors and the mechanisms through which they exert their effects. We found that GluN3A bi-directionally affects mice performance in contextual and associative learning tasks: deleting GluN3A enhances mice performance while increasing its expression impairs mice ability to form associative memories. To expand our investigation, we utilized genetic tools to further elucidate the role of GluN3A in memory processes. Through these tools, we were able to demonstrate that GluN3A exerts its influence on memory by being expressed in excitatory neurons. Importantly, we discovered that the impact of GluN3A on memory is not limited to critical periods of development but continues to be significant throughout adulthood. We also discovered

that GluN3A limits cognitive behaviors by constraining mTORC1-signaling and that its deletion enhances long-term potentiation (LTP) *in vivo*.

To further our understanding, we studied postnatal and aged mice with ablated GluN3A expression. We found that removing GluN3A-NMDARs increased protein synthesis and accelerated the ontogeny of memories, limiting the temporal window of infantile amnesia and that GluN3A ablation protects against age-related memory loss.

The findings presented in this thesis significantly contribute to our comprehension of the mechanisms through which GluN3A-NMDARs, impact the brain and influence behaviors essential for our interaction with the environment. These results pave the way for novel avenues of research aimed at enhancing our understanding of NMDARs function. Moreover, our experiments provide compelling evidence supporting the therapeutic prospects of targeting GluN3A-NMDARs as a means to develop memory-enhancing treatments.

Durante el desarrollo temprano del cerebro se produce un exceso de producción de sinapsis, lo que resulta en el establecimiento de conexiones débiles entre neuronas. Posteriormente, la actividad neuronal refina el circuito inicial, fortaleciendo y manteniendo conexiones específicas, al tiempo que suprimen (podan) otras. Este proceso lleva en última instancia a la formación de conexiones más precisas y duraderas. Existen pruebas convincentes de que incluso desequilibrios sutiles en la maduración y poda de sinapsis pueden contribuir a diversos trastornos cerebrales graves, como el autismo, la esquizofrenia, el trastorno bipolar y las enfermedades neurodegenerativas que se manifiestan en la edad adulta. Los receptores NMDA que contienen la subunidad GluN3A (GluN3A-NMDARs) han surgido como reguladores cruciales de este refinamiento sináptico. Por lo general, los GluN3A-NMDARs se expresan antes y durante los períodos críticos del desarrollo posnatal. Su papel es la prevención de la maduración y estabilización prematura de las sinapsis hasta que se produzca la experiencia sensorial, y posteriormente se dirigen a las sinapsis menos utilizadas o inactivas para su poda.

En trabajos anteriores, nuestro laboratorio demostró que los GluN3A-NMDARs exhiben una inhibición selectiva de un subconjunto específico de vías de señalización reguladas por la actividad y los NMDARs. Entre estas vías, destaca la vía mTOR, en particular el complejo multiproteico mTORC1, debido a su papel crucial en la estimulación de la síntesis de proteínas dendríticas en respuesta a señales sinápticas.

Basándonos en este trabajo, investigamos si los GluN3A-NMDARs afectan los comportamientos relacionados con la cognición y los mecanismos a través de los cuales ejercen sus efectos. Descubrimos que los GluN3A-NMDAR afectan el desempeño de los ratones en tareas de aprendizaje contextual y asociativo de manera bidireccional: la eliminación de GluN3A-NMDARs mejora el rendimiento de los ratones, mientras que el aumento de su expresión perjudica la capacidad de los ratones para formar memorias asociativas. Para ampliar nuestra investigación, utilizamos herramientas genéticas que nos permitieran conocer mejor el papel de GluN3A en los procesos de memoria. Mediante estas herramientas, pudimos demostrar que GluN3A ejerce su influencia en la

memoria mediante su expresión en neuronas excitatorias. Es importante destacar que descubrimos que el impacto de GluN3A en la memoria no se limita a períodos críticos del desarrollo, sino que sigue siendo significativo durante toda la edad adulta. También descubrimos que GluN3A restringe la señalización de mTORC1 y que su eliminación mejora la potenciación a largo plazo (LTP) *in vivo*.

Para profundizar en nuestra comprensión de estos procesos, estudiamos ratones con la expresión de GluN3A eliminada en el período posnatal y en la vejez. Descubrimos que la eliminación de GluN3A-NMDARs aumentaba la síntesis de proteínas y aceleraba la ontogenia de las memorias, limitando los efectos de la amnesia infantil, y que la eliminación de GluN3A protege contra la pérdida de memoria relacionada con la edad.

Los hallazgos presentados en esta tesis contribuyen significativamente a nuestra comprensión de los mecanismos a través de los cuales los GluN3A-NMDARs modelan el cerebro e influyen en comportamientos esenciales para nuestra interacción con el entorno. Estos resultados abren nuevas vías de investigación destinadas a mejorar nuestra comprensión de la función de los NMDARs. Además, nuestros experimentos proporcionan pruebas convincentes que respaldan el potencial terapéutico de manipular los GluN3A-NMDARs como medio para desarrollar tratamientos que mejoren la memoria.

Introduction and objectives



1. The study of memory

Memory has been a central topic of study and discussion since the very moment our brain was developed enough to study and discuss topics. According to Hesiod's *Theogony* (VIII-VII B.C.), memory was of such importance in the ancient Greek mythology that it was embodied in the goddess Mnemosyne, mother of the seven muses, sources of all art and knowledge. However, in the fourth century B. C., Aristotle considered the brain to be an organ of secondary importance that served as a cooling agent for the heart. Centuries later, the Roman physician Galen, based on his observations of the effect of brain injuries, concluded that mental functions such as willed action or cognition occurred in the brain rather than the heart. His ideas started the study of the brain as locus of memory. Thus, in this work, philosophy will be left aside and the emphasis will be on the more concrete biomedical study of memory and its mechanisms.

We could define memory as the process that allows us to incorporate and retain new information about the world, permitting us to connect experiences and learn about our surrounding world, an essential skill for survival. Being memory an intricate process and a broad term, the first approaches relevant to current neuroscience date from the late 19th century, when James (1890) distinguished primary and secondary memory. Some years later, Maine de Biran (1929) classified mechanical memory, sensitive memory and representative memory. Currently, the scientific community agrees in classifying memory in three types that will be explained below: sensory memory, short-term memory (STM)(sometimes referred to as working memory due to its functions) and long-term memory (LTM).

1.1 Sensory memory

Sensory memory is the capacity to briefly store the large amount of information that we encounter in our day to day. It is subdivided in echoic memory, that retains auditory information; haptic memory, related to touch; and iconic memory, that keeps

information from the visual system and it's the most widely studied of the three. This type of memory will not be studied in depth in this work.

1.2 Short-term memory

Short-term memory (STM) allows us to maintain a small amount of information for brief periods of time. This type of memory is thought to have different components, being Atkinson and Shiffrin's modal model one of the most widely accepted explanation (Atkinson & Shiffrin, 1968). They proposed the existence of a short-term storehouse that receives inputs from sensory registers and from a long-term storage. Due to its limited capacity, the short-term storehouse also sends information to the long-term storage. (Fig. 1A). The short-term storehouse plays a key role in this model, generating reasoning and new deductions from existing ones, hence it's capable of manipulating information (functioning as working memory). However, this model was criticized for implying that items that were stored in memory were more likely to be moved to the long-term storage, but some studies refuted this hypothesis (Tulving & Pearstone, 1966; Craik and Watkins, 1973).

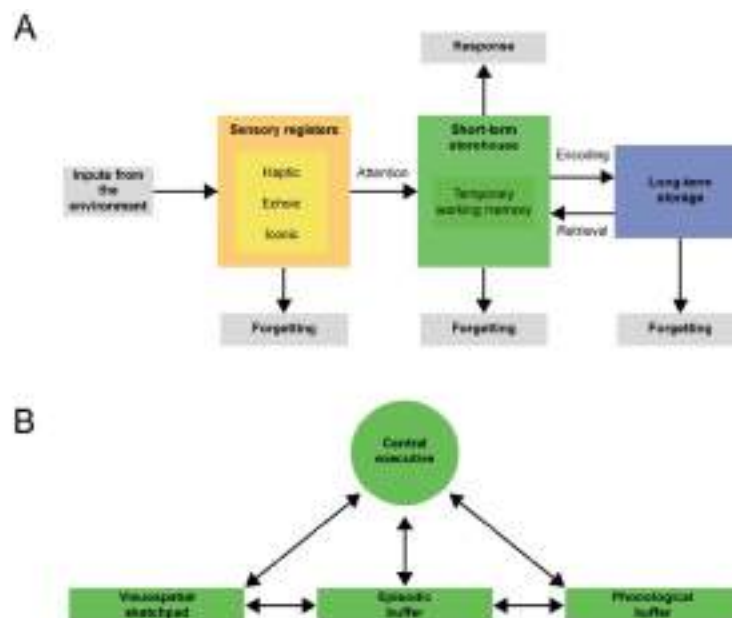


Figure 1. Memory models. A) Atkinson & Shiffrin's modal model. B) Baddeley & Hitch's structural model.

Baddeley and Hitch (1974) proposed the structural model that is currently the most accepted one and its composed by a central executive, a visuospatial sketchpad, a phonological buffer and, introduced later (Baddeley, 2000) an episodic buffer (Fig. 1B). The central executive is a system of attention control that uses long-term information to weigh options and respond accordingly to novel situations. The visuospatial sketchpad creates and maintains representations of visual information. The phonological buffer provides the ability to store words before their consolidation into long-term memory. Lastly, the episodic buffer is a temporary storage with capacity to integrate information from different sources, and likely controlled by the central executive.

1.3 Long-term memory

Long-term memory stores information for extended periods of time, even for life. It's subdivided into declarative or explicit memory, term that includes the information that can be consciously evoked; and non-declarative or implicit memory, referring for example to abilities or skills that are unconscious.

1.3.1 Declarative or explicit memory

This type of memory is also subdivided in two categories: one that stores personal experiences (episodic memory) and one that encompasses information about facts (semantic memory). Episodic memory involves details about life events such as what, when, and where (Tulving, 1972). Previously thought to be restricted to humans (Roberts, 2002) Ergorul and Eichenbaum (2004) published a study investigating this matter in rats, and demonstrated that these rodents are indeed capable of using a combination of where and what data to elucidate the timing of events. They also proved that damaging the hippocampus caused impairments in the recovery of memories.

The ability of humans to represent concepts in language allow us to combine these concepts, manipulate them and also to disseminate conceptual knowledge to other humans. That is why “semantic memory generally encompasses matters widely

construed as common knowledge, which are neither exclusively nor immediately drawn from personal experience” (McRae & Jones, 2013).

1.3.2 Non-declarative or implicit memory

Implicit memory is the kind of memory that includes all unconscious memories, as well as certain skills. It is divided in four subtypes: procedural memory, associative memory, non-associative memory and priming. Procedural memory is acquired by repeating a certain complex activity and is defined as the recall of executive and motor skills required to perform that task.

Associative memory refers to the ability to store and retrieve information based on the relationship between concepts and not only on the particular concepts themselves. Associative memory can be achieved through either classical conditioning or operant conditioning. The first one has its main exponent in the Pavlov’s dog experiment (Pavlov, 1927) and is based in the close association between two stimuli in time. By repeating a conditioned stimulus (CS) before an unconditioned stimulus (US), the CS acquires characteristics from the US. Meanwhile, according to the operant conditioning paradigm, behaviors develop depending on their consequences: whenever a behavior is followed by a positive outcome, it will be repeated and reinforced; whereas if the behavior carries negative consequences, it will not be repeated over time. Thorndike (1932) first called this instrumental conditioning, while the current term was coined by Skinner (1938) whose research was built upon Thorndike’s law of effect (Thorndike, 1898).

Non-associative memory can be classified depending on their response to the repetition of a stimulus: sensitization (when the response to the repeated stimulus increases) and habituation (when the repetition of the stimulus causes a decrease in the response to it). These two processes are present in both, animals and human beings, and have greatly contributed to the advance in the knowledge of the learning process, thanks mainly, but not solely to the work of Eric Kandel (Castellucci & Kandel, 1976).

Introduction and objectives

Lastly, the fourth modality of implicit memory is priming, an effect that occurs when the presentation of a stimuli influences the response given to a later stimulus.

2. Features of memory

Most of memory-related research has focused on how memories are formed, stored, and retrieved in the brain. Specifically, researchers have been interested in understanding the best system for storing and retrieving memories - in other words, the most efficient and effective way for our brains to remember things. Some studies, however, pointed out the importance of forgetting for maintaining a healthy memory system. Aleksandr Lúriya described the case of Patient S (Luriya, 1968), a man whose memory had “no distinct limits”: While he was able to remember the smallest detail of every situation, this apparent super memory made him unable to generalize information across contexts and situations, pointing out the importance of forgetting (or transience of memory).

2.1 Persistence of memory

Many neuroscientists coincide in the neural definition of remembering as a reactivation of the patterns that were active during encoding (Josselyn *et al.*, 2015; Tonegawa *et al.*, 2015). For encoding, a cell assembly (or engram) is formed by strengthening of connections between groups of neurons that are active during an event. The engram is further strengthened by the consolidation process, which transforms engrams from an initially labile state to a more permanent state through posttranslational modifications, modulation of gene expression, and morphological synaptic remodeling (Dudai & Eisenberg, 2004). This reinforced spatiotemporal pattern of neural activity is thus more likely to be reactivated (retrieved) at a later time.

This definition follows the logic of Hebbian Learning, which proposes that: “When an axon of cell A is near enough to excite a cell B and repeatedly or persistently takes part in firing it, some growth process or metabolic change takes place in one or both cells such that A's efficiency, as one of the cells firing B, is increased’ (Hebb, 1949).

According to this theory, the stronger the connection between neurons, the stronger memories would be, as Carla Shatz paraphrased: “what fires together, wires together” (Shatz, 1992). Hebb’s affirmation was backed by the discovery that a stimulation of high-

frequency induces long-lasting synaptic strengthening between neurons (long-term potentiation or LTP, to be described later in this section) (Bliss & Gardner-Medwin, 1973; Bliss & Lomo, 1973). This provided the framework for the modern understanding for how engrams might be formed.

The idea that remembering requires the activation of the cells active during encoding is supported by recent genetic tagging experiments during amygdala- and hippocampus-dependent tasks, that have shown that the neurons that were active during the encoding of a memory are more likely to be activated during a “natural” recall of that memory (Denny *et al.*, 2014; Reijmers *et al.*, 2007; Tanaka *et al.*, 2014). Following the same line, blocking the activation of those cells during memory retrieval impairs recall (Berndt *et al.*, 2016; Denny *et al.*, 2014; Han *et al.*, 2009; Hsiang *et al.*, 2014; Park *et al.*, 2016; Rashid *et al.*, 2016; Tanaka *et al.*, 2014; Zhou *et al.*, 2009). Conversely, artificially activating the tagged cell populations out of context induces recall (Cowansage *et al.*, 2014; Liu *et al.*, 2013; Ohkawa *et al.*, 2015; Ramirez *et al.*, 2013; Rogerson *et al.*, 2016; Yiu *et al.*, 2014).

The formation and posterior modification of these neuronal assemblies is possible due to synaptic plasticity mechanisms that include the elimination of some synapses and the formation or strengthening of new ones (Holtmaat & Caroni, 2016). In this context, protein synthesis is thought to be a critical mechanism that confers stability to long-term synaptic changes underlying the consolidation of long-term memory and will be explored in greater detail later on.

2.2 Transience of memory

Conversely to the persistence of memory, that occurs when changes in synaptic connectivity and structure are long-lasting, modifications in that stability lead to forgetting. Likewise, manipulations that promote circuit dynamism are prone to cause transience of memories. This hypothesis is supported, for example, by the effects of Zeta (ζ) Inhibitory Peptide (ZIP). ZIP inhibits the atypical protein kinase C (PKC) isoform PKM- ζ , which plays a key role in maintaining LTP and memory (Sacktor, 2011) and its

infusion after LTP induces depotentiation and erases memory (Pastalkova *et al.*, 2006; Tsokas *et al.*, 2016).

Another study that induced memory loss was performed by Hayashi-Takagi and colleagues (2015). In this study, they generated a photoactivable form of Rac1 (a key GTPase regulating actin cytoskeletal dynamics) to induce spine shrinkage *in vivo*, which allowed them to control synaptic strength with light. After rotarod training, they eliminated the learning-induced synaptic growth, causing mice to lose the acquired motor skills. Although these manipulations caused very rapid memory loss, natural forgetting is much more gradual (Ebbinghaus, 1913). Supporting this idea, Dong and colleagues (2015) found that rats trained with a weak protocol in the inhibitory avoidance test showed robust avoidance 1 hour after training but not after 24 hours, in contrast to the weeks-lasting avoidance generated by a strong training (Inda *et al.*, 2011). However, preventing GluA2 endocytosis, a central mechanism for LTM maintenance (Hardt *et al.*, 2014) prolonged this initially weak memory (Dong *et al.*, 2015).

It is then clear that some endogenous processes impact transience, as is the continuous turnover of synaptic spines. Other processes such as neurogenesis have also been invoked. In the adult brain, neurogenesis occurs at least in the subgranular and subventricular zones of the dentate gyrus (DG). These new neurons facilitate the formation of hippocampal memories. However, these cells establish new connections and integrate in hippocampal circuits. Several studies have hypothesized that integration of newly-generated neurons overwrite existing memory and promote forgetting (Akers *et al.*, 2014; Epp *et al.*, 2016; Ishikawa *et al.*, 2016; Kitamura *et al.*, 2009).

Although seemingly menacing for a healthy memory at first, certain levels of transience, in equilibrium with persistence are key for a balanced practical use of our brain. Forgetting is necessary for the flexibility of our behavior. For one example, preventing forgetting in rats led to impairments in generalization, leading to the hypothesis that the same mechanisms that lead to forgetting promote memory generalization (Migues *et al.*, 2016). Memory generalization was also detected by Eric

Introduction and objectives

Klann's team using a cell-type specific chemogenetic approach that increased protein synthesis by manipulation of the eukaryotic initiation factor 2 α (eIF2 α). The phosphorylation of eIF2 α prevents the activity of eIF2B, inhibiting general new protein synthesis. Their strategy was to virally deliver Camk2 α .Cre.eGFP bilaterally to the lateral amygdala of floxed phosphomutant eIF2 α mice, since constitutive heterozygous phosphomutant eIF2 α mice have enhanced LTM in several memory paradigms including contextual and auditory threat conditioning and conditioned taste aversion (Costa-Mattioli *et al.*, 2007). They found that this manipulation increased protein synthesis and enhanced memory strength but reduced memory fidelity and behavioral flexibility (Shrestha *et al.*, 2020a). In another study, Paul Frankland's lab examined the role of neurogenesis-mediated forgetting in the Morris water maze (Epp *et al.*, 2016). They trained mice to find a submerged platform in a pool and promoted neurogenesis after training by allowing mice with free access to a running wheel. Wheel access fostered mice exercise, enhanced hippocampal neurogenesis and facilitated forgetting: when the platform was moved to the opposite quadrant of the pool, the mice with enhanced hippocampal neurogenesis found the new platform location more rapidly. Conversely, post-training suppression of neurogenesis by inducing apoptosis in newly generated neurons with vanganciclovir, led to a better memory of the first platform location, but interfered with learning the new location.

2.3 Memory ontogeny

Often considered to be an immature version of the adult brain, the infant brain's neural network is indeed rudimentary and its cognitive abilities are limited. Yet although immature, the infant brain is capable of plasticity and learning and supports complex cognitive operations. However, adults retain very little information of events that happened during infancy, a phenomenon for which Freud coined the term of infantile amnesia (Freud, 1914). Infantile amnesia has been modeled in rodents using contextual fear conditioning (Akers *et al.*, 2012) and inhibitory avoidance (Travaglia *et al.*, 2016). The use of both paradigms showed that rodents trained before the third postnatal week

undergo rapid forgetting, while training after the fourth week caused long-lasting memories (Fig. 2).

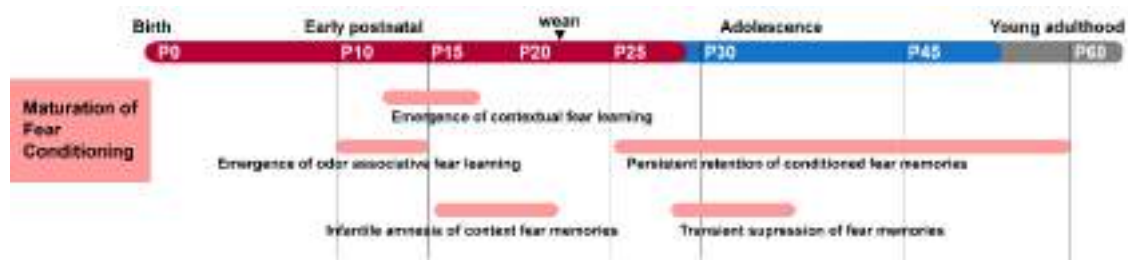


Figure 2. Timeline of fear conditioning-associated major events during rodent development. Odor associative fear learning emerges early in life, behaviors such as contextual fear learning and persistent retention of conditioned fear require a more mature brain. The emergence of these behaviors corresponds with the maturation of relevant neural circuits. Adapted from Klune *et al.*, 2021.

Learning from experience is one of the most important functions for our survival. It relies heavily on the hippocampus-dependent memory system, but even when infancy and childhood are periods characterized by the need for a rapid learning, the structural and functional maturation of the hippocampus extends beyond these periods. This led to Campbell and Campbell's (1962) postulate that infantile amnesia is due to the restricted ability of the developing hippocampus to process information. Indeed, hippocampal circuits, such as the entorhinal-hippocampal circuit, mature late during brain development and at distinct rates. For instance, in rodents, the medial entorhinal cortex has matured by the third postnatal week (Donato *et al.*, 2017; Ray & Brecht, 2016) while the lateral entorhinal cortex does not mature until the end of the fourth week (Donato *et al.*, 2017). Prefrontal circuits end their maturation at six weeks, corresponding to adolescence in humans (Chini & Hanganu-Opatz, 2021; Kolk & Rakic, 2022).

Connections between the medial prefrontal cortex (mPFC), the hippocampus and the amygdala play key roles in adaptive behaviors such as conditioned fear. Thus, it is likely that the maturation of these pathways is also necessary for the emergence of related behavioral functions. During early postnatal weeks, mPFC cells exhibit immature

Introduction and objectives

morphological and functional characteristics, like more dendritic spines and higher spine turnover than in adults (Johnson *et al.*, 2016); or higher levels of the immediately early genes (IEGs) *Arc*, *c-Fos* and *Zif268* (Jia *et al.*, 2018), a reflection of an immature regulatory mechanisms.

3. Substrates of memory

3.1 Long-term potentiation (LTP)

As outlined in section 2.1, Bliss and Lomo discovered that high-frequency stimulation of the fibers of the hippocampus results in a long-lasting enhancement of synaptic transmission efficacy (Bliss & Lomo, 1973) and coined the term long-term potentiation. Hippocampal LTP attracted enormous attention since its discovery, has been studied in depth and is considered the biological substrate of learning and memory (Bliss and Dolphin, 1982; Goddard 1980; Voronin, 1983). Supporting evidence included the early findings that rhythmic bursts of activity that lead to LTP induction mimic naturally occurring rhythms in the hippocampus during exploratory behavior (Greenstein *et al.*, 1988; Larson *et al.*, 1986) or that LTP-inhibitors, such as AP5, block hippocampal learning (Morris *et al.*, 1986).

LTP is divided in two phases: an early phase (E-LTP) which lasts 2-3 hours; and a later phase (long-lasting LTP, L-LTP) which lasts weeks. A key feature is that E-LTP, like short-term memory, is independent of protein synthesis, while L-LTP, as long-term memory, requires protein synthesis for its persistence. A crucial trigger for LTP is postsynaptic calcium influx which is necessary and sufficient to induce LTP (Bliss & Collingridge, 1993). This event is mediated by the activation of NMDARs, thus making these receptors critical for LTP.

3.2 NMDARs

NMDARs are ionotropic glutamate receptors that mediate fast excitatory synaptic transmission in the central nervous system. They are heterotetrameric assemblies of two mandatory GluN1 subunit and combinations of GluN2 (A-D) and GluN3 (A-B) (Monyer *et al.*, 1992; Schorge *et al.*, 2003). The specific subunit composition of NMDAR subtypes confers specific biophysical properties and protein interactions which will determine the unique trafficking, localization, signaling and functions of the receptor (Lau *et al.*, 2007; Paoletti *et al.* 2013). NMDARs are essential mediators of brain plasticity and convert

specific neuronal activity patterns into long-term changes in synapse structure. In higher brain structures of adult and juvenile mice, such as the cortex and hippocampus, GluN2A and GluN2B-containing NMDARs have central roles in synaptic plasticity and function (Monyer *et al.*, 1994) and mediate LTP.

During the period of postnatal refinement, the transition from juvenile to mature NMDAR subtypes which differ in subunits composition and properties is thought to be a key driver of the maturation and stabilization of excitatory synapses (Hansen *et al.*, 2017; Paoletti *et al.*, 2013). At early postnatal and juvenile stages, synapses throughout the CNS are mainly composed of di-heteromeric GluN1/2B and tri-heteromeric GluN1/2B or 2A/3A NMDARs (Paoletti *et al.*, 2013). Pure GluN2A or 3A-containing NMDARs are progressively replaced by mature di-heteromeric GluN1/2A or tri-heteromeric GluN1/2B/2A receptors in most brain regions (Sheng *et al.*, 1994; Watanabe *et al.*, 1992).

3.2.1 Properties and expression pattern of GluN3A-NMDARs

GluN3A-containing tri-heteromeric NMDARs (from now on referred to as GluN3A-NMDARs) respond to glutamate and NMDA and display atypical biophysical and trafficking properties relative to classical NMDARs composed of GluN1 and GluN2 subunits (Burzomato *et al.*, 2010; Das *et al.*, 1998; Matsuda *et al.*, 2003; Perez-Otano *et al.*, 2001; Roberts *et al.*, 2009; Sasaki *et al.*, 2002; Tong *et al.*, 2008), gaining the term of “non-conventional NMDARs”. Compared to GluN1/GluN2 NMDARs, GluN3A-NMDARs exhibit smaller single-channel conductance (Perez-Otano *et al.*, 2001; Sucher *et al.*, 1995), lower Ca²⁺ permeability (Sasaki *et al.*, 2002), a lower open probability but longer mean open times (Perez-Otano *et al.*, 2001), and a relative insensitivity to voltage-dependent Mg²⁺ block (Burzomato *et al.*, 2010; Chatterton *et al.*, 2002; McClymont *et al.*, 2012; Roberts *et al.*, 2009; Sasaki *et al.*, 2002).

Current data pinpoints the relevance of GluN3A-NMDARs as key players on the postnatal development of synapse plasticity and on the stabilization of neural circuits. GluN3A subunits are highly expressed in the brain during a narrow temporal window of

postnatal development when massive synapse stabilization and elimination occur, and their expression drops markedly in most brain regions after these periods (Pérez-Otaño *et al.*, 2006; Wong *et al.*, 2002). Molecular manipulations in mice show that prolonging GluN3A expression beyond its natural time window (Fig. 3A) inhibits synapse maturation and promotes pruning (Fig. 3B), whereas GluN3A deletion accelerates synapse maturation and leaves hyperconnected circuits (Henson *et al.*, 2012; Kehoe *et al.*, 2014; Roberts *et al.*, 2009). Specifically, ablation of GluN3A expression at CA3-CA1 synapses accelerates the postnatal onset of LTP (Roberts *et al.*, 2009). Another study found that overexpressing GluN3A inhibits LTP and reduces spine density by increasing spine turnover and elimination, and decreasing spine stability. By contrast, GluN3A deletion reduced spine turnover and favored stability, both features of mature brains (Kehoe *et al.*, 2014). Previous work had shown that GluN3A deletion increases the expression of GluN2A or AMPA receptors (AMPA receptors) considered markers of synaptic maturation (Henson *et al.*, 2012) The characteristic time window of GluN3A expression coincides with critical periods of postnatal experience-driven refinement of neural circuits.

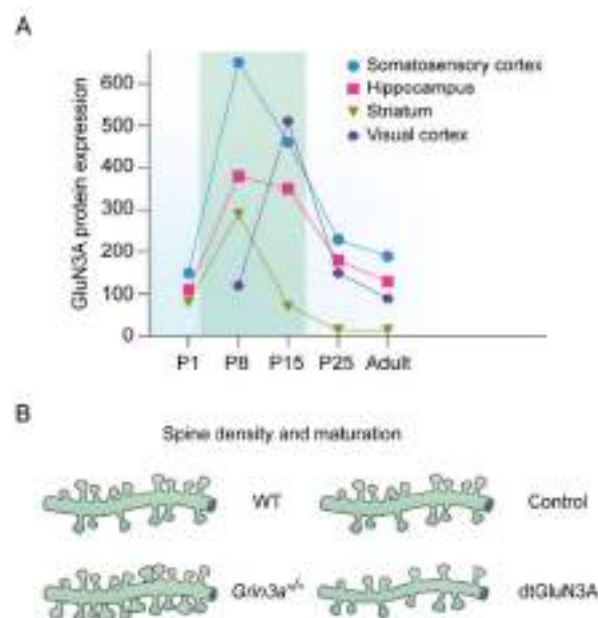


Figure 3. GluN3A temporal expression and effect on spine density. A) GluN3A protein expression during rodent brain development. Graph shows GluN3A peak of expression during the critical circuit refinement period (shaded area) in different brain areas in the first postnatal days (P5-P10) of development. After that, sharp

Introduction and objectives

decrease expression occurs into adulthood. B) Drawing shows dendritic segments from cortical neurons of *Grin3a*^{-/-} mice (left) which had increased density of spines compared to neurons from WT mice, indicative of a mature morphology. Conversely, dendritic spine size and density were reduced in transgenic mice with GluN3A prolonged expression (dtGluN3A) (right). Modified from Perez-Otaño *et al.*, 2016.

Recent work from our lab mapped *Grin3a* (rodent gene encoding GluN3A, homologue to human *GRIN3A*) mRNA expression in the mouse brain from embryonic to postnatal and adult stages (Murillo *et al.*, 2021). Though heavily downregulated in the adult brain, significant GluN3A levels were found to be retained in areas with high plasticity needs, like amygdala nuclei, the medial habenula, association cortices, the olfactory system or the claustrum (Fig. 4).

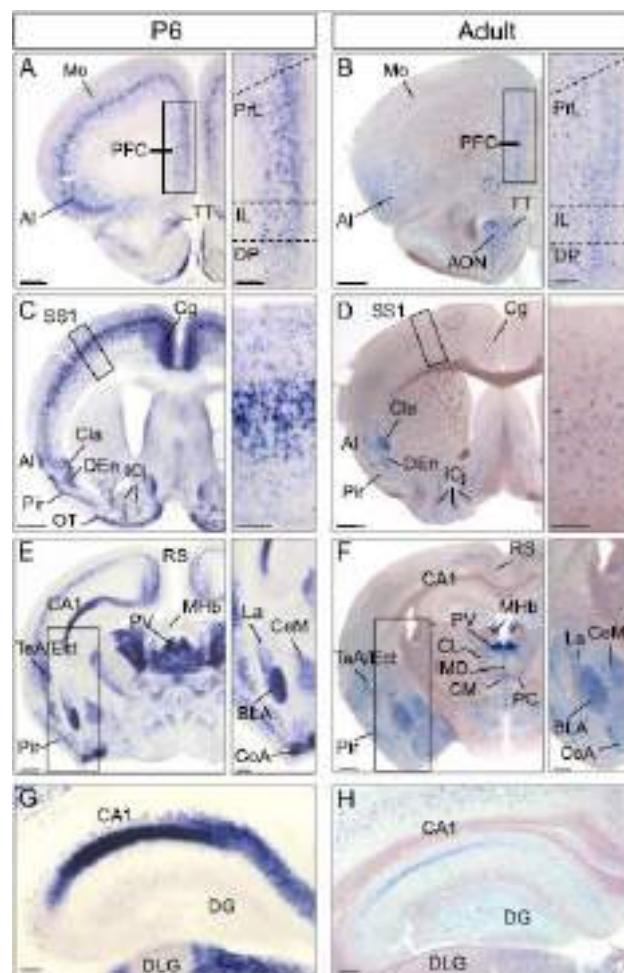


Figure 4. Differential *Grin3a* expression through mouse lifespan. *In situ* hybridizations showing *Grin3a* mRNA expression in P6 (A, C, E, G) and adult mouse brain (B, D, F, H). Higher magnification images of the boxed areas are

shown on the right. AI, agranular insular cortex; AON, anterior olfactory nucleus; BLA, basolateral amygdala; CA1, Cornu Ammonis 1; CeM, central amygdala; Cg, cingulate cortex; CL, centrolateral thalamic nucleus; Cla, claustrum; CM, centromedial thalamic nucleus; CoA, cortical amygdala; DEn, dorsal endopiriform nucleus; DG, dentate gyrus; DLG, dorsal lateral geniculate nucleus; DP, dorsal peduncular cortex; Ect, ectorhinal cortex; ICj, islands of Calleja; IL, infralimbic cortex; IMD, intermediodorsal thalamic nucleus; La, lateral amygdala; MHb, medial habenula nucleus; Mo, motor cortex; OT, olfactory tubercle; PC, paracentral thalamic nucleus, PFC, prefrontal cortex; Pir, piriform cortex; PrL, prelimbic cortex; PV, paraventricular thalamic nucleus; RS, retrosplenial cortex; SS1, somatosensory cortex 1; TeA, temporal association cortex; TT, tenia tecta. Scale bars: 500 μm (A-F); 200 μm (G-H and insets). (Adapted from Murillo *et al.*, 2021).

Regarding cell types, GluN3A levels are particularly high in somatostatin interneurons (Fig. 5A) of the neocortex and hippocampus (Murillo *et al.*, 2021, Pfeffer *et al.*, 2013). GluN3A is also prominently expressed in excitatory pyramidal neurons in the cortex and hippocampus, retinal ganglion cells and cerebellar Purkinje neurons (Fig. 5B) (Henson *et al.*, 2010; Pachernegg *et al.*, 2012).

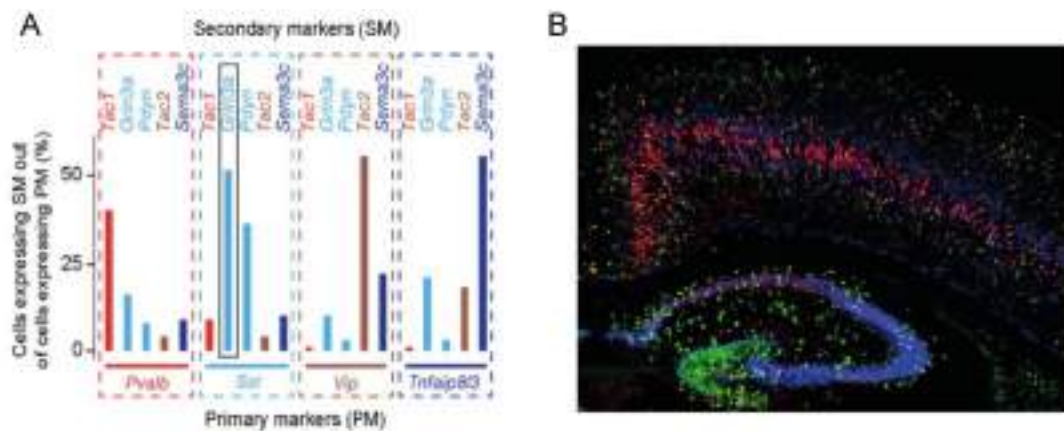


Figure 5. GluN3A expression patterns. A) Single-cell transcriptomic analyses of mouse somatosensory and visual cortex interneurons (Pfeffer *et al.* 2013) showing high levels of *Grin3a* expression in *SST* interneurons (adapted from Crawley *et al.*, 2021). B) *Grin3a* expression in excitatory and inhibitory neurons: Representative coronal section from a P6 wild-type mouse brain labeled by RNAscope for *Grin3a* mRNA (red) and markers of inhibitory (green: *Gad1* mRNA) and excitatory neurons (blue: *vGlut1* mRNA) (adapted from Murillo *et al.*, 2021).

3.2.2 GluN3A links to CNS disorders

Alteration in synaptic NMDARs function, either hyperactivity or hypofunction, can cause synaptopathies such as Alzheimer's disease, Parkinson's disease, depression, autism

Introduction and objectives

spectrum disorders, among others (Paoletti *et al.*, 2013). This is the case of GluN3A-NMDARs, which have been implicated in schizophrenia due to its elevated levels or gene variants found in the brains of schizophrenic patients at autopsy (Mueller & Meador-Woodruff, 2004; Yu *et al.*, 2018). *GRIN3A* gene variants and changes in GluN3A expression have also been linked to addiction to alcohol, heroin or opioids (Roozafzoon *et al.*, 2010; Liu *et al.*; 2021), findings coherent with the observation that a single cocaine injection elevates levels of GluN3A-NMDARs in the synapses of reward-related regions (Yuan *et al.*, 2013). Another example of the relation between GluN3A and disease came out of a series of discoveries from the lab of Prof. Isabel Perez-Otaño. First, Marco and colleagues (2013) found an aberrant reactivation of GluN3A in the adult striatum of mouse models of Huntington's Disease (HD) due to a specific trafficking defect caused by mutant huntingtin. Genetic deletion of GluN3A prevented the observed HD-like phenotype, suggesting putative translational value. Later development of a gene therapy strategy using AAV-mediated RNAi in HD mouse models demonstrated that GluN3A suppression reversed the disease phenotype (Marco *et al.*, 2018). Further studies reported that *Grin3a*^{-/-} mice display increased pain sensation (Mohamad *et al.*, 2013), or impaired social behavior (Lee *et al.*, 2018).

A number of studies provide insights on the role of GluN3A in cognition. Object recognition, spatial memory and learning are apparently enhanced in adult *Grin3a*^{-/-} mice (Mohamad *et al.*, 2013). Whereas memory consolidation in adult GluN3A overexpressing mice is impaired, memory acquisition remains unaffected (Roberts *et al.*, 2009). Lastly, a recent study implicated glycine-gated GluN1/GluN3A receptors in the media habenula (MHb) in the control of aversive behaviors (Otsu *et al.*, 2019).

The evidence above suggested that reducing GluN3A expression seems of therapeutic potential. However, reduced levels of mRNA and GluN3A protein were found in bipolar disorder patients (Mueller & Meador-Woodruff, 2004) and, as mentioned before, *Grin3a* knockout mice have shown deficits in social behavior, a hallmark of Autism Spectrum Disorder (Lee *et al.*, 2018).

Regarding Alzheimer's Disease (AD), the most prevalent neurodegenerative disease (Arrondo *et al.*, 2022) and leading cause of dementia worldwide (Ferri *et al.*, 2005), *GRIN3A* genetic variants have been associated with and increased risk of developing AD (Crawley *et al.*, 2021). Interestingly, a recent study by Zhong *et al.* (2021) indicated that old mice lacking *GluN3A* showed slower learning and memory deficits, in shocking contrast with earlier evidence of the improvements in cognition-related tasks listed above and endorsed by their own laboratory as well as ours (Conde-Dusman *et al.*, 2021; Verhaeghe *et al.*, 2023). More research is needed in the field to shed light on this specific matter.

3.3 The mTOR pathway and protein synthesis

The mechanistic (formerly “mammalian”) Target of Rapamycin (mTOR) is a serine-threonine kinase that regulates signal transduction and it is implicated in cellular homeostasis and control of cell growth, survival and proliferation in many cell types (Sabatini, 2017). It is also a main actor in autophagy, cytoskeletal reorganization and lipid, nucleotide and *de novo* protein synthesis (Liu and Sabatini, 2020), key processes in the long-lasting changes needed in the neural system. To carry out these functions, mTOR forms two functionally and structurally distinct multiprotein complexes: mTOR complex 1 (mTORC1) and mTOR complex 2 (mTORC2) (Fig. 6). While mTORC2 is crucial in cell survival and proliferation or actin cytoskeleton dynamics, this work will focus on the role of mTORC1 and protein synthesis.

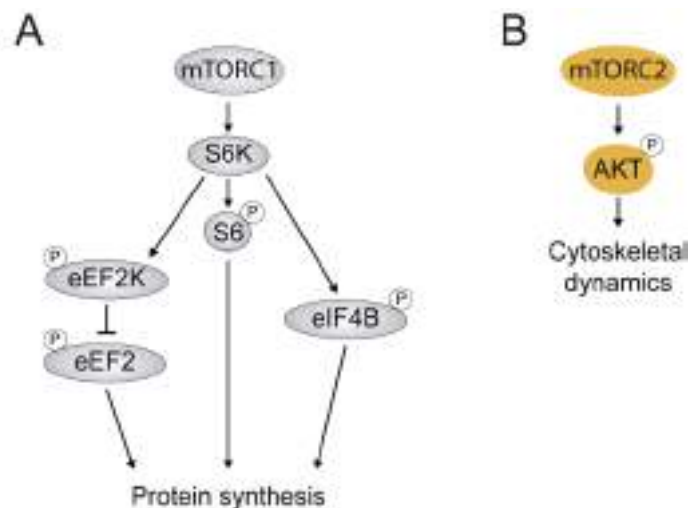


Figure 6. Schematic overview of mTORC1 and mTORC2 signaling pathways. A) mTORC1 regulates protein translation through activation of S6K, and inhibition of eEF2, and enhances RNA translation via S6. B) mTORC2 regulates cell survival and cytoskeletal organization primarily by phosphorylating its substrates.

mTORC1 regulates protein synthesis by phosphorylation of its downstream effector ribosomal S6 kinase (S6K) at Thr³⁸⁹ (Ma *et al.*, 2008). S6K promotes protein synthesis by phosphorylating three main targets: the 40S ribosomal protein S6 (S6), the eukaryotic elongation factor 2 kinase (eEF2K), and the eukaryotic initiation factor 4B (eIF4B). S6 phosphorylation is essential for ribosomal biogenesis and protein synthesis initiation (Fenton and Gout, 2010). eEF2K phosphorylation suppresses its ability to phosphorylate the eukaryotic elongation factor 2 (eEF2). eEF2 dephosphorylation further stimulates the elongation of nascent peptide chains (Ma and Blenis, 2009). Lastly, eIF4B phosphorylation promotes the activity of the RNA helicase eIF4A and permits the translation of mRNAs with longer 5'-UTRs (Lipton and Sahin, 2014).

A large body of evidence supports the role of mTOR in LTP and memory. First, Tang *et al* (2002) found mTOR to be localized at synapses and that is necessary for LTP. They also discovered that rapamycin, the main mTOR inhibitor, decreased L-LTP, data supported by Cammalleri and colleagues (2003). At the same time, a study by Takei *et al* (2001) found that the protein synthesis initiation stimulated by brain-derived

neurotrophic factor (BDNF) relies on mTOR signaling. Complementing their study, they discovered that local protein synthesis is mTOR-dependent (Takei *et al.*, 2004).

More controversial evidence is available on the specific implication of mTOR complexes in synaptic plasticity. A study discovered that only mTORC1 is required for hippocampal L-LTP, LTM consolidation and reconsolidation of contextual fear conditioning memory (Stoica *et al.*, 2011). In this study, they used a low dose rapamycin treatment (10nM) to inhibit mTORC1 signaling without affecting mTORC2 in mTOR heterozygous mice (mTOR^{+/-}). Years later, the same lab used a mTORC2-deficient mouse in which *Rictor* was postnatally deleted in the forebrain and found that both L-LTP and LTM were impaired in hippocampal slices from mTORC2-deficient mice (Huang *et al.*, 2013).

It was recently found that enriched environment enhanced LTP in a mTOR-dependent manner (Hullinger *et al.*, 2015), while sleep deprivation, which reduces mTORC1 activation, impaired hippocampal protein synthesis in vivo (Tudor *et al.*, 2016).

Although again controversial, particularly in regard to the roles of different subtypes, evidence links mTOR and NMDARs. For example, Cammalleri and colleagues (2003) shown NMDAR-dependent phosphorylation of the mTORC1 effector S6K in dendrites upon depolarization with KCl or glutamate, while in another study, pharmacological blockade of NMDARs with APV or MK-801 increased phosphorylation of S6 and 4E-BP, indicating mTOR activation (Huang *et al.*, 2007). Pharmacological blockade of NMDARs with ketamine also led to mTOR activation and protein synthesis with therapeutic effects in depression-like behaviors (Li *et al.*, 2010). Whether discrepancies reflect differences in subunit composition is yet to be addressed.

4. Objectives

Building upon previous work from our laboratory, which demonstrated that GluN3A-NMDARs are key players in the postnatal refinement of neural circuits, the goal of this thesis was to perform a comprehensive analysis of the extent and the impact of GluN3A-mediated refinements in cognition-related behaviors. A major objective was to dissect out the roles of postnatal GluN3A expression in shaping mature circuits versus the roles of adult GluN3A expression, to validate the possibility of targeting GluN3A-NMDARs for therapeutic purposes. The work was structured into three specific objectives:

1. To test how GluN3A expression impacts cognition-related behaviors through the mouse lifespan: from the emergence of memory to adult memory domains or potential influences on age-dependent cognitive decline.
2. To use mouse genetics to determine whether GluN3A-linked behavioral changes arise from altered synapse development or are a feature of adult synapses, and to identify the cell populations involved.
3. To unveil the mechanisms underlying GluN3A-related alterations in behavior.

Materials & methods



1. Experimental animals

Mice were the animals of choice because they provide a powerful tool to link specific genes to changes in behavior. Animals were housed four to five per cage with *ad libitum* access to food and water and maintained in a temperature-controlled environment on a 12-hr dark/light cycle at the RMG (Spanish for genetically modified mice) vivarium of the Miguel Hernández University. All procedures were conducted in accordance with the European and Spanish regulations (2010/63/UE; RD 53/2013) and were approved by the Ethical Committee of the Generalitat Valenciana. Mice backcrossed for 10–12 generations into a C57Bl6/J background were used.

Constitutive Grin3a^{-/-} mice

B6;129X1-Grin3a^{tm1Nnk}/J (JAX:029974) mice (hereafter *Grin3a^{-/-}*) were kindly provided by Nobuki Nakanishi and Stuart Lipton (Das *et al.*, 1998) and bred with *wild type* C57Bl6/J mice (JAX:000664) for 10 generations. Heterozygous *Grin3a^{+/-}* mice were used for breeding purposes while *Grin3a^{-/-}* and their *Grin3a^{+/+}* (hereafter wild type, WT) littermates were used for experimental purposes.

dtGFPGluN3A mice

Mice overexpressing GluN3A were generated by generated and characterized in the Pérez-Otaño lab (Roberts *et al.*, 2009). In brief, a GFP-tagged version of the rat GluN3A open-reading frame (Perez-Otaño *et al.*, 2001) was cloned into pMM400 (kindly provided by Mark Mayford). The NotI fragment was isolated and injected into pronuclei of B6SJLF1/J F2 oocytes. Resulting mice were backcrossed to C57BL/6J mice to establish founder lines, that were subsequently crossed with mice expressing the tTA transgene under the control of the CaMKII α promoter (Mayford *et al.*, 1996).

1.2 Generation of cell type-specific GluN3A-lacking mice

For ablation of GluN3A in specific cell types, *Grin3atm1a*^{(EUCOMM)Hmgu/H} (hereafter *Grin3a^{ff}*) mice were crossed with different Cre-driver mouse lines. This mouse line was generated by inserting the L1L2_Bact_P cassette at position 49793582 of Chromosome 4 upstream the critical exons. This cassette is composed of a flipase recognition target (FRT) site followed by lacZ sequence and a loxP site. This first loxP site is followed by a neomycin resistance gene under the control of the human beta-actin promoter, SV40 polyA, a second FRT site and a second loxP site. A third loxP site is inserted downstream of the targeted exon at position 49793582. The critical exon is thus flanked by loxP sites. Subsequent Cre expression results in a knockout mouse.

Selective ablation of Grin3a from excitatory neurons

Grin3a^{ff} mice were crossed (Fig. 7) with tamoxifen inducible CaMKII α -Cre^{ERT2+/-} mice (Erdmann *et al.*, 2007) to generate *Grin3a^{ff}* x CaMKII α -Cre^{ERT2+/-} mice, where selective deletion from projection neurons in the cortex and hippocampus can be induced with tamoxifen, and *Grin3a^{ff}* x CaMKII α -Cre^{ERT2-/-} controls.

Materials & methods

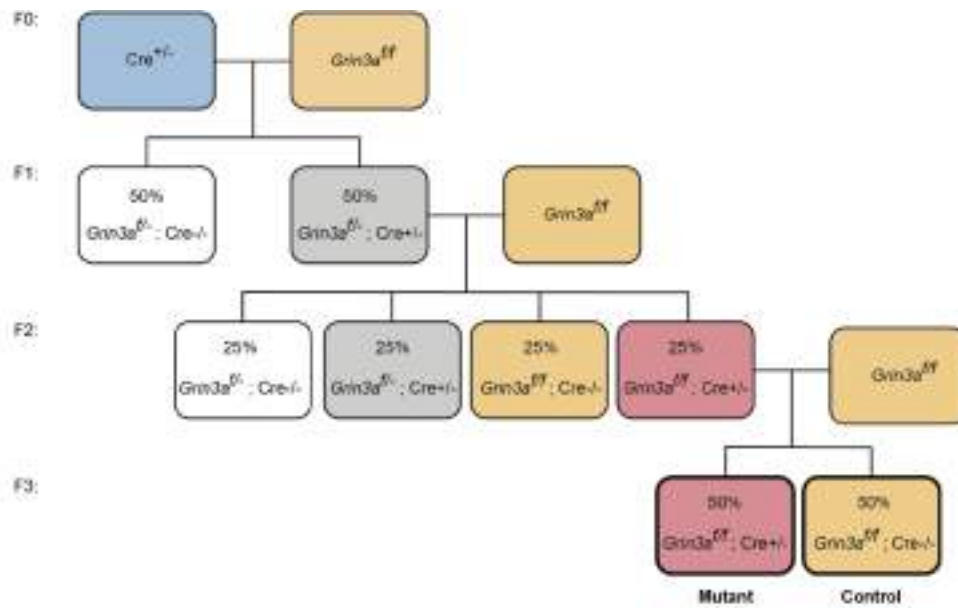


Figure 7. Breeding scheme used for the generation of cell-type specific *GluN3A*-lacking mice. Note that following F3, all animals are suitable for experimentation. Littermate cohorts were used.

To trigger ablation of *Gln3a*, tamoxifen (TMX; Sigma-Aldrich; T5680) was administered in two different ways depending on mice age:

- For adult animals, tamoxifen was dissolved at a concentration of 20mg/ml in corn oil and 200µl of solution was given to each mouse via oral gavage, every other day for 10 consecutive days. 20 days were then additionally allowed for recombination to occur (Fig. 8A)
- For postnatal mice, tamoxifen was dissolved at a concentration of 1mg/ml in corn oil and 50µl of solution was given to each mouse via intraperitoneal injection every day for 3 consecutive days (Fig. 8B).

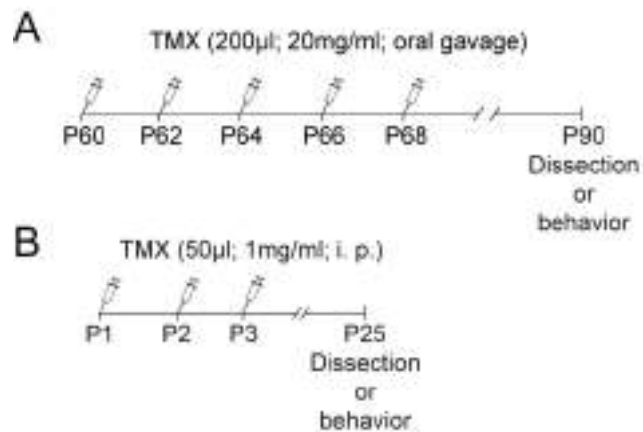


Figure 8. Tamoxifen administration regimes. A) Tamoxifen regime used for adult mice. B) Regime used for ablation of GluN3A in postnatal mice. Volume administered, tamoxifen concentration and administration method are indicated.

Selective ablation of Grin3a from inhibitory neurons

Grin3a^{ff} mice were selectively crossed with *Sst-IRES-Cre* (JAX:018973), following the previously shown reproductive strategy (Fig. 7) to generate *Grin3a^{ff} x Sst-IRES-Cre^{+/-}* and *Grin3a^{ff} x Sst-IRES-Cre^{-/-}* controls.

2. Behavioral tests

2.1- Spatial learning: Morris water maze (MWM)

This behavioral test was first described in 1981 (Morris, 1981) to assess spatial learning and memory in rats. It has since been adapted for use in mice and it is the most widely used for this. The Morris water maze is based on the idea that rodents find water aversive, thus escaping from water is a positive reinforcer. For this test, a circular tank (190 cm diameter) is filled with water made opaque with non-toxic white tempera paint (1g/10l) and maintained at a controlled temperature of $25 \pm 1^\circ\text{C}$. The tank is virtually divided into 4 quadrants, and a platform is placed in one of the quadrants. The goal is for mice to learn the location of the platform using contextual cues placed around the tank. Mice are tracked throughout the whole protocol using the video-tracking software SMART (Panlab S.L.). The protocol is divided into different phases:

Materials & methods

- Visual platform phase: this first phase is used to check the locomotor and visual capacities of mice. During this phase there is no external contextual cues and the platform is signaled with a black pole. The platform is located in a random quadrant and each mouse has 120 seconds to find it. If it fails to do so, it is gently guided to it and allowed 10 seconds to explore it. Once every mouse has completed one trial, the platform is relocated and the protocol is repeated. Four trials per day are performed.
- Hidden platform phase: this phase is used to test contextual memory. During this phase, external contextual cues are located in four cardinal points around the tank. The platform is submerged 1 cm into the opaque water and stays in the same quadrant for the whole length of the protocol. Each mouse is given 120 seconds to find the platform and it is gently guided to it if it fails to do so. Each mouse is given 10 seconds to explore its surroundings once it is on the platform. The number of trials per day can be adjusted to increase the difficulty of the task, four trials per day being the standard protocol. Here four and two trials per day were used. Intertrial interval was 45 minutes. In order to avoid a mechanical-learning induced bias, mice were introduced in the water from a different quadrant every trial.
- Reversal phase: this phase tests behavioral flexibility, the ability to readapt a memory to a new context. For this phase, the hidden platform is relocated to the opposite quadrant of the tank and mice are trained as during the hidden platform phase.
- Probe tests: at the end of hidden platform and reversal phases, sixty-second-long test tests in which the platform was removed from the water were performed to test contextual memory. Time spent in the target quadrant (the quadrant where the platform used to be) was compared to the average time spent in all other quadrants.

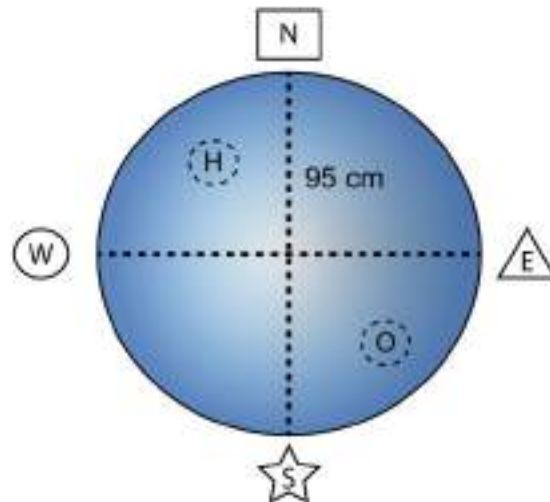


Figure 9. Schematic representation of the Morris water maze. Distinct external cues signal four cardinal points (N: North; S: South; W: West; E: East; these cardinal points are for indicative purposes only and do not correspond with actual cardinal points) and divide the pool in four equal quadrants. Mice are first trained to find the submerged platform in location H. During reversal platform phase, the platform location is switched to the opposite quadrant (location O). Platform is removed for probe trials.

2.2- Y-maze spontaneous alternation task

The Y-maze spontaneous alternation task is used to assess repetitive behaviors in mice (Lalonde, 2002). It is based in the innate willingness of rodents to explore new environments. Testing occurs in a Y-shaped maze with three transparent plexiglass arms (10x10x50cm) at a 120° angle from each other. During testing, mice are introduced one by one in the maze and allowed to freely explore the three arms for 5 min. If the animal chooses a different arm than the one it arrived from twice, this is called a triad. This is considered the correct response, whereas returning to the previous arm is considered an error. The total number of arm entries and the sequence of entries are recorded in order to calculate the percentage of alternation. Correct triad scores were noted when all three arms were sequentially entered. Alternation indices were calculated as correct triads/possible triads. Maze was cleaned between animals with a water-based soap solution.

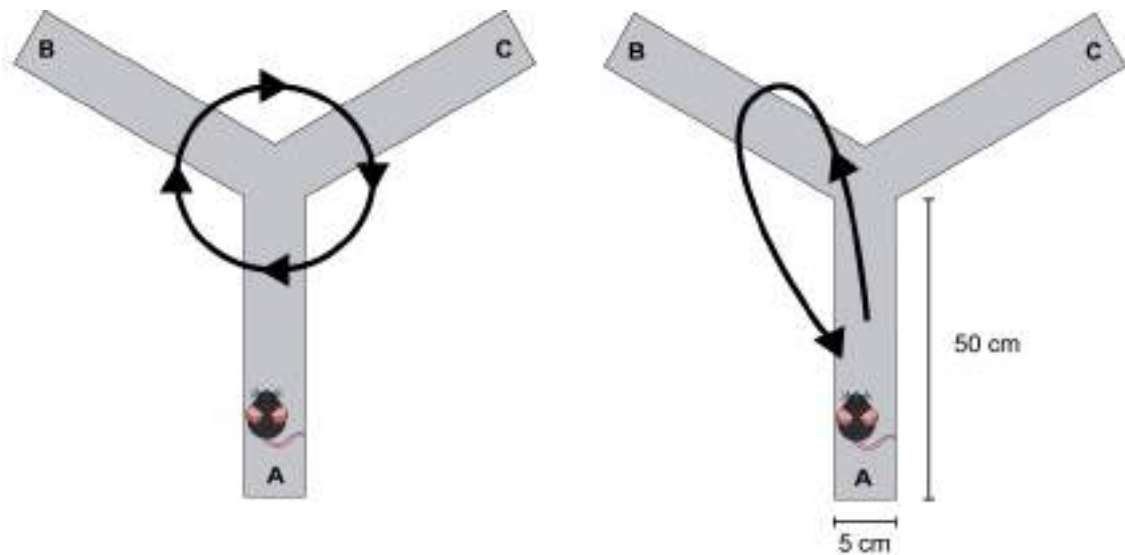


Figure 10. Schematic of the Y-maze. A sequential entrance to all three arms of the maze is considered a correct trial (left panel), while failing to enter one of the arms during the sequence is considered an incorrect trial (right panel). Arm measurements are indicated, walls are 10cm tall to prevent mice from escaping.

2.3- Fear conditioning

Fear conditioning (FC) is a type of associative learning task in which mice learn to associate a primarily neutral Conditional Stimulus (CS; in this case, a context) with an aversive Unconditional Stimulus (US; in this case, an electrical foot shock) (Crawley, 2007). After pairing the CS and US, the animal learns to fear the CS. Though US can be modified in intensity and number to adjust the difficulty of the learning paradigm, FC is learned rapidly, and after one conditioning session, a very stable and long-lasting behavioral change is often produced.

Fear conditioning was carried out with a computerized Fear and Startle system (Panlab-Harvard, Barcelona, Spain). Tones and shocks were delivered and controlled using Freezing v1.3.04 software (Panlab-Harvard, Barcelona, Spain). The fear chambers consisted of a black methacrylate box with a transparent front door (25x25x25cm) inside a sound-attenuating cubicle (67x53x55cm). The chambers were carefully cleaned before and after each mouse. Freezing behavior, a rodent's natural response to fear defined as the absence of movement except respiration, was scored by a high sensitivity weight

transducer system located at the bottom of the experimental chambers which records and analyses the signal generated by the movement of the animal.

Three different protocols were used:

- *Weak fear conditioning*: Animals were habituated to the chambers for 5 min/day during two consecutive days prior to FC. During training day, mice were placed in the fear chambers and allowed to explore a context (CS) (metal grid floor, dim light) for 2 minutes. Mice were then presented with a foot shock (US) (0.3 mA, 2s). Sixty seconds later, they were returned to their home cage. Conditioning was assessed at 1 (short-term memory), 24 and 48 hours (long-term memory) or 7 days (remote memory) by re-introducing mice in the conditioning context for 5 minutes.
- *Strong fear conditioning*: Animals were introduced in the conditioning chambers and allowed to explore the context (CS) (metal grid floor, dim light) for 2 minutes. Mice were then presented with three strong foot-shocks (US) (0.5 mA, 2s) sixty seconds apart. Sixty seconds after the last shock, they were returned to their home cage. Conditioning was assessed at 24 hours and 7 days by re-introducing mice in the conditioning context for 5 minutes.
- *Mixed (contextual and cued) fear conditioning*: Animals were introduced in the conditioning chambers and allowed to explore the context (CS) (metal grid floor, dim light) for 2 minutes. Mice were then presented with a 30-second long tone (85dB; 2800kHz) co-terminated with one foot-shock (US) (0.3 mA, 2s). Sixty seconds after the shock, they were returned to their home cage. Conditioning was assessed at desired time points by re-introducing mice in the conditioning context for 5 minutes.

2.4- Contextual fear discrimination

The use of fear conditioning paradigms can lead to fear generalization, the transfer of conditioned responses to stimuli that perceptually differ from the original conditioned stimulus. Our contextual fear discrimination paradigm addresses the reaction of mice to

Materials & methods

four different contexts. Mice are first repeatedly trained in a context, then context discrimination is assessed when subtle differences are introduced on the context during subsequent trials while freezing response is measured. High levels of freezing are expected when testing mice in the training context and in contexts similar to it. Freezing responses should be lower in each trial when mice are tested in contexts that are progressively different to the training context.

Training consisted in three consecutive days during which mice were placed in the conditioning chambers and allowed to explore a context (Context A: metal grid floor, black walls, bright light, 70% ethanol scent) for 2 minutes. Mice were then presented with a foot shock (0.4 mA, 2s). Sixty seconds later, they were returned to their home cage. On day 4, mice were introduced in different contexts for 5 minutes and their freezing was measured.

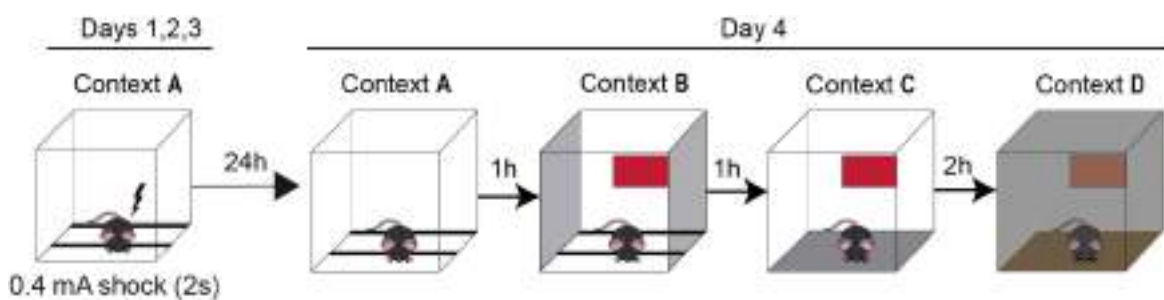


Figure 11. Context discrimination paradigm. Mice are trained during three days in the same context (Context A). On day 4, mice are first reintroduced in Context A which is sequentially altered with slight cumulative modifications for testing discrimination.

Mice were first introduced in Context A (training context). One hour later, mice were introduced in Context B (metal grid floor, black walls with color inserts, bright light, soap solution scent). One hour after Context B, mice were introduced in Context C (plain metal floor, white walls with color inserts, medium light, azahar water scent). Lastly, after two hours mice were introduced in Context D (bedding floor, white walls with color inserts, dim light, citric scent).

3. Protein quantification by Western blotting

Mouse brain dissection

Mice were sacrificed by decapitation, then the skin and skull were removed and regions of interest (prefrontal cortex and hippocampus) were micro-dissected. Dissected tissue was immediately snap-frozen by immersion in liquid nitrogen and stored at -80°C until protein isolation.

Protein sample preparation

Tissues were homogenized in 15 (wt/vol) volumes of modified ice-cold RIPA buffer (50 mM Tris-HCl pH 7.5, 150 mM NaCl, 1% NP40, 0.01 % SDS) supplemented with cOmplete™ protease inhibitor cocktail [Roche; 4693116001] and PhosSTOP™ phosphatase inhibitors [Roche; 4906837001] using 12 strokes of a glass-Teflon douncer (Heidolph RZR-1 600-800rpm). Then mechanical lysis (sonication with 20 pulses with a Branson-tip-sonicator; duty cycle 20, amplitude 15%) was performed to increase the proportion of lysed cells and extract the maximum of proteins. The suspension was centrifuged for 20 minutes at 16200xg and 4°C. The resulting supernatant was aliquoted and stored at -80°C for further use. Protein content was estimated using a Pierce BCA Assay kit (Thermo Fisher) before immunoblotting.

SDS-PAGE electrophoresis

Proteins were resolved using sodium dodecyl sulfate – polyacrylamide gel electrophoresis (SDS-PAGE). Gels were casted manually using the Criterion™ System (BioRad® 1656025). The resolving gel (Acrylamide/bisacrylamide from 7 to 12 %, 10% SDS; 1.5 M Tris-HCl pH 8.8; 10% ammonium persulfate; 0.05% TEMED) was smoothly added to commercial cassettes (Bio-Rad®). The solution was covered with isopropanol to better alignment of the upper border and left to polymerize. Once polymerized, isopropanol was removed, the gel surface was carefully rinsed with distilled water and the stacking gel the stacking gel (4% Acrylamide/bisacrylamide; 10% SDS; 0.5 M Tris-HCl pH 6.8; 10% ammonium persulfate; 0.05% TEMED) was poured over it. The comb, with a

Materials & methods

variable number of wells was then carefully inserted in the cassette and left to polymerize for 15-20 minutes.

Polymerized gels were placed into the electrophoresis module filled with electrophoresis buffer (25 mM Tris-HCl; 0.1% SDS; 192 mM glycine). Samples were dissolved in 4x Laemmli sample buffer (125 mM Tris-HCl; 4% SDS; 20% β -mercaptoethanol; 20% glycerol; 0.004% bromophenol blue), heated at 65°C for 10 minutes and loaded into the wells along with a molecular weight marker (Nippon Genetics #MWP04). Electrophoresis was carried out at 100V until the samples entered the resolving gel and then at 120V until the front reached the bottom of the gel.

Protein transfer

Criterion™ cassettes were carefully divided and following manufacturer instructions and gels were then equilibrated for 10 minutes in Transfer Buffer (10 mM glycine; 10 mM Tris-HCl; 5% methanol). Simultaneously, 0.45 μ M PDVF membranes (GE Healthcare® 10600023) were activated in 100% methanol for 5 minutes. Transfer cassettes sandwiches were prepared sequentially adding one fiber pad, three Whatman® filter papers, the gel, the activated PDVF membrane, three Whatman® filter papers and another fiber pad in a Criterion Blotter set. The cassettes were placed into the electrode module with the gels facing the cathode end and filled with cold Transfer Buffer. Transference was carried out at constant 300 mA for 2 hours at 4°C. Once the proteins were transferred to the membrane this was briefly rinsed in distilled water and stained in Ponceau S solution [0.1% (w/v) Ponceau S (Sigma-Aldrich® P3504) in 5% (v/v) acetic acid] for 10 minutes.

Immunodetection

Membranes were blocked with 5% Bovine Serum Albumin (BSA; Sigma-Aldrich® A9647) in Tris-buffer saline pH 7.6 (50 mM Tris-Cl; 150 mM NaCl; 0.05% Tween-20) (TBS-T) at room temperature (RT) for 1 hour and then incubated overnight at 4°C in primary antibody solution (TBS-T + 2% BSA) (Table 1).

Table 1. Primary antibodies used for immunoblotting.

Antibody	Supplier	Catalog number	Host	Working dilution
GluN3A	Merck-Millipore	07-356	Rabbit	1:1000
Synapsin 1	Synaptic Systems	106011	Mouse	1:5000
CamKII	Merck-Millipore	C6974	Rabbit	1:1000
PSD95	NeuroMab	73-028	Mouse	1:1000
GluN1 (clone R1JHL)	Merck-Millipore	MAB1586	Mouse	1:1000
Phospho-mTOR (Ser2448)	CST	2971S	Rabbit	1:1000
mTOR	CST	2972S	Rabbit	1:1000
Phospho-S6 ribosomal protein (Ser240/244)	CST	2215S	Rabbit	1:1000
S6 ribosomal protein (clone 5G10)	CST	2217S	Rabbit	1:1000
Phospho-AKT (Ser473)	CST	9271S	Rabbit	1:1000
AKT	CST	9272S	Rabbit	1:1000
GluN2A (clone A12W)	Merck-Millipore	05-901R	Rabbit	1:1000
GluN2B (clone BWJHL)	Merck-Millipore	05-920	Rabbit	1:1000
Puromycin (clone 12D10)	Merck-Millipore	MABE343	Mouse	1:2000

Materials & methods

The following day, the blot was rinsed with TBS-T for 30 minutes and incubated with horseradish secondary antibodies (Table 2) in TBS-T + 2% BSA for 1 hour at RT. Blots were then washed with TBS-T (20 minutes) and with TBS (10 minutes). Proteins were visualized using an Enhanced Chemiluminescence (ECL) Western Blotting Detection Reagent (GE Healthcare® RPN2209 & ThermoFisher® Scientific™ 32132) and scanned with a High-sensitivity digital Blot chemiluminescence imager (Amersham™ Imager 680). Individual bands were quantified after background subtraction using Image Studio™ Lite (LI-COR Biosciences) software.

Table 2. Secondary antibodies used for immunoblotting.

Antibody	Supplier	Catalog number	Host	Working dilution
HRP-mouse IgG	GE-Healthcare®	NA931V	Sheep	1:10000
HRP-rabbit IgG	GE-Healthcare®	NA934V	Donkey	1:10000

4. Protein synthesis measurements

Intracerebroventricular injections

Mice were anesthetized with isoflurane and placed in a Stoelting 51730 stereotaxic frame. The scalp was shaved and a longitudinal incision was made to expose the skull surface. Two burr holes were drilled above the infusion sites with a hand drill. 0.7µl of 50µg/µl puromycin solution (Sigma-Aldrich; P8833 dissolved in sterile PBS) were stereotaxically injected with a 5 µL Hamilton syringe into both lateral ventricles of anesthetized mice according to the Paxinos and Franklin mouse brain atlas (Paxinos *et al.*, 2001). The infusion rate was 200 nL per minute with a World Precision Instruments single-syringe infusion pump (SP100iZ), and the needle remained in place for 5 minutes after infusion for vector absorption before removal of the syringe. Finally, the site was glued closed with

Cicastick (Chemical Iberica). After surgery, mice were placed in a Vetario TS intensive care unit for one hour.

Protein sample preparation

Protein synthesis was measured by the surface sensing of translation (SUnSET) method. After intracerebroventricular injection, mice were sacrificed by cervical dislocation and brains were removed and the hippocampi were rapidly dissected and immersed in liquid nitrogen until further use. Hippocampi were homogenized in a prechilled glass homogenizer with 300 µl of lysis buffer containing 0.5M EDTA and 1M HEPES supplemented with cOmplete™ protease inhibitor cocktail (Roche; 4693116001) and PhosSTOP™ phosphatase inhibitors (Roche; 4906837001) using 12 strokes of a glass-Teflon douncer (Heidolph RZR-1 600-800rpm). Samples were centrifuged for 5 min at 500g at 4°C. The resulting supernatant was aliquoted and stored at -80°C for further use. Protein content was estimated using a Pierce BCA Assay kit (Thermo Fisher) before immunoblotting. SDS-PAGE electrophoresis, protein transfer and immunodetection were performed as described above. Puromycin incorporation was detected by western blotting using 12D10 antibody for puromycin (1:2000, Sigma-Aldrich) and Ponceau S staining was used for protein normalization.

5. In vivo electrophysiological recordings

Long-term potentiation (LTP) was evoked and recorded at medial prefrontal cortex (mPFC) – basolateral amygdala (BLA) synapses (Sánchez-Hidalgo *et al.*, 2021). For this, animals were anesthetized with 0.8-1% isoflurane delivered from a calibrated Fluotec 5 (Fluotec-Ohmeda, Tewksbury, MA) vaporizer at a flow rate of 1-1.2 L/min oxygen (AstraZeneca, Madrid, Spain) and placed in stereotaxic frame (David Kopf Instruments, Tujunga, CA, USA). Additional anesthesia during surgery was provided across an adaptable mouse mask (also from David Kopf Instruments). Following their stereotaxic coordinates (Franklin and Paxinos, 2007), animals were implanted with a bipolar stimulating electrode aimed to the superficial mPFC (anterior to Bregma: 1.8 mm; right

Materials & methods

lateral: 0.3 mm; depth from brain surface: 2.2 mm)—namely, to layers II-III where mPFC neurons projecting to BLA are located (McDonald, 1998). Animals were also implanted with two recording electrodes in the dorsomedial BLA (posterior to Bregma: 1.6 mm; right lateral: 3 mm; depth from brain surface: 4 mm), where the target neurons to mPFC projections are located (McGarry and Carter, 2017). Electrodes were made of 50 μm , Teflon-coated tungsten wire (Advent Research Materials Ltd., Eynsham, UK). The final position of the recording electrodes was determined using as a guide the presence of short-latency field excitatory post-synaptic potentials (fEPSPs) evoked by single pulses presented at the mPFC (Sánchez-Hidalgo *et al.*, 2021). Two bare silver wires (0.1 mm) were affixed to the skull as a ground with the help of two small screws. All these wires were soldered to a 6-pin socket and the socket was fixed to the skull with the help of dental cement. Animals were allowed a minimum of a week before the start of the recording sessions.

fEPSPs were recorded across a high-impedance probe ($2 \times 10^{12} \Omega$, 10 pF) with Grass P511 differential amplifiers (Grass-Telefactor, West Warwick, RI, USA), at a bandwidth of 0.1 Hz-10 kHz. Electrical stimulus applied to the mPFC area consisted of 100 μs , square, biphasic (positive-negative) pulses presented alone, paired, or in trains. Stimulus intensities were $\leq 0.4 \text{ mA}$.

Prior to LTP induction, we have 15 min of baseline recordings (3 per min). Here, the stimulus intensity was set $< 40\%$ of peak fEPSP values. Then, each animal was presented with a high frequency stimulation (HFS) protocol consisting of five trains (200 Hz, 100 ms) of pulses at a rate of 1/s. This protocol was presented 6 times in total, at intervals of 1 min. Evolution of fEPSPs after the HFS protocol was followed for 60 min at the same stimulation rate (3 per min). Additional post-HFS sessions (30 min) were carried out for three additional days. Further details of this chronic preparation can be found elsewhere (Gruart *et al.*, 2006; Hasan *et al.*, 2013).

Field EPSPs and 1-volt rectangular pulses corresponding to stimulus presentations were stored digitally on a computer via an analog/digital converter (CED

1401 Plus, Cambridge, UK) at a sampling frequency of 11-22 kHz and with an amplitude resolution of 12 bits. Electrophysiological data were analyzed off-line for quantification of fEPSP amplitudes with the help of commercial (Spike 2 and SIGAVG from CED) programs. For this, five successive fEPSPs were averaged, and the mean value of the amplitude was determined. Computed results were processed for statistical analysis using the Signal program (Systat Software, San Jose, CA, USA).

6. Histology

For immunohistochemistry, mice were perfused with 4% paraformaldehyde (PFA) in phosphate-buffered saline (PBS) (0.01M; pH 7.4) using a Masterflex L/S complete pump system. The brain was removed and post-fixed overnight in the same fixative. Fixed brains were embedded with 4% agarose in PBS solution, sectioned coronally with a cryotome in 30 μ m-thick slices and stored in cryoprotectant solution at -20°C.

Immunohistochemistry was performed by first counterstaining free-floating brain sections with the fluorescent nuclear dye 4',6-diamidino-2-phenylindole (DAPI) (Sigma-Aldrich; D9542). Slices were then fixed with 4% PFA in PBS at RT for 50 minutes. After thorough rinsing with PBS, slices were incubated with 2 N HCl at 37°C for 30 min, followed by an incubation with borax buffer at room temperature. Slices were incubated for 2 hours at room temperature in a blocking solution containing 1% BSA, 4% normal serum, and 0.1% Triton X-100 in 0.01 M PBS and subsequently incubated overnight at 4°C with anti-BrdU (Abcam; 6326). Next day slices were incubated for 2 hours at room temperature with the appropriate secondary antibody in a solution containing PBST + 1% BSA. Sections were mounted and images were acquired with a Leica Thunder Imager inverted microscope.

Results



1. Testing cognition-related behaviors on constitutive *Grin3a*^{-/-} mice

Although better-known for its roles in activity-dependent refinements during early postnatal stages, significant expression of GluN3A persists into adulthood in a variety of regions of the mouse brain. However, the physiological role of adult GluN3A control of plasticity on mouse behavior is still unknown. Previous work showed that GluN3A-overexpressing mice present deficits in hippocampal-dependent learning tasks such as the Morris water maze (Roberts *et al.*, 2009). Defects were specifically observed in long-term memory while memory acquisition was intact, suggesting GluN3A interference with mechanisms mediating memory persistence. In line with this, work in our lab found that GluN3A inhibits the activation of mTORC1, a key pathway for translational control implicated in long-lasting synaptic plasticity and memory encoding. Thus, in this chapter, we undertook a comprehensive analysis of how lack of GluN3A impacts different types of memory in adult mice and directly addressed the involvement of enhanced mTORC1 function.

1.1 *Grin3a*^{-/-} mice perform as wild-type littermates under standard testing conditions

We first used the Morris water maze for assessing spatial learning abilities in constitutive knockout mice that lack GluN3A in all regions and neuronal populations. We hypothesized that GluN3A deletion, by lifting limits on mTORC1 activation, might facilitate long-lasting memory formation and have a pro-cognitive effect, in contrast with the learning deficits of GluN3A overexpressing mice.

During the visible platform phase of the test (V1-V3), mice have to search for a flagged platform located in the circular swimming pool and swim towards it as a form of escaping water. No differences were observed between WT and *Grin3a*^{-/-} mice (Fig. 12A), indicating that neither visual nor motor function are affected by GluN3A deletion. Swim speed was also measured throughout the whole protocol to assess motor performance, showing no differences (Fig. 12B). We then tested the memory capacity of

Results

Grin3a^{-/-} and WT littermates (WT) in the hidden platform phase of the Morris water maze (H1-H7) in which every mouse has two minutes to locate the hidden platform in the swimming pool using the visual cues surrounding them.

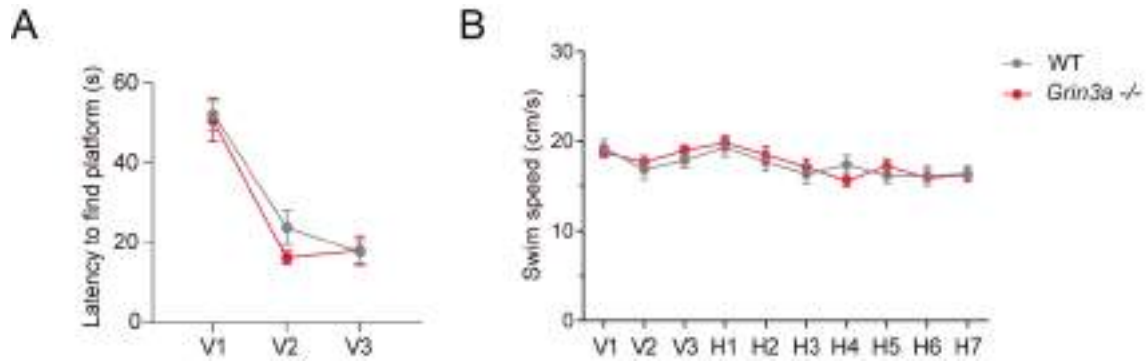


Figure 12. Intact visual and locomotive abilities in *Grin3a*^{-/-} mice. A) Male WT and *Grin3a*^{-/-} mice (3-4 months old) show no differences in times to reach a visible platform. B) Swimming speed over the training period showed no effects related to GluN3A deletion (n= 11-13 mice per group).

Every mouse was trained using four trials per day, a standard protocol used for assessing learning that mimics the conditions previously used in GluN3A overexpressors (Roberts et al 2009). No difference in learning curves of WT and *Grin3a*^{-/-} mice were observed (Fig. 13A). This was confirmed 24 hours after the last training session (H7) during a probe trial where the platform was removed from the pool: both genotypes displayed similar preferences (above 25% chance, dotted line) for the target quadrant where the platform used to be, indicating a correct memory of its location (Fig. 13B).

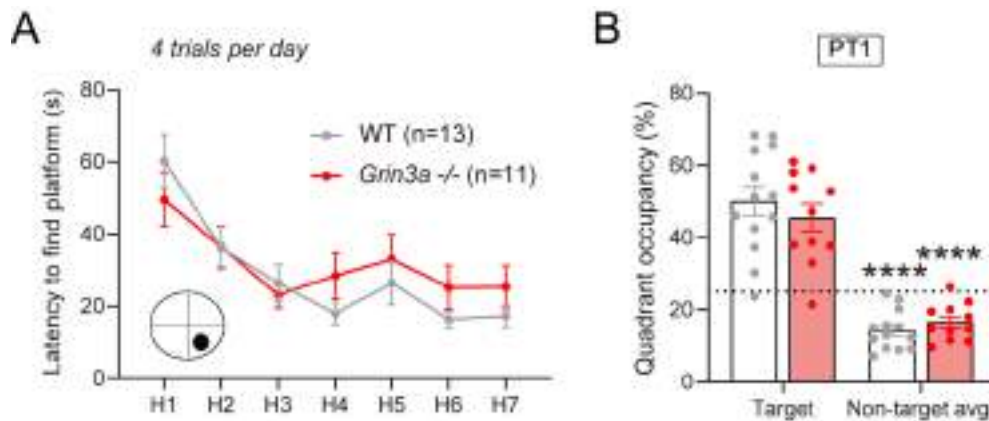


Figure 13. Standard MWM testing conditions do not reveal learning nor memory differences. A) Escape latencies of male WT and *Grin3a*^{-/-} mice (3-4 months old) over the time-course of training on a standard hidden platform version of the Morris water maze (7 days, four trials per day). B) On the probe trial for memory acquisition performed 24 hr after day 7 (PT1), both groups showed similar preference for the target quadrant. Dashed lines indicate chance levels (25%) (n= 11-13 mice per group; two-way ANOVA, **** p<0.001).

1.2 *Grin3a*^{-/-} mice perform better on demanding memory tasks

One advantage of the Morris water maze is that difficulty level can be regulated by increasing or lowering the number of trials per day. With shorter training, forming stable memories becomes more difficult. We therefore adapted our protocol to two trials per day and tested a second cohort of *Grin3a*^{-/-} and WT mice.

The weaker protocol unveiled significant differences between genotypes. *Grin3a*^{-/-} mice reached the platform significantly faster than WTs (Fig. 14A), with shorter latencies by day 4 of training. In addition, only *Grin3a*^{-/-} mice showed preference for the target quadrant during a probe trial conducted 24 hours after day 7 (Fig. 14B), indicating a better memory of the platform location. As with our previous mice cohort, the visible platform phase performed beforehand showed no differences, ruling out influences of motor or perceptual differences in these results.

Results

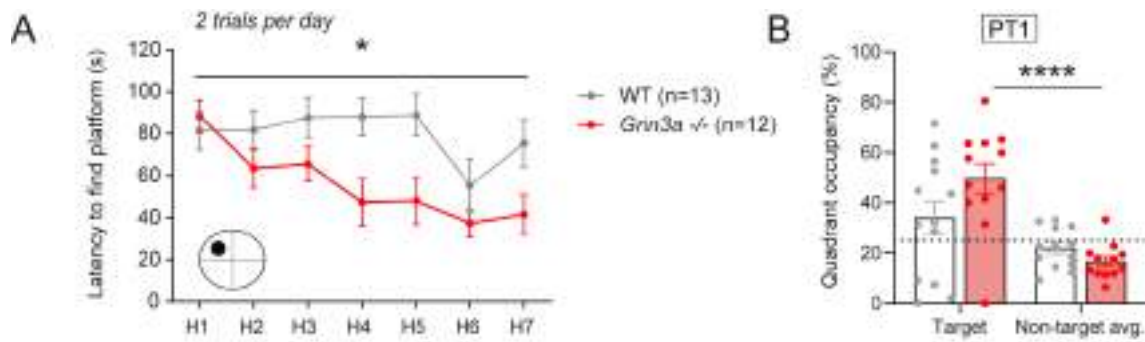


Figure 14. GluN3A deletion facilitates spatial learning in male mice. A) Escape latencies of male WT and *Grin3a*^{-/-} mice (4 months old) over the time-course of training on a weak hidden platform version of the Morris water maze (7 days, two trials per day). *Grin3a*^{-/-} mice learn to correctly locate the platform significantly faster than WT mice (Repeated measurements two-way ANOVA, **** $p < 0.001$). B) On the probe trial performed 24 hr after H7, only *Grin3a*^{-/-} mice showed a correct distinction between target and non-target quadrants. Dashed lines indicate chance levels (25%) ($n = 12$ -13 mice per group; two-way ANOVA, **** $p < 0.001$).

To address potential sexual dimorphisms, we performed the test in female mice under the same conditions. Female *Grin3a*^{-/-} mice showed no advantage over WT mice during training (Fig. 15A), but showed greater preference for the target quadrant during the probe trial (Fig. 15B), as well as correct distinction between target and non-target quadrants, replicating our results obtained in male mice.

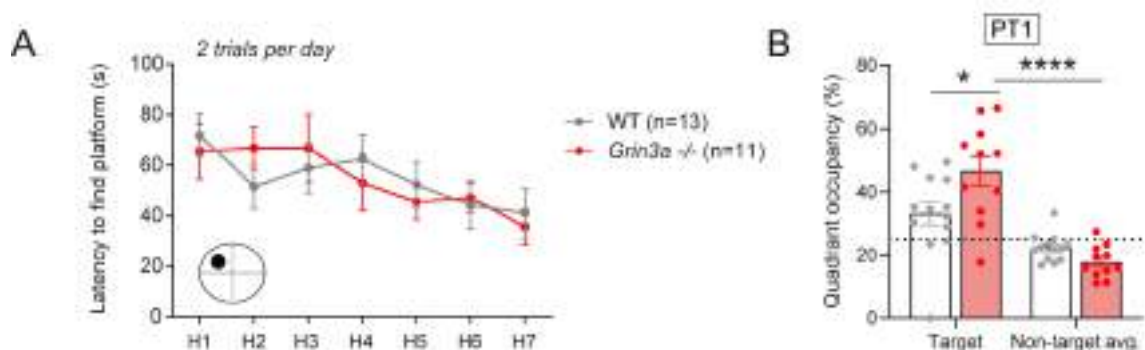


Figure 15. GluN3A deletion also facilitates spatial learning in female mice. A) Escape latencies of female WT and *Grin3a*^{-/-} mice (4 months old) over the time-course of training on a weak hidden platform version of the Morris water maze (7

days, two trials per day). B) On the probe trial for memory acquisition performed 24 hr after H7, female *Grin3a*^{-/-} mice showed increased preference for the target quadrant and a correct distinction between target and non-target quadrants. Dashed lines indicate chance levels (25%) (n= 11-13 mice per group; two-way ANOVA, * p<0.05; **** p<0.001).

1.3 Associative memory is enhanced in *Grin3a*^{-/-} mice

We then assessed associative memory. We used a task that elicits memories using a single pairing of a conditioned stimulus with an unconditioned stimulus. In this case, contextual fear conditioning is based on the relation between a specific context (CS) and a foot-shock (US) that can be regulated in length and intensity to adjust the difficulty of the task. Once the conditioning is performed, this paradigm allows testing mice at several time points and can be used to distinguish short-term memory and long-term memory.

Because previous work had not assessed associative memory in conditions of GluN3A overexpression, here we conducted experiments upon bidirectional GluN3A manipulation: mice overexpressing GluN3A (dtGFPGluN3A) and *Grin3a*^{-/-} mice. Guided by the results obtained in the Morris water maze, we chose a weak conditioning protocol (single pairing of a tone with a 2 second-long 0.3 mA foot-shock; Fig. 16A).

Before the delivery of the foot-shock, neither dtGFPGluN3A mice nor control mice showed freezing behavior (Fig. 16B, left) indicating that the context itself is not aversive. We observed significant differences between the groups when mice were tested 24 hours after the fear conditioning. Specifically, dtGFPGluN3A mice exhibited a significant decrease in freezing behavior compared to control mice (Fig. 16B). This suggested that GluN3A expression of GluN3A plays a role in constraining associative memory formation as previously observed for spatial learning.

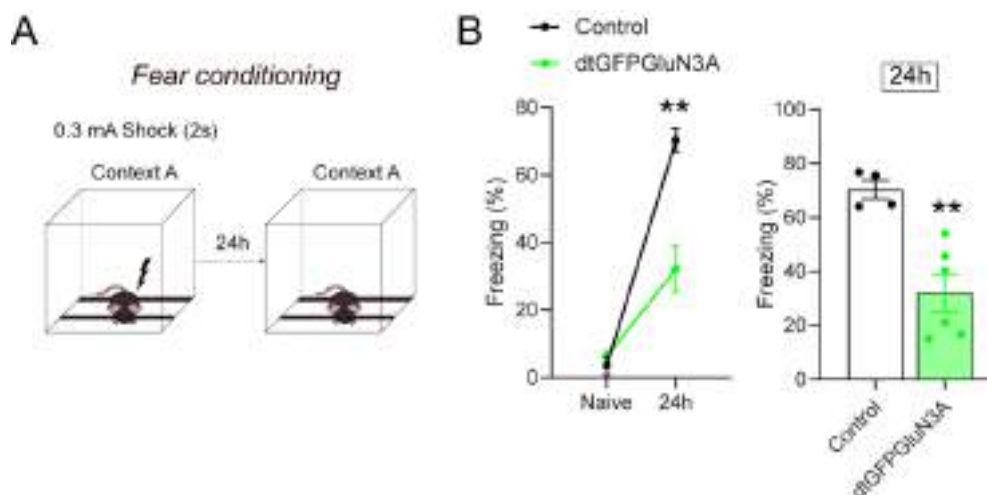


Figure 16. Adult transgenic mice overexpressing GluN3A display impairments in contextual fear conditioning. A) Contextual fear conditioning paradigm. B-C) In the test performed 24h after conditioning, male dtGFPGluN3A mice (6 months old) showed reduced freezing in comparison with control mice (n= 4-6 mice per group; two-tailed unpaired t-test ** p<0.01).

We then assessed *Grin3a*^{-/-} mice using the same fear conditioning protocol (Fig. 17A). As in the previous experiment (Fig. 16) before the delivery of the foot-shock, neither *Grin3a*^{-/-} nor WT mice showed freezing behavior (Fig. 17B, left). However, in contrast to the effects of GluN3A overexpression, removal of GluN3A improved the performance of mice in contextual fear conditioning, as shown in Figure 17B. These findings suggest that the absence of GluN3A facilitates memory formation and enhances mice ability to form associations between a particular context and the foot-shock.

Our study did not detect differences in short-term memory between the experimental groups when tested 1 hour after training, as shown in Figure 17C. Taken together with mechanistic information on GluN3A regulation of mTORC1, the findings suggest that the enhancement in memory observed in *Grin3a*^{-/-} mice might reflect alterations in protein synthesis, which is critical for the formation of long-term, but not short-term, memory.

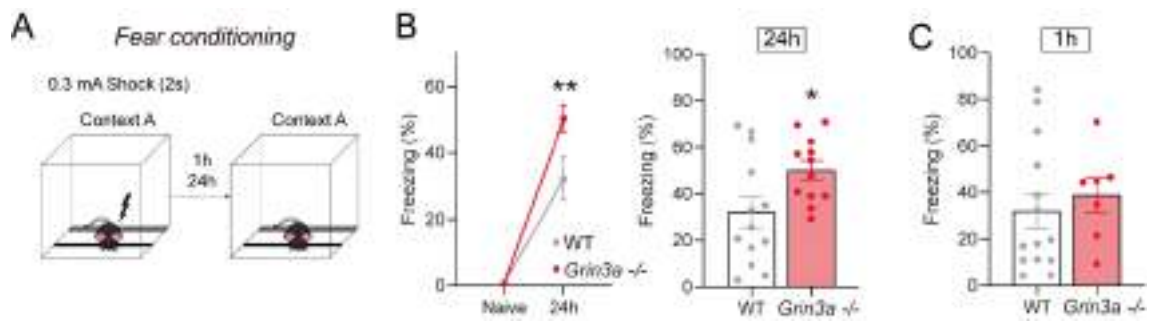


Figure 17. GluN3A deletion enhances contextual fear conditioning. A) Contextual fear conditioning paradigm. B-C) Enhanced contextual fear conditioning in male *Grin3a*^{-/-} mice (4 months old) 24 hr but not 1 hr after training (n = 9–13 male mice per group; left: repeated measurements two-way ANOVA, **p = 0.004; right: two-tailed unpaired t-test, *p < 0.05).

1.4 *Grin3a*^{-/-} mice enhanced memory is mTOR dependent

We thus asked whether the enhanced memory in *Grin3a*^{-/-} mice is related to differences in mTORC1 signaling using pharmacological blockade with rapamycin. Mice were treated with a subthreshold dosing regime of rapamycin consisting of five injections of rapamycin (20mg/kg; i.p.) every other day, finishing 24 hours before training (Stoica *et al.*, 2011; Conde-Dusman *et al.*, 2021) and then subjected to the weak fear conditioning protocol (Fig. 17A). Rapamycin erased the enhanced memory in *Grin3a*^{-/-} mice (Fig. 18), supporting the notion that disinhibited mTOR signaling causes the cognitive enhancement.

Results

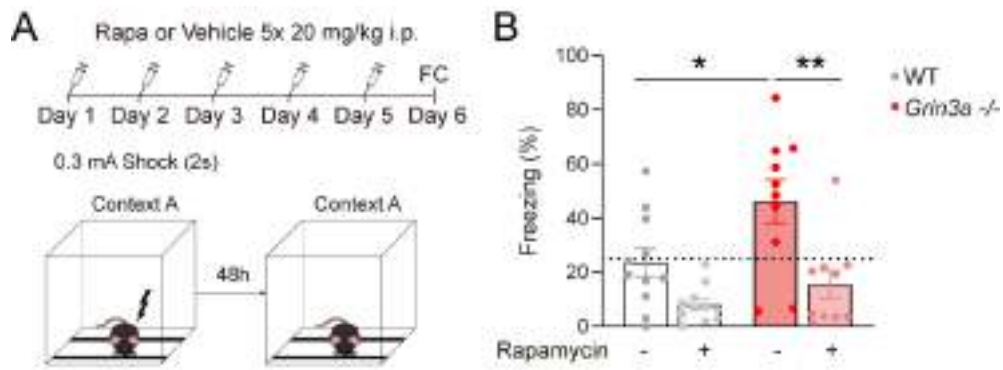


Figure 18. Enhanced contextual fear conditioning in *Grin3a*^{-/-} mice at 48 hr is reversed by rapamycin. A) Rapamycin administration regime and fear conditioning paradigm. Rapamycin was injected 5 × 20 mg/kg i.p., 24 hr apart, prior to training. B) Enhanced contextual fear conditioning in male *Grin3a*^{-/-} mice (3-5 months old) at 48 hr is reversed by rapamycin (n = 10–11 mice per group; *p < 0.05; **p < 0.01, two-way ANOVA with Bonferroni post hoc test).

2. Generation and characterization of cognition phenotypes in population specific GluN3A-lacking mice

As mentioned above, specific areas of the adult brain continue to express GluN3A into adulthood. Therefore, the phenotypes described in Chapter 1 could be caused by lack of GluN3A during postnatal development or could be due to lack of a yet unknown GluN3A function in the mature brain. Moreover, GluN3A is expressed by excitatory neurons and somatostatin interneurons, both recently implicated in protein synthesis-dependent memory consolidation of fear memories (Sharma *et al.*, 2020; Shrestha *et al.*, 2020a). In order to answer these questions, we took advantage of the Cre-LoxP system to study the role of GluN3A on different neuronal populations and developmental timepoints.

2.1 *Grin3a^{ff}* × *Camk2a-Cre^{ERT2}*

Developed and characterized by Erddman *et al.* (2007), *CamK2a-Cre^{ERT2}* mice allow selective deletion of the floxed protein in CamKII-expressing neurons when mice are administered with tamoxifen (TMX). Following the reproductive scheme explained in methods, we bred *Grin3a^{ff}* × *CamK2a-Cre^{ERT2}* in a manner that permitted us to use 100% of the mice produced, being the control and experimental subjects littermates, to avoid potential confounds arising from differences in genetic background.

In a first set of experiments, we validated inducible GluN3A deletion by TXF using quantitative immunoblotting. At two months of age, TMX was administered to mice of both genotypes via oral gavage (Fig. 19A). After allowing one month for recombination, we dissected the hippocampi and prefrontal cortices of *Grin3a^{ff}* × *CamK2a-Cre^{ERT2+/-}* and *Grin3a^{ff}* × *CamK2a-Cre^{ERT2-/-}* and assessed GluN3A deletion by western blot.

Results

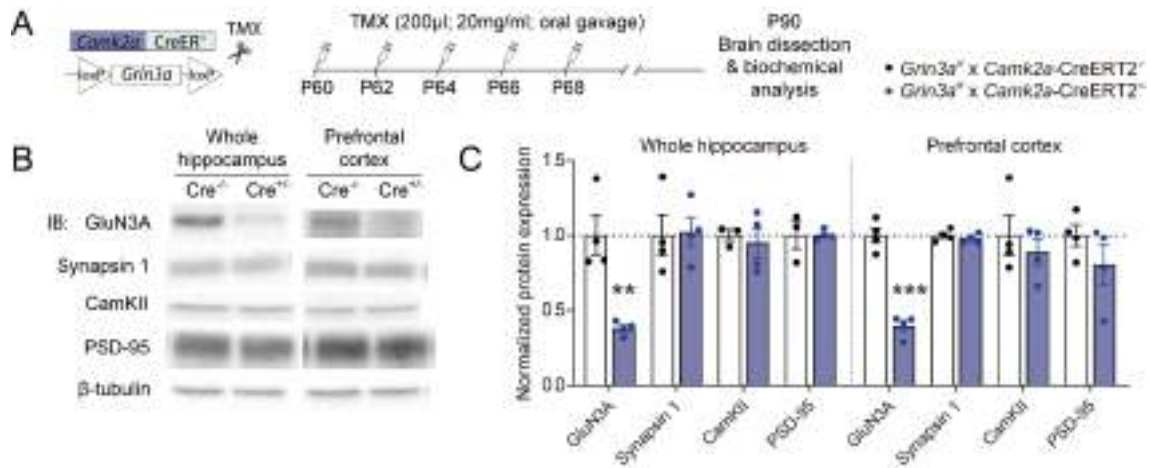


Figure 19. Expression of GluN3A and other synaptic proteins in *Grin3a^{ff} x CamK2a-Cre^{ERT2}*. A) TMX administration regime. B) Representative immunoblots of hippocampal and prefrontal cortex lysates of P90 mice from the indicated genotypes after TXF administration. C) TMX administration results in a significant reduction in GluN3A levels without affecting other synaptic proteins (n = 4 mice per group; unpaired two-tailed t-test, **p < 0.01, ***p < 0.0001). Expression was normalized to tubulin and expressed as ratio of control mice.

A significant reduction in GluN3A levels was observed in total protein lysates of both hippocampus and prefrontal cortex (Fig. 19B-C) without significant changes in other synaptic proteins (Hippocampus: 62 ± 0.02% decrease; prefrontal cortex: 61 ± 0.03%). Once we had corroborated the reduction in GluN3A levels we proceeded with the behavioral testing.

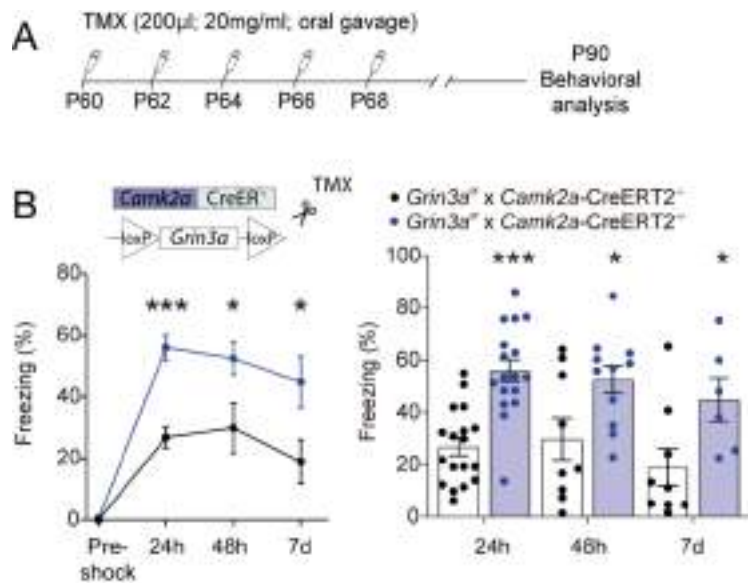


Figure 20. Conditional deletion of GluN3A from adult excitatory neurons is sufficient to enhance long-term contextual fear memory. A) Tamoxifen administration regime. B) Male *Grin3a^{ff} x CamK2a-Cre^{ERT2}^{+/-}* mice (3 months old) showed enhanced freezing at 24 and 48h as well as at 7d after training. (n= 6-18 mice per group; *p < 0.05; ***p < 0.001 two-tailed unpaired t-test).

Using the weak fear conditioning protocol used on *Grin3a*^{-/-} mice (Fig. 17) we found that adult deletion of GluN3A on principal excitatory neurons was enough to recapitulate the enhanced performance seen in constitutive *Grin3a*^{-/-} mice (Fig. 20B). In order to better characterize the effect of GluN3A deletion on CamKII-expressing neurons, we extended our testing period to 48h, finding the same enhanced performance that at 24h (Fig. 20B). Indeed, the phenotype was still detected, 7 days after conditioning demonstrating that weak associative stimuli are encoded over long periods of time in absence of GluN3A (Fig. 20B).

2.2 *Grin3a^{ff} x Sst-Ires-Cre*

Developed and characterized by Taniguchi *et al.* (2011), *Sst-Ires-Cre* mice allow deletion of the floxed protein in somatostatin interneurons. Following the same reproductive strategy as with *Grin3a^{ff} x CamK2a-Cre^{ERT2}* we achieved a 100% efficiency in 3 generations. We then proceeded to the dissection of the hippocampus and prefrontal

Results

cortex for western blotting (Fig. 21A). In this case, the reduction observed in GluN3A levels was of $20\pm 0.05\%$ in the hippocampus and $50\pm 0.04\%$ in the prefrontal cortex with no changes in other synaptic proteins in any of the structures analyzed (Fig. 21B). This is expected as the population of SST interneurons is much smaller in hippocampus, where it is mostly restricted to interneurons located in the stratum oriens (Murillo *et al.*, 2021), than in prefrontal cortex.

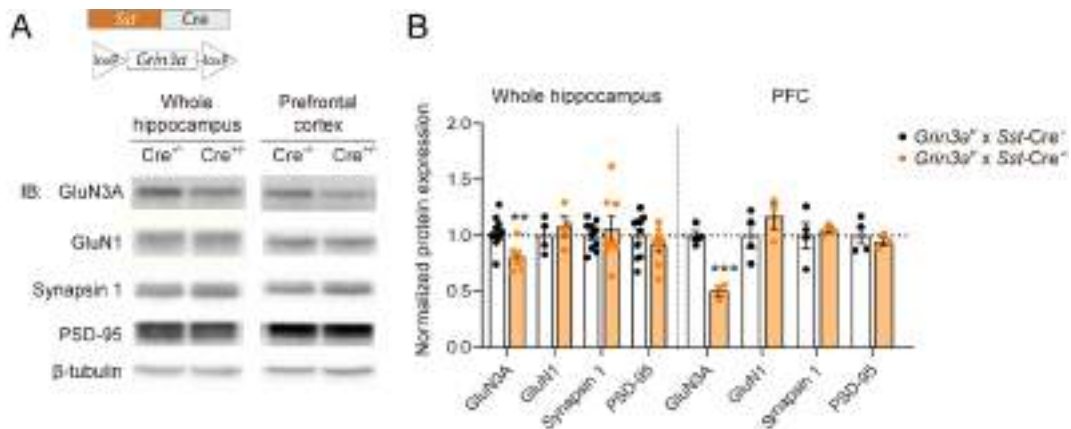


Figure 21. Expression of GluN3A and other synaptic proteins in *Grin3a*^{fl/fl} x *Sst-Ires-Cre* mice. A) Representative immunoblots of hippocampal and prefrontal cortex lysates of 3 months old mice (male and female) from the indicated genotypes. B) Immunoblot quantification indicating reduction in GluN3A levels without affecting other synaptic proteins (n = 4–8 mice per group; unpaired two-tailed t-test, **p < 0.01, ***p < 0.0001). Expression was normalized to tubulin and expressed as ratio of control mice.

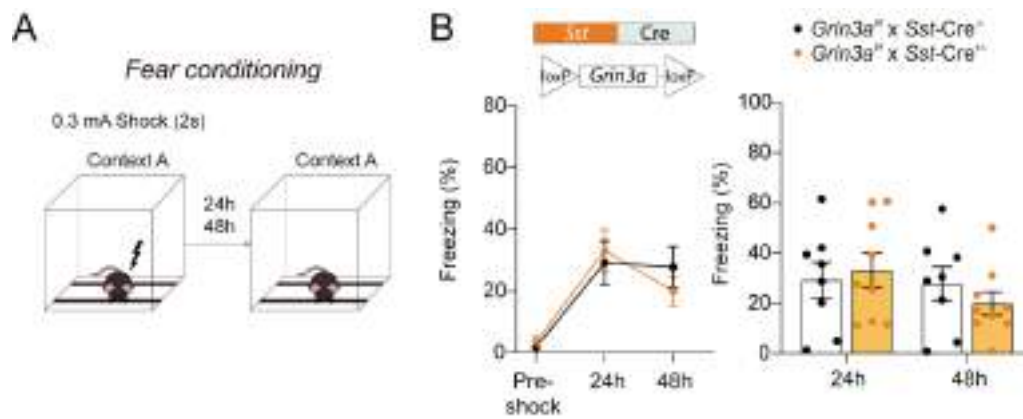


Figure 22. Deletion of GluN3A from somatostatin (*Sst*) interneurons does not affect associative memory. A) Contextual fear conditioning paradigm. B) No differences were found at any of the time points studied in 4 months old male mice ($n = 8-9$ mice per group).

We then assessed *Grin3a^{fl/fl}* x *Sst-Ires-Cre* mice performance using the weak fear conditioning paradigm (Fig. 22A) to directly compare phenotypes in both GluN3A-lacking mouse lines. We observed no differences between control and SST-specific GluN3A knockouts (Fig. 22B). Altogether, the results obtained by using population specific GluN3A-lacking mice indicate that the role of GluN3A on gating long-term memory formation depends on its expression on principal excitatory neurons.

2.3 Validation of enhanced associative memory using a second, context specific, fear conditioning paradigm

In the above-mentioned fear conditioning experiments, the foot-shock was presented as co-termination of a 30-second long tone (85dB, 2.8kHz). The protocol was originally developed for simultaneous assessment of hippocampal-dependent context fear conditioning, and amygdala-dependent cued (or auditory) fear conditioning (Fig. 23).

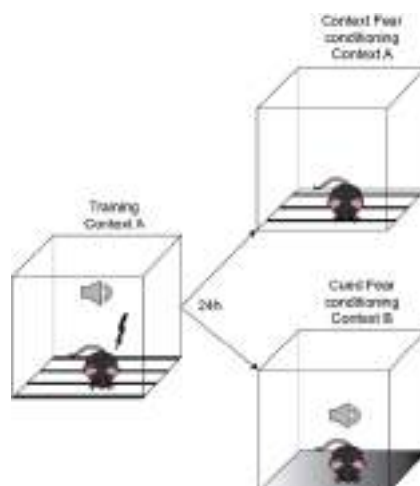


Figure 23. Schematic of the mixed fear conditioning paradigm. This paradigm allows the differential assessment of Context fear conditioning by reintroducing mice in the training context and of Cued fear conditioning by changing the context and sounding the same tone as during training.

However, the sound before the shock makes the correct association between the context and the foot shock harder to form. In order to dissect specific effects of GluN3A on pure contextual fear conditioning and isolate influences from the tone, we adapted the paradigm by introducing two five-minutes long habituation sessions to the conditioning boxes and skipping the tone (Fig. 24).

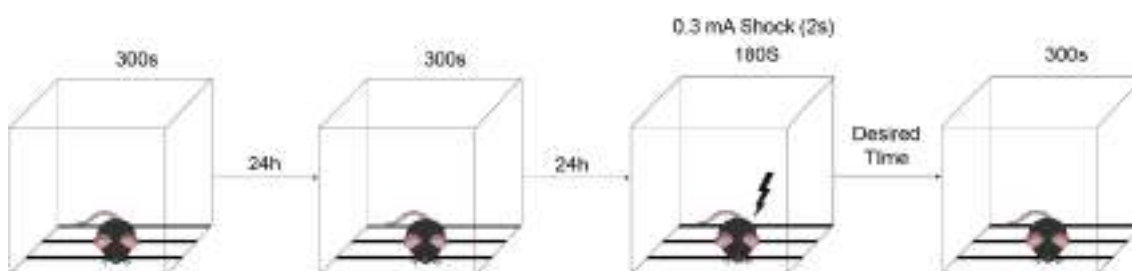


Figure 24. Pure context-specific fear conditioning paradigm. This paradigm includes two 5-minute long habituation sessions (24 hr apart) prior to training. The training context remains intact during the whole duration of the protocol but becomes aversive upon shock application.

It has been described that the introduction of habituation sessions before training increases freezing levels during testing (Fanselow, 1990; Frankland *et al.*, 2004; McHugh

& Tonegawa, 2007). Once the protocol was set up, we performed fear conditioning experiments on both Cre lines to directly compare both fear conditioning protocols and lines. In line with the previous studies, the new protocol caused higher levels of freezing in control mice at both 24 and 48 hours after conditioning (Table 3).

Table 3. Comparison of freezing levels between FC paradigms.

Freezing levels in control mice with full GluN3A expression in the different fear conditioning paradigms.

Genotype	Freezing at 24h (%)		Freezing at 48h (%)	
	Mixed protocol	Context-specific protocol	Mixed protocol	Context-specific protocol
<i>Grin3a^{fl/x}</i> <i>CamK2a-Cre^{ERT2-/-}</i>	26.77 (3.38)	60.80 (5.5)	29.82 (8.13)	44.93 (6.06)
<i>Grin3a^{fl/x}</i> <i>Sst-Ires-Cre^{ERT2-/-}</i>	29.20 (7.05)	44.32 (7.76)	27.79 (6.65)	39.05 (6.62)

Data are expressed as mean (s. e. m.).

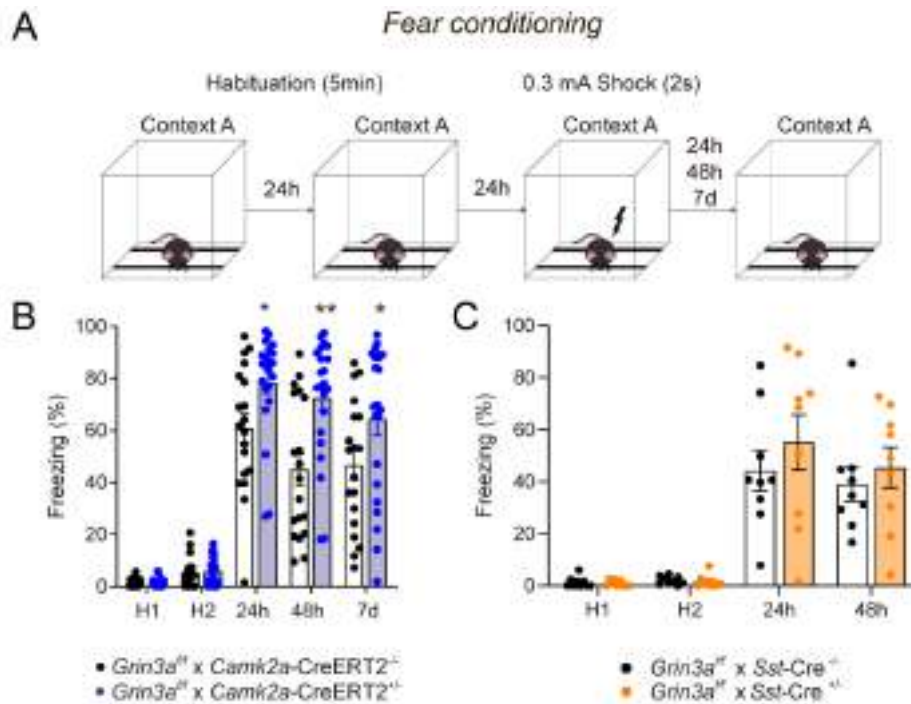


Figure 25. Deletion of GluN3A from excitatory but not inhibitory neurons enhances long-term and remote hippocampal memories. A) Experimental design. B) Conditional deletion of GluN3A from adult (3 months old mice; males and females pooled) excitatory neurons but enhances long-term contextual fear memory (n=19-22 mice per group; repeated measurements two-way ANOVA, *p<0.05; ** p< 0.01). C) Deletion of GluN3A from inhibitory neurons do not affect contextual memory in male mice (4 months old). (n= 9 mice per group).

Using the pure context fear conditioning protocol (Fig. 25A) we confirmed the results previously obtained despite the stronger freezing shown by control mice: *Grin3a^{fl/fl} x CamK2a-Cre^{ERT2+/+}* scored higher levels of freezing relative to *Grin3a^{fl/fl} x CamK2a-Cre^{ERT2-/-}* littermates at 24h, 48 h and until 7 days after training (Fig. 25B); while *Grin3a^{fl/fl} x Sst-Ires-Cre^{+/-}* mice performed at the same level as their littermates with unmodified GluN3A expression (Fig. 25C). Moreover, the experiment on *Grin3a^{fl/fl} x CamK2a-Cre^{ERT2}* mice was performed in separate cohorts of male and female mice which yielded identical results pooled in Figure 25B.

2.4 GluN3A gates memory through limiting mTORC1-dependent protein synthesis in excitatory synapses

We finally asked whether enhanced cognition in CamKII-conditional GluN3A mice exhibits mTOR-dependence, as seen in constitutive GluN3A knockouts. Here we titrated down the rapamycin dose used, since high doses of rapamycin could also affect mTORC2 (Sarbasov *et al.*, 2005; Sarbasov *et al.*, 2006; Stoica *et al.*, 2011). We injected mice with two doses of 10 mg/kg rapamycin i.p. (vs the 5 x 20 mg/kg i.p. in Figure 18) and assessed selectivity over mTORC1 versus mTORC2 inhibition in hippocampal lysates using western blotting. S6 phosphorylation was used as a read-out of mTORC1 activity and the phosphorylation of AKT in serine 473 was used as a proxy for mTORC2 (Fig. 26A). We found that two doses of 10mg/kg rapamycin effectively blocked the phosphorylation of mTOR and S6 without affecting the phosphorylation of AKT^{S473} in total protein lysates of hippocampal samples (Fig. 26B). Furthermore, analysis of hippocampal synaptic fraction extracts corroborated that this treatment completely blocked S6 phosphorylation in synaptic compartments without altering AKT in serine 473. (Fig. 26B)

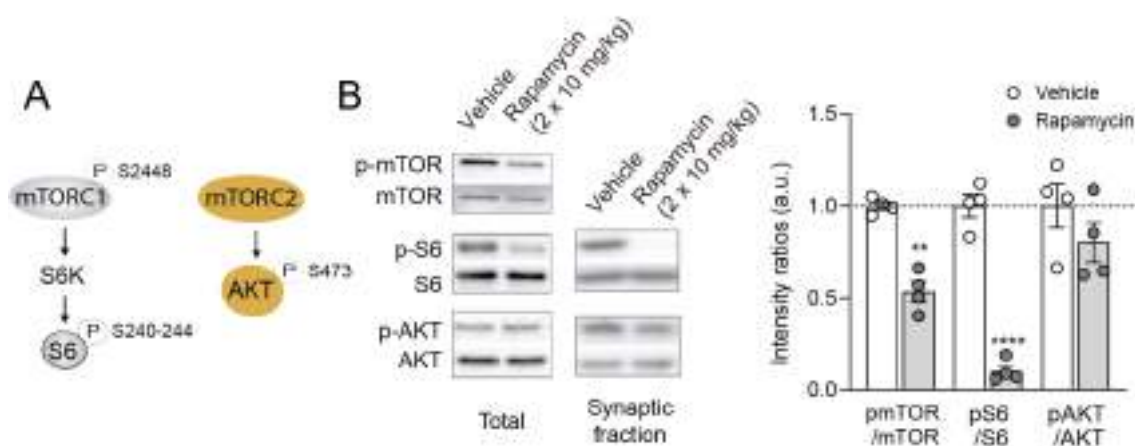


Figure 26. Selective inhibition of mTORC1 signaling. A) Scheme illustrating downstream readouts of mTORC1 and mTORC2 pathway activation. B) The selected rapamycin treatment blocks mTORC1 activation in adult mice (3 months old) without affecting the normal function of mTORC2 (n= 4 mice per group; unpaired two-tailed t-test, **p < 0.01, ****p < 0.0001).

Results

Once the correct rapamycin dose for selective inhibition of mTORC1 was determined, we performed the experiment on *Grin3a^{ff} x CamK2a-Cre^{ERT2}* mice using our pure context-specific fear conditioning protocol. To further establish the protein synthesis dependence of our phenotype, a third group of *Grin3a^{ff} x CamK2a-Cre^{ERT2}* was treated with the general protein synthesis inhibitor anisomycin (Fig 27, A). Based on previous results from Alcino Silva's lab (Ehninger *et al.*, 2008) we selected a dose of anisomycin that was expected to significantly impair performance in this test if the observed phenotype was indeed dependent on protein synthesis.

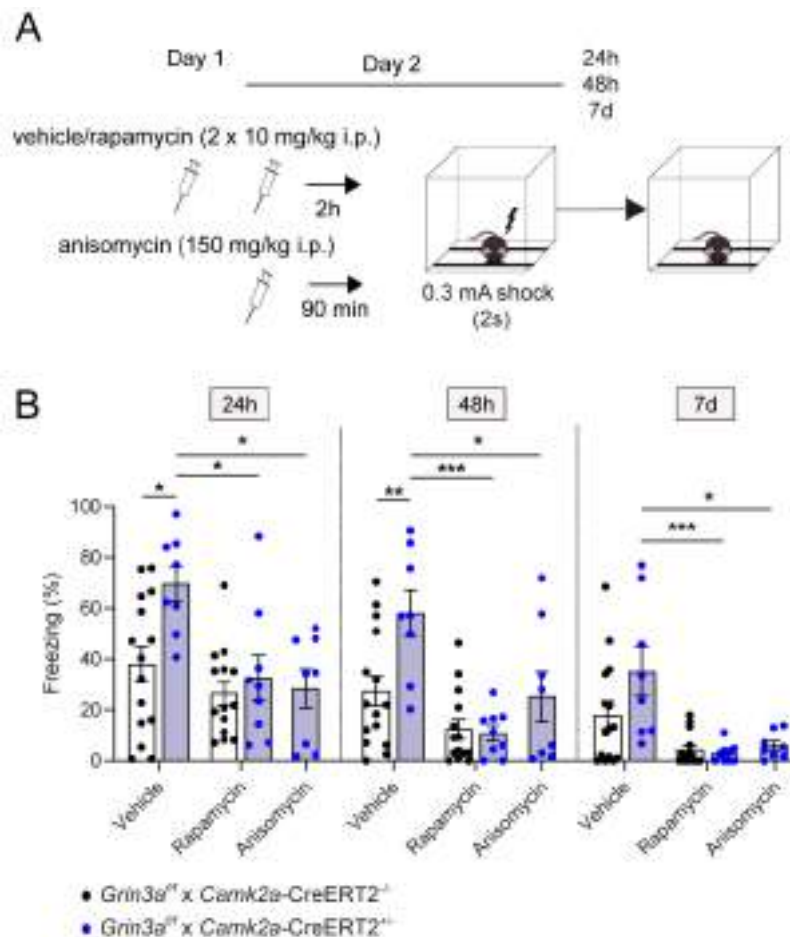


Figure 27. Blocking mTORC1-mediated protein synthesis reverses enhanced fear conditioning in *Grin3a^{ff} x CamK2a-Cre^{ERT2}^{+/-}* mice. A) Experimental design: Drug administration regime and fear conditioning protocol. B) *Grin3a^{ff} x CamK2a-Cre^{ERT2}^{+/-}* mice (3-5 months old) showed enhanced fear conditioning at

24 and 48 hours that was occluded by rapamycin and anisomycin treatments (n= 8-15 mice per group; Two-way ANOVA, **p < 0.01, ***p < 0.0001).

The results from this experiment validated our previous data. *Grin3a^{fl/fl}* x *CamK2a-Cre^{ERT2+/-}* mice outperformed their *Grin3a^{fl/fl}* x *CamK2a-Cre^{ERT2-/-}* littermates and showed enhanced memory of the foot-shock at 24 and 48 hours (Fig. 27B), as well as a tendency to keep memories of it 7 days after the shock (Fig. 27B, p = 0.13). Both the rapamycin and anisomycin treatments blocked the enhanced performance, making the treated *Grin3a^{fl/fl}* x *CamK2a-Cre^{ERT2+/-}* perform the test at the same levels as their littermates. These results demonstrate that the expression of GluN3A on excitatory neurons gates protein synthesis by inhibiting mTORC1 signaling, hence limiting long-term memory formation. GluN3A removal lifts limits on synaptic mTORC1 signaling, lowering learning thresholds and expanding memory capacity.

3. GluN3A deletion is not associated with common side effects of translation manipulations

Similarly, reduced learning thresholds have been reported in mice with elevated activity of mTOR or other pathways controlling general translation (Banko *et al.*, 2007; Costa-Mattioli *et al.*, 2007; Hoeffler *et al.*, 2008; Stern *et al.*, 2013). However, the pro-cognitive effects upon elevated mTOR activity often came at the cost of impairments in mouse ability to respond to changed environments or readapt to new learning. For instance, deletion of the translational repressor 4E-BP, one of mTORC1 downstream targets, enhanced memory for conditioned taste aversion at the cost of the appearance of perseverative behaviors on a spontaneous alternation task (Banko *et al.*, 2007). In another study, Eric Klann's lab discovered that conditional knockout mice with ablated FKB12 (which binds rapamycin and regulates mTOR signaling) displayed enhanced contextual fear memory and autistic/obsessive-compulsive-like perseveration in several assays including the water maze, Y-maze reversal task, and the novel object recognition test (Hoeffler *et al.*, 2008). These studies suggest that, although apparently beneficial for

Results

memory, mTOR-related increases in general protein translation also have cognitive disadvantages.

3.1. Behavioral flexibility

Having confirmed that the enhanced memory observed in GluN3A-lacking mice was due to mTORC1-related increases in protein translation (see Figures 18 and 27), we asked whether cognitive flexibility was affected in mice lacking GluN3A. Three different paradigms were used: platform location reversal in the Morris water maze, Y-maze alternation and fear extinction.

First, we trained *Grin3a*^{-/-} mice in the Morris water maze (2 trials per day for 7 days). We then evaluated cognitive flexibility by switching the platform location to the opposite side of the pool and re-training the mice to learn the new location (Fig. 28A). *Grin3a*^{-/-} mice were better at shifting their preference relative to WT controls as seen in the probe trial performed after seven days of training (Fig. 28B).

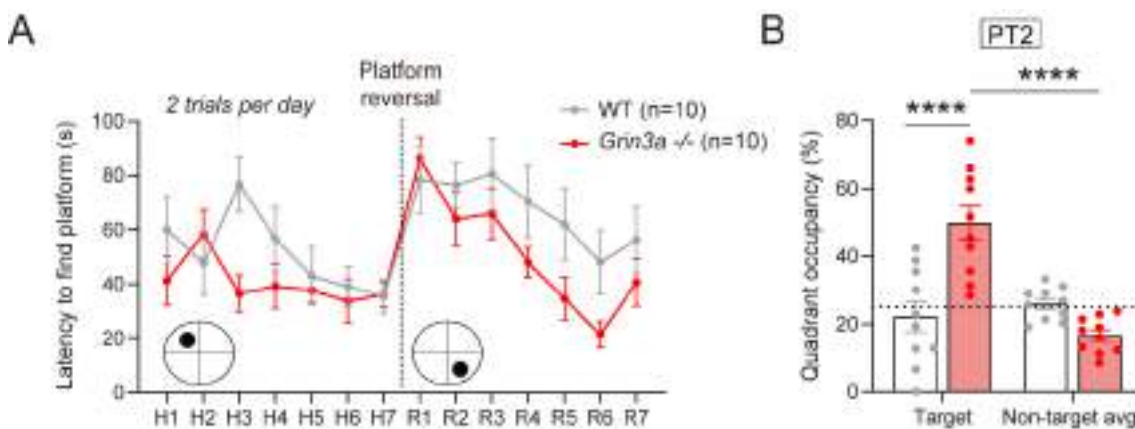


Figure 28. Removal of GluN3A enhances cognitive flexibility in male mice. A) Escape latencies of WT and *Grin3a*^{-/-} mice (4-5 months old) over the time-course of reversal training on a weak version of the Morris water maze (7 days, two trials per day). C) During the probe trial performed 24 hr after R7 (PT2), *Grin3a*^{-/-} mice showed a correct distinction between target and non-target quadrants as well as an enhanced preference for the target quadrant. Dashed lines indicate chance levels (25%) (two-way ANOVA, *** $p < 0.001$).

Similar to male mice, after seven days of training (Fig. 29A) female *Grin3a*^{-/-} mice learnt the new platform location, whereas female WT mice did not (Fig. 29B).

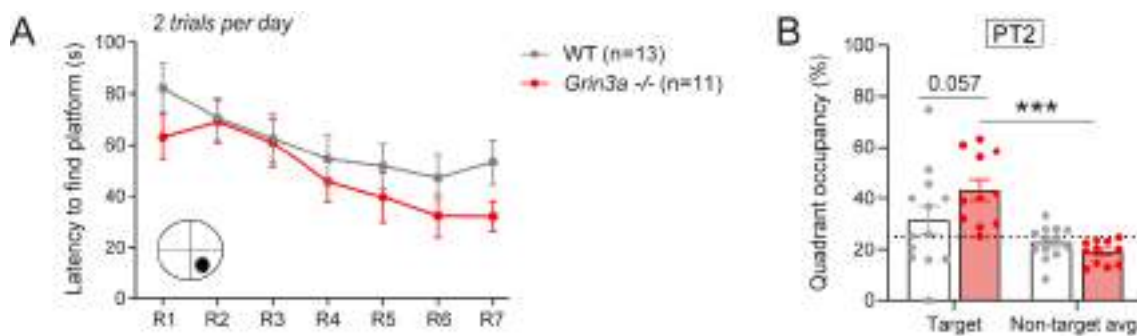


Figure 29. Removal of GluN3A enhances cognitive flexibility in female mice. A) Escape latencies of female WT and *Grin3a*^{-/-} mice (4 months old) over the time-course of reversal training on a weak version of the Morris water maze (7 days, two trials per day; see Fig. 4 for Hidden platform phase and PT1). B) During the probe trial performed 24 hr after R7, female *Grin3a*^{-/-} mice showed a correct distinction between target and non-target quadrants. Dashed lines indicate chance levels (25%) (n= 11-13 mice per group; two-way ANOVA, *** p<0.001).

We then tested for the existence of perseverative behaviors using a Y-maze spontaneous alternation task. In this test, mice are introduced in a transparent Y-shaped Plexiglass maze, with all three arms of the maze being open to explore during 5 minutes (Fig. 30A). A healthy mouse would enter the three arms in an alternating manner, without preference nor aversion for any of the arms. Mice presenting perseverative behaviors would enter one of the arms significantly more than the others, leaving one or two of the other arms nearly unvisited. No perseverative behavior was observed in the Y-maze task as both *Grin3a*^{-/-} and WT mice correctly alternated their entries to all three arms of the maze (Fig. 30B).

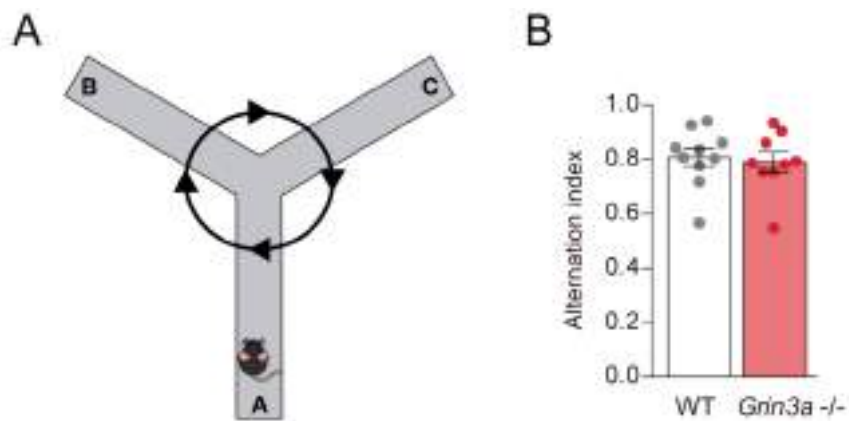


Figure 30. *Grin3a*^{-/-} mice do not show perseverative behaviors. A) Drawing of the Y-maze. B) Alternation index of male WT and *Grin3a*^{-/-} mice (3-5 months old) in the Y-maze showing no differences nor perseverative behaviors (n = 9–10 mice per genotype).

To complete our behavioral flexibility assessment in *Grin3a*^{-/-} mice we addressed cued fear extinction (FE). Fear extinction requires protein synthesis and is another indicator of behavioral flexibility that has been shown to be impaired after manipulation of general elements of translation. For this test, mice are conditioned to fear a tone by pairing the tone (CS) with a foot shock (US) five times during four days of training (Fig. 31A). Once this association is made, the repeated presentation of the CS without reinforcement (15 times a day over four days) leads to the extinction of the acquired fear memory (Fig. 31A).

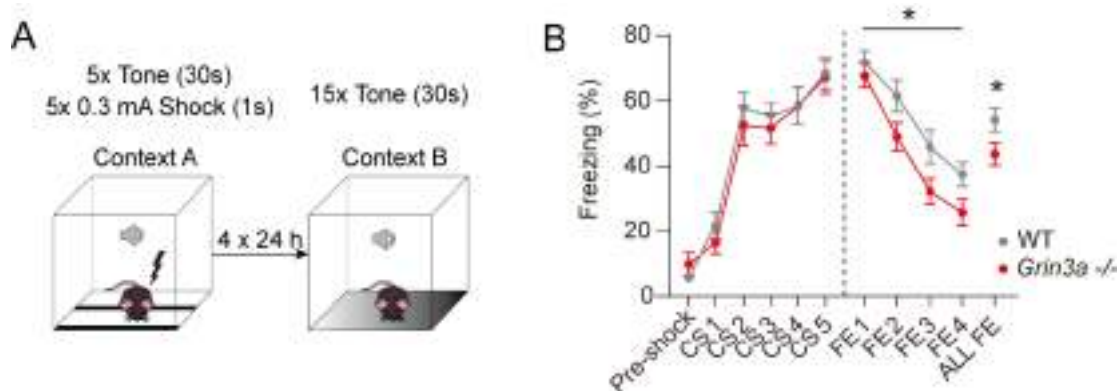


Figure 31. Enhanced cued fear extinction in male *Grin3a*^{-/-} mice. A) Experimental design for FE. B) Cued-fear extinction in *Grin3a*^{-/-} and WT

littermates (4 months old) over a four-day fear extinction paradigm (n = 14–13 mice per group; * p < 0.05, two-way repeated measurements ANOVA). Freezing levels were not different between phenotypes in FE1.

Fear memory acquisition was similar between WT and *Grin3a*^{-/-} littermates (Fig. 20B, CS1-5) but fear extinction was enhanced in *Grin3a*^{-/-} mice with differences starting by the second day of extinction (Fig. 31B), demonstrating that GluN3A deletion does not compromise the updating of memories but rather facilitates the extinction of fear memories, matching the results obtained in the reversal phase of the Morris water maze (Figs. 28 & 29).

3.2 Memory precision

Another potential main adverse effect of manipulating translation as a means to enhance memory is the loss of accuracy in the memory formed. Examples previously cited (Shrestha *et al.*, 2020b) indicate that enhancing the reaction to a conditioned stimulus can be associated with an inability to discriminate that stimulus from an innocuous but similar one.

To test whether GluN3A-lacking mice suffer these consequences, we set up a context discrimination test following the method by McAvoy *et al.*, (2016) (Fig. 32A), and evaluated the performance of *Grin3a*^{-/-} and *Grin3a*^{ff} x *CamK2a*-Cre^{ERT2} mice. This test consists of a three-day training in which mice are introduced in the conditioning boxes and receive a foot shock. This intensive training causes elevated levels of freezing specific to the training context (Taha *et al.*, 2020). On the fourth day, their reaction to the conditioning box (Context A) is measured. To test mice ability to differentiate contexts, we introduced subtle changes every session (Contexts B, C & D). Contexts were increasingly different from Context A as more contextual cues are changed every session.

In line with our previous studies, mice lacking GluN3A exhibited an accelerated learning of the aversive memory, showing differences after the two first training days (Fig. 32B, Day 3) that disappeared after the third training day (Fig. 32C, Context A).

Results

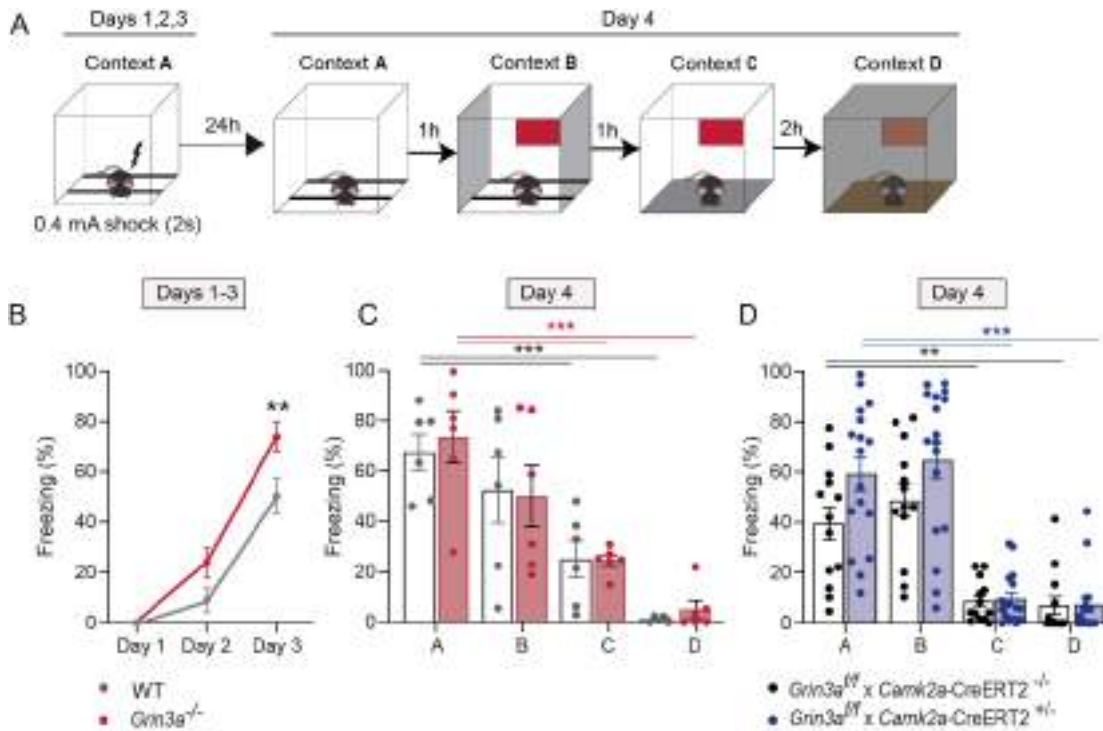


Figure 32. GluN3A deletion does not affect contextual fear discrimination. A) Protocol for contextual fear discrimination. Mice were trained (one shock, 0.4mA, 2s) for three days in context. A) On day 4, context discrimination was assessed by reintroducing mice into context A and in the sequentially modified contexts. B) Acquisition of conditioned fear in male WT and *Grin3a*^{-/-} mice (3 months old). After two training session, *Grin3a*^{-/-} mice show an enhanced fear conditioning that is matched by WT mice after the third session. Note that measures were taken before daily shock delivery (n= 6 mice per group; repeated measurements two-way ANOVA, ** p<0.01). C-D) *Grin3a*-ablated and mice with unmodified *Grin3a* expression of both sexes correctly distinguished Contexts C and D (n= 6-17 mice per group; two-way ANOVA, ** p<0.01, *** p<0.001).

As shown in Figure 32 (C & D), GluN3A-lacking mice did not show alterations in memory fidelity relative to WT controls. Mice performance did not differ between phenotypes in any of the contexts, with reduced levels of aversion in every session, reaching close to no freezing in Context D, which is drastically different to Context A. Importantly, we used both male and female mice in these experiments and again found no evidence of sexual dimorphism (Fig. 32D).

These results altogether showed that GluN3A deletion facilitates spatial learning and memory without the unwanted side effects seen when manipulating other modulators of translation.

4. Removal of GluN3A-NMDARs enhances LTP *in vivo*

The basal and lateral nuclei of the amygdala (together the BLA) have been established as crucial loci in fear memory acquisition (Pape and Pare, 2010). BLA is thought to rely on bidirectional synaptic connections with the hippocampus and the mPFC. Electrophysiological approaches support the involvement of the mPFC and BLA in fear conditioning and extinction: for example, increased neural activity in the prelimbic area of the mPFC was observed in rats in response to CS presentation (Burgos-Robles et al, 2009). Similarly, enhanced LTP in the BLA was associated with fear conditioning (LeDoux, 2000). Vouimba and Maroun (2011) discovered that fear conditioning increased evoked field potentials (EFPs) in the mPFC–BLA pathway, finding supported by a study which demonstrated that fear encoding involves strengthening of BLA synapses from a specific group of neurons in the mPFC (Arruda-Carvalho & Clem, 2014).

Since circuits including mPFC projections are involved in associative learning and other complex behavioral processes (Jurado-Parras *et al.*, 2012; Conde-Moro *et al.*, 2019; Sánchez-Hidalgo *et al.*, 2022), we analyzed LTP induction and duration at mPFC to BLA synapses in awake behaving *Grin3a*^{-/-} mice and their WT littermates (Fig. 33A). In order to collect baseline values, animals were stimulated in the mPFC area each for 15 min with single pulses at a rate of 3/min. Then, a high frequency stimulation (HFS) protocol was applied as described in methods. Following HFS trains, responses to single pulses (3/min) were recorded for 1 h. Recording sessions were repeated for 3 additional days (30 min each). Although the two groups of mice increased the amplitude of collected field excitatory postsynaptic potential (fEPSP) responses following the HFS session, the WT mice increase in synaptic strength was weak and transient compared to the *Grin3a*^{-/-} group (Fig. 33B). Indeed, the enhanced synaptic strength persisted for up to 4 days in

Results

Grin3a^{-/-} mice. Thus, absence of GluN3A facilitates the induction of “super” lasting LTP, at least at mPFC-BLA glutamatergic synapses.

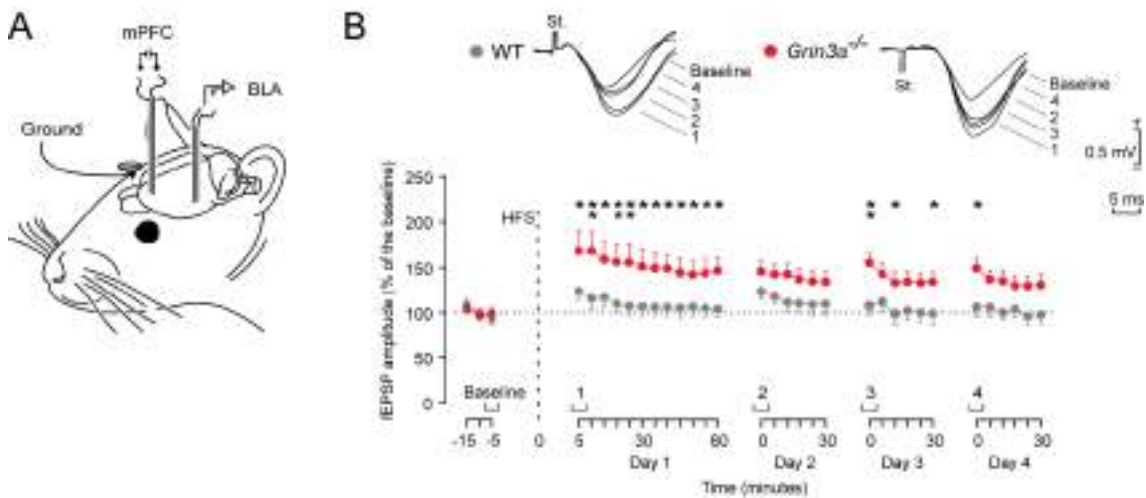


Figure 33. GluN3A removal facilitates *in vivo* LTP. A) Adult males (4 months old) were implanted with stimulating electrodes at the mPFC and with two recording electrodes at the BLA. B) Time course of LTP evoked at the mPFC-BLA synapse in the two experimental groups. Following 15 min of baseline recordings, animals were presented with the HFS protocol described in methods and illustrated by the dashed line. LTP evolution was followed for four days. At the top are illustrated representative examples (averaged five times) of fEPSPs collected at the times indicated in the bottom graph collected from a representative animal per group. Although the two groups presented a significant increase in fEPSP amplitudes following the HFS session the LTP evoked in *Grin3a*^{-/-} mice was significantly larger and longer lasting than that evoked in the control group (n = 13 mice per group; two-way repeated measurements ANOVA *, p < 0.05; **, p < 0.01).

5. Testing GluN3A effect on memory ontogeny

The results in sections 1-4 demonstrate a role of GluN3A in limiting memory formation in the adult brain, far from postnatal critical periods when GluN3A expression is most prevalent and when receptors containing this subunit play crucial roles in synapse maturation and refinements. They further attribute the effect to inhibitory effects of GluN3A on mTORC1 signaling.

Molecular and cell biology approaches in our eLife paper (see Appendix 1) shed insight on how GluN3A controls mTORC1 activity. The mechanism involves direct binding of the C-terminal domain of GluN3A to the postsynaptic scaffold GIT1, which impedes the assembly of GIT1-mTORC1 complexes that are normally localized to synapses and nucleate the production of plasticity-related proteins upon neuronal activation. GIT1-mTORC1 complex formation is regulated through development, first appearing in WT hippocampi around P16 and progressively increasing in abundance into juvenile-adult stages (Conde-Dusman *et al.*, 2021). Sharing time window with activity-dependent down-regulation of GluN3A expression and formation of GIT1-mTORC1 complexes, the mouse brain becomes capable of storing (24h) fear memories around P14 (Akers *et al.*, 2012).

We further found that GIT1-mTORC1 complex formation is accelerated in *Grin3a*^{-/-} mice (Conde-Dusman *et al.*, 2021), providing a mechanism for GluN3A deletion to promote a plasticity switch of synapses from a labile state to a state capable of lasting structural and functional potentiation. We thus asked whether the earlier appearance of GIT1-mTORC1 complexes in GluN3A knockouts affects the timing of emergence of mature protein translation and in turn, the ontogeny of memories. Both rely on the maturation of synaptic signaling pathways, most prominently mTORC1.

5.1 The emergence of memory is not altered in mice lacking GluN3A

We started by comparing the timing of emergence of contextual fear memory in young WT and GluN3A knockout mice. Paul Frankland's & Sheena Josselyn's laboratory

Results

defined a timeline for the ontogeny of fear conditioning memories in mice, with mice becoming capable of storing fear conditioning memories for 24 hours at P14 (Akers *et al.*, 2012). In order to implement their protocol to test fear ontogeny in our lab, we exposed P13 and P15 *Grin3a*^{-/-} and WT mice (before and after the P14 milestone) to three foot-shocks of 0.5mA and two seconds of duration. Age-matched groups of mice were exposed to the conditioning context but no shocks were delivered as a control for spontaneous freezing not related to memory formation (no shock group; Fig. 34A).

We were able to replicate the results of the Frankland lab: At P13, shocked and non-shocked mice showed similar levels of freezing (Fig. 34B). Hence freezing at P13 cannot be attributed to contextual fear memory but rather to spontaneous freezing in juveniles. By P15, spontaneous freezing declined in both genotypes, revealing fear memory-related significant differences between shocked and non-shocked mice but no differences between genotypes (Fig. 34B).

These results validated our protocol for assessing fear memory ontogeny, and showed that GluN3A deletion does not impact the emergence of the ability of mice to form lasting associations between context and shock.

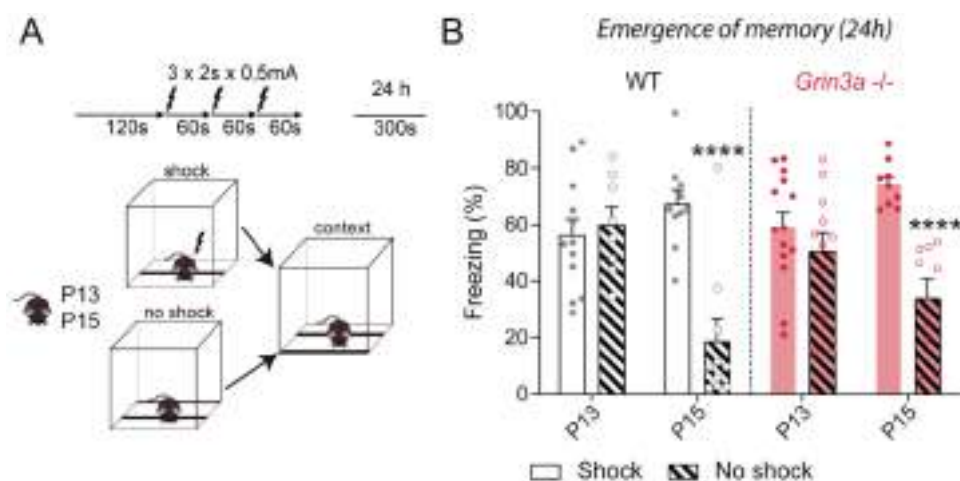


Figure 34. GluN3A deletion does not affect the developmental timing of memory formation. A) Experimental design for testing the ontogeny of fear conditioned memories at 24 hours. B) Shocked mice showed high levels of freezing regardless of age, while nonshocked mice showed a gradual decline in spontaneous

freezing from P13 to P15. P13 mice showed no evidence of fear memory. (n= 8-13 mice per group; two-way ANOVA, **** p<0.001).

5.2 Challenging paradigms unveil increased fear responses in postnatal *Grin3a*^{-/-} mice

Although we found no acceleration in the ontogeny of fear memories in GluN3A-lacking mice using the methods from Frankland's lab (Fig. 34), a prediction of our results in adult mice would be that weaker stimuli might unveil enhanced memory. Thus, we tested P15 mice using a weaker fear conditioning protocol adapted to postnatal mice. For this protocol, we subjected mice to a milder, single CS-US exposure in the conditioning box, using a single shock of 0.5mA, two-second long, rather than the triple pairing of context-shock (Fig. 35A). Here, P15 *Grin3a*^{-/-} mice showed higher levels of freezing relative to WT's 24 & 48 hours after exposure to the context, revealing an earlier emergence of fear memory mechanisms in GluN3A-lacking mice (Fig. 35B & C).

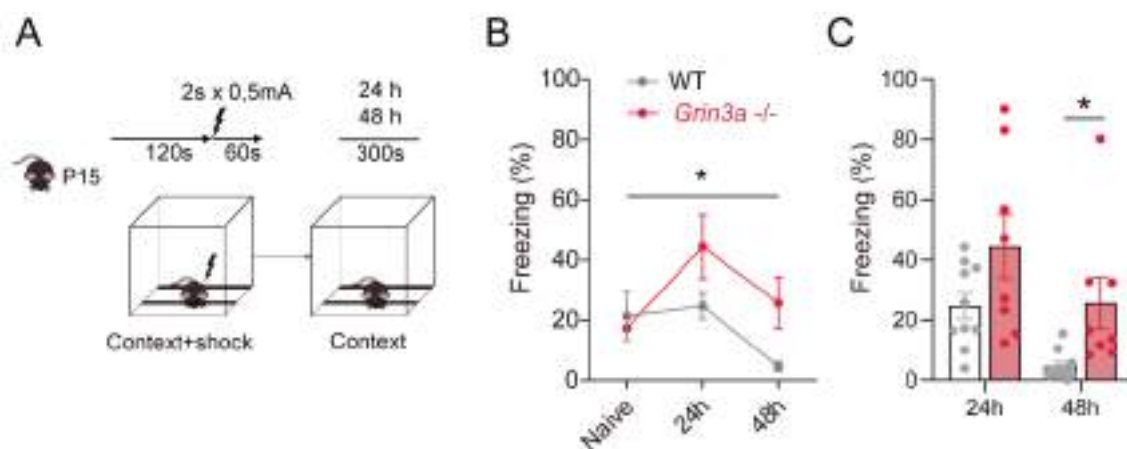


Figure 35. Postnatal *Grin3a*^{-/-} mice show enhanced memory of a weak conditioning. A) Weak protocol used for testing fear ontogeny in P15 mice. B-C) *Grin3a*^{-/-} mice exhibit an increased conditioned fear at 24 and 48 hours after training. (B: Repeated measurements two-way ANOVA, * p < 0.05; C: two-tailed unpaired t-test, * p < 0.05; n= 8-10 mice per group).

5.3 Removing GluN3A accelerates the emergence of the persistence of memory

Our results indicated enhanced memory at 24 hours in GluN3A-lacking postnatal mice when trained with weak stimuli but no differences at the same time point when trained strongly. Following the path marked by these results, and those obtained in adult mice where the enhanced fear conditioning could be observed at least 7 days after training, we went on to test the onset of remote memories in *Grin3a*^{-/-} mice. While mice become capable of storing fear memories at P14, they do not show signs of memory persistence (defined as high levels of freezing 7 days after training) until P30 (Akers *et al.*, 2012). We hypothesized that the earlier emergence of fear memories in *Grin3a*^{-/-} mice would be associated with earlier emergence of memory persistence.

For this experiment, we trained WT and *Grin3a*^{-/-} mice with three foot shocks at four different postnatal stages (Fig. 36A): from P15, a time point in which no memory persistence had been found in WT mice; to P25, close to when the persistence of memory starts in WT mice (Akers *et al.*, 2012; Klune *et al.*, 2021). Consistent with previous reports in rats and mice (Spear, 1979; Akers *et al.*, 2012) P15 mice showed no freezing at 7d (Fig. 36B). Thus, we concluded that none of the genotypes had developed persistent memories at that stage. As expected, WT mice did not show freezing at P17. At this age however, *Grin3a*^{-/-} mice started to show signs of memory persistence (Fig. 36B). Differences between genotypes became more evident by P20 into P25 (Fig. 36B). Our findings indicate that in both postnatal stages, *Grin3a*^{-/-} mice consistently outperformed their WT littermates, exhibiting strong memory persistence one week after training.

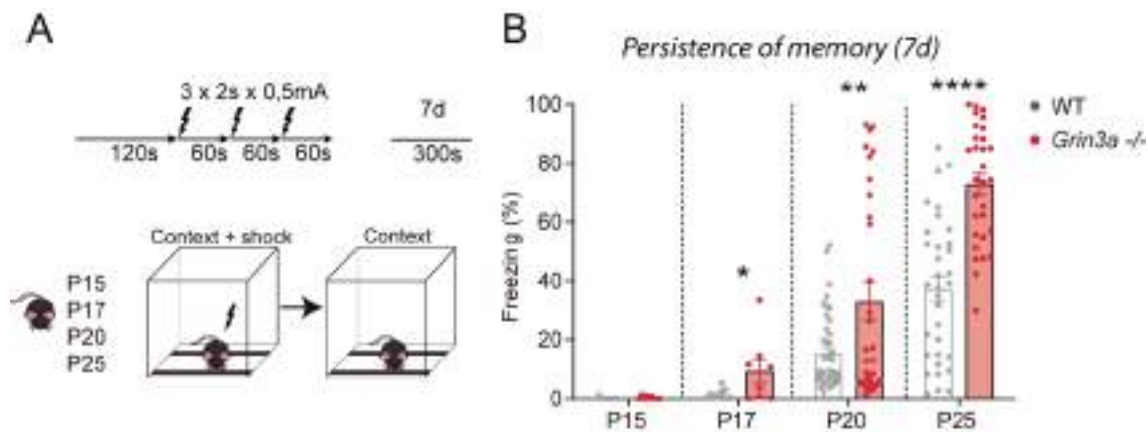


Figure 36. Ontogeny of memory persistence is accelerated in *Grin3a*^{-/-} mice. A) Protocol used for testing the ontogeny of memory persistence. Postnatal ages in which mice were trained are indicated. B) WT mice show little or no freezing until P20. In contrast, *Grin3a*^{-/-} mice exhibit higher levels of freezing 7 days post-training starting at P17. (Unpaired two-tailed t-test, * $p < 0.05$, ** $p < 0.01$, **** $p < 0.0001$).

Therefore, these results provide evidence of an accelerated emergence of memory persistence in *Grin3a*^{-/-} mice and support a regulatory role of GluN3A in memory ontogeny.

5.4 Selective ablation of GluN3A from principal excitatory neurons is sufficient to accelerate fear ontogeny

We then asked whether the effect was due to GluN3A expression in excitatory neurons, as was the case in adult mice. We focused on the hippocampus, since many studies are currently trying to unveil the mechanisms by which infants can make the types of memories that in adult brains are processed by the hippocampus-dependent memory system (Akers *et al.*, 2014; Donato *et al.*, 2021).

5.4.1 Early postnatal ablation of GluN3A from excitatory neurons

We first designed and tested a tamoxifen administration protocol to drive efficient GluN3A deletion in postnatal mice (Fig. 37A). Administration to *Grin3a*^{ff} x *CamK2a*-Cre^{ERT2} mice of 50 μ g of TXF via i.p. every day during postnatal days 1-3 resulted in a

Results

significant reduction on hippocampal GluN3A levels tested at P25 ($69.41 \pm 0.043\%$) with a survival ratio of 100% in postnatal mice (Fig. 37B). Note that the decrease in juveniles was similar to the observed in adult mice (see Fig. 19).

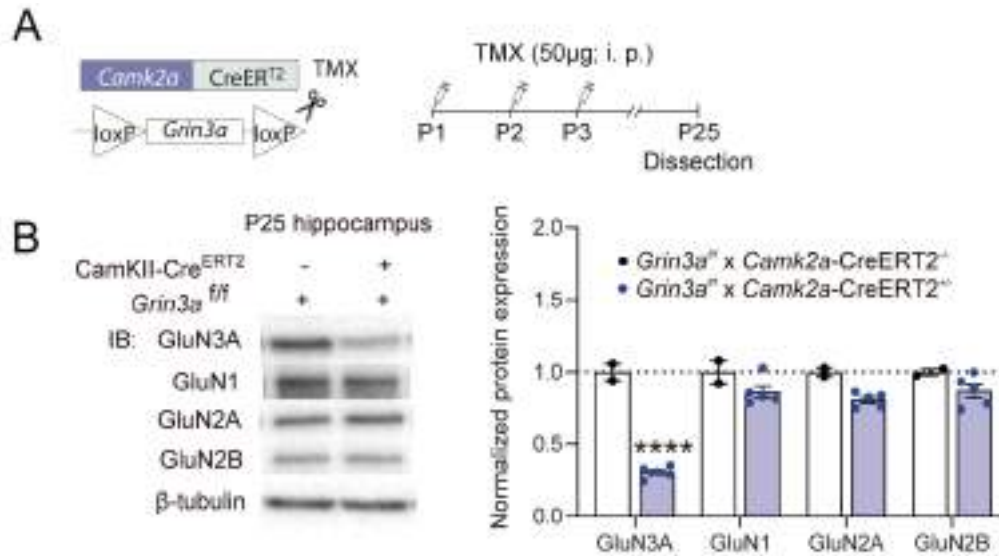


Figure 37. Biochemical characterization of postnatal *Grin3a^{ff}* x *CamK2a-Cre^{ERT2}* mice. A) Experimental design. B) Hippocampal lysates of P25 mice were analyzed by sodium dodecyl sulfate polyacrylamide gel electrophoresis (SDS-PAGE) and immunoblotted for the indicated proteins (n= 2-5 mice per group; unpaired two-tailed t-test, ****p < 0.0001).

5.4.2 Postnatal GluN3A expression in excitatory neurons controls the ontogeny of memory persistence

Since our approach showed that it is possible to delete GluN3A in postnatal *Grin3a^{ff}* x *CamK2a-Cre^{ERT2+/-}* mice, we investigated how the expression of GluN3A in excitatory neurons affects the development of long-term memory. We administered TXF and then trained P25 *Grin3a^{ff}* x *CamK2a-Cre^{ERT2+/-}* mice and littermate controls with three strong foot shocks (Fig. 38A & B). We tested their responses 7 days after training.

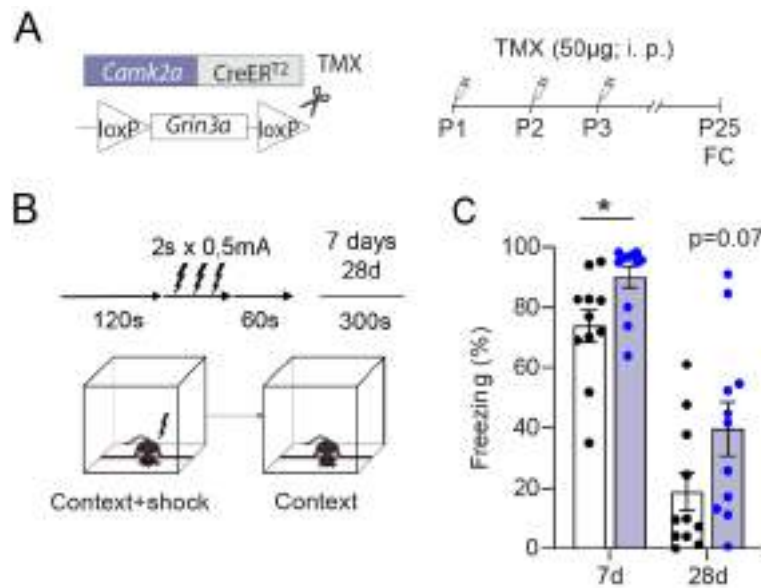


Figure 38. Conditional deletion of GluN3A from postnatal excitatory neurons accelerates the ontogeny of memory persistence. A-B) Experimental design. C) GluN3A deletion from excitatory neurons mimics the effect of constitutive GluN3A deletion. (n= 11 male and female mice per group; repeated measurements two-way ANOVA *p < 0.05).

In line with our results in adult mice, P25 *Grin3a^{ff}* x *CamK2a-Cre^{ERT2+/-}* mice showed higher levels of freezing than *Grin3a^{ff}* x *CamK2a-Cre^{ERT2-/-}* controls one week after training (Fig. 38C). Moreover, when we extended our period of testing to 28d, we continue to detect a trend towards enhanced memory persistence in GluN3A-lacking mice (Fig. 38C). These results altogether indicate that ablation of GluN3A from excitatory neurons at early stages in development is enough to accelerate the ontogeny of memory persistence.

6. Unveiling the mechanisms underlying accelerated memory ontogeny

Once we had confirmed the role of GluN3A in memory ontogeny and located its origin to excitatory neurons, we investigated the mechanism behind this acceleration in the emergence of memories.

6.1 GluN3A ablation promotes protein synthesis in postnatal mice

As mentioned, GluN3A deletion allows the nucleation of GIT1/mTORC1 complexes and enables or facilitates mTORC1-mediated synthesis of plasticity proteins (Conde-Dusman *et al.*, 2021). Because long-term memory requires protein synthesis, we asked whether this facilitation could be responsible for the phenotypes observed in postnatal mice as was in adults (see Figs. 17 & 36). To test this, we first analyzed protein translation rates in P20 WT and *Grin3a*^{-/-} mice using a method for labeling *de novo* translated proteins, surface sensing of translation (SUnSET), which measures translation elongation and is amenable for *in vivo* labeling.

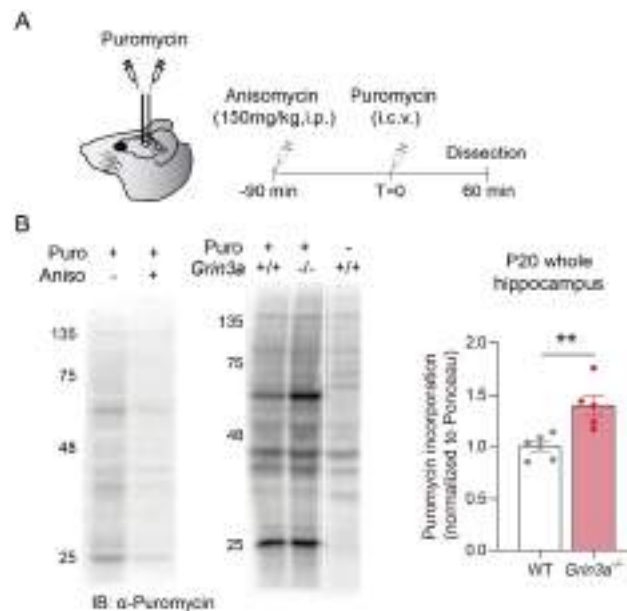


Figure 39. Increased protein synthesis in postnatal *Grin3a*^{-/-} mice. A) Diagram and timeline of intracerebroventricular (i.c.v.) puromycin injections. The protein synthesis inhibitor anisomycin was used as positive control. B) *De novo* translation labeled at the carboxy terminus (C terminus) in awake behaving mice (male and female) using SUnSET showed a significant increase in translation in P20 *Grin3a*^{-/-} mice (n= 5-6 mice per group, unpaired two-tailed t-test, ** p< 0.01).

By injecting puromycin into the lateral ventricles of postnatal mice (Fig. 39A) we could measure the levels of *de novo* protein synthesis in microdissected brain regions of WT and *Grin3a*^{-/-} mice *in vivo* by quantifying the levels of puromycin incorporation. The

read-out was validated by a significant decrease in puromycin labeling in the presence of the general protein synthesis inhibitor anisomycin (Fig. 39B, left blots). Puromycin immunoblotting showed that *Grin3a*^{-/-} mice exhibit a robust increase ($39.92 \pm 0.10\%$) in protein synthesis (Fig. 39B, right blots), supporting the notion that an increased proteins synthesis underlies the accelerated memory ontogeny in GluN3A-lacking mice.

6.2 Blocking enhanced mTORC1-signaling occludes GluN3A effects on fear memory ontogeny

We then asked whether enhanced protein synthesis mediated by mTORC1 is responsible for the earlier emergence of memory capacity in GluN3A-lacking mice. To test this, we blocked mTORC1 signaling in postnatal mice with rapamycin. As in adult mice, we titrated the rapamycin dose to target mTORC1 without impairing mTORC2 signaling.

We injected three different rapamycin doses (i.p. daily for three days), microdissected mice hippocampi two hours after the last injection and evaluated mTOR signaling by western blotting (Fig. 40). We found that three doses of 2 mg/kg rapamycin were sufficient to block the phosphorylation of mTOR and its effector S6 without affecting the phosphorylation of the mTORC2 downstream target AKT^{S473} (Fig. 40).

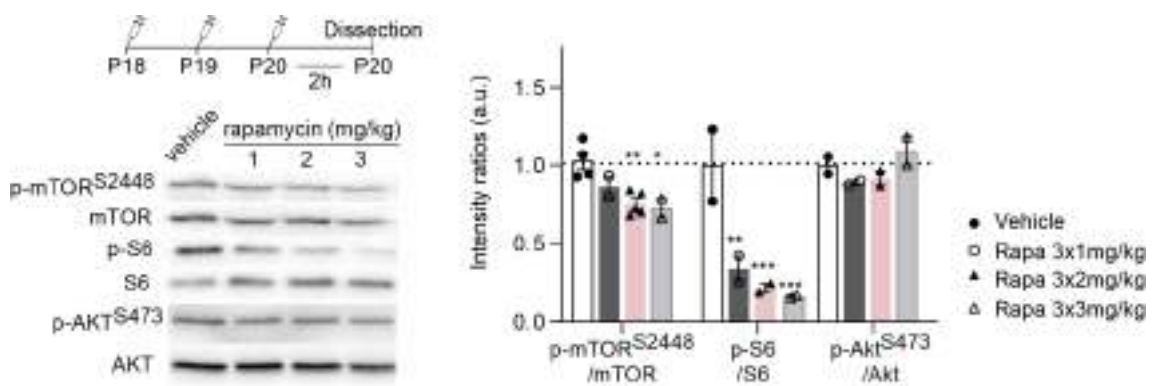


Figure 40. Rapamycin dose titration in postnatal mice. Rapamycin regime, representative immunoblots and quantification of blots showing reduction in the phosphorylation of mTORC1-related proteins. Note that phosphorylation of AKT at S473 remains unaffected (n=2-4 mice per group; one-way ANOVA, * p<0.05, ** p<0.01, *** p<0.001)

Results

Once we had selected the dose for the experiment, we assessed the relationship between mTORC1 and GluN3A in the ontogeny of memory persistence. We trained postnatal WT and *Grin3a*^{-/-} mice in context fear conditioning and administered rapamycin following the selected regime (Fig. 41A). One week after training, rapamycin-treated *Grin3a*^{-/-} mice were comparable to WT mice in learning the association between the context and the foot shock. By contrast, *Grin3a*^{-/-} mice treated with vehicle exhibited a marked increase in memory persistence (Fig. 41B).

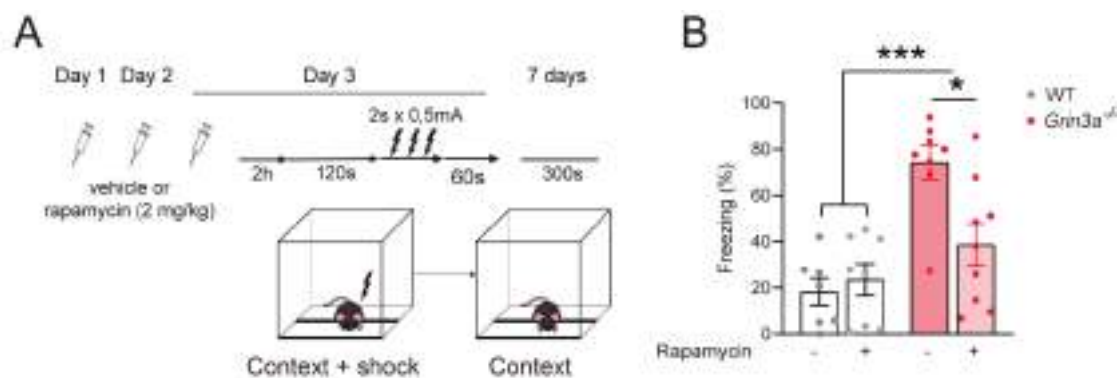


Figure 41. mTORC1-dependent effects of GluN3A on the ontogeny of memory persistence. A) Rapamycin administration regime and fear conditioning paradigm. B) Enhanced contextual fear conditioning in postnatal *Grin3a*^{-/-} mice (male and females) 7 days after training is reversed by rapamycin (n=8-9 mice per group; two-way ANOVA, * p<0.05, *** p<0.001).

These results confirmed our hypothesis that enhanced mTORC1 signaling underlies the accelerated memory ontogeny seen in *Grin3a*^{-/-} mice. The results are also in line with those obtained in adult mice where we demonstrated a mTORC1-dependent enhanced associative memory.

6.3 Neurogenesis levels remain unchanged in *Grin3a*^{-/-} mice

Neurogenesis (the birth of new neurons) was thought to be negligible once the brain had developed. However, neurogenic niches exist in the brain that are capable of generating new neurons through life and are active during postnatal stages (Zhao *et al.*, 2008; Ming *et al.*, 2005). This newly generated neurons are thought to reconfigure memory circuits

and overwrite previous hippocampus-dependent memories, reducing the ability of the brain to reinvoke the pattern of activity that initially encoded the existing memory (Akers *et al.*, 2014). The idea is that high levels of neurogenesis lead to weaker memories, because a higher number of newly generated neurons are integrated into the circuit and disrupt the initial memory pattern. Conversely, a lower number of newly generated neurons may result in a more negligible reconfiguration of the memory circuit, thus making recall easier.

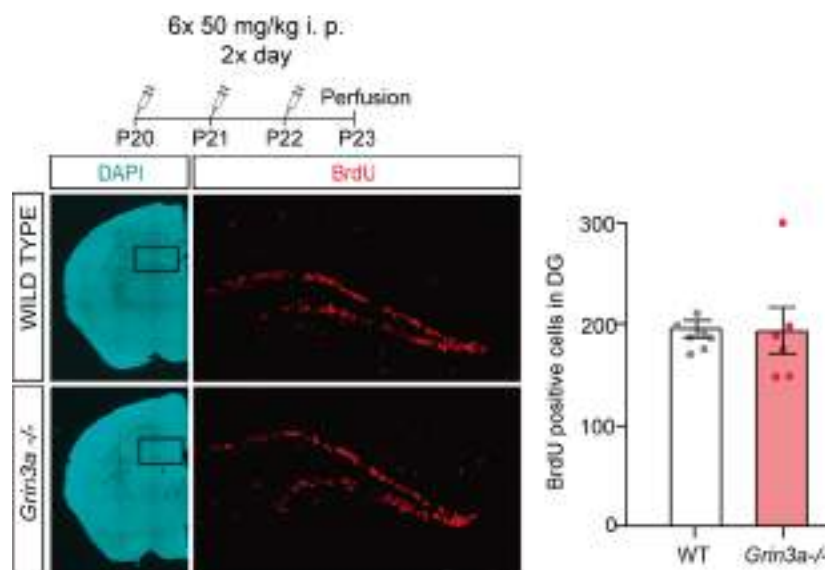


Figure 42. Normal neurogenesis levels in postnatal *Grin3a*^{-/-} mice. BrdU labeling of granule cells in the DG in WT and *Grin3a*^{-/-} mice (males and females) showing the same rate of postnatal neurogenesis. BrdU administration regime is indicated. (n= 6-7 mice per group).

To address potential contributions of altered neurogenesis to the accelerated fear ontogeny in GluN3A knockouts, we injected BrdU two times a day for three days (P20-P22) (Fig. 31). This protocol allowed labeling of every cell proliferating during those days. We found no differences in BrdU⁺ cells in *Grin3a*^{-/-} mice (Fig. 42), ruling out less neurogenesis as the cause of the earlier emergence of memory persistence in GluN3A-lacking mice.

7. GluN3A-related memory enhancement is lifelong

In the previous chapters we characterized the effects of GluN3A on cognition-related behaviors in postnatal and adult mice. In this chapter, we studied whether the impact of GluN3A on memory persists in aged mice. Mice are considered of old age when they reach an age of 12 months, hence we started our characterization past that point.

Our first step was characterizing age-related differences using young adult and aged mice. For that purpose, we tested in parallel mice aged 3-4 months and 20 months old. We started with the weak paradigms used in previous chapters. For fear conditioning, we used a single, weak CS-US pairing (Fig. 43A). However, neither aged *Grin3a*^{-/-} nor WT mice learnt the association, showing that enhanced performance of younger *Grin3a*^{-/-} mice in demanding tasks was lost with age (Fig. 43B).

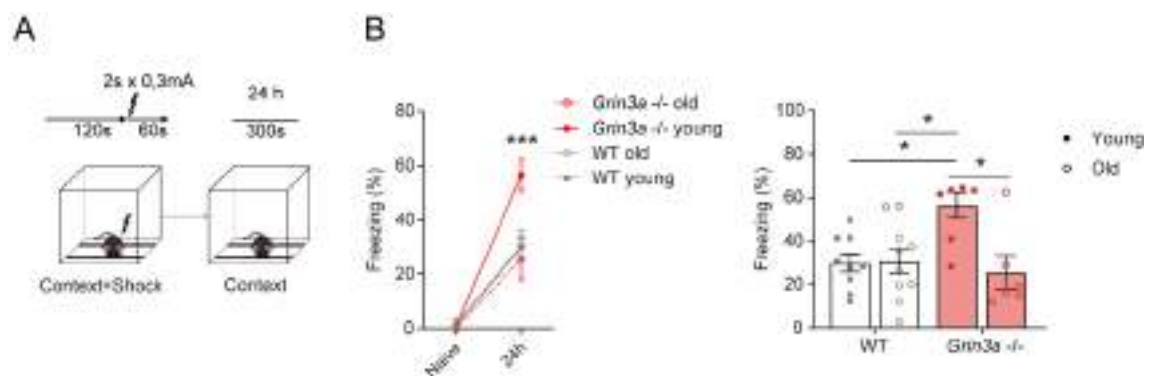


Figure 43. Age-associated decline of enhanced contextual memory in *Grin3a*^{-/-} males. A) Contextual fear conditioning paradigm. B) Enhanced contextual fear conditioning in young adult *Grin3a*^{-/-} mice (3-4 months old) is lost with age. Old *Grin3a*^{-/-} mice (20 months old) perform at WT levels. (n = 9–13 mice per group; left: repeated measures two-way ANOVA; right: two-way ANOVA, * p<0.05, *** p<0.001).

We continued our study by performing the 2 trial per day Morris water maze. Based on our fear conditioning results (Fig. 43), we decided to extend the training phase of the Morris water maze (from 7 to 10 days) to facilitate aged mice performance. No differences were found during visible platform phase, ruling out a decline in visual or

motor performance (Fig. 44A). No differences in learning were found during hidden platform phase (Fig. 44A). However, results on the probe trial replicated those of the fear conditioning and previous experiments: young *Grin3a*^{-/-} mice spent more time in the target quadrant, and correctly distinguished it, outperforming all other three groups that were incapable to correctly locate the target quadrant (Fig. 44B).

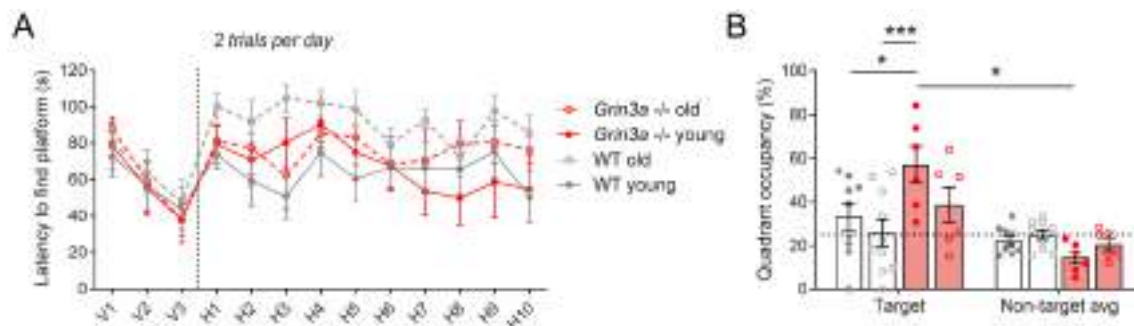


Figure 44. *Grin3a*^{-/-} mice enhanced associative memory declines with age. A) Escape latencies over the time-course of training on a 2 trials per day version of the Morris water maze. Visible platform phase (V1-V3) shown as control. B) On the probe trial for memory acquisition performed 24 hr after H10, only young *Grin3a*^{-/-} mice (3-4 vs. 20 months old) demonstrated a correct distinction between target and non-target quadrants. Dashed lines indicate chance levels (25%) (n= 6-9 mice per group; two-way ANOVA, *p<0.05, *** p<0.001).

These experiments showed that because of the cognitive decline that accompanies age in both WT and knockout mice, the weak protocols used in Figures 43 & 44 are unfit to unveil genotype differences in aged mice. We thus decided to study aged mice on the standard version of the Morris water maze (4 trials per day). No differences were found during the visible platform phase, ruling out visual and perceptual deficits (Fig. 45A). *Grin3a*^{-/-} mice showed no advantage over WT mice during training (Fig. 45A). However, they showed correct distinction between target and non-target quadrants in the probe trial while WT mice did not (Fig. 45, B), indicating enhanced hippocampal-dependent contextual memory.

Results

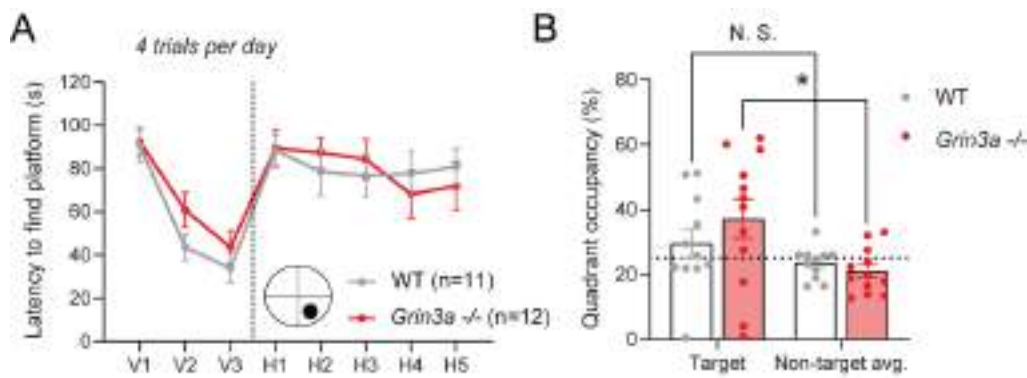


Figure 45. Enhanced associative memory in old *Grin3a*^{-/-} female mice. A) Escape latencies of aged WT and *Grin3a*^{-/-} mice over the time-course of training on a 4 trials per day version of the Morris water maze. Visible platform phase (V1-V3) is also showed as control. B) On the probe trial for memory acquisition performed 24 hr after H5, aged *Grin3a*^{-/-} mice demonstrated a correct distinction between target and non-target quadrants. Dashed lines indicate chance levels (25%) (n=11-12 mice per group; two-way ANOVA, *p<0.05).

We then continued our behavioral characterization of aged mice by using the fear conditioning paradigm. We switched to a strong training protocol (Fig. 46A), since the performance of aged mice upon weak training was poor indicating the need of stronger stimuli.

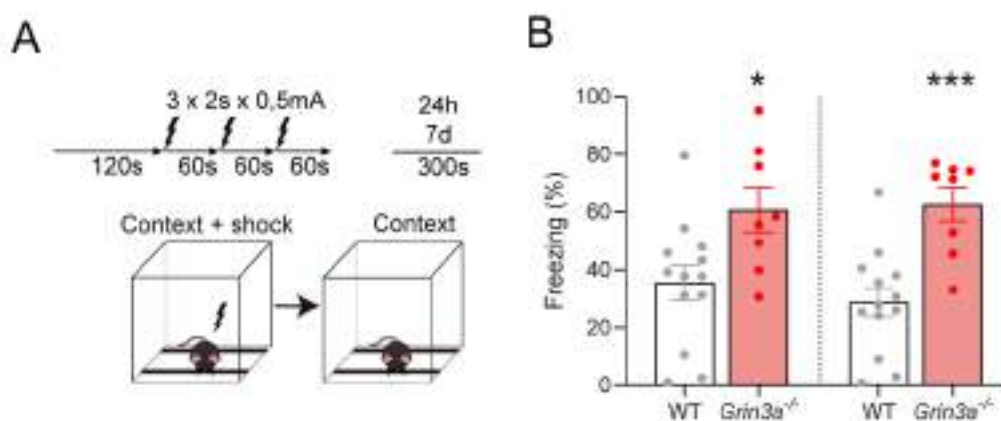


Figure 46. Enhanced contextual fear memory in aged *Grin3a*^{-/-} males. A) Experimental design. B) Aged (15-16 months old) *Grin3a*^{-/-} males exhibit an increased conditioned fear at 24 and 7 days after training (n= 8-13 per group, unpaired two-tailed t-test, * p<0.05, *** p<0.001).

We discovered that aged *Grin3a*^{-/-} outperform their WT littermates at both, 24 hours and 7 days post-training (Fig. 46B), indicating that the phenotype observed in younger mice persists during late adulthood.

In summary, the results show that *Grin3a*^{-/-} mice, despite presenting age-related memory decline, keep outperforming their WT littermates and show no pathological features, hence, reinforcing the possible role of GluN3A as a therapeutic target for enhancing memory throughout the entire lifespan of mice.

Discussion



The goal of this Thesis work was to investigate the effects that the refinement of synapses and neural circuits driven by GluN3A-NMDARs have on cognition-related behaviors, in hopes of finding a novel therapeutic target for ameliorating memory loss. To do so, we assessed the performance of GluN3A-lacking mice in learning and memory tasks through their entire lifespan: from young postnatal stages (P13-P25) through adulthood and into aging. In postnatal mice, we found that removing GluN3A-NMDARs accelerated the ontogeny of memories, limiting the temporal window of infantile amnesia. In adult mice, genetic ablation of GluN3A-NMDARs enhances mice performance in spatial navigation and associative memory tasks upon weak training protocols, while their performance under standard training conditions is normal.

In an effort to map the cellular loci of GluN3A effects, we obtained and characterized genetically modified mice lacking GluN3A in either somatostatin interneurons or principal excitatory neurons, the two major cellular populations where GluN3A is prominently expressed. The use of these genetic tools allowed us to attribute the memory-enhancing effects of GluN3A deletion to its expression on excitatory neurons. By using an inducible Cre-line, we further demonstrated that the memory enhancement is due to adult expression rather than to altered brain developmental trajectories due to lack of GluN3A during critical refinement periods. Upon reaching old age, mice without GluN3A expression retain their advantage in learning and memory tasks, indicating that antagonizing GluN3A might indeed be of therapeutic potential for the treatment of memory-loss associated disorders.

Overall, the data presented in this thesis open new avenues for a better understanding of how NMDARs in general and GluN3A-NMDARs in particular exert their effect on the brain and affect behaviors crucial for our relationship with the environment. Our experiments also evidence the therapeutic potential of targeting GluN3A-NMDARs for memory-enhancing treatments. Future experiments targeting specific temporo-spatial expression of GluN3A or pharmacological manipulations of its

effects will help furthering a more accurate characterization of its role in our brain and its therapeutic potential.

GluN3A constrains memory by inhibiting mTORC1 signaling

Research conducted previously in our laboratory demonstrated that mice overexpressing GluN3A exhibit impairments in hippocampal learning tasks, such as the Morris water maze, novel object recognition or social transmission of food preference (Roberts *et al.*, 2009). The deficiencies observed were specific to long-term memory, while memory acquisition remained unaffected, indicating that GluN3A interferes with brain mechanisms responsible for memory persistence. Studies conducted in our laboratory revealed that GluN3A expression inhibits the activation of mTORC1, a crucial pathway for translational control that is thought to be involved in long-lasting synaptic plasticity and memory encoding (Conde-Dusman *et al.*, 2021). We hypothesized that, if this were the case, removal of GluN3A would enhance long-term plasticity and memory formation by removing the constraints it imposes on mTORC1 activation.

While no differences were found in the Morris water maze when *Grin3a*^{-/-} mice were tested under standard conditions (Fig. 13), male and female *Grin3a*^{-/-} mice showed a better performance in more challenging versions of the test when training was spaced out (Figs. 14 & 15). Similar results were obtained in associative memory tests conducted in mice overexpressing GluN3A and *Grin3a*^{-/-} mice. Since better spatial learning only emerged as test difficulty was higher, we adapted the fear conditioning protocol to assess mouse responses to weak training. The strategy unveiled an interesting bidirectional phenotype in which GluN3A deletion facilitates long-term memory (Fig. 17) while its overexpression impairs the ability of mouse to form CS-US associations (Fig. 16). In line with the work by Roberts *et al.*, (2009) we found short-term memory to be unaffected in *Grin3a*^{-/-} mice .

It is important to consider that the cognitive enhancement could result from lack of GluN3A during development rather than adult stages. In addition, GluN3A is highly

expressed in both excitatory neurons and somatostatin interneurons, both of which have recently been implicated in protein synthesis-dependent memory consolidation (Sharma *et al.*, 2020; Shrestha *et al.*, 2020a). We addressed these issues using cell-type-specific and inducible *Grin3a* knockout mice and demonstrated that: 1) GluN3A regulation of cognitive processing is due to adult expression, suggesting that GluN3A functions extend beyond the well-recognized roles in shaping postnatal neural circuit refinements (Figs. 17-20), and 2) excitatory neurons are the site of GluN3A's actions in gating cognitive processing (Fig. 20).

As explained previously, a fundamental mechanism for long-term memory storage involves lasting changes in synaptic strength associated to structural modifications in synapse and spine morphology that rely on local protein synthesis for persistence. Thus, in parallel to our behavioral assessment we analyzed the induction and duration of LTP in mPFC to amygdala synapses of awake, behaving *Grin3a*^{-/-} mice and WT counterparts. This particular synapse was chosen because of its implication in a variety of complex behavioral processes including the encoding of aversive memories (Jurado-Parras *et al.*, 2012; Conde-Moro *et al.*, 2019; Sánchez-Hidalgo *et al.*, 2022). While both groups of mice exhibited LTP after HFS, *Grin3a*^{-/-} mice displayed a stronger and much more prolonged increase in synaptic strength compared to WT mice. Remarkably, while LTP was transient in WTs it lasted up to 3-4 days in the knockouts.

We then tested the second part of our hypothesis, i.e. the involvement of mTORC1-mediated protein synthesis. The idea was supported by two lines of evidence. First, protein synthesis is a crucial process for the consolidation of synapses and memories, as demonstrated in previous studies (Monné A, 1948), being mTORC1 one of its key regulators. Studies dating from the early 1970's already pointed out that general protein synthesis inhibitors, such as cycloheximide or anisomycin (Squire and Barondes, 1974) prior to training impair memory capacities. Later evidence supports the role of mTORC1 in protein synthesis: Pereyra *et al.*, (2018) showed that infusion of rapamycin into the dorsal hippocampus reversibly disrupted memory expression in the inhibitory

Discussion

avoidance test. Years before, Powell's lab had found that systemic administration of rapamycin before training blocked fear memory at 24h (Blundell *et al.*, 2008). Second, a recent study conducted by our laboratory (Conde-Dusman *et al.*, 2021) revealed a direct link between GluN3A-NMDARs and the postsynaptic GIT1 adaptor that allows GluN3A to tune protein synthesis selectively at synapses.

By using a subthreshold regime of rapamycin (Stoica *et al.*, 2011; Conde-Dusman *et al.*, 2021) in *Grin3a*^{-/-} mice, we confirmed that enhanced mTORC1 activity underlied the enhanced fear conditioning phenotype that we had discovered in GluN3A-lacking mice. However, a wide variety of rapamycin doses and treatments have been used to test its role in memory: from bilateral cannulation aimed at the amygdala (Parsons *et al.*, 2006), to i.p. injections starting at 1mg/kg, up to 150 mg/kg (Ehninger *et al.*, 2008). Another concern was that high doses of rapamycin have been shown to affect mTORC2 (Sarbassov *et al.*, 2005; Sarbassov *et al.*, 2006; Stoica *et al.*, 2011). mTORC2 implication in memory was confirmed by Costa-Mattioli's team in 2013: They ablated the key mTORC2 component *Rictor* in a forebrain-specific manner by crossing *Rictor*^{loxP/loxP} mice with *Camk2a*-Cre mice (Huang *et al.*, 2013). By using these mice, they avoided the abnormal brain development described in mice constitutively lacking *Rictor* (Carson *et al.*, 2013) and described that both L-LTP and LTM were impaired in hippocampal slices from mTORC2-lacking mice due to defective actin polymerization dynamics (Huang *et al.*, 2013). Years later, this same lab found that mTORC2-deficient mice displayed impaired novel object recognition (Zhu *et al.*, 2018). Interestingly, this study found no impairments in mTORC1-deficient mice.

In order to achieve specificity in blocking mTORC1 activity, we employed a titration strategy to decrease the dosage of rapamycin so only mTORC1-dependent signaling was inhibited. To validate the implication of mTORC1-mediated effects on protein synthesis, we further administered the general protein inhibitor anisomycin to a cohort of mice prior to their training in a fear conditioning paradigm.

Taken together, our findings (Figs. 25-27) demonstrate that GluN3A expression on excitatory neurons modulates protein synthesis and long-term memories via inhibition of mTORC1 signaling. Downregulation of GluN3A expression removes the inhibitory effects of GluN3A on mTORC1 signaling, thereby lowering the threshold for learning and expands memory capacity.

Manipulating translation via GluN3A is safe

Protein synthesis regulation is crucial for proper cognitive function and dysregulated translation has been linked to cognitive impairment in neurodevelopmental disorders such as autism spectrum disorders and intellectual disability. Unchecked translation due to loss of negative regulators of translation such as FMR1, MECP2, or the mTORC1 suppressors NF1, TSC1/2, or PTEN has been implicated (Kelleher and Bear, 2008). Intriguingly, a subset of individuals with autism exhibit enhanced cognitive skills in specific domains as mental calculation or music (Heaton and Wallace, 2004). In line with this, some experimental manipulations that enhance translation such as inhibition of eIF2 α phosphorylation or enhancement of mTORC1 activity through FKBP12 removal lower memory thresholds. However, the memory enhancement is often at the expense of reduced memory fidelity and cognitive flexibility, even with cell-type-specific modulation attempts (Santini *et al.*, 2013; Shrestha *et al.*, 2020a; Trinh *et al.*, 2012).

Thus, at present, available data suggests that deviation from the physiological translation range can both impair or enhance cognition. If the latter, specific features of cognition or memory can be compromised. To evaluate whether enhanced mTORC1 translation by removing GluN3A is accompanied by those undesired effects, a battery of behavioral tests demonstrated that *Grin3a*^{-/-} mice show no deficits in behavioral flexibility (Figs. 28-32) nor perseverative behaviors (Fig. 30). Interestingly, fear extinction, another type of memory which is also dependent on protein synthesis, was found to be enhanced in *Grin3a*^{-/-} mice. This indicates that the absence of GluN3A does not compromise memory updating, that is required for cognitive flexibility, but instead

facilitates the extinction of fear memories. Similar results were obtained during the reversal phase of the Morris water maze (Figs. 28 & 29).

Another drawback of targeting translation to improve memory is a reduction in precision of the resulting memory. For instance, decreasing eIF2 α phosphorylation (Shrestha *et al.*, 2020b) increased mice fear responses to a conditioned stimulus but impaired the ability to differentiate that stimulus from a similar, innocuous one. A context discrimination test revealed that GluN3A deletion did not alter memory accuracy when compared to WT controls, indicating that GluN3A manipulations do not lead to the loss of memory fidelity often associated with other translation manipulations.

The differences might be related to the higher specificity of GluN3A deletion that specifically targets synaptic translation and is expressed in selected cell populations and brain regions. By contrast, negative regulators of mTORC1 such as FMRP, PTEN, or Tsc1/2 are expressed ubiquitously in many cell types and neuronal subpopulations, and their dysregulation has been linked to abnormal cell growth and tumorigenesis (Lipton and Sahin, 2014). Moreover, constitutive activation of translation may reach a plateau and interfere with the ability of cells to respond to extrinsic signals. Our experiments showed that this is not the case with loss of GluN3A, which does not impede mTORC1 activation but rather appears to facilitate the mTORC1 response to incoming synaptic inputs. Ultimately, the cognitive benefits observed upon GluN3A deletion suggest that targeting GluN3A expression or signaling pathways could be a promising therapeutic strategy.

Removal of GluN3A-NMDARs accelerates memory ontogeny

Learning from experience as an adaptation to the environment is a key feature for our survival, and is of utmost importance during infancy. During this stage the brain undergoes massive rearrangements of synaptic connections that remodel rudimentary neural circuits formed by the concerted action of intrinsic wiring programs. The synaptic remodeling is fundamental because it sets connectivity and plasticity patterns that will allow the individual to encode behaviors to adapt to the environment at hand. Because

GluN3A is highly expressed postnatally, we asked whether and how it contributes to the emergence of long-term memory abilities.

We focused on the hippocampus, main hub of the memory system, which maturation extends past infancy until the third postnatal week. This delay in development is thought to be the cause of infantile amnesia: the rapid forgetting and inability to recall early life memories that characterizes this life stage. Several mechanisms have been invoked to underlie infantile amnesia, including high levels of postnatal neurogenesis or immaturity of glutamatergic signaling in the hippocampus. The latter was proposed by Cristina Alberini's group. They further proposed that critical period mechanisms triggered by early experiences would later drive the maturation of glutamatergic signaling in the hippocampus and other brain areas so that can express long-term memories (Travaglia *et al.*, 2016, 2018). At least two maturation mechanisms seem to be engaged: the postnatal switch between GluN2B and GluN2A receptors and the incorporation of AMPARs into synapses. Specifically, at birth, NMDARs throughout the brain are composed predominantly of GluN2B subunits, which negatively regulate AMPA receptor expression and mature synapse formation (Gray *et al.*, 2011; Kelsch *et al.*, 2014; Wang *et al.*, 2011). After the second postnatal week, GluN2A subunits are progressively incorporated to NMDARs, establishing "mature" NMDAR function and signaling (Yashiro and Philpot, 2008).

In a series of studies testing the role of glutamatergic transmission maturation, Travaglia, Alberini and colleagues observed that GluN2A/GluN2B ratios in the hippocampi of infant mice that had learned the inhibitory avoidance task were higher compared to naïve infants (Travaglia *et al.*, 2016, 2018). The increased ratio indicates stronger expression of GluN2A subunits compared to GluN2B, a molecular phenotype characteristic of mature hippocampi from juveniles and adults able to form long-term memories (Travaglia *et al.*, 2016). The findings suggested that learning during infancy actively promotes the expression of GluN2A subunits and mature NMDA receptor function, thereby improving the ability to form long-term memories. Further

mechanistic insight in Travaglia *et al.*, (2016) revealed an involvement of BDNF and mGluR5 signaling in the GluN2B to GluN2A switch.

Similarly, GluN3A controls the synaptic trafficking of NMDARs and delays the developmental GluN2B to GluN2A switch during critical postnatal windows (González-González *et al.*, 2023). Supporting this concept, GluN3A deletion increases the expression of GluN2A-containing NMDARs and enhances AMPAR expression (Henson *et al.*, 2012). It was then reasonable that GluN3A deletion could induce an earlier maturation in the hippocampal circuits responsible of memory, hence, accelerating memory ontogeny. Our thorough analyses of the performance of postnatal GluN3A-lacking mice on the ontogeny of contextual fear conditioning confirmed this hypothesis.

Our first observation was that postnatal (P13 & P15) *Grin3a*^{-/-} mice present no alterations in the emergence of aversive memories at 24h (Fig. 34), matching the results described by Akers *et al.*, (2012) that located the ontogeny of contextual fear conditioning at P14. However, when we switched the training paradigm to a subtler one, in which just one shock was delivered instead of the classical three shocks necessary for training conditioning in postnatal mice, we unveiled an earlier emergence of aversive memories (Fig. 35), coherent with the earlier brain maturation previously described in GluN3A-lacking mice (Perez-Otaño *et al.*, 2016).

We then proceeded to test the effects of GluN3A on the ontogeny of remote memories, given that adult mice with ablated GluN3A expression outperform their WT littermates in this test. By testing GluN3A-ablated mice at different postnatal stages, we demonstrated that, contrary to WTs, *Grin3a*^{-/-} mice were capable of retaining remote memories starting at P17, and that this acceleration promoted memory in a stable manner over time (Fig. 36). Our experiments testing remote memory in postnatal mice support the hypothesis that GluN3A acts as a brake of brain maturation that affects the ontogeny of memories.

Following the path marked by our results obtained in adult mice, we developed and characterized postnatal mice with ablated GluN3A expression limited to excitatory neurons, which allowed us to find that, coherently with previous results, GluN3A exerts its role by its function in CamKII-expressing neurons.

Finally, two experiments provided a causal link between enhanced mTORC1-dependent protein synthesis and the enhanced memory capacity and earlier fear ontogeny in postnatal mice. First, SUnSET analyses showed increased levels of protein translation in young GluN3A knockout mice relative to WT. Second, pharmacological block with rapamycin was sufficient to prevent the earlier emergence of fear ontogeny. Here we faced the same problem we had during our analyses of adult brain behavior: high doses of rapamycin could affect mTORC2 signaling (Sarbasov *et al.*, 2005; Sarbasov *et al.*, 2006; Stoica *et al.*, 2011). Since no other study had ever characterized the effects of rapamycin in such an early age, we titrated the dose of rapamycin that blocked mTORC1 signaling without affecting mTORC2 (Fig. 40).

Using that well-titrated rapamycin dose, we demonstrated that mTORC1 signaling also underlies the enhanced cognitive performance of postnatal mice with ablated GluN3A expression. This result, together with those that later confirmed no alteration in the level of neurogenesis in *Grin3a*^{-/-} mice, allowed us to conclude that GluN3A deletion enhances cognitive performance in postnatal mice by promoting an earlier maturation of brain circuits that favors an enhanced protein synthesis via mTORC1 signaling.

GluN3A deletion permanently enhances memory

Memory loss is arguably one of the main negative features of aging in humans, and thus one of the most studied phenomena in Neuroscience. Both the reasons for memory decline and the mechanisms for maintaining a competent memory through our lifespan have been and continue to be the subject of intense study.

Discussion

There is growing recognition that synaptic defects and dysfunction of NMDARs are associated with various neuropsychiatric disorders. Both NMDAR hyperactivity and NMDAR hypofunction can be harmful (Paoletti *et al.*, 2013). Following brain insults, such as stroke and traumatic brain injury, the elevation of glutamate levels directly contributes to neuronal death by activating NMDARs. Therefore, for decades, antagonists of NMDARs have been researched as a potential solution. Additionally, chronically increased glutamate levels can lead to a loss of synapses and neurons in degenerative conditions that implicate memory loss, like Alzheimer's disease (Paoletti *et al.*, 2013).

According to Zhong *et al.*, (2021) the absence of GluN3A could be a contributing factor in the development of sporadic Alzheimer's disease by enhancing NMDAR function that eventually becomes toxic. This proposal was based on findings that the deficiency induced signs of degenerative excitotoxicity and cognitive decline in adult/aging mice lacking GluN3A. This conclusion seemed at odds with previous results by that same research group and ours (Results chapters 1 & 6 of this Thesis) in which GluN3A-lacking mice performed significantly better in a variety of spatial and associative learning tasks (Mohamad *et al.*, 2013; Conde-Dusman *et al.*, 2021).

The global annual economic cost of dementia supposes an amount of one billion US dollars and it will increase up to 2 billion in 2030 (Prince *et al.*, 2015). In addition, it is estimated that a 1-year delay on AD onset would reduce the number of cases in 12 million by 2050 (Brookmeyer *et al.*, 2007). Because of the critical importance for identifying targets and developing therapies for AD, as a last step in our characterization of the effects of GluN3A on cognition we analyzed the performance of aged WT mice and littermates lacking GluN3A, from the last age used in Zhong *et al.*, (2021) and onto later stages (Verhaeghe *et al.*, 2023; Annex 2). We found that memory declines between young and old mice but GluN3A lacking mice maintain their enhanced performance relative to WT mice in standard cognitive tests (Figs. 43-46). The findings demonstrate that GluN3A places limits on certain aspects of cognitive performance from infant age to late adulthood and that its deletion might be of therapeutic benefit for age-associated memory decline.

Although the exact reason for the discrepancy between our results and those of Yu's group remains unclear, one possible factor is the genetic background of the experimental subjects used. In our study, we utilized a congenic *Grin3a* knockout strain that was generated through over 12 generations of backcrossing F1 hybrids into a C57Bl6/J background. This approach was taken to minimize any potential ambiguities. In addition, all experiments were conducted using knockout and WT littermates from heterozygote crosses. In contrast, our understanding is that Zhong *et al.* maintained the knockout and control strains as separate homozygous colonies. Such approach could have introduced genetic drift or flanking gene effects that were not related to GluN3A function, and may have ultimately contributed to the observed disease phenotype.

Conclusions/ Conclusiones

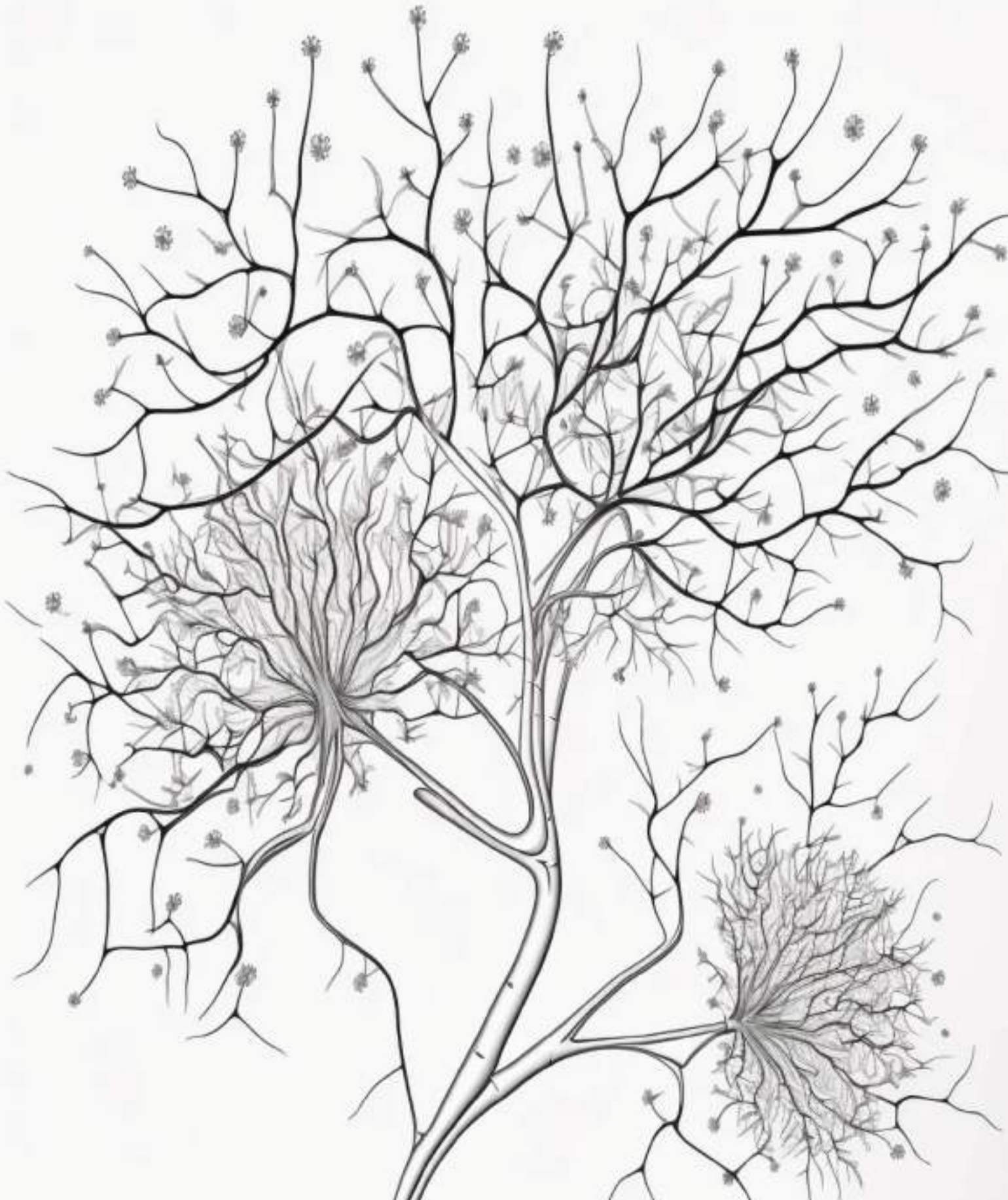


Conclusions/Conclusiones

1. Removing GluN3A-NMDARs in postnatal mice accelerates the ontogeny of fear memories limiting the effects of infantile amnesia.
2. Genetic ablation of GluN3A-NMDARs enhances adult mice performance in associative memory and memory flexibility tasks. The memory-enhancing effects associated with GluN3A deletion depend on its expression on excitatory neurons.
3. GluN3A deletion at adult stages is sufficient for the cognitive enhancement, demonstrating that inhibitory effects on memory extend beyond the critical period and their peak of expression and continue to be relevant through the lifespan.
4. Mechanistically, the memory enhancement in postnatal and adult stages caused by GluN3A removal is due to removal of brakes in mTORC1-dependent protein synthesis.
5. GluN3A deletion does not impair other cognitive domains tested here, providing an advantage over other manipulations of translation currently investigated for memory enhancement or treatment of emotional disorders such as anxiety or depression.
6. Thus, targeting GluN3A-NMDARs presents a potential avenue for developing memory-enhancing treatments.

1. La eliminación de los GluN3A-NMDARs en ratones postnatales acelera la ontogenia de la memoria, limitando los efectos de la amnesia infantil.
2. La ablación de los GluN3A-NMDAR mejora el rendimiento de ratones adultos en tareas de memoria asociativa y flexibilidad de la memoria. La mejoría asociada a la eliminación de GluN3A depende de su expresión en neuronas excitatorias.
3. La eliminación de GluN3A en etapas adultas es suficiente para mejorar las funciones cognitivas, demostrando que sus efectos inhibitorios en la memoria se extienden más allá del período crítico y su pico de expresión, y siguen siendo relevantes a lo largo de la vida.
4. Mecánicamente, la mejora de la memoria en etapas postnatales y adultas causada por la eliminación de GluN3A-NMDARs se debe a la eliminación del freno que estos receptores ejercen en la síntesis de proteínas dependientes de mTORC1.
5. La eliminación de GluN3A no afecta a otros dominios cognitivos, lo que proporciona una ventaja sobre otras manipulaciones de la traducción actualmente investigadas para mejorar la memoria o tratar trastornos emocionales como la ansiedad o la depresión.
6. Por lo tanto, los GluN3A-NMDARs presentan una vía factible para el desarrollo de tratamientos que mejoren la memoria.

References



- Akers, K. G., Arruda-Carvalho, M., Josselyn, S. A., & Frankland, P. W. (2012). Ontogeny of contextual fear memory formation, specificity, and persistence in mice. *Learning & Memory*, *19*(12), 598–604.
- Akers, K. G., Martinez-Canabal, A., Restivo, L., Yiu, A. P., De Cristofaro, A., Hsiang, H.-L. (Liz), Wheeler, A. L., Guskjolen, A., Niibori, Y., Shoji, H., Ohira, K., Richards, B. A., Miyakawa, T., Josselyn, S. A., & Frankland, P. W. (2014). Hippocampal Neurogenesis Regulates Forgetting During Adulthood and Infancy. *Science*, *344*(6184), 598–602.
- Arrondo, P., Elía-Zudaire, Ó., Martí-Andrés, G., Fernández-Seara, M. A., & Riverol, M. (2022). Grey matter changes on brain MRI in subjective cognitive decline: a systematic review. *Alzheimer's Research & Therapy*, *14*(1), 98.
- Arruda-Carvalho, M., & Clem, R. L. (2014). Pathway-Selective Adjustment of Prefrontal-Amygdala Transmission during Fear Encoding. *The Journal of Neuroscience*, *34*(47), 15601–15609.
- Atkinson, R. C., & Shiffrin, R. M. (1968). *Human Memory: A Proposed System and its Control Processes* (K. W. Spence & J. T. Spence (eds.); Vol. 2, pp. 89–195). Academic Press.
- Baddeley, A. (2000). The episodic buffer: a new component of working memory? *Trends in Cognitive Sciences*, *4*(11), 417–423.
- Baddeley, A. D., & Hitch, G. (1974). *Working Memory* (G. H. Bower (ed.); Vol. 8, pp. 47–89). Academic Press.
- Banko, J. L., Merhav, M., Stern, E., Sonenberg, N., Rosenblum, K., & Klann, E. (2007). Behavioral alterations in mice lacking the translation repressor 4E-BP2. *Neurobiology of Learning and Memory*, *87*(2), 248–256.
- Barondes, S. H. (1970). Cerebral Protein Synthesis Inhibitors Block Long-Term Memory. In *International review of neurobiology* (Vol. 12, pp. 177–205).
- Berndt, A., Lee, S. Y., Wietek, J., Ramakrishnan, C., Steinberg, E. E., Rashid, A. J., Kim, H., Park, S., Santoro, A., Frankland, P. W., Iyer, S. M., Pak, S., Ährlund-Richter, S., Delp, S. L., Malenka, R. C., Josselyn, S. A., Carlén, M., Hegemann, P., & Deisseroth, K. (2016). Structural foundations of optogenetics: Determinants of channelrhodopsin ion selectivity. *Proceedings of the National Academy of Sciences*, *113*(4), 822–829.
- Bliss, T. V. P., & Dolphin, A. C. (1982). What is the mechanism of long-term potentiation in the hippocampus? *Trends in Neurosciences*, *5*(C), 289–290.

References

- Bliss, T. V. P., & Gardner-Medwin, A. R. (1973). Long-lasting potentiation of synaptic transmission in the dentate area of the unanaesthetized rabbit following stimulation of the perforant path. *The Journal of Physiology*, 232(2), 357–374.
- Bliss, T. V. P., & Lømo, T. (1973). Long-lasting potentiation of synaptic transmission in the dentate area of the anaesthetized rabbit following stimulation of the perforant path. *The Journal of Physiology*, 232(2), 331–356.
- Blundell, J., Kouser, M., & Powell, C. M. (2008). Systemic inhibition of mammalian target of rapamycin inhibits fear memory reconsolidation. *Neurobiology of Learning and Memory*, 90(1), 28–35.
- Brookmeyer, R., Johnson, E., Ziegler-Graham, K., & Arrighi, H. M. (2007). Forecasting the global burden of Alzheimer's disease. *Alzheimer's & Dementia*, 3(3), 186–191.
- Burgos-Robles, A., Vidal-Gonzalez, I., & Quirk, G. J. (2009). Sustained Conditioned Responses in Prelimbic Prefrontal Neurons Are Correlated with Fear Expression and Extinction Failure. *Journal of Neuroscience*, 29(26), 8474–8482.
- Cammalleri, M., Lütjens, R., Berton, F., King, A. R., Simpson, C., Francesconi, W., & Sanna, P. P. (2003). Time-restricted role for dendritic activation of the mTOR-p70 S6K pathway in the induction of late-phase long-term potentiation in the CA1. *Proceedings of the National Academy of Sciences of the United States of America*, 100(SUPPL. 2), 14368–14373.
- Campbell, B. A., & Campbell, E. H. (1962). Retention and extinction of learned fear in infant and adult rats. *Journal of Comparative and Physiological Psychology*, 55(1), 1–8.
- Carson, R. P., Fu, C., Winzenburger, P., & Ess, K. C. (2013). Deletion of Rictor in neural progenitor cells reveals contributions of mTORC2 signaling to tuberous sclerosis complex. *Human Molecular Genetics*, 22(1), 140–152.
- Castellucci, V., & Kandel, E. R. (1976). Presynaptic Facilitation as a Mechanism for Behavioral Sensitization in *Aplysia*. *Science*, 194(4270), 1176–1178.
- Chini, M., & Hanganu-Opatz, I. L. (2021). Prefrontal cortex development in health and disease: lessons from rodents and humans. *Trends in Neurosciences*, 44(3), 227–240.
- Conde-Dusman, M. J., Dey, P. N., Elía-Zudaire, Ó., Rabaneda, L. G., García-Lira, C., Grand, T., Briz, V., Velasco, E. R., Andero, R., Niñerola, S., Barco, A., Paoletti, P., Wesseling, J. F., Gardoni, F., Tavalin, S. J., & Perez-Otaño, I. (2021). Control of

protein synthesis and memory by GluN3A-NMDA receptors through inhibition of GIT1/mTORC1 assembly. *ELife*, *10*, e71575.

Conde-Moro, A. R., Rocha-Almeida, F., Sánchez-Campusano, R., Delgado-García, J. M., & Gruart, A. (2019). The activity of the prelimbic cortex in rats is enhanced during the cooperative acquisition of an instrumental learning task. *Progress in Neurobiology*, *183*, 101692.

Costa-Mattioli, M., Gobert, D., Stern, E., Gamache, K., Colina, R., Cuello, C., Sossin, W., Kaufman, R., Pelletier, J., Rosenblum, K., Krnjević, K., Lacaille, J.-C., Nader, K., & Sonenberg, N. (2007). eIF2 α Phosphorylation Bidirectionally Regulates the Switch from Short- to Long-Term Synaptic Plasticity and Memory. *Cell*, *129*(1), 195–206.

Cowansage, K. K., Shuman, T., Dillingham, B. C., Chang, A., Golshani, P., & Mayford, M. (2014). Direct Reactivation of a Coherent Neocortical Memory of Context. *Neuron*, *84*(2), 432–441.

Craik, F. I. M., & Watkins, M. J. (1973). The role of rehearsal in short-term memory. *Journal of Verbal Learning and Verbal Behavior*, *12*(6), 599–607.

Crawley, J. N. (2007). *What's wrong with my mouse?: behavioral phenotyping of transgenic and knockout mice*. John Wiley & Sons.

Crawley, O., Conde-Dusman, M. J., & Pérez-Otaño, I. (2022). GluN3A NMDA receptor subunits: more enigmatic than ever? *The Journal of Physiology*, *600*(2), 261–276.

Das, S., Sasaki, Y. F., Rothe, T., Premkumar, L. S., Takasu, M., Crandall, J. E., Dikkes, P., Conner, D. A., Rayudu, P. V., Cheung, W., Chen, H.-S. V., Lipton, S. A., & Nakanishi, N. (1998). Increased NMDA current and spine density in mice lacking the NMDA receptor subunit NR3A. *Nature*, *393*(6683), 377–381.

Denny, C. A., Kheirbek, M. A., Alba, E. L., Tanaka, K. F., Brachman, R. A., Laughman, K. B., Tomm, N. K., Turi, G. F., Losonczy, A., & Hen, R. (2014). Hippocampal Memory Traces Are Differentially Modulated by Experience, Time, and Adult Neurogenesis. *Neuron*, *83*(1), 189–201.

Donato, F., Jacobsen, R. I., Moser, M.-B., & Moser, E. I. (2017). Stellate cells drive maturation of the entorhinal-hippocampal circuit. *Science*, *355*(6330), eaai8178.

Dong, Z., Han, H., Li, H., Bai, Y., Wang, W., Tu, M., Peng, Y., Zhou, L., He, W., Wu, X., Tan, T., Liu, M., Wu, X., Zhou, W., Jin, W., Zhang, S., Sacktor, T. C., Li, T., Song, W., & Wang, Y. T. (2015). Long-term potentiation decay and memory loss are mediated by AMPAR endocytosis. *Journal of Clinical Investigation*, *125*(1), 234–247.

References

- Dudai, Y., & Eisenberg, M. (2004). Rites of Passage of the Engram. *Neuron*, *44*(1), 93–100.
- Ebbinghaus, H. (1913). Memory: A contribution to experimental psychology. In *Memory: A contribution to experimental psychology*. Teachers College Press.
- Ehninger, D., Han, S., Shilyansky, C., Zhou, Y., Li, W., Kwiatkowski, D. J., Ramesh, V., & Silva, A. J. (2008). Reversal of learning deficits in a Tsc2+/- mouse model of tuberous sclerosis. *Nature Medicine*, *14*(8), 843–848.
- Epp, J. R., Silva Mera, R., Köhler, S., Josselyn, S. A., & Frankland, P. W. (2016). Neurogenesis-mediated forgetting minimizes proactive interference. *Nature Communications*, *7*(1), 10838.
- Erdmann, G., Schütz, G., & Berger, S. (2007). Inducible gene inactivation in neurons of the adult mouse forebrain. *BMC Neuroscience*, *8*(1), 63.
- Ergorul, C., & Eichenbaum, H. (2004). The Hippocampus and Memory for “What,” “Where,” and “When.” *Learning & Memory*, *11*(4), 397–405.
- Fanselow, M. S. (1990). Factors governing one-trial contextual conditioning. *Animal Learning & Behavior*, *18*(3), 264–270.
- Ferri, C. P., Prince, M., Brayne, C., Brodaty, H., Fratiglioni, L., Ganguli, M., Hall, K., Hasegawa, K., Hendrie, H., Huang, Y., Jorm, A., Mathers, C., Menezes, P. R., Rimmer, E., & Sczufca, M. (2005). Global prevalence of dementia: a Delphi consensus study. *Lancet (London, England)*, *366*(9503), 2112–2117.
- Frankland, P. W., Bontempi, B., Talton, L. E., Kaczmarek, L., & Silva, A. J. (2004). The Involvement of the Anterior Cingulate Cortex in Remote Contextual Fear Memory. *Science*, *304*(5672), 881–883.
- Frankland, P. W., Josselyn, S. A., Anagnostaras, S. G., Kogan, J. H., Takahashi, E., & Silva, A. J. (2004). Consolidation of CS and US representations in associative fear conditioning. *Hippocampus*, *14*(5), 557–569.
- Freud, S. (1915). *Psychopathology of everyday life*. MacMillan.
- González-González, I. M., Gray, J. A., Ferreira, J., Conde-Dusman, M. J., Bouchet, D., Perez-Otaño, I., & Groc, L. (2023). GluN3A subunit tunes NMDA receptor synaptic trafficking and content during postnatal brain development. *Cell Reports*, *42*(5), 112477.
- Gruart, A., Muñoz, M. D., & Delgado-García, J. M. (2006). Involvement of the CA3-CA1 synapse in the acquisition of associative learning in behaving mice. *The Journal*

of Neuroscience: The Official Journal of the Society for Neuroscience, 26(4), 1077–1087.

Han, J. H., Kushner, S. A., Yiu, A. P., Hsiang, H. L., Buch, T., Waisman, A., Bontempi, B., Neve, R. L., Frankland, P. W., & Josselyn, S. A. (2009). Selective erasure of a fear memory. *Science (New York, N.Y.)*, 323(5920), 1492–1496.

Hardt, O., Nader, K., & Wang, Y.-T. (2014). GluA2-dependent AMPA receptor endocytosis and the decay of early and late long-term potentiation: possible mechanisms for forgetting of short- and long-term memories. *Philosophical Transactions of the Royal Society B: Biological Sciences*, 369(1633), 20130141.

Hasan, M. T., Hernández-González, S., Dogbevia, G., Treviño, M., Bertocchi, I., Gruart, A., & Delgado-García, J. M. (2013). Role of motor cortex NMDA receptors in learning-dependent synaptic plasticity of behaving mice. *Nature Communications*, 4(1), 2258.

Hayashi-Takagi, A., Yagishita, S., Nakamura, M., Shirai, F., Wu, Y. I., Loshbaugh, A. L., Kuhlman, B., Hahn, K. M., & Kasai, H. (2015). Labelling and optical erasure of synaptic memory traces in the motor cortex. *Nature*, 525(7569), 333–338.

Heaton, P., & Wallace, G. L. (2004). Annotation: The savant syndrome. *Journal of Child Psychology and Psychiatry and Allied Disciplines*, 45(5), 899–911.

Hebb, D. O. (2005). *The organization of behavior: A neuropsychological theory*. Psychology Press.

Henson, M. A., Larsen, R. S., Lawson, S. N., Pérez-Otaño, I., Nakanishi, N., Lipton, S. A., & Philpot, B. D. (2012). Genetic deletion of NR3A accelerates glutamatergic synapse maturation. *PloS One*, 7(8), e42327.

Henson, M. A., Roberts, A. C., Pérez-Otaño, I., & Philpot, B. D. (2010). Influence of the NR3A subunit on NMDA receptor functions. *Progress in Neurobiology*, 91(1), 23–37.

Hoeffler, C. A., Tang, W., Wong, H., Santillan, A., Patterson, R. J., Martinez, L. A., Tejada-Simon, M. V., Paylor, R., Hamilton, S. L., & Klann, E. (2008). Removal of FKBP12 Enhances mTOR-Raptor Interactions, LTP, Memory, and Perseverative/Repetitive Behavior. *Neuron*, 60(5), 832–845.

Holtmaat, A., & Caroni, P. (2016). Functional and structural underpinnings of neuronal assembly formation in learning. *Nature Neuroscience*, 19(12), 1553–1562.

References

- Hsiang, H. L. L., Epp, J. R., van den Oever, M. C., Yan, C., Rashid, A. J., Insel, N., Ye, L., Niibori, Y., Deisseroth, K., Frankland, P. W., & Josselyn, S. A. (2014). Manipulating a “cocaine engram” in mice. *The Journal of Neuroscience: The Official Journal of the Society for Neuroscience*, *34*(42), 14115–14127.
- Huang, W., Zhu, P. J., Zhang, S., Zhou, H., Stoica, L., Galiano, M., Krnjević, K., Roman, G., & Costa-Mattioli, M. (2013). mTORC2 controls actin polymerization required for consolidation of long-term memory. *Nature Neuroscience*, *16*(4), 441–448.
- Huang, Y., Kang, B. N., Tian, J., Liu, Y., Luo, H. R., Hester, L., & Snyder, S. H. (2007). The cationic amino acid transporters CAT1 and CAT3 mediate NMDA receptor activation-dependent changes in elaboration of neuronal processes via the mammalian target of rapamycin mTOR pathway. *The Journal of Neuroscience: The Official Journal of the Society for Neuroscience*, *27*(3), 449–458.
- Hullinger, R., O’Riordan, K., & Burger, C. (2015). Environmental enrichment improves learning and memory and long-term potentiation in young adult rats through a mechanism requiring mGluR5 signaling and sustained activation of p70s6k. *Neurobiology of Learning and Memory*, *125*, 126–134.
- Huynh, T. N., Santini, E., & Klann, E. (2014). Requirement of Mammalian Target of Rapamycin Complex 1 Downstream Effectors in Cued Fear Memory Reconsolidation and Its Persistence. *The Journal of Neuroscience*, *34*, 9034–9039.
- Inda, M. C., Muravieva, E. V., & Alberini, C. M. (2011). Memory retrieval and the passage of time: from reconsolidation and strengthening to extinction. *The Journal of Neuroscience: The Official Journal of the Society for Neuroscience*, *31*(5), 1635–1643.
- Ishikawa, R., Fukushima, H., Frankland, P. W., & Kida, S. (2016). Hippocampal neurogenesis enhancers promote forgetting of remote fear memory after hippocampal reactivation by retrieval. *ELife*, *5*(September).
- Jia, M., Travaglia, A., Pollonini, G., Fedele, G., & Alberini, C. M. (2018). Developmental changes in plasticity, synaptic, glia, and connectivity protein levels in rat medial prefrontal cortex. *Learning & Memory*, *25*(10), 533–543.
- Johnson, C. M., Loucks, F. A., Peckler, H., Thomas, A. W., Janak, P. H., & Wilbrecht, L. (2016). Long-range orbitofrontal and amygdala axons show divergent patterns of maturation in the frontal cortex across adolescence. *Developmental Cognitive Neuroscience*, *18*, 113–120.
- Jones, F. N., & Skinner, B. F. (1939). The Behavior of Organisms: An Experimental Analysis. *The American Journal of Psychology*, *52*(4), 659.

- Josselyn, S. A., Köhler, S., & Frankland, P. W. (2015). Finding the engram. *Nature Reviews Neuroscience*, *16*(9), 521–534.
- Jurado-Parras, M. T., Gruart, A., & Delgado-García, J. M. (2012). Observational learning in mice can be prevented by medial prefrontal cortex stimulation and enhanced by nucleus accumbens stimulation. *Learning & Memory (Cold Spring Harbor, N.Y.)*, *19*(3), 99–106.
- Kehoe, L. A., Bellone, C., De Roo, M., Zanduetta, A., Dey, P. N., Pérez-Otaño, I., & Muller, D. (2014). GluN3A promotes dendritic spine pruning and destabilization during postnatal development. *The Journal of Neuroscience: The Official Journal of the Society for Neuroscience*, *34*(28), 9213–9221.
- Keysers, C., & Gazzola, V. (2014). Hebbian learning and predictive mirror neurons for actions, sensations and emotions. *Philosophical Transactions of the Royal Society B: Biological Sciences*, *369*(1644), 20130175.
- Kitamura, T., Saitoh, Y., Takashima, N., Murayama, A., Niibori, Y., Ageta, H., Sekiguchi, M., Sugiyama, H., & Inokuchi, K. (2009). Adult neurogenesis modulates the hippocampus-dependent period of associative fear memory. *Cell*, *139*(4), 814–827.
- Klune, C. B., Jin, B., & DeNardo, L. A. (2021). Linking mPFC circuit maturation to the developmental regulation of emotional memory and cognitive flexibility. *Elife*, *10*.
- Kolk, S. M., & Rakic, P. (2022). Development of prefrontal cortex. *Neuropsychopharmacology*, *47*(1), 41–57.
- Lalonde, R. (2002). The neurobiological basis of spontaneous alternation. *Neuroscience & Biobehavioral Reviews*, *26*(1), 91–104.
- LeDoux, J. E. (2000). Emotion Circuits in the Brain. *Annual Review of Neuroscience*, *23*(1), 155–184.
- Lee, J. H., Zhang, J. Y., Wei, Z. Z., & Yu, S. P. (2018). Impaired social behaviors and minimized oxytocin signaling of the adult mice deficient in the N-methyl-D-aspartate receptor GluN3A subunit. *Experimental Neurology*, *305*(October 2017), 1–12.
- Li, N., Lee, B., Liu, R.-J., Banasr, M., Dwyer, J. M., Iwata, M., Li, X.-Y., Aghajanian, G., & Duman, R. S. (2010). mTOR-Dependent Synapse Formation Underlies the Rapid Antidepressant Effects of NMDA Antagonists. *Science*, *329*(5994), 959–964.
- Liu, G. Y., & Sabatini, D. M. (2020). mTOR at the nexus of nutrition, growth, ageing and disease. *Nature Reviews Molecular Cell Biology*, *21*(4), 183–203.

References

- Liu, S. X., Gades, M. S., Swain, Y., Ramakrishnan, A., Harris, A. C., Tran, P. V., & Gewirtz, J. C. (2021). Repeated morphine exposure activates synaptogenesis and other neuroplasticity-related gene networks in the dorsomedial prefrontal cortex of male and female rats. *Drug and Alcohol Dependence*, *221*, 108598.
- Luriya, A. R. (1987). *The Mind of a Mnemonist: A Little Book about a Vast Memory, With a New Foreword by Jerome S. Bruner*. Harvard University Press.
- Marco, S., Giralt, A., Petrovic, M. M., Pouladi, M. A., Martínez-Turrillas, R., Martínez-Hernández, J., Kaltenbach, L. S., Torres-Peraza, J., Graham, R. K., Watanabe, M., Luján, R., Nakanishi, N., Lipton, S. A., Lo, D. C., Hayden, M. R., Alberch, J., Wesseling, J. F., & Pérez-Otaño, I. (2013). Suppressing aberrant GluN3A expression rescues synaptic and behavioral impairments in Huntington's disease models. *Nature Medicine*, *19*(8), 1030–1038.
- Marco, S., Murillo, A., & Pérez-Otaño, I. (2018). RNAi-Based GluN3A Silencing Prevents and Reverses Disease Phenotypes Induced by Mutant huntingtin. *Molecular Therapy*, *26*(8), 1965–1972.
- McAvoy, K. M., Scobie, K. N., Berger, S., Russo, C., Guo, N., Decharatanachart, P., Vega-Ramirez, H., Miake-Lye, S., Whalen, M., Nelson, M., Bergami, M., Bartsch, D., Hen, R., Berninger, B., & Sahay, A. (2016). Modulating Neuronal Competition Dynamics in the Dentate Gyrus to Rejuvenate Aging Memory Circuits. *Neuron*, *91*(6), 1356–1373.
- McDonald, A. J. (1998). Cortical pathways to the mammalian amygdala. *Progress in Neurobiology*, *55*(3), 257–332.
- McGarry, L. M., & Carter, A. G. (2017). Prefrontal Cortex Drives Distinct Projection Neurons in the Basolateral Amygdala. *Cell Reports*, *21*(6), 1426–1433.
- McHugh, T. J., & Tonegawa, S. (2007). Spatial exploration is required for the formation of contextual fear memory. *Behavioral Neuroscience*, *121*(2), 335–339.
- McRae, K., & Jones, M. (2013). Semantic Memory. In *The Oxford handbook of cognitive psychology*. Oxford University Press.
- Migues, P. V., Liu, L., Archbold, G. E. B., Einarsson, E., Wong, J., Bonasia, K., Ko, S. H., Wang, Y. T., & Hardt, O. (2016). Blocking Synaptic Removal of GluA2-Containing AMPA Receptors Prevents the Natural Forgetting of Long-Term Memories. *The Journal of Neuroscience: The Official Journal of the Society for Neuroscience*, *36*(12), 3481–3494.

- Ming, G., & Song, H. (2005). Adult neurogenesis in the mammalian central nervous system. *Annual Review of Neuroscience*, *28*, 223–250.
- Mohamad, O., Song, M., Wei, L., & Yu, S. P. (2013). Regulatory roles of the NMDA receptor GluN3A subunit in locomotion, pain perception and cognitive functions in adult mice. *The Journal of Physiology*, *591*(Pt 1), 149.
- Morris, R. G. M. (1981). Spatial localization does not require the presence of local cues. *Learning and Motivation*, *12*(2), 239–260.
- Morris, R. G. M., Anderson, E., Lynch, G. S., & Baudry, M. (1986). Selective impairment of learning and blockade of long-term potentiation by an N-methyl-D-aspartate receptor antagonist, AP5. *Nature*, *319*(6056), 774–776.
- Mueller, H. T., & Meador-Woodruff, J. H. (2004). NR3A NMDA receptor subunit mRNA expression in schizophrenia, depression and bipolar disorder. *Schizophrenia Research*, *71*(2–3), 361–370.
- Murillo, A., Navarro, A. I., Puelles, E., Zhang, Y., Petros, T. J., & Pérez-Otaño, I. (2021). Temporal Dynamics and Neuronal Specificity of Grin3a Expression in the Mouse Forebrain. *Cerebral Cortex (New York, N.Y. : 1991)*, *31*(4), 1914–1926.
- Ohkawa, N., Saitoh, Y., Suzuki, A., Tsujimura, S., Murayama, E., Kosugi, S., Nishizono, H., Matsuo, M., Takahashi, Y., Nagase, M., Sugimura, Y. K., Watabe, A. M., Kato, F., & Inokuchi, K. (2015). Artificial association of pre-stored information to generate a qualitatively new memory. *Cell Reports*, *11*(2), 261–269.
- Otsu, Y., Darcq, E., Pietrajtis, K., Mátyás, F., Schwartz, E., Bessaih, T., Abi Gerges, S., Rousseau, C. V., Grand, T., Dieudonné, S., Paoletti, P., Acsády, L., Agulhon, C., Kieffer, B. L., & Diana, M. A. (2019). Control of aversion by glycine-gated GluN1/GluN3A NMDA receptors in the adult medial habenula. *Science*, *366*(6462), 250–254.
- Pachernegg, S., Strutz-Seeböhm, N., & Hollmann, M. (2012). GluN3 subunit-containing NMDA receptors: not just one-trick ponies. *Trends in Neurosciences*, *35*(4), 240–249.
- Paoletti, P., Bellone, C., & Zhou, Q. (2013). NMDA receptor subunit diversity: Impact on receptor properties, synaptic plasticity and disease. *Nature Reviews Neuroscience*, *14*(6), 383–400.
- Pape, H.-C., & Pare, D. (2010). Plastic synaptic networks of the amygdala for the acquisition, expression, and extinction of conditioned fear. *Physiological Reviews*, *90*(2), 419–463.

References

- Park, S., Kramer, E. E., Mercaldo, V., Rashid, A. J., Insel, N., Frankland, P. W., & Josselyn, S. A. (2016). Neuronal Allocation to a Hippocampal Engram. *Neuropsychopharmacology: Official Publication of the American College of Neuropsychopharmacology*, *41*(13), 2987–2993.
- Parsons, R. G., Gafford, G. M., & Helmstetter, F. J. (2006). Translational Control via the Mammalian Target of Rapamycin Pathway Is Critical for the Formation and Stability of Long-Term Fear Memory in Amygdala Neurons. *Journal of Neuroscience*, *26*(50), 12977–12983.
- Pastalkova, E., Serrano, P., Pinkhasova, D., Wallace, E., Fenton, A. A., & Sacktor, T. C. (2006). Storage of spatial information by the maintenance mechanism of LTP. *Science (New York, N.Y.)*, *313*(5790), 1141–1444.
- Pavlov, P. I. (2010). Conditioned reflexes: an investigation of the physiological activity of the cerebral cortex. *Annals of Neurosciences*, *17*(3), 136.
- Pereyra, M., Kathe, C., de Landeta, A. B., & Medina, J. H. (2018). mTORC1 controls long-term memory retrieval. *Scientific Reports*, *8*.
- Pérez-Otaño, I., Larsen, R. S., & Wesseling, J. F. (2016). Emerging roles of GluN3-containing NMDA receptors in the CNS. *Nature Reviews Neuroscience*, *17*(10), 623–635.
- Pérez-Otaño, I., Luján, R., Tavalin, S. J., Plomann, M., Modregger, J., Liu, X.-B., Jones, E. G., Heinemann, S. F., Lo, D. C., & Ehlers, M. D. (2006). Endocytosis and synaptic removal of NR3A-containing NMDA receptors by PACSIN1/syndapin1. *Nature Neuroscience*, *9*(5), 611–621.
- Pfeffer, C. K., Xue, M., He, M., Huang, Z. J., & Scanziani, M. (2013). Inhibition of inhibition in visual cortex: the logic of connections between molecularly distinct interneurons. *Nature Neuroscience* 2013 16:8, *16*(8), 1068–1076.
- Prince, M. J., Wimo, A., Guerchet, M. M., Ali, G. C., Wu, Y.-T., & Prina, M. (2015). *World Alzheimer Report 2015 - The Global Impact of Dementia: An analysis of prevalence, incidence, cost and trends*. Alzheimer's Disease International.
- Ramirez, S., Liu, X., Lin, P. A., Suh, J., Pignatelli, M., Redondo, R. L., Ryan, T. J., & Tonegawa, S. (2013). Creating a false memory in the hippocampus. *Science (New York, N.Y.)*, *341*(6144), 387–391.
- Rashid, A. J., Yan, C., Mercaldo, V., Hsiang, H. L., Park, S., Cole, C. J., De Cristofaro, A., Yu, J., Ramakrishnan, C., Lee, S. Y., Deisseroth, K., Frankland, P. W., & Josselyn,

- S. A. (2016). Competition between engrams influences fear memory formation and recall. *Science (New York, N.Y.)*, 353(6297), 383–387.
- Ray, S., & Brecht, M. (2016). Structural development and dorsoventral maturation of the medial entorhinal cortex. *Elife*, 5, e13343.
- Reijmers, L. G., Perkins, B. L., Matsuo, N., & Mayford, M. (2007). Localization of a stable neural correlate of associative memory. *Science (New York, N.Y.)*, 317(5842), 1230–1233.
- Roberts, W. A. (2002). Are animals stuck in time? *Psychological Bulletin*, 128(3), 473.
- Rogerson, T., Jayaprakash, B., Cai, D. J., Sano, Y., Lee, Y.-S., Zhou, Y., Bekal, P., Deisseroth, K., & Silva, A. J. (2016). Molecular and Cellular Mechanisms for Trapping and Activating Emotional Memories. *PLOS ONE*, 11(8), e0161655.
- Roozafzoon, R., Goodarzi, A., Vousooghi, N., Sedaghati, M., Yaghmaei, P., & Zarrindast, M.-R. (2010). Expression of NMDA receptor subunits in human peripheral blood lymphocytes in opioid addiction. *European Journal of Pharmacology*, 638(1–3), 29–32.
- Sabatini, D. M. (2017). Twenty-five years of mTOR: Uncovering the link from nutrients to growth. *Proceedings of the National Academy of Sciences*, 114(45), 11818–11825.
- Sacktor, T. C. (2011). How does PKM ζ maintain long-term memory? *Nature Reviews. Neuroscience*, 12(1), 9–15.
- Sánchez-Hidalgo, A. C., Arias-Aragón, F., Romero-Barragán, M. T., Martín-Cuevas, C., Delgado-García, J. M., Martínez-Mir, A., & Scholl, F. G. (2022). Selective expression of the neurexin substrate for presenilin in the adult forebrain causes deficits in associative memory and presynaptic plasticity. *Experimental Neurology*, 347, 113896.
- Sarbassov, D. D., Ali, S. M., Sengupta, S., Sheen, J.-H., Hsu, P. P., Bagley, A. F., Markhard, A. L., & Sabatini, D. M. (2006). Prolonged Rapamycin Treatment Inhibits mTORC2 Assembly and Akt/PKB. *Molecular Cell*, 22(2), 159–168.
- Sarbassov, D. D., Guertin, D. A., Ali, S. M., & Sabatini, D. M. (2005). Phosphorylation and Regulation of Akt/PKB by the Rictor-mTOR Complex. *Science*, 307(5712), 1098–1101.
- Sharma, V., Sood, R., Khlaifia, A., Eslamizade, M. J., Hung, T.-Y., Lou, D., Asgarihafshejani, A., Lalzar, M., Kiniry, S. J., Stokes, M. P., Cohen, N., Nelson, A. J.,

References

- Abell, K., Possemato, A. P., Gal-Ben-Ari, S., Truong, V. T., Wang, P., Yiannakas, A., Saffarzadeh, F., Sonenberg, N. (2020). eIF2 α controls memory consolidation via excitatory and somatostatin neurons. *Nature*, 586(7829), 412–416.
- Shatz, C. J. (1992). The Developing Brain. *Scientific American*, 267(3), 60–67.
- Shrestha, P., Ayata, P., Herrero-Vidal, P., Longo, F., Gastone, A., LeDoux, J. E., Heintz, N., & Klann, E. (2020a). Cell-type-specific drug-inducible protein synthesis inhibition demonstrates that memory consolidation requires rapid neuronal translation. *Nature Neuroscience*, 23(2), 281–292.
- Shrestha, P., Shan, Z., Mamcarz, M., Ruiz, K. S. A., Zerihoun, A. T., Juan, C.-Y., Herrero-Vidal, P. M., Pelletier, J., Heintz, N., & Klann, E. (2020b). Amygdala inhibitory neurons as loci for translation in emotional memories. *Nature*, 586(7829), 407–411.
- Spear, N. E. (1979). Memory storage factors leading to infantile amnesia. In *Psychology of learning and motivation* (Vol. 13, pp. 91–154). Elsevier.
- Squire, L. R., & Barondes, S. H. (1974). Anisomycin, like other inhibitors of cerebral protein synthesis, impairs ‘long-term’ memory of a discrimination task. *Brain Research*, 66, 301–308.
- Stern, E., Chinnakkaruppan, A., David, O., Sonenberg, N., & Rosenblum, K. (2013). Blocking the eIF2 α kinase (PKR) enhances positive and negative forms of cortex-dependent taste memory. *The Journal of Neuroscience: The Official Journal of the Society for Neuroscience*, 33(6), 2517–2525.
- Stoica, L., Zhu, P. J., Huang, W., Zhou, H., Kozma, S. C., & Costa-Mattioli, M. (2011). Selective pharmacogenetic inhibition of mammalian target of Rapamycin complex I (mTORC1) blocks long-term synaptic plasticity and memory storage. *Proceedings of the National Academy of Sciences*, 108(9), 3791–3796.
- Taha, E., Patil, S., Barrera, I., Panov, J., Khamaisy, M., Proud, C. G., Bramham, C. R., & Rosenblum, K. (2020). eEF2/eEF2K Pathway in the Mature Dentate Gyrus Determines Neurogenesis Level and Cognition. *Current Biology*, 30(18), 3507–3521.e7.
- Takei, N. (2004). Brain-Derived Neurotrophic Factor Induces Mammalian Target of Rapamycin-Dependent Local Activation of Translation Machinery and Protein Synthesis in Neuronal Dendrites. *Journal of Neuroscience*, 24(44), 9760–9769.
- Takei, N., Kawamura, M., Hara, K., Yonezawa, K., & Nawa, H. (2001). Brain-derived neurotrophic factor enhances neuronal translation by activating multiple initiation

processes: comparison with the effects of insulin. *The Journal of Biological Chemistry*, 276(46), 42818–42825.

Tanaka, K. Z., Pevzner, A., Hamidi, A. B., Nakazawa, Y., Graham, J., & Wiltgen, B. J. (2014). Cortical representations are reinstated by the hippocampus during memory retrieval. *Neuron*, 84(2), 347–354.

Tang, S. J., Reis, G., Kang, H., Gingras, A.-C., Sonenberg, N., & Schuman, E. M. (2002). A rapamycin-sensitive signaling pathway contributes to long-term synaptic plasticity in the hippocampus. *Proceedings of the National Academy of Sciences of the United States of America*, 99(1), 467–472.

Taniguchi, H., He, M., Wu, P., Kim, S., Paik, R., Sugino, K., Kvitsiani, D., Fu, Y., Lu, J., Lin, Y., Miyoshi, G., Shima, Y., Fishell, G., Nelson, S. B., & Huang, Z. J. (2011). A resource of Cre driver lines for genetic targeting of GABAergic neurons in cerebral cortex. *Neuron*, 71(6), 995–1013.

Thorndike, E. L. (1898). Animal intelligence: An experimental study of the associative processes in animals. *The Psychological Review: Monograph Supplements*, 2(4), i–109.

Thorndike, E. L. (2006). The fundamentals of learning. *The Fundamentals of Learning*.

Tonegawa, S., Liu, X., Ramirez, S., & Redondo, R. (2015). Memory Engram Cells Have Come of Age. *Neuron*, 87(5), 918–931.

Travaglia, A., Bisaz, R., Sweet, E. S., Blitzer, R. D., & Alberini, C. M. (2016). Infantile amnesia reflects a developmental critical period for hippocampal learning. *Nature Neuroscience*, 19(9), 1225–1233.

Trinh, M. A., Kaphzan, H., Wek, R. C., Pierre, P., Cavener, D. R., & Klann, E. (2012). Brain-specific disruption of the eIF2 α kinase PERK decreases ATF4 expression and impairs behavioral flexibility. *Cell Reports*, 1(6), 676–688.

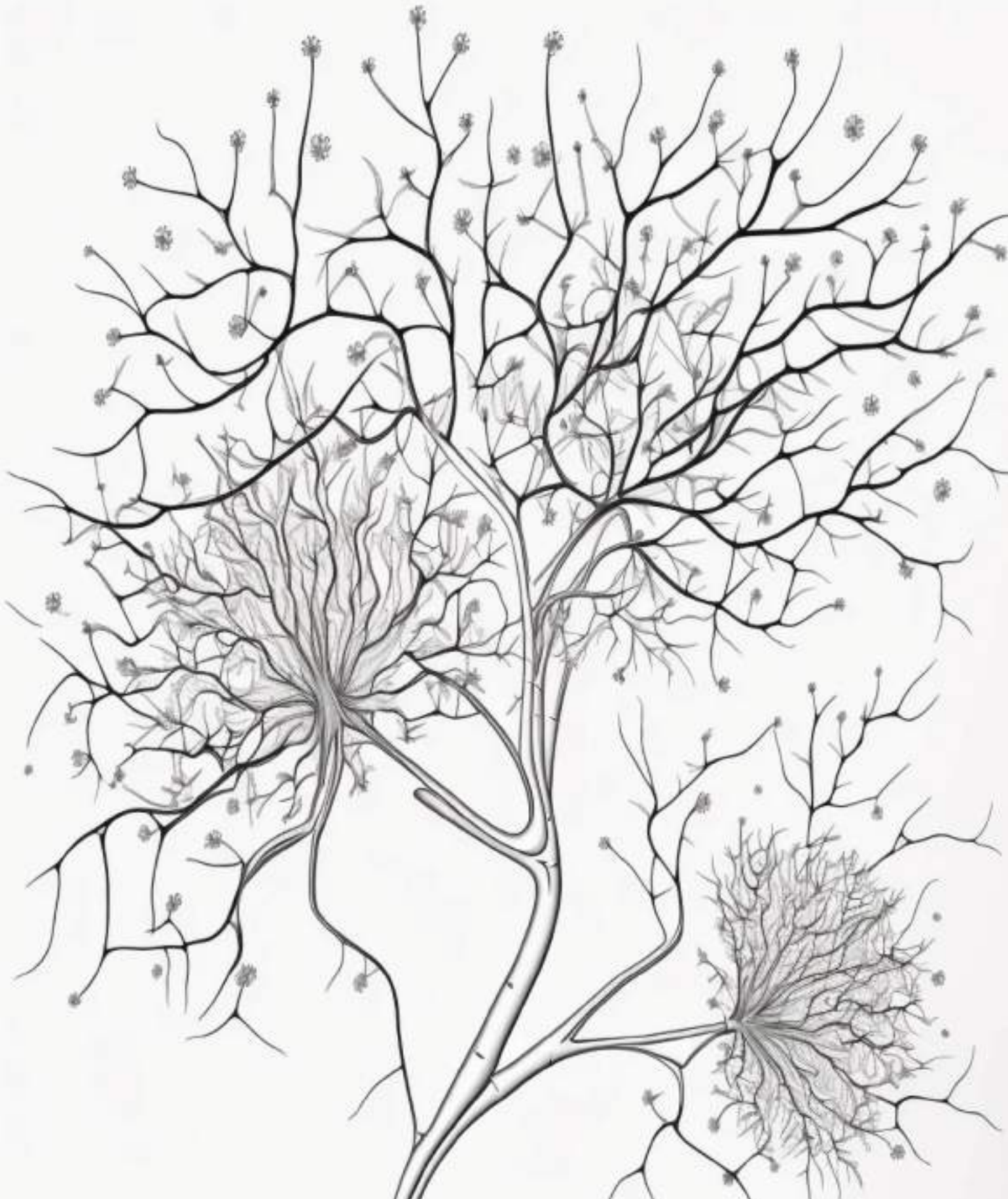
Tsokas, P., Hsieh, C., Yao, Y., Lesburguères, E., Wallace, E. J. C., Tcherepanov, A., Jothianandan, D., Hartley, B. R., Pan, L., Rivard, B., Farese, R. V., Sajan, M. P., Bergold, P. J., Hernández, A. I., Cottrell, J. E., Shouval, H. Z., Fenton, A. A., & Sacktor, T. C. (2016). Compensation for PKM ζ in long-term potentiation and spatial long-term memory in mutant mice. *ELife*, 5(MAY2016).

Tudor, J. C., Davis, E. J., Peixoto, L., Wimmer, M. E., van Tilborg, E., Park, A. J., Poplawski, S. G., Chung, C. W., Havekes, R., Huang, J., Gatti, E., Pierre, P., & Abel, T. (2016). Sleep deprivation impairs memory by attenuating mTORC1-dependent protein synthesis. *Science Signaling*, 9(425), ra41.

References

- Tulving, E. (1972). *Episodic and semantic memory*.
- Tulving, E., & Pearlstone, Z. (1966). Availability versus accessibility of information in memory for words. *Journal of Verbal Learning and Verbal Behavior*, 5(4), 381–391.
- Verhaeghe, R., Elía-Zudaire, O., Escamilla, S., Sáez-Valero, J. & Pérez-Otaño, I (2023). No evidence for cognitive decline or neurodegeneration in strain-matched GluN3A knockout mice. *Alzheimer's & Dementia* (accepted for publication).
- Vouimba, R.-M., & Maroun, M. (2011). Learning-Induced Changes in mPFC–BLA Connections After Fear Conditioning, Extinction, and Reinstatement of Fear. *Neuropsychopharmacology*, 36(11), 2276–2285.
- Wong, H.-K., Liu, X.-B., Matos, M. F., Chan, S. F., Pérez-Otaño, I., Boysen, M., Cui, J., Nakanishi, N., Trimmer, J. S., Jones, E. G., Lipton, S. A., & Sucher, N. J. (2002). Temporal and regional expression of NMDA receptor subunit NR3A in the mammalian brain. *Journal of Comparative Neurology*, 450(4), 303–317.
- Yiu, A. P., Mercaldo, V., Yan, C., Richards, B., Rashid, A. J., Hsiang, H. L. L., Pressey, J., Mahadevan, V., Tran, M. M., Kushner, S. A., Woodin, M. A., Frankland, P. W., & Josselyn, S. A. (2014). Neurons are recruited to a memory trace based on relative neuronal excitability immediately before training. *Neuron*, 83(3), 722–735.
- Yuan, T., Mamei, M., O'Connor, E. C., Dey, P. N., Verpelli, C., Sala, C., Perez-Otano, I., Lüscher, C., & Bellone, C. (2013). Expression of Cocaine-Evoked Synaptic Plasticity by GluN3A-Containing NMDA Receptors. *Neuron*, 80(4), 1025–1038.
- Zhao, C., Deng, W., & Gage, F. H. (2008). Mechanisms and functional implications of adult neurogenesis. *Cell*, 132(4), 645–660.
- Zhong, W., Wu, A., Berglund, K., Gu, X., Jiang, M. Q., Talati, J., Zhao, J., Wei, L., & Yu, S. P. (2022). Pathogenesis of sporadic Alzheimer's disease by deficiency of NMDA receptor subunit GluN3A. *Alzheimer's & Dementia*, 18(2), 222–239.
- Zhou, Y., Won, J., Karlsson, M. G., Zhou, M., Rogerson, T., Balaji, J., Neve, R., Poirazi, P., & Silva, A. J. (2009). CREB regulates excitability and the allocation of memory to subsets of neurons in the amygdala. *Nature Neuroscience*, 12(11), 1438–1443.
- Zhu, P. J., Chen, C.-J., Mays, J., Stoica, L., & Costa-Mattioli, M. (2018). mTORC2, but not mTORC1, is required for hippocampal mGluR-LTD and associated behaviors. *Nature Neuroscience*, 21(6), 799–802.

Annex



Control of protein synthesis and memory by GluN3A-NMDA receptors through inhibition of GIT1/mTORC1 assembly

María J Conde-Dusman^{1,2,3†}, Partha N Dey^{2,4†}, Óscar Elía-Zudaire^{1†}, Luis G Rabaneda^{1,2,5}, Carmen García-Lira¹, Teddy Grand⁶, Victor Briz⁷, Eric R Velasco⁸, Raül Andero^{9,10,11}, Sergio Niñerola¹, Angel Barco¹, Pierre Paoletti⁶, John F Wesseling¹, Fabrizio Gardoni¹², Steven J Tavalin¹³, Isabel Perez-Otaño^{1,2*†}

¹Instituto de Neurociencias (UMH-CSIC), Alicante, Spain; ²Centro de Investigación Médica Aplicada (CIMA), University of Navarra, Pamplona, Spain; ³Centre for Developmental Neurobiology, Institute of Psychiatry, King's College London, London, United Kingdom; ⁴National Eye Institute, National Institutes of Health, Bethesda, United States; ⁵Institute of Science and Technology Austria, Klosterneuburg, Austria; ⁶Institut de Biologie de l'Ecole Normale Supérieure/CNRS/INSERM, Paris, France; ⁷Centro de Biología Molecular Severo Ochoa (UAM-CSIC), Madrid, Spain; ⁸Institut de Neurociències, Universitat Autònoma de Barcelona, Bellaterra, Spain; ⁹Institut de Neurociències, Departament de Psicobiologia i de Metodologia de les Ciències de la Salut, Unitat de Neurociència Traslacional, Parc Taulí Hospital Universitari, Institut d'Investigació i Innovació Parc Taulí (I3PT), Universitat Autònoma de Barcelona, Bellaterra, Spain; ¹⁰Centro de Investigación Biomédica en Red de Salud Mental (CIBERSAM), Instituto de Salud Carlos III, Madrid, Spain; ¹¹ICREA, Barcelona, Spain; ¹²Department of Pharmacological and Biomolecular Sciences, University of Milan, Milan, Italy; ¹³Department of Pharmacology, Addiction Science, and Toxicology, University of Tennessee Health Science Center, Memphis, United States

*For correspondence: otano@umh.es

†These authors contributed equally to this work

Competing interest: The authors declare that no competing interests exist.

Funding: See page 24

Received: 23 June 2021

Preprinted: 05 September 2021

Accepted: 13 October 2021

Published: 17 November 2021

Reviewing Editor: Mary B Kennedy, California Institute of Technology, United States

© Copyright Conde-Dusman et al. This article is distributed under the terms of the [Creative Commons Attribution License](https://creativecommons.org/licenses/by/4.0/), which permits unrestricted use and redistribution provided that the original author and source are credited.

Abstract De novo protein synthesis is required for synapse modifications underlying stable memory encoding. Yet neurons are highly compartmentalized cells and how protein synthesis can be regulated at the synapse level is unknown. Here, we characterize neuronal signaling complexes formed by the postsynaptic scaffold GIT1, the mechanistic target of rapamycin (mTOR) kinase, and Raptor that couple synaptic stimuli to mTOR-dependent protein synthesis; and identify NMDA receptors containing GluN3A subunits as key negative regulators of GIT1 binding to mTOR. Disruption of GIT1/mTOR complexes by enhancing GluN3A expression or silencing GIT1 inhibits synaptic mTOR activation and restricts the mTOR-dependent translation of specific activity-regulated mRNAs. Conversely, GluN3A removal enables complex formation, potentiates mTOR-dependent protein synthesis, and facilitates the consolidation of associative and spatial memories in mice. The memory enhancement becomes evident with light or spaced training, can be achieved by selectively deleting GluN3A from excitatory neurons during adulthood, and does not compromise other aspects of cognition such as memory flexibility or extinction. Our findings provide mechanistic insight into synaptic translational control and reveal a potentially selective target for cognitive enhancement.

Introduction

Memories are thought to be encoded through formation and modification of the synaptic connections between neurons. Lasting memory encoding requires de novo mRNA and protein synthesis in response to neuronal activity and sensory experience. It entails the transcription of immediate-early genes (IEGs) to mRNA, and the protein products of some IEG transcripts mediate structural and functional modifications of synapses (*Yap and Greenberg, 2018*). However, transcription occurs in the cell body and generates a neuron-wide pool of mRNAs, whereas only a fraction of synapses of any individual neuron are modified by a given memory (*Holtmaat and Caroni, 2016; Josselyn and Tonegawa, 2020*). To ensure input specificity, transcription is coupled to local mechanisms that restrict the effects of activity-induced gene products to selected synapses (*Wang et al., 2010*).

One of these mechanisms is thought to be the local, synapse-specific translation of mRNA into protein (*Holt et al., 2019; Klann and Dever, 2004; Sossin and Costa-Mattioli, 2019*). The main rate-limiting step in translation is initiation, which is regulated by the phosphorylation of two separate proteins: the eukaryotic initiation factor 2 α (eIF2 α) and the mTOR ('mechanistic target of rapamycin') serine/threonine kinase. Manipulations of eIF2 α phosphorylation have been implicated in synapse plasticity and memory (*Costa-Mattioli et al., 2007; Sharma et al., 2020; Shrestha et al., 2020b*), but evidence for a role in local translation is lacking. mTOR could in principle afford more selective translational control. mTOR forms at least two distinct multiprotein complexes, mTORC1 and mTORC2. mTORC1 is defined by the presence of Raptor, an adaptor protein which recruits mTOR substrates to promote the translation of specific mRNAs, and compartmentalized activation has been shown to be essential for mTORC1 responses to nutrients in nonneuronal cells (*Liu and Sabatini, 2020*). In neurons, components of mTORC1 localize to axons, dendrites, and synapses (*Pouloupoulos et al., 2019; Takei et al., 2004; Tang et al., 2002*), and pharmacological inhibition of mTORC1 with rapamycin blocks long-lasting synaptic plasticity and memory formation (*Cammalleri et al., 2003; Hou and Klann, 2004; Stoica et al., 2011; Tang et al., 2002*). Moreover, dysregulated translation is a feature in diseases of cognition, from autism to intellectual disability, and many of the mutations associated with these diseases affect genes encoding negative regulators of mTORC1 (*Costa-Mattioli and Monteggia, 2013; Lipton and Sahin, 2014*). However, it is currently unclear how mTOR activation might be controlled at specific synapses and linked to mechanisms that gate learning and memory.

The most intensively studied mechanism gating learning and memory involves the NMDA-type glutamate receptor (NMDAR). NMDARs contain multiple subunits, including an obligatory GluN1 subunit, various GluN2 (A–D) and, for some subtypes, one of the GluN3 (A–B) subunits (*Paoletti et al., 2013*). Conventional subtypes containing GluN1 and GluN2 trigger gene expression programs that mediate the strengthening and stabilization of active synapses and the persistent storage of information (*Lyons and West, 2011*). By contrast, nonconventional subtypes containing the GluN3A subunit (GluN3A-NMDARs) inhibit many of these synaptic modifications (*Pérez-Otaño et al., 2016*). Synapses that express GluN3A are resistant to the induction of long-lasting functional and structural plasticity, and memories fade more quickly in mutant mice with enhanced GluN3A expression (*Kehoe et al., 2014; Roberts et al., 2009*). In line with this work in mice, human genetic studies correlate enhanced cognitive performance with low GluN3A levels or variations in *GRIN3A* (human gene encoding GluN3A) (*Gallinat et al., 2007; Papenberg et al., 2014; Sadat-Shirazi et al., 2019*); and GluN3A dysregulation in humans is linked to cognitive impairment in schizophrenia (*Greenwood et al., 2019; Mueller and Meador-Woodruff, 2004; Ohi et al., 2015; Takata et al., 2013*), Huntington's disease (*Marco et al., 2013; Marco et al., 2018*), addiction, and other pathologies (*Huang et al., 2017; Pérez-Otaño et al., 2016; Sarker et al., 2019; Yang et al., 2015; Yuan et al., 2013*). We reasoned that understanding the underlying mechanisms would yield insight into the brain processes that constrain long-term memory formation and might uncover targets for therapeutic intervention.

Here, we report that GluN3A-NMDARs selectively and negatively regulate synaptic mTORC1-dependent translation without affecting neuron-wide transcriptional activation. The negative regulation is mediated by inhibition of the assembly of mTOR complexes that contain the postsynaptic adaptor GIT1 (G-protein-coupled receptor kinase-interacting protein) and Raptor. GIT1/mTORC1 complexes are located at or near synaptic sites, and couple mTORC1 kinase activity to synaptic stimulation. Through biochemical, mouse genetics, and behavioral approaches, we further show that GluN3A deletion increases the availability of GIT1/mTORC1 complexes, boosts mTORC1-dependent protein synthesis, and facilitates long-term memory formation. The advantage is selectively evident

when mice are subjected to weak training behavioral paradigms; can be reversed by the mTORC1 inhibitor rapamycin; and unlike the memory enhancement seen after manipulations of general translational regulators, is not associated with deficits in memory flexibility or extinction (*Shrestha et al., 2020a*). Our findings identify a novel regulatory mechanism whereby GluN3A/GIT1 interactions set local modes of protein synthesis and gate memory formation, and reveal a potentially selective target for correcting cognitive impairment in pathological contexts.

Results

Selective inhibition of activity-dependent gene expression by GluN3A at the post-transcriptional level

GluN3A expression is pervasive during postnatal brain development, and regulated removal allows for the activity-dependent stabilization or elimination of excess synapses (*Pérez-Otaño et al., 2016*). To assess whether GluN3A-NMDARs modulate activity-dependent gene expression, we expressed GluN3A in cultured cortical neurons over the stage when endogenous downregulation normally occurs (days in vitro [DIV] 9–14, ~ postnatal days P8–P16 in vivo, *Figure 1A*; *Figure 1—figure supplement 1*; *Kehoe et al., 2014*). We used lentiviral vectors where expression is targeted to neurons by the synapsin 1 promoter and induced synaptic activity with bicuculline, which inhibits γ -aminobutyric acid (GABA) transmission and triggers bursts of action potential firing (*Hardingham et al., 2002*).

As expected, bicuculline induced a robust expression of IEGs implicated in the consolidation of synaptic modifications and memories, including *Arc*, *Fos*, and *Zif268/Egr1* (*Flavell and Greenberg, 2008*; *Figure 1B*). Enhancing GluN3A expression largely reduced the induction of *Arc* and *Fos* proteins while *Zif268* induction was unaffected, indicating that GluN3A selectively inhibits specific activity-dependent signaling pathways (*Figure 1B*). Analysis at the mRNA level demonstrated that modulation occurs downstream of gene transcription: *Arc*, *Fos*, and *Zif268* mRNA levels were strongly induced by bicuculline in both control and GluN3A-infected neurons, and no differences were observed in the time-courses or magnitude of induction (*Figure 1C*). Unchanged transcription was in-line with intact activation of the phosphorylation of extracellular signal-regulated kinase (ERK1/2) and CREB (*Figure 1—figure supplement 1B*), the two major pathways for activity-dependent transcription (*Flavell and Greenberg, 2008*). By contrast, the general NMDAR antagonist D-2-amino-5-phosphonovaleric acid (APV) inhibited all signaling pathways analyzed and the induction of IEGs at both mRNA and protein levels (*Figure 1—figure supplement 1C, D*).

An analogous dissociation between protein and transcript levels of a subset of IEGs was observed when GluN3A-infected neurons were stimulated with the neurotrophin BDNF (*Figure 1—figure supplement 1E, F*), a potent inducer of gene expression at both transcriptional and translational levels (*Rao et al., 2006*). Whole transcriptome RNAseq analyses confirmed that transcriptional responses to bicuculline or BDNF were unaffected by GluN3A expression (*Figure 1D*; *Figure 1—figure supplement 2*). Together these results indicated that GluN3A-NMDARs repress the translation of specific activity-regulated mRNAs without affecting global transcriptional programs of gene expression. Inhibited induction of IEGs by GluN3A was not rescued by pretreatment with the proteasome inhibitor MG-132 (*Figure 1E*), ruling out alternative mechanisms such as enhanced proteasome-dependent degradation (*Rao et al., 2006*).

GluN3A inhibits mTORC1-dependent translation of IEGs

We thus turned to protein synthesis pathways to search for mechanisms underlying the selective inhibition of gene expression by GluN3A. We focused on mTORC1 because it has been shown to couple synaptic signals including BDNF and NMDAR activation to translation of specific mRNAs in dendrites and synapses (*Takei et al., 2004*; *Tang et al., 2002*). mTORC1 signaling was strongly activated by bicuculline in DIV14 cortical neurons, as shown by phosphorylation of mTOR on Ser²⁴⁴⁸ (a reliable readout of mTORC1 kinase activity; see *Chiang and Abraham, 2005*) and of its downstream effectors, the p70-kDa ribosomal protein S6 kinase (S6K, Thr³⁸⁹) and the ribosomal protein S6 (Ser²⁴⁰⁻⁴, *Figure 2A and B*). The effects were blocked by APV and the NMDAR open-channel blocker MK-801, confirming NMDAR dependence in our model (*Figure 2—figure supplement 1*).

The phosphorylation of mTOR, S6K, and S6 following bicuculline treatment was significantly reduced in GluN3A-infected neurons, indicating that GluN3A interferes with synaptic mTORC1 activation

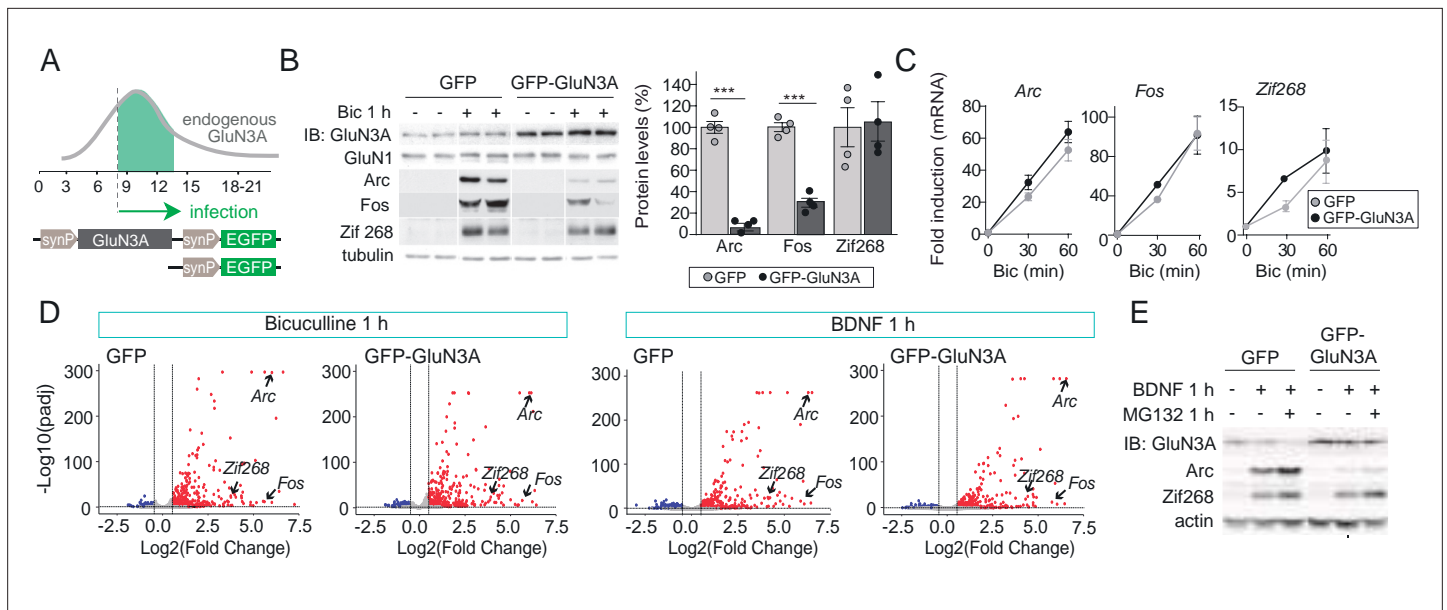


Figure 1. GluN3A inhibits the activity-dependent induction of a subset of immediate-early genes (IEGs). **(A)** Timeline of endogenous GluN3A expression and downregulation and of lentiviral infections. Rat cortical neurons in primary culture were infected on days in vitro (DIV) 9 with lentiviruses where Green fluorescent protein (GFP) or GluN3A and GFP (GFP-GluN3A) expression is driven by the human synapsin 1 promoter (synP). **(B, C)** DIV14 neurons were treated with bicuculline (50 μ M, 1 hr) and matching samples collected for immunoblot and mRNA analyses ($n = 4$ from two independent cultures; $***p < 0.001$, two-tailed unpaired t -test). **(B)** Left, representative western blots show that GluN3A inhibits the induction of the IEGs Arc and Fos but not Zif268. Right, signal intensities of indicated proteins as percentage of stimulated GFP-infected neurons. **(C)** quantitative Reverse Transcription-Polymerase Chain Reaction (qRT-PCR) analysis of IEG mRNA induction. Plotted values are fold-induction relative to non-stimulated neurons. **(D)** Volcano plots presenting the RNAseq-based differential expression analysis in DIV14 neurons treated with bicuculline or Brain-derived neurotrophic factor (BDNF) for 1 hr ($n = 2-4$ from two independent cultures). **(E)** DIV14 neurons were treated with MG132 (30 μ M). A representative western blot probed with the indicated antibodies is shown. In immunoblot analyses, tubulin or actin was used as a loading control and GluN1 as a measure of potential effects of GluN3A on overall NMDAR numbers. Histograms in this and subsequent figures are mean \pm standard error of the mean (SEM).

The online version of this article includes the following figure supplement(s) for figure 1:

Source data 1. Western blots for immediate-early gene (IEG) induction in GFP and GFP-GluN3A-infected neurons after bicuculline treatment.

Source data 2. Western blots for bicuculline induction of immediate-early genes (IEGs) in GFP and GFP-GluN3A-infected neurons in the presence of MG132.

Figure supplement 1. Selective versus global effects of GluN3A expression and general NMDAR blockade on activity-dependent signaling.

Figure supplement 1—source data 1. Annotated western blots and original scans.

Figure supplement 1—source data 2. Annotated western blots and original scans.

Figure supplement 1—source data 3. Annotated western blots and original scans.

Figure supplement 1—source data 4. Annotated western blots and original scans.

Figure supplement 2. RNAseq analysis of activity-dependent gene expression.

(Figure 2B). Two experiments linked mTORC1 inhibition to the altered production of IEGs. First, low concentrations of rapamycin (100 nM) that inhibit mTORC1 but not mTORC2 (Zhu et al., 2018), blocked Arc and Fos translation in response to bicuculline without affecting Zif268, demonstrating selective mTORC1 dependence (Figure 2C). By contrast, the general protein synthesis inhibitor anisomycin fully suppressed Arc, Fos, and Zif268 induction (Figure 2—figure supplement 1B). Second, restoring mTORC1 signaling in GluN3A-infected neurons by expressing a constitutively active form of Rheb, the main upstream activator of mTORC1, was sufficient to normalize IEG induction (Figure 2D).

Conversely, lentiviral knockdown of GluN3A in cortical neurons with a validated short hairpin RNA (Kehoe et al., 2014) enhanced mTORC1 activity (Figure 3A and B) and potentiated the induction of Arc and Fos by bicuculline or BDNF (Figure 3C and D). Increased phosphorylation of S6K and S6 was additionally detected in hippocampal lysates from mice lacking GluN3A (*Grin3a*^{-/-}) relative to wild-type littermates (Figure 3E), confirming a role of GluN3A in limiting mTORC1 signaling in vivo.

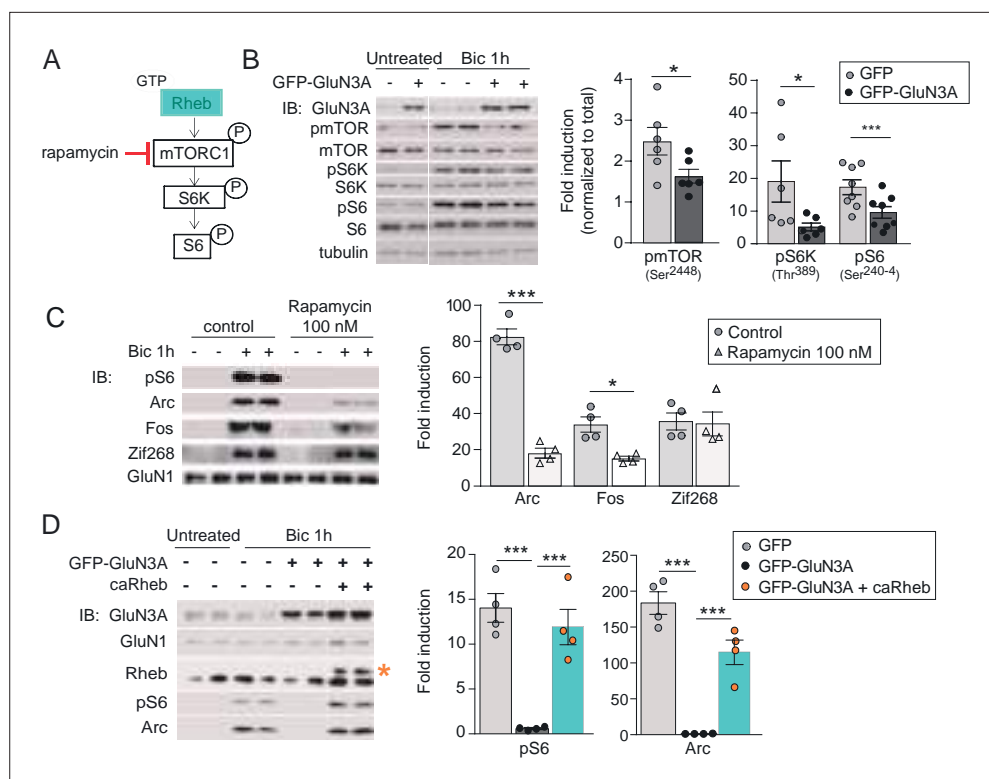


Figure 2. GluN3A inhibits the activation of mTORC1 signaling by synaptic stimuli. **(A)** Schematic of the mTORC1 signaling pathway. **(B)** Left, representative western blots of primary rat cortical neurons infected with GFP and GFP-GluN3A (days in vitro [DIV] 9) and treated with bicuculline at DIV14. Right, fold-induction of phosphorylated mTOR, S6 kinase (S6K), and S6 normalized to total protein ($n = 6-8$ from three to four independent cultures; $*p < 0.05$, $***p < 0.001$, two-tailed paired t -test). **(C)** mTOR is required for activity-dependent induction of Arc and Fos but not Zif268. Left, representative western blots of DIV14 neurons stimulated with bicuculline after preincubation with rapamycin (100 nM, 1 hr before and during bicuculline treatment). Right, fold-induction of immediate-early genes (IEGs) in response to bicuculline ($n = 4$ from two independent cultures; $*p < 0.05$, $***p < 0.001$, two-tailed paired t -test). **(D)** Reactivation of mTOR in GFP-GluN3A-infected neurons by adeno-associated virus (AAV) driven constitutively active Rheb (caRheb) rescues Arc induction. Left, representative western blots of neurons infected with lentiviral GFP-GluN3A and AAV-caRheb and treated with bicuculline. Right, fold-induction by bicuculline of pS6 and Arc in the indicated conditions ($n = 4$ from two independent cultures; $***p < 0.001$, one-way analysis of variance [ANOVA] followed by Tukey's test).

The online version of this article includes the following figure supplement(s) for figure 2:

Source data 1. Western blots for mTOR and downstream effector phosphorylation in GFP and GFP-GluN3A-infected cortical neurons after bicuculline treatment.

Source data 2. Western blots for rapamycin dependence of immediate-early gene (IEG) induction in DIV14 cortical neurons by bicuculline treatment.

Source data 3. Western blots for S6 phosphorylation and Arc induction by bicuculline in GFP and GFP-GluN3A-infected cortical neurons in the presence of caRheb.

Figure supplement 1. General inhibition of the activity induction of immediate-early genes (IEGs) by anisomycin.

Figure supplement 1—source data 1. Annotated western blots and original scans.

Figure supplement 1—source data 2. Annotated western blots and original scan.

mTORC1 inhibition requires GluN3A C-terminal domain interactions

GluN3A subunits confer unique biophysical properties to NMDARs, including reduced channel conductance and calcium permeability, and enable distinct interactions with signaling/scaffolding proteins via their intracellular C-terminal tail (Pérez-Otaño *et al.*, 2016). To dissect their contribution to inhibited mTORC1 signaling, we derived primary cortical neurons from *Grin3a*^{-/-} mice and reexpressed full-length GluN3A, a mutant where the distal 33 amino acids of the GluN3A C-terminus

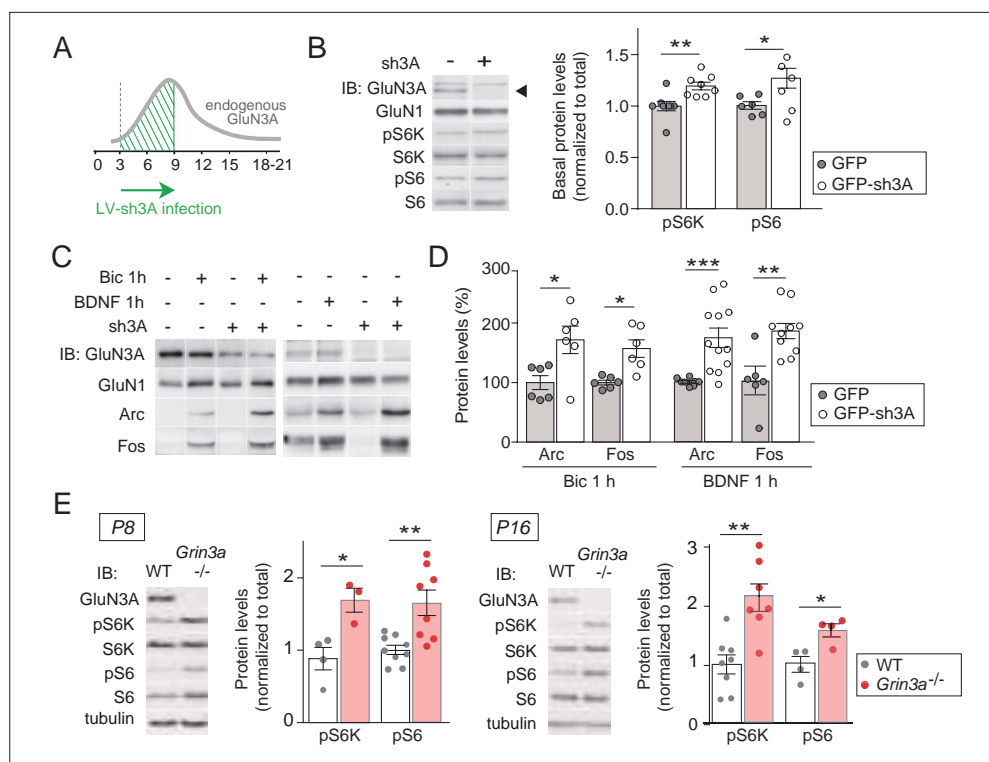


Figure 3. GluN3A deletion potentiates synaptic mTORC1 signaling. **(A)** Primary rat cortical neurons were infected on days in vitro (DIV) 3 with lentiviruses expressing GFP alone or along with a small hairpin RNA (shRNA) against GluN3A (GFP-sh3A) and collected at DIV7–9, when GluN3A expression is maximal. **(B)** Representative blots and quantification of phosphorylated S6 kinase (S6K) and S6 normalized to total protein ($n = 6–8$ from three to four independent cultures; * $p < 0.05$, ** $p < 0.01$ two-tailed paired t -test). Arrow marks specific GluN3A band. **(C, D)** Representative western blots and quantification of immediate-early gene (IEG) induction by bicuculline or BDNF ($n = 6–12$ from three independent cultures; * $p < 0.05$, ** $p < 0.01$, *** $p < 0.001$, two-tailed paired t -test). Data plotted as percentage of stimulated control GFP-infected neurons. **(E)** Immunoblots and quantification of S6K and S6 phosphorylation in lysates from wild-type (WT) and *Grin3a*^{-/-} hippocampi ($n = 4–8$ mice; * $p < 0.05$, ** $p < 0.01$, two-tailed unpaired t -test).

The online version of this article includes the following figure supplement(s) for figure 3:

Source data 1. Western blots for S6 kinase (S6K) and S6 phosphorylation in control and sh3A-infected days in vitro (DIV) 7 cortical neurons.

Source data 2. Western blots for Arc and Fos induction by bicuculline and BDNF in control and sh3A-infected days in vitro (DIV) 7 cortical neurons.

Source data 3. Western blots for S6 kinase (S6K) and S6 phosphorylation in lysates from P8 and P16 wild-type and *Grin3a*^{-/-} hippocampi.

have been deleted and lacks synapse destabilizing activity (GluN3A1082 Δ) (Fiuza *et al.*, 2013; Kehoe *et al.*, 2014), or GFP as a control (Figure 4A). While full-length GluN3A rescued the enhanced mTOR activation and hyperinduction of Arc and Fos proteins by bicuculline or BDNF in *Grin3a*^{-/-} cultures, the GluN3A1082 Δ mutant failed to do so (Figure 4B–E). Neither GluN3A nor GluN3A1082 Δ modified the activation of other signaling pathways such as ERK1/2 phosphorylation or the induction of Zif268 in *Grin3a*^{-/-} neurons (Figure 4D).

Since GluN3A and GluN3A1082 Δ display similar distributions and cell surface targeting (Fiuza *et al.*, 2013), the differences we observed are unlikely to stem from altered subcellular localization. We evaluated whether the deletion alters ion fluxes via GluN3A-NMDARs by analyzing electrophysiological responses to glutamate of GluN3A and GluN3A1082 Δ when coexpressed with GluN1 and GluN2A in HEK293 cells. The relative calcium permeability was estimated by measuring the shift in reversal potential (ΔE_{rev}) of recombinant NMDAR currents induced by changing extracellular Ca^{2+} (Perez-Otano *et al.*, 2001). GluN3A and GluN3A1082 Δ yielded similarly reduced shifts in ΔE_{rev} relative

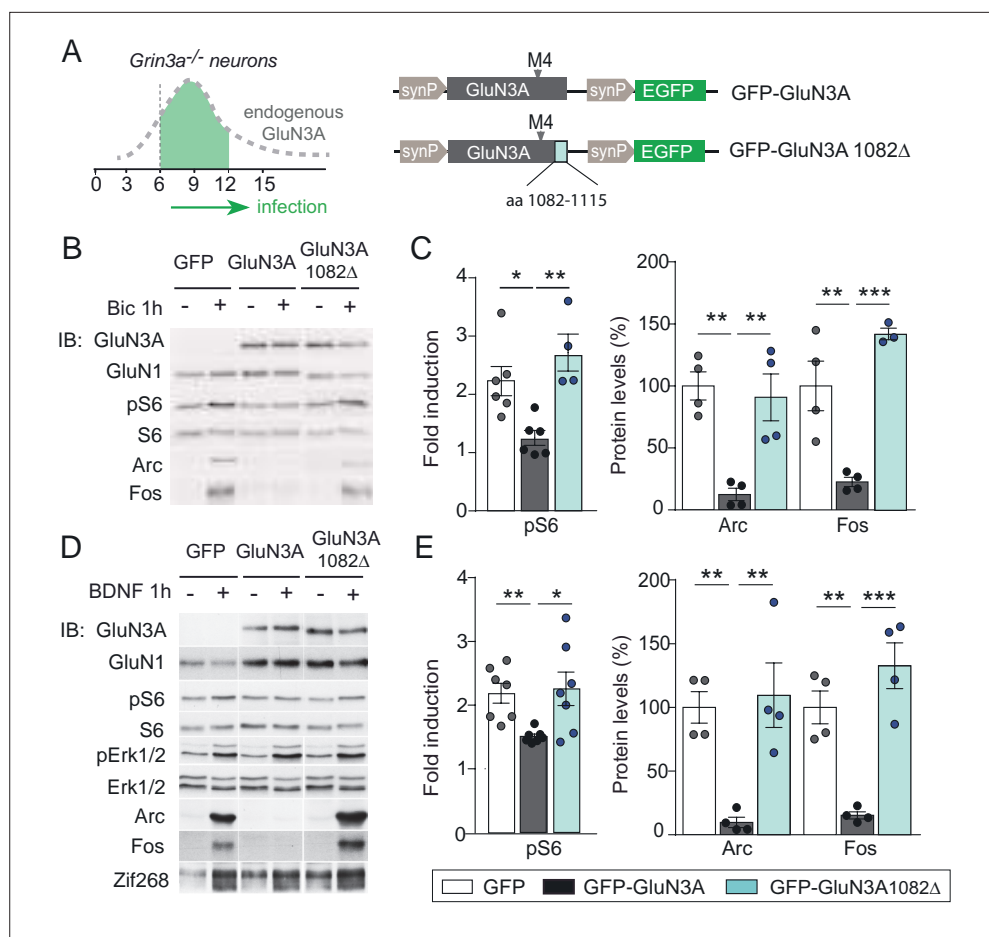


Figure 4. mTORC1 inhibition is mediated by GluN3A C-terminal domain interactions. **(A)** Cortical neurons from *Grin3a*^{-/-} mice were infected on days in vitro (DIV) 6 with lentiviruses expressing GFP, GFP-GluN3A, or GFP-GluN3A1082Δ, and stimulated with bicuculline or BDNF at DIV12. **(B, D)** Representative western blots of lysates from bicuculline or BDNF-treated neurons probed for the indicated antibodies. **(C, E)** Induction of phosphorylated S6 (normalized to total levels), Arc and Fos by bicuculline or BDNF ($n = 3-7$ from two to four independent cultures, * $p < 0.05$, ** $p < 0.01$, *** $p < 0.001$ analysis of variance [ANOVA] followed by Tukey's test).

The online version of this article includes the following figure supplement(s) for figure 4:

Source data 1. Western blots for mechanistic target of rapamycin (mTOR) effector phosphorylation and Arc and Fos induction in GFP, GFP-GluN3A, and GFP-GluN3A1082Δ-infected cortical neurons after bicuculline treatment.

Source data 2. Western blots for mechanistic target of rapamycin (mTOR) effector phosphorylation and Arc and Fos induction in GFP, GFP-GluN3A, and GFP-GluN3A1082Δ-infected cortical neurons after BDNF treatment.

Figure supplement 1. Electrophysiological properties of recombinant NMDA and excitatory glycine receptors containing full-length or truncated GluN3A.

to conventional GluN1/GluN2A NMDARs, confirming that the mutant incorporated into functional triheteromeric GluN3A-NMDARs and arguing against differences in Ca^{2+} permeability (**Figure 4—figure supplement 1**). In addition, both GluN3A versions drove comparable reductions in current densities relative to conventional NMDARs (**Figure 4—figure supplement 1B**). Along with nonconventional NMDARs, GluN3A subunits can form glycine-gated diheteromeric GluN1/GluN3 receptors (**Pérez-Otaño et al., 2016**). Thus, we additionally examined whether the deletion modified responses to glycine of GluN1/GluN3 receptors taking advantage of the CGP-78608 compound (**Grand et al., 2018**), but no differences were found (**Figure 4—figure supplement 1C**). The absence of ionotropic differences favored the hypothesis that the inhibition of mTOR signaling requires metabotropic interactions of GluN3A-NMDARs, possibly modulating its association with synaptic adaptors or scaffolds.

GluN3A expression modulates the assembly of synaptic GIT1/mTORC1 complexes

A leading candidate is the multifunctional adaptor GIT1. GIT1 is enriched in postsynaptic compartments and binds the 33 amino acids of the GluN3A C-terminus that we show above are required for mTORC1 inhibition (Fiuza *et al.*, 2013). Although best known for its role in actin signaling (Zhang *et al.*, 2003), GIT1 has been detected in mTOR immunoprecipitates from mouse astrocytes by mass spectrometry (Smithson and Gutmann, 2016) though a function for this association could not be established. Using reciprocal immunoprecipitation with GIT1 and mTOR antibodies, we isolated GIT1/mTOR complexes from lysates of microdissected hippocampal (Figure 5A) and cortical (not shown) tissue. We chose detergent conditions that preserve mTOR interactions with Raptor and Rictor (0.3 % CHAPS) to further characterize the composition of the complex, and were able to identify Raptor (but not the mTORC2 component Rictor) in GIT1 immunoprecipitates. The mTOR antibody pulled down both, validating our assay conditions (Figure 5A). The GIT1-binding protein and Rac1 activator β PIX was also pulled down by the mTOR antibody while the control presynaptic protein synaptophysin was not (Figure 5A). We additionally detected phosphorylated mTOR at Ser²⁴⁴⁸ in GIT1 immunoprecipitates, demonstrating GIT1/mTORC1 complex functionality (Figure 5B).

We then examined the subcellular localization of GIT1/mTORC1 complexes using in situ proximity ligation assay (PLA) with antibodies against GIT1 and mTOR. PLA puncta were present along dendritic shafts often localized within or at the base of dendritic spines (Figure 5C), suggesting that GIT1 positions mTORC1 near synaptic sites to mediate dendritic translation in response to synaptic signals. To test this, we stimulated cortical neurons with bicuculline or BDNF and quantified mTOR phosphorylation in total lysates and GIT1 immunoprecipitates. Both bicuculline and BDNF induced large increases in the phosphorylation of GIT1-bound mTOR on Ser²⁴⁴⁸ (Figure 5D and E). Importantly, the phosphorylation of GIT1-bound mTOR was much higher than phosphorylation of the total cellular mTOR pool (BDNF: 1.98 ± 0.38 - fold increase in total lysates vs. 4.2 ± 1.15 in GIT1 immunoprecipitates; bicuculline: 1.42 ± 0.15 vs. 4.63 ± 1.24), consistent with a role for GIT1 in nucleating synaptic mTORC1 activation. Further evidence came from GIT1 loss-of-function experiments. Lentiviral knockdown of GIT1 blunted the activation of mTORC1 by BDNF, as shown by reduced phosphorylation of S6 and S6K (Figure 5F and G), and inhibited mTORC1-dependent protein synthesis assessed using a non-radioactive puromycin-labeling assay (SUnSET) (Figure 5H). Arc translation was also reduced, as judged by loss of rapamycin sensitivity relative to control neurons, while Zif268 which is mTORC1 independent was unaffected (Figure 5F and G). Collectively, these experiments demonstrated the existence of mTORC1 complexes composed of GIT1, mTOR, and Raptor that mediate mTORC1 signaling in response to synaptic stimuli.

GluN3A/GIT1 interactions control the emergence of mTORC1-dependent protein synthesis

We further found that the abundance of GIT1/mTORC1 complexes is regulated throughout post-natal development. GIT1/mTORC1 complexes were readily observed in P16, but not P7 or P10, hippocampus or cortex of wild-type mice (Figure 6A; Figure 6—figure supplement 1). Because this time-course matches the timing of synaptic GluN3A downregulation in vivo (Henson *et al.*, 2012), we asked whether GluN3A expression influences GIT1/mTORC1 assembly. Biochemical analysis of GIT1 immunoprecipitates from hippocampi of P10 wild-type and *Grin3a*^{-/-} showed that GluN3A removal enables the formation of GIT1/mTORC1 complexes at earlier stages, as judged by enhanced GIT1/mTOR and GIT1/Raptor binding (Figure 6B). Reciprocally, reexpression of full-length GluN3A (but not the GluN3A1082 Δ mutant) in *Grin3a*^{-/-} neurons was sufficient to prevent the GIT1/mTOR association, indicating that GluN3A-bound GIT1 cannot incorporate into the complex (Figure 6C). Taken together, the results support a model where GluN3A expression regulates the abundance of synaptic GIT1/mTORC1 complexes by directly binding GIT1, impeding its association with mTOR and limiting mTORC1 activation and downstream protein synthesis of plasticity factors. Conversely, developmental or genetic GluN3A downregulation enables GIT1/mTORC1 formation and primes synapses for mTORC1-dependent translation (Figure 6D).

To test this model, we asked whether genetic manipulations of GluN3A/GIT1 interactions affect the timing and magnitude of mTORC1-dependent protein synthesis. A first set of experiments showed that protein synthesis in young cortical neurons (DIV7–9) is not dependent on mTORC1 activation,

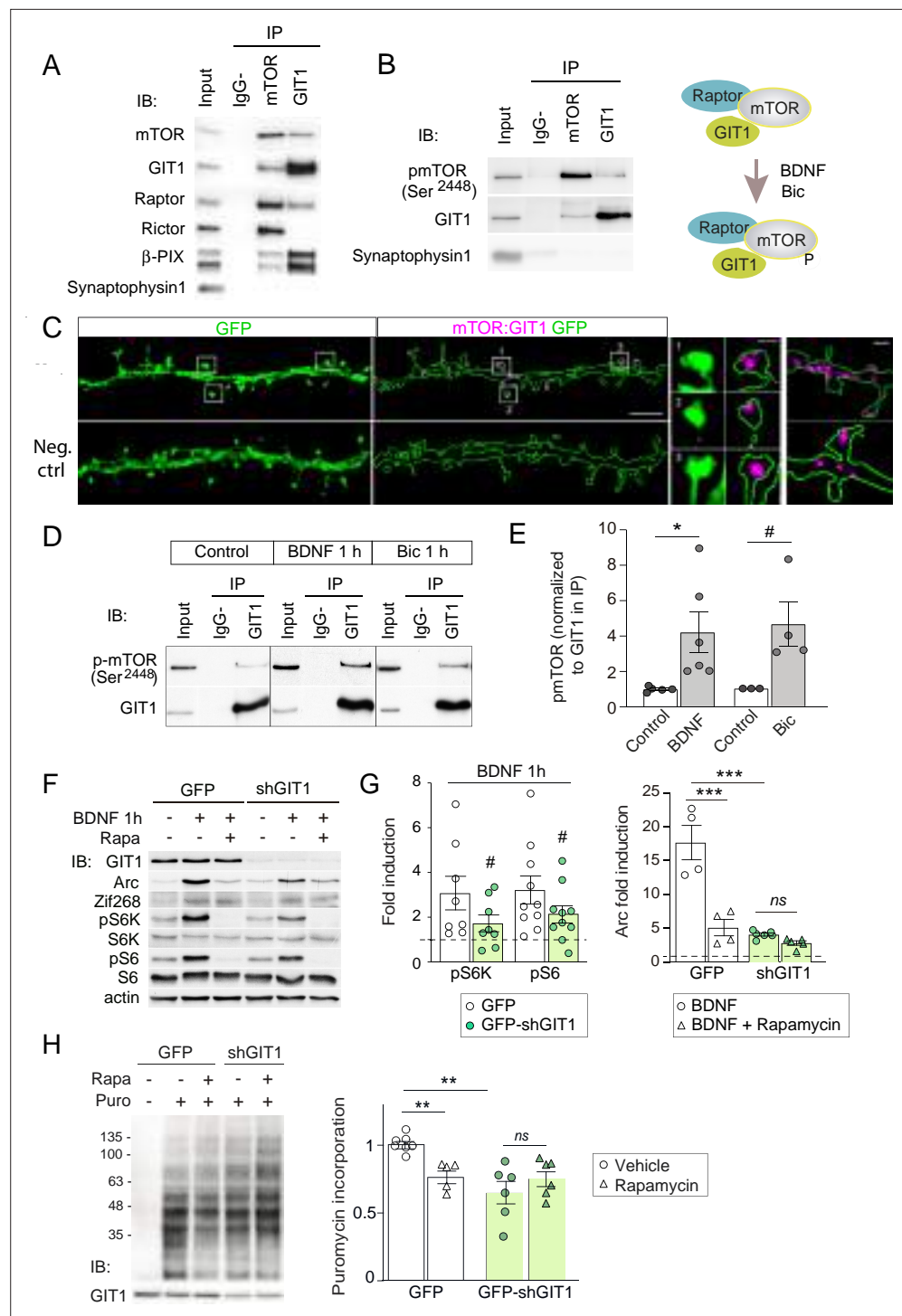


Figure 5. GIT1/mechanistic target of rapamycin (mTOR)/Raptor complexes couple synaptic activation to mTORC1-dependent protein synthesis. (A, B) Protein extracts from P16 mouse hippocampus were solubilized with 0.3 % CHAPS buffer, incubated with antibodies against mTOR or GIT1 (IP), and immunoprecipitated proteins analysed by immunoblot (IB). Input: 10 % of lysate used for immunoprecipitation. IgG–: no antibody control. A cartoon of the interactions and regulation by activity (see panel D) is shown. (C) Representative images of proximity ligation assay for rat mTOR: GIT1 (magenta) in days in vitro (DIV) 17 rat hippocampal neurons transfected with GFP (green) to visualize dendritic morphology (scale bar, 5 μm). High magnification examples of spines and dendrites (scale bars, 0.5 and 1 μm) are shown. As negative control, only mTOR primary antibody was used. (D, E) Rat cortical neurons stimulated with BDNF or bicuculline were solubilized with 0.3 % CHAPS and incubated with GIT1 antibody

Figure 5 continued on next page

Figure 5 continued

(IP). Representative immunoblots (D) and quantification of mTOR phosphorylation in GIT1 immunoprecipitates (E) are shown ($n = 3-6$ from three independent cultures; $*p < 0.05$, $\# = 0.06$, two-tailed unpaired t-test). (F–H) Primary mouse cortical neurons were infected with lentiviruses expressing GFP or GFP-shGIT1 on DIV7. mTOR responses to BDNF (F, G) and puromycin incorporation (H) in the presence or absence of 100 nM rapamycin were analyzed at DIV14. Quantification of phosphorylated S6K and S6 and Arc induction ($\#pS6K: p = 0.13$, $\#pS6: p = 0.05$, two-tailed paired; $***p < 0.001$, two-way analysis of variance [ANOVA] followed by Tukey's test) (G) and puromycin levels normalized to Ponceau S ($n = 5-7$ from four independent cultures, $**p < 0.01$, two-way ANOVA followed by Tukey's test) (H) are shown.

The online version of this article includes the following figure supplement(s) for figure 5:

Source data 1. Coimmunoprecipitation assays of GIT1 with mechanistic target of rapamycin (mTOR), Raptor, and Rictor in P16 mouse hippocampus.

Source data 2. Coimmunoprecipitation of GIT1 with phosphorylated mechanistic target of rapamycin (mTOR) in Ser²⁴⁴⁸ in P16 mouse hippocampus.

Source data 3. Coimmunoprecipitation of GIT1 and phosphorylated mechanistic target of rapamycin (mTOR) in days in vitro (DIV) 17 hippocampal neurons after bicuculline and BDNF treatment.

Source data 4. Western blots of mechanistic target of rapamycin (mTOR) effectors and immediate-early gene (IEG) induction by BDNF in the presence or absence of rapamycin in days in vitro (DIV) 14 cortical neurons infected with control or shGIT1-expressing lentiviruses.

Source data 5. Western blots of puromycin incorporation in days in vitro (DIV) 14 cortical neurons infected with control or shGIT1-expressing lentiviruses.

with strong rapamycin sensitivity emerging at later stages (DIV14) (Figure 6—figure supplement 2). Knockdown of GluN3A resulted in a large increase in protein synthesis in DIV7–9 neurons, which exhibited a rapamycin dependence typical of mature neurons (Figure 6E). Robust rapamycin-dependent protein synthesis was also observed in *Grin3a*^{−/−} neurons (Figure 6F). Reexpression of GluN3A, but not GluN3A1082Δ, reduced protein synthesis rates and was sufficient to block mTORC1 dependence, reinstating a juvenile mode of protein synthesis (Figure 6F). Thus GluN3A, via binding to GIT1, controls the age-dependent switch between mTORC1-independent and mTORC1-dependent protein synthesis.

Long-term memory formation is enhanced in *Grin3a*-deficient mice in a rapamycin-dependent manner

While GluN3A expression is typical of immature synapses at early postnatal stages as illustrated in our model, electron microscopy analyses demonstrate that subsets of synapses continue to express GluN3A into adulthood in areas such as the hippocampal CA1 (Roberts et al., 2009); and a recent mRNA expression study revealed that significant GluN3A levels are retained in a variety of brain regions (Murillo et al., 2021). Previous work showed that transgenic GluN3A overexpression impairs memory consolidation in hippocampal-dependent paradigms such as the Morris water maze (Roberts et al., 2009), but whether endogenous GluN3A expression has a physiological role in memory formation is unknown. We hypothesized that GluN3A modulation of synaptic mTORC1 signaling might provide a mechanism to set modes of translational control participating in memory encoding.

We reasoned that, if so, GluN3A deletion would create a permissive environment for stable memory formation and tested this by assessing mice learning in increasingly demanding tasks. Testing of *Grin3a*^{−/−} mice in a standard version of the Morris water maze (four trials per day) did not reveal differences in the latencies to reach the hidden platform relative to wild-type controls (Figure 7—figure supplement 1). Wild-type and *Grin3a*^{−/−} mice displayed similar preferences for the target quadrant in probe trials where the platform was removed from the pool at the end of training, confirming that both had learnt the platform location (PT1; Figure 7—figure supplement 1C). Differences emerged with a more demanding version of the task (two trials per day): both male and female *Grin3a*^{−/−} mice reached the platform significantly faster than wild types, with shorter latencies by day 3 of training and greater preference for the target quadrant in probe trials (PT1; Figure 7A and B; Figure 7—figure supplement 1B, D). No differences were observed in a visible version of the maze or in swim velocities, suggesting that motor or perceptual differences do not account for the phenotype (Figure 7—figure supplement 1E, F).

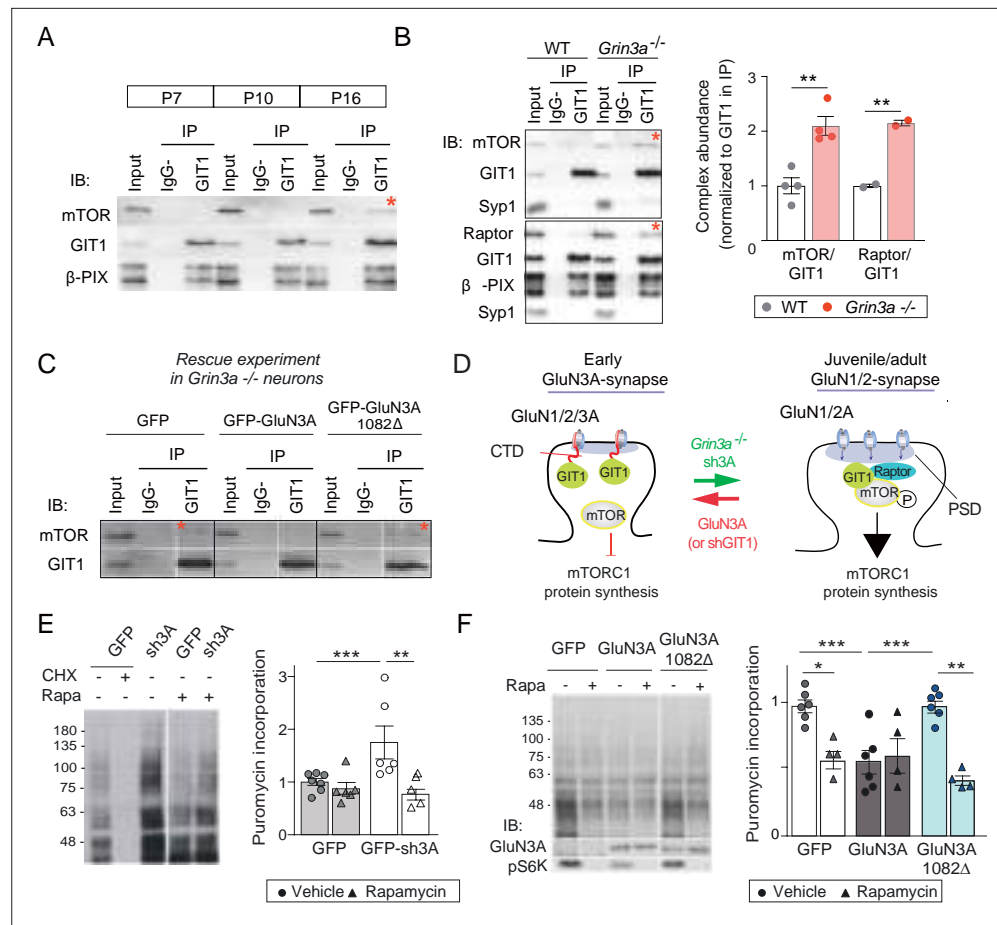


Figure 6. GluN3A/GIT1 interactions control the age-dependent onset of mTORC1-dependent protein synthesis. **(A)** Hippocampi from P7, P10, and P16 wild-type mice were lysed, immunoprecipitated with GIT1 antibody and probed for the indicated antibodies. Input: 10 % of the lysate used for immunoprecipitation. IgG–: negative control without antibody. Red asterisks here and other panels indicate mechanistic target of rapamycin (mTOR)- and Raptor bound to GIT1. **(B)** GIT1/mTORC1 complex formation is enhanced in P10 *Grin3a*^{–/–} hippocampus. Representative blots of GIT1 immunoprecipitates and quantifications are shown (*n* = 2–4 mice; ***p* < 0.01 unpaired *t*-test). Bound mTOR and Raptor are normalized to immunoprecipitated GIT1. Syp1: synaptophysin 1. **(C)** *Grin3a*^{–/–} cortical neurons infected with GFP, GFP-GluN3A, or GFP-GluN3A1082Δ were solubilized and GIT1 immunoprecipitates blotted as indicated (IB). **(D)** GIT1/GluN3A control mTORC1 translation. Left: at early postnatal stages, immature synapses express GluN3A-NMDARs, which bind the postsynaptic scaffold GIT1 via their C-terminal tail preventing the nucleation of GIT1/mTORC1 and the mTORC1-mediated synthesis of plasticity proteins. Right: at juvenile/adult stages, GluN3A downregulation enables GIT1/mTOR/Raptor complex assembly and primes synapses for mTORC1 translation of mRNAs involved in synapse and memory consolidation. The genetic manipulations shown here to alter the age-dependent switch from mTORC1-independent to mTORC1-dependent modes of translation are indicated. Note that GluN3A expression is retained by subsets of synapses in adult brains and might play roles in selecting synapses that will be recruited to stably encode memory traces (see Discussion). **(E)** Mouse cortical neurons were infected with lentiviruses expressing GFP or GFP-sh3A on days in vitro (DIV) 3 and protein synthesis analyzed at DIV7–9. Representative blots and quantification of puromycin incorporation in infected neurons treated with rapamycin (100 nM), cycloheximide (CHX, 25 μM), or vehicle. **(F)** *Grin3a*^{–/–} cortical neurons were infected with GFP, GFP-GluN3A, or GFP-GluN3A1082Δ lentiviruses, and protein synthesis analyzed at DIV12. GluN3A expression and mTOR activation were monitored with the indicated antibodies (IB). In panels D–E, *n* = 4–7 from three to four independent cultures (**p* < 0.05, ***p* < 0.01, ****p* < 0.001, two-way analysis of variance [ANOVA] followed by Tukey’s test).

The online version of this article includes the following figure supplement(s) for figure 6:

Source data 1. Coimmunoprecipitation of GIT1 and mechanistic target of rapamycin (mTOR) in lysates from P7, P10, and P16 mouse hippocampus.

Figure 6 continued on next page

Figure 6 continued

Source data 2. Coimmunoprecipitation of GIT1 with mechanistic target of rapamycin (mTOR) and Raptor in hippocampal lysates from P10 wild-type and *Grin3a*^{-/-} mice.

Source data 3. Coimmunoprecipitation of GIT1 with mechanistic target of rapamycin (mTOR) in *Grin3a*^{-/-} cortical neurons infected with GFP, GFP-GluN3A, and GFP-GluN3A1082Δ lentiviruses.

Source data 4. Western blots of puromycin incorporation in neurons infected with control or sh3A-expressing lentiviruses.

Source data 5. Western blots of puromycin incorporation in the presence or absence of rapamycin in *Grin3a*^{-/-} cortical neurons infected with GFP, GFP-GluN3A, and GFP-GluN3A1082Δ.

Figure supplement 1. Postnatal regulation of GIT1/mTORC1 complexes in mouse somatosensory cortex.

Figure supplement 1—source data 1. Annotated western blots and original scans.

Figure supplement 2. Age-dependent emergence of mTORC1-dependent protein synthesis in cultured rat cortical neurons.

Figure supplement 2—source data 1. Annotated western blots and original scans.

Similarly reduced learning thresholds had been reported in mice with elevated activity of mTOR or other pathways controlling translation (Banko et al., 2007; Costa-Mattioli et al., 2007; Hoeffler et al., 2008; Stern et al., 2013), often at the expense of impaired ability to respond to changed environments, altered memory fidelity, or appearance of perseverant and repetitive behaviors (Banko et al., 2007; Hoeffler et al., 2008; Santini et al., 2013; Shrestha et al., 2020b; Trinh et al., 2012). Thus, we evaluated cognitive flexibility by retraining the mice to learn a new platform location ('reversal'). *Grin3a*^{-/-} mice were better at shifting their preference relative to wild-type controls as evident in probe trials conducted 7 days after reversal (PT2; Figure 7A and B, Figure 7—figure supplement 1B, D). No perseverative behavior was observed either in a Y-maze spontaneous alternation task (Figure 7—figure supplement 1G). These results showed that GluN3A deletion facilitates spatial learning and memory without the unwanted effects associated to other modulators of translation.

We then assessed associative memory formation using two tasks that depend on new protein synthesis and can be achieved with the single pairing of a conditioned (CS) and unconditioned stimulus (US): conditioned taste aversion (CTA) and contextual fear conditioning (FC). In CTA, a novel taste (saccharin, CS) is associated with an aversive US (LiCl, which induces nausea). The LiCl dose (US) and temporal contiguity between CS–US can be regulated to evaluate standard memory (Figure 7C), or 'enhanced' memory by using a weaker paradigm (Figure 7F; Adaikkan and Rosenblum, 2015). Transgenic mice with prolonged GluN3A expression into adulthood (dt GluN3A) displayed deficits in a standard CTA paradigm (US, LiCl 0.15 M i.p.) as judged by their similar preference for saccharin 24 hr after saline or LiCl injections (Figure 7D, green bars). This result was inline with the memory deficits reported in other behavioral paradigms (Roberts et al., 2009). Control experiments ruled out the possibility that the defect was due to insensitivity to LiCl or to defects in distinguishing flavors (Figure 7—figure supplement 2). By contrast, *Grin3a*^{-/-} mice did not show differences relative to wild types in a standard paradigm of CTA memory (Figure 7E). We then used a weak CTA paradigm where the strength of the US was reduced (LiCl 0.025 M), and US–CS were separated by 5 hr (Figure 7F). Under these conditions, only *Grin3a*^{-/-} mice formed an association between CS–US, as shown by their significantly reduced preference for saccharin after LiCl injection but intact preference in wild-type controls. The negative association was long-lasting as it could be observed 24 (Figure 7G) and 48 hr after conditioning (data not shown). To determine whether it was mTOR dependent, we treated mice with a subthreshold dosing regime of rapamycin (Stoica et al., 2011) that does not affect standard CTA memory (Figure 7—figure supplement 2). Rapamycin erased the weak CTA memory in *Grin3a*^{-/-} mice (Figure 7H), supporting the notion that disinhibited mTOR signaling causes the cognitive enhancement.

In contextual FC, a particular environment (CS) is associated with a foot-shock (US) (Figure 8A). Wild-type and *Grin3a*^{-/-} littermates showed similar freezing responses before the delivery of the foot-shock (Figure 8B). However, freezing was significantly stronger in *Grin3a*^{-/-} mice 24 and 48 hr after a weak training protocol (single pairing of a tone with a 0.3 mA foot-shock, Figure 8B and C), demonstrating enhanced and lasting memory formation. No differences were observed in short-term (1 hr) memory that is protein synthesis independent (Figure 8B). As in CTA, rapamycin occluded the

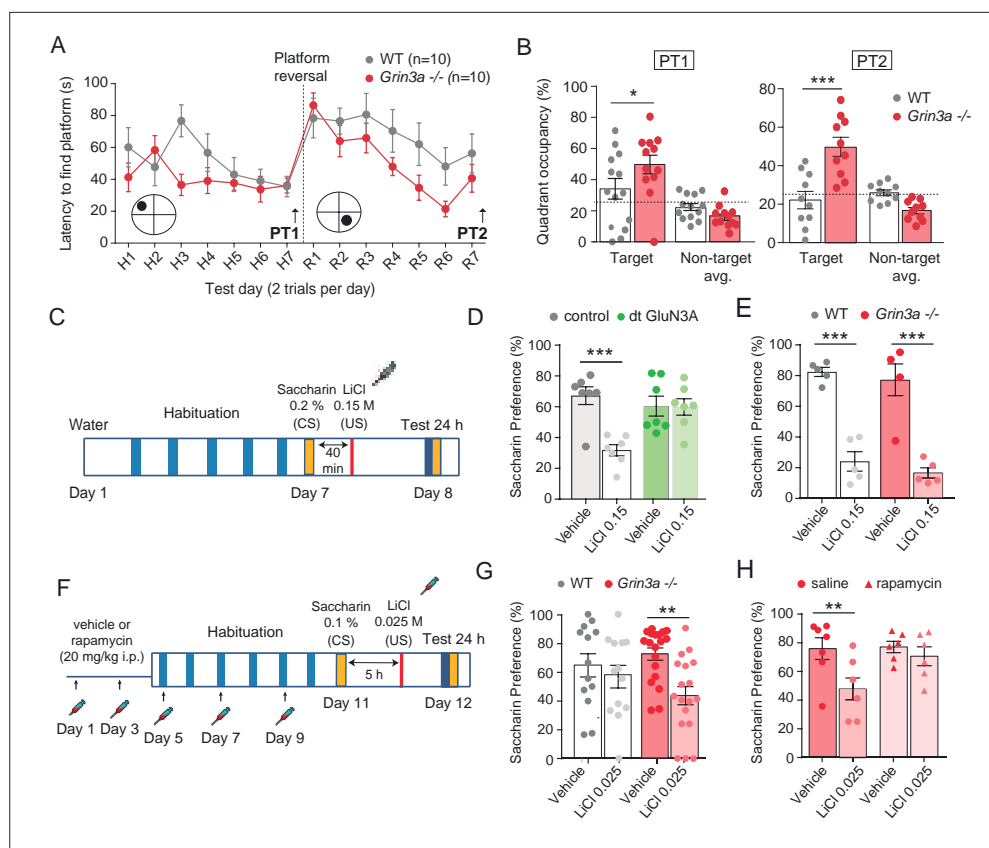


Figure 7. GluN3A deletion facilitates spatial and associative learning. **(A)** Escape latencies of male wild-type (WT) and *Grin3a*^{-/-} mice on a weak version of the Morris water maze (two trials per day) during 7-day training and after platform reversal on day 8. **(B)** Probe trials performed 24 hr after day 7 (PT1), or 24 hr after reversal training (PT2) ($n = 10$ – 13 mice per genotype; two-way analysis of variance [ANOVA] with Bonferroni post hoc test, $*p < 0.05$, $***p < 0.0001$). **(C)** Conditioned taste aversion (CTA) paradigm. **(D)** Saccharin preference of control and double transgenic (dt) GluN3A mice, and **(E)** WT and *Grin3a*^{-/-} mice after vehicle or LiCl injection ($n = 5$ – 7 mice per group; $***p < 0.001$, two-way ANOVA followed by Bonferroni post hoc test). **(F–H)** Weak CTA paradigm and rapamycin treatment regime. Decreased saccharin preference of *Grin3a*^{-/-} mice on the weak CTA **(G)** was reversed by rapamycin **(H)** ($**p < 0.01$, two-way ANOVA followed by Bonferroni post hoc test).

The online version of this article includes the following figure supplement(s) for figure 7:

Figure supplement 1. Behavior of male and female *Grin3a*^{-/-} mice in the Morris water maze.

Figure supplement 2. Controls for conditioned taste aversion (CTA) experiments.

difference between wild-type and *Grin3a*^{-/-} mice (**Figure 8C**). Taken together, our behavioral results demonstrate that GluN3A deletion lowers the threshold for stable memory storage and provide pharmacological evidence linking the enhanced learning to a relief of GluN3A constraints on mTORC1 signaling.

Yet the cognitive enhancement could have been due to lack of GluN3A during development rather than adult stages. Also, GluN3A is expressed by excitatory neurons and somatostatin interneurons, both recently implicated in protein synthesis-dependent memory consolidation (**Sharma et al., 2020; Shrestha et al., 2020a**). We therefore selectively ablated *Grin3a* from excitatory neurons or somatostatin-expressing interneurons by crossing floxed *Grin3a* mice (*Grin3a*^{fl/fl}) with mice that express Cre recombinase under the control of the Ca²⁺ calmodulin kinase II α (*Camk2a*-Cre^{ERT2}) or somatostatin (*Sst*-Cre) promoter. The first strategy allowed conditional deletion of GluN3A at adult stages by injecting tamoxifen (**Figure 8D**). Biochemical analysis of adult hippocampal lysates confirmed effective deletion of GluN3A, and revealed that $\sim 70\%$ and $\sim 20\%$ of GluN3A protein is expressed by excitatory and somatostatin interneurons, respectively (**Figure 8—figure supplement 1**). We then subjected the mice to the weak FC protocol. Adult deletion of GluN3A from excitatory neurons was

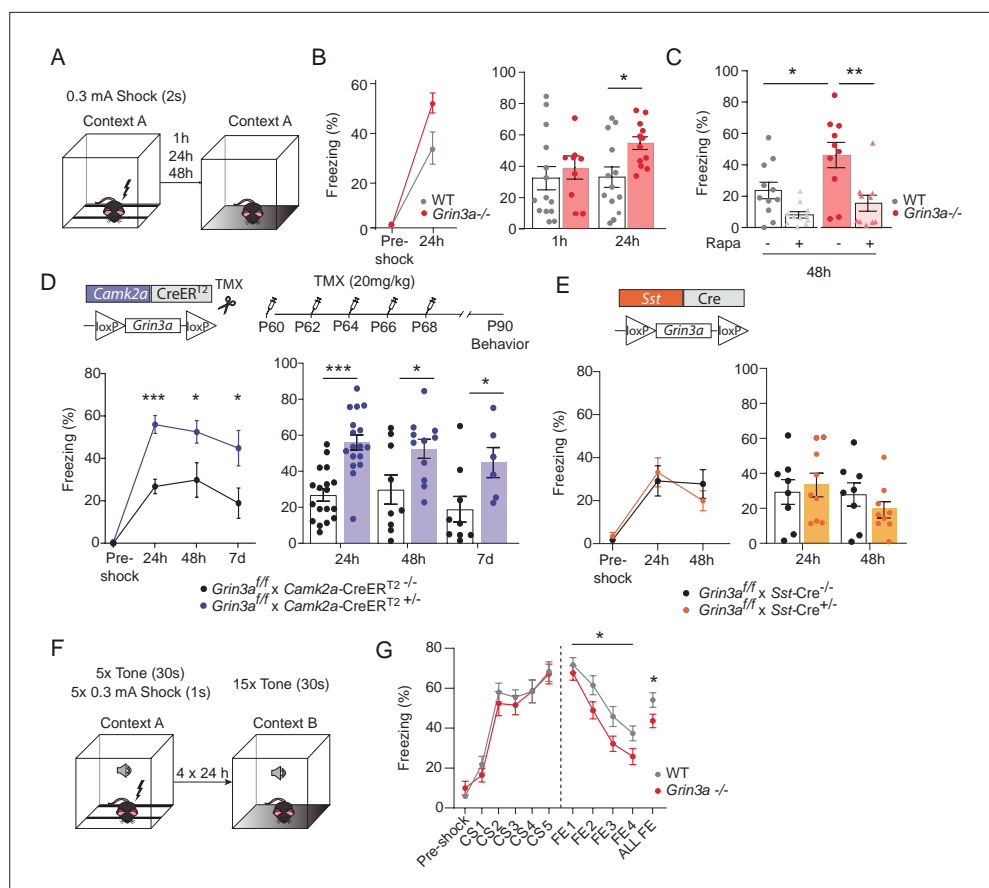


Figure 8. GluN3A deletion from excitatory neurons in adult mice is sufficient for memory enhancement. **(A)** Contextual fear conditioning test. **(B)** Enhanced contextual fear conditioning in *Grin3a*^{-/-} mice 24 hr but not 1 hr after training ($n = 9$ – 13 mice per group; left: repeated measures two-way analysis of variance [ANOVA] with Bonferroni post hoc test, $p = 0.004$; right: two-tailed unpaired t -test, $*p < 0.05$). **(C)** Enhanced contextual fear conditioning in *Grin3a*^{-/-} mice at 48 hr is reversed by rapamycin (2×20 mg/kg i.p., 24 hr apart, prior to training) ($n = 10$ – 11 mice per group; $*p < 0.05$; $**p < 0.01$, two-way ANOVA with Bonferroni post hoc test). **(D, E)** Conditional deletion of GluN3A from adult excitatory neurons, but not somatostatin (*Sst*) interneurons, enhances long-term contextual fear memory. The regime for tamoxifen (TMX) injection is indicated ($*p < 0.05$; $***p < 0.001$ two-tailed unpaired t -test). **(F, G)** Cued-fear extinction in *Grin3a*^{-/-} and wild-type littermates over a four-day fear extinction paradigm ($n = 14$ – 13 mice per group; $*p = 0.0461$ between-subjects effect, repeated measures ANOVA). Freezing levels were not different between phenotypes in FE1 ($t(25) = 0.760$, $p = 0.455$).

The online version of this article includes the following figure supplement(s) for figure 8:

Figure supplement 1. Expression of GluN3A and other synaptic proteins in conditional *Grin3a* knockout mice.

Figure supplement 1—source data 1. Annotated western blots and original scans.

Figure supplement 1—source data 2. Annotated western blots and original scans.

sufficient to enhance long-term memory, as shown by stronger freezing of *Grin3a*^{fl/fl} \times *Camk2a-Cre*^{ERT2} mice 24, 48 hr, and even 7 days after training (**Figure 8D**). In contrast, *Grin3a*^{fl/fl} \times *Sst-Cre* and control mice exhibited similar freezing levels 24 and 48 hr after training (**Figure 8E**). Thus, adult GluN3A expression in excitatory neurons gates long-term memory formation.

Finally, we evaluated fear extinction (FE), a form of memory where repeated presentation of a CS without reinforcement leads to the extinction of the acquired fear memory (**Andersson and Ressler, 2012**). FE requires protein synthesis and is another indicator of behavioral flexibility that has been shown to be impaired after manipulation of general elements of translation. Mice were subjected to a strong auditory cued-FC protocol (five pairings of a tone [CS] with a 0.3 mA foot-shock) followed by four cued-FE sessions (15 CS alone, no foot-shock) (**Figure 8F**). Fear memory acquisition was similar between WT and *Grin3a*^{-/-} littermates but FE was enhanced in *Grin3a*^{-/-} mice (**Figure 8G**),

demonstrating that GluN3A deletion does not compromise the updating of memories but rather facilitates the extinction of fear memories.

Discussion

In this study, we report a regulatory mechanism that affords spatiotemporal control of mTORC1-dependent translation in response to synaptic stimulation. Specifically we identify GIT1/mTORC1 complexes as key mediators of synaptic mTORC1 responses, and demonstrate that GluN3A-NMDARs, through direct association with GIT1, impede GIT1/mTORC1 assembly and negatively regulate synaptic mTORC1 activation and mTORC1-dependent translation. Using in vitro and in vivo genetic approaches, we further show that negative regulation by GluN3A determines the emergence of mature mTORC1-dependent protein synthesis in developing brains, and continues to play a role in adult life by placing boundaries on long-term memory storage. More broadly, our findings suggest that neuronal GIT1/mTORC1 complexes might provide a central site for the regulation and dysregulation of synaptic translation in other physiological and disease contexts.

Modulation by GluN3A of GIT1/mTORC1 complex assembly

mTORC1 is a ubiquitous protein kinase complex that promotes protein synthesis and cell growth in response to a variety of signals including nutrient availability, energy levels, insulin, growth factors, and synaptic inputs. Coupling such diverse signals to mTORC1 activation requires regulated targeting to specific subcellular compartments. For instance, mTORC1 responses to amino acids require its recruitment by the Ragulator–Rag complex to lysosomal membranes, where interactions between positive (Rheb) and negative (Tsc1/2 complex) mTOR regulators take place (*Benjamin and Hall, 2014; Sancak et al., 2010*). Our observations suggest that GIT1 could play an analogous scaffolding role to position mTORC1 such that it senses synaptic signals, with negative regulation by GluN3A limiting mTORC1-dependent translation at specific developmental times and/or in specific subsets of synapses in adult brains.

First, GIT1/mTORC1 complexes are located at dendritic/synaptic sites and respond to synaptic stimuli, as shown by phosphorylation of GIT1-bound mTOR on Ser²⁴⁴⁸, an event that is stimulated by NMDARs (*Figure 2—figure supplement 1*) and is amplified by feedback from the downstream mTORC1 substrate S6K (*Chiang and Abraham, 2005*). Second, knocking-down GIT1 blunts synaptic mTORC1 signaling and mTORC1-dependent translation of specific activity-regulated genes. Third, GIT1/mTORC1 abundance increases during postnatal development and is bidirectionally modulated by GluN3A expression. Fourth, the association of GIT1 with GluN3A is required for mTORC1 modulation, as demonstrated by the fact that expression in the *Grin3a* knockout of a GluN3A mutant lacking the GIT1-binding site does not rescue the increased assembly of GIT1 with mTOR (*Figure 6*) nor the increased activation of synaptic mTORC1 (*Figure 4*). Given that GluN3A and mTOR bind overlapping regions in GIT1 (*Fiuza et al., 2013; Smithson and Gutmann, 2016*), the most parsimonious explanation is that GluN3A competes with mTOR for binding to GIT1.

We previously reported that GluN3A modulates the formation of GIT1 complexes with β PIX (*Fiuza et al., 2013*), and might coordinately inhibit two central mechanism in spines that are necessary for memory consolidation—actin cytoskeletal rearrangements and protein synthesis. This action would be analogous to the translational repression by FMRP/CYFIP1 complexes (*De Rubeis et al., 2013*). Our results here (see *Figure 6B*) indicate that GluN3A exerts a more potent regulation over GIT1/mTORC1 than GIT1/ β PIX complexes and suggest that mTOR modulation might be the primary event. Of note, rare coding variants in GIT1 have been identified in schizophrenic patients (*Kim et al., 2017*) and GIT1 knockout mice display deficits that resemble those seen in mice with elevated GluN3A expression, including reduced spine size and poor learning and memory (*Martyn et al., 2018*). Additional phenotypes reported in mice and flies upon GIT1 deletion, such as microcephaly, reduced neuronal size or hyperactivity, might also be related to mTOR modulation (*Hong and Mah, 2015; Won et al., 2011*).

Our RNAseq analyses indicate that GluN3A acts at the level of translation and would thus preserve the supply of activity-induced plasticity mRNAs but restrict their active translation to specific synapses, in contrast to classical NMDARs that work at both transcriptional and translational levels. Nevertheless, GluN3A knockdown in cultured neurons has been shown to enhance the transcription of a subset

of mRNAs (*Chen et al., 2020*) upon prolonged periods of synaptic activation (6–8 vs. 1 hr in the present study), and we cannot rule out later regulation by GluN3A of compensatory or homeostatic responses. Of note, tonic repression of mTOR-dependent protein synthesis by GluN2B-containing NMDARs has also been reported (*Wang et al., 2011*). However, the molecular determinants of stimulation or repression of protein synthesis were not addressed. It remains to be established whether GluN3A and GluN2B share common mechanisms.

A role for GluN3A in restricting translation for precise circuit refinements and long-term memory storage

GluN3A-NMDARs are highly expressed during critical periods of experience-dependent neural circuit refinements, when they have been proposed to determine which synapses will be maintained or eliminated, and at lower levels in specific regions of the adult brain (*Murillo et al., 2021*). We propose a model whereby the lack or presence of GluN3A at postsynaptic sites contributes to spine-specific translation by setting an enhanced or repressed biochemical environment for mTORC1 signaling that will depend on the stage of brain development (*Figure 6D*) and the activity history of individual synapses. This is: synaptic GluN3A levels are downregulated by sensory experience and can be controlled at the level of individual synapses by activity-dependent endocytosis (*Pérez-Otaño et al., 2006*). The removal of GluN3A-NMDARs from active synapses would drive formation of nearby GIT1/mTORC1 complexes. This would locally increase the potential for dendritic translation of activity-regulated mRNAs, giving active inputs an advantage for consolidation versus less-active neighbors. Hence, competition for active mTORC1 would provide a means for selective synapse stabilization and memory storage. Defects in mTORC1 regulation might permit the consolidation of otherwise lost synaptic changes.

Such a competition-based model is supported by the localization of GluN3A to subsets of adult synapses (*Roberts et al., 2009*). It is also supported by the observations that in *Grin3a*^{-/-} mice, the levels of GIT1/mTORC1 are increased and these mice exhibit enhanced capacity for memory storage, as shown by their performance in weak training protocols that are normally insufficient for stable memory formation in wild-type mice. Importantly, the restriction of dendritic translation to sites near active synapses is thought to underlie phenomena such as the competition between spines for lasting LTP expression (*Fonseca et al., 2004*) or the potentiation of synapses in clusters along the dendrite (*Fonseca et al., 2004; Govindarajan et al., 2011*). Incorporation into these models of the molecular components unveiled here might open avenues for testing how the above phenomena determine memory capacity and efficiency and for correcting cognitive dysfunction.

Our experiments using cell-type-specific and -inducible *Grin3a* knockout mice demonstrate a role of GluN3A in gating cognitive processing in the adult brain beyond its better recognized functions in postnatal neural circuit refinements, and identify excitatory neurons as the locus of GluN3A actions. In relation to memory, negative regulators are thought to provide an advantage by ensuring that only salient features are learnt and irrelevant events or associations are filtered out (*Abel et al., 1998; Cho et al., 2015*). For instance, temporal contiguity of events is required for many forms of associative learning; within the scale of seconds or minutes for classical conditioning paradigms, longer in other types of memory. In CTA, the CS and US can be hours apart, with temporal boundaries set by the strength of the US (*Adaikkan and Rosenblum, 2015*). Our results show that the absence of GluN3A broadens this temporal limit and facilitates learning of demanding tasks, i.e. where training is spaced apart or the presented stimuli are weaker. The reversal by rapamycin is consistent with the notion that the enhanced readiness of the mTORC1 translational machinery in GluN3A-deficient mice expands the range for consolidation of memory traces. While we used a subthreshold dose of rapamycin that does not alter memory or mTOR signaling in wild-type mice (*Stoica et al., 2011*), we cannot rule out potential nonsynaptic effects. Definitive proof will require the development of tools that directly disrupt GluN3A/GIT1 or GIT1/mTOR association or synaptic localization.

As far as tested here, GluN3A deletion does not impair other aspects of cognition such as memory flexibility or extinction. Yet significant GluN3A levels are retained in areas of the mouse and human adult brain with strong plasticity or functional integration needs (*Fulcher et al., 2019; Murillo et al., 2021*), and a recent study linked adult GluN3A expression to the control of emotional states (*Otsu et al., 2019*). In addition, genetic variations in *GRIN3A* have been shown to modulate prefrontal cortex activity (*Gallinat et al., 2007*) and episodic memory (*Papenberg et al., 2014*). Future investigations

should determine whether domains of cognition other than the ones we tested are compromised by GluN3A deletion.

GluN3A and synaptic protein synthesis as selective therapeutic targets

The stabilization of memories requires de novo protein expression. Nevertheless, the effects on cognition of enhancing mTOR signaling or protein synthesis are perplexing. Loss of constraints on protein synthesis due to mutations in negative regulators of translation (*FMR1*, *MECP2*, or mTORC1 suppressors including *NF1*, *TSC1/2*, or the phosphatase *PTEN*) are associated with cognitive impairment and high incidence of autism spectrum disorders and intellectual disability (*Kelleher and Bear, 2008*), although a fraction of autistic individuals exhibit enhanced cognitive skills within specific domains (*Heaton and Wallace, 2004*). On the other hand, inhibiting the phosphorylation of eIF2 α , which generally increases translation (*Costa-Mattioli et al., 2007; Stern et al., 2013*), or enhancing mTORC1 activity by removal of FKBP12 (*Hoeffler et al., 2008*) have been reported to lower memory thresholds. However, the cognitive enhancement came at the cost of reduced memory fidelity and cognitive flexibility even when cell-type-specific modulation was attempted (*Santini et al., 2013; Shrestha et al., 2020a; Trinh et al., 2012*), which we did not observe here. Key differences could be that other negative regulators of mTOR such as FMRP, PTEN, or Tsc1/2 are expressed in multiple cell types and neuronal locations, as demonstrated by their linkage to altered cell growth and appearance of tumors (*Lipton and Sahin, 2014*). Also, in some of the above situations, translation is constitutively activated and responses to incoming signals might be obliterated. By contrast, lack of GluN3A does not occlude mTORC1 activation but rather seems to prime mTOR activation by synaptic stimuli. At present, the enhancement of learning and memory produced by loss of GluN3A suggests that targeting GluN3A expression or signaling functions might be of therapeutic benefit. For instance, small molecules that perturb the GluN3A/GIT1 association might work in subtler ways than general translation regulators by specifically modulating synaptic mTORC1 signaling.

Materials and methods

Animals

Adult (3–6 months old) *Grin3a*^{−/−}, *Grin3a*^{tm1a(EUCOMM)Hmgu/H} (*Grin3a*^{fl/fl}) and double-transgenic GFP-GluN3A (dtGluN3A) mice backcrossed for 10–12 generations into a C57Bl6/J background were used. Single transgenic mice were used as controls for dtGluN3A mice, and wild-type littermates from heterozygote crosses were controls for *Grin3a*^{−/−} mice. Commercial C57BL6/J mice were purchased from Charles River Laboratories. For time-specific knockout of *Grin3a* in excitatory neurons, tamoxifen-inducible CaMKII α -CreERT2^{+/-} mice (*Erdmann et al., 2007*) were crossed with *Grin3a*^{fl/fl} mice. Tamoxifen (Sigma-Aldrich T5648, 20 mg/ml dissolved in corn oil) was administered via oral gavage (five alternate days). For inhibitory neuron-specific knockout of *Grin3a*, Sst-IRES-Cre^{+/-} mice (JAX Stock No. 018973) were backcrossed with C57BL/6J mice for 12 generations and then bred with *Grin3a*^{fl/fl} mice. Male mice were used for behavioral experiments unless indicated. Animals were housed four to six per cage with ad libitum access to food and water and maintained in a temperature-controlled environment on a 12-hr dark/light cycle. All procedures were conducted in accordance with the European and Spanish regulations (2010/63/UE; RD 53/2013) and were approved by the Ethical Committee of the Generalitat Valenciana (2017/VSC/PEA/00196). For the cued-FC experiments, ethic protocols were approved by the Committee of Ethics of the Universitat Autònoma de Barcelona and the Generalitat de Catalunya.

Primary neuronal cultures

Cortical and hippocampal neurons in primary culture were prepared as described (*Pérez-Otaño et al., 2006*). Briefly, cortices were dissected from E19 rat pups or E17.5 mice pups and dissociated with papain (Worthington Biochemical). Mouse primary neurons were used for rescue experiments in the *Grin3a*-null background shown in **Figures 4 and 6**, and for shGIT1 experiments in **Figure 5**. Neurons were plated at 75,000 cells per well on 12-well plates, 500,000 cells per well on 6-well plates and 1,000,000 cells/ dish on 60 mm dishes coated with laminin and poly-D-lysine and grown in Neurobasal Medium supplemented with B27 (Thermo Fisher).

Neurons were infected with lentiviruses 5 days prior to collection (timing of infection is indicated in figure legends). Neurotrophic factors and other drugs were used at the following concentrations: anisomycin (0.8 μ M, Sigma-Aldrich A5892), recombinant human BDNF (100 ng/ml, PeproTech 450-02), bicuculline (50 μ M, Abcam Ab120108), cycloheximide (25 μ M, Sigma Aldrich C7698), (D,L)-APV (50 μ M, Tocris 3693), MK801 (10 μ M, Tocris 0924), rapamycin (100 nM, Alfa Aesar J62473), and puromycin (10 ng/ml, Sigma Aldrich P8833).

Lentiviral vectors

For the generation of lentiviral constructs, full-length GluN3A and GluN3A1082 Δ cDNAs were subcloned into a dual lentiviral vector Syn-WPRE-Syn-GFP kindly provided by Dr. Francisco G Scholl, University of Sevilla, Spain. For knockdown experiments, 19–20 base pairs (bp)-long small hairpin RNAs (shRNAs) directed to GluN3A (shGluN3A1185, target sequence: CTACAGCTGAGTTTAGAAA) or GIT1 (shGIT1, target sequence: TGATCACAAGAATGGGCATTA) were cloned into the pLentilox 3.7-GFP vector downstream the U6 promoter. The AAV encoding constitutively active human Rheb (AAV-caRheb, S16H) was kindly provided by Dr. Beverly Davidson, Children’s Hospital of Philadelphia, University of Pennsylvania.

RNA isolation, qRT-PCR, and RNAseq analyses

Total RNA from cultured cortical neurons was isolated using the Nucleospin RNA (Macherey-Nagel). RNA concentration and purity were assessed with NanoDrop. RNA quality was determined by the RNA Integrity Number (RIN) algorithm using the Agilent 2100 Bionalyzer Instrument; only samples with RIN >9 matched our standard.

For qRT-PCR experiments, first-strand cDNA was synthesized from 1 μ g of total RNA using the Invitrogen SuperScript IV First-Strand cDNA Synthesis System (Thermo Fisher). Quantitative real-time PCR (qPCR) was performed using the Applied Biosystems QuantStudio 3 Real-Time PCR system and analyzed with the QuantStudio 3 Design and Analysis software (v1.5.1, Thermo Fisher). Briefly, real-time qPCR was assayed in a total volume of 20 μ l reaction mixture containing the ready-to-use PyroTaq EvaGreen qPCR Mix Plus ROX (Cmb), 5 pmol of forward and reverse (rv) primers (detailed in key resource table) and cDNA. PCR thermal conditions included an initial hold stage with 5 min at 50 $^{\circ}$ C and 15 min at 95 $^{\circ}$ C followed by 40 cycles of denaturation for 30 s at 95 $^{\circ}$ C, annealing for 32 s at 60 $^{\circ}$ C and primer elongation for 32 s at 72 $^{\circ}$ C. All qPCR reactions were run in triplicates. Mean cycle threshold (Ct) values for each reaction were recorded and the relative RNA expression levels were calculated referring to *Gapdh*, encoding glyceraldehyde 3-phosphate dehydrogenase: $\Delta Ct = Ct_{GAPDH} - Ct_{(target\ gene)}$. The gene expression fold change normalized to GAPDH and relative to control sample was calculated as $2^{\Delta Ct}$.

Key resources table

Reagent type (species) or resource	Designation	Source or reference	Identifiers	Additional information
Antibody	GIT-1 (mouse monoclonal, clone A-1)	Santa Cruz Biotechnology	Cat# sc-365084; RRID: AB_10850059	PLA 1:150
Antibody	Arc (mouse monoclonal, clone C-7)	Santa Cruz Biotechnology	Cat# sc-17839; RRID: AB_626696	WB 1:100
Antibody	beta-Tubulin III (mouse monoclonal)	Sigma-Aldrich	Cat# T8660; RRID: AB_477590	WB 1:20,000
Antibody	NMDAR1, all splice variants (mouse monoclonal, clone R1JHL)	Millipore	Cat# MAB1586; RRID: AB_11213180	WB 1:1000
Antibody	NR2B (mouse monoclonal, clone BWJHL)	Millipore	Cat# 05–920; RRID: AB_417391	WB 1:1000
Antibody	NR3A (mouse monoclonal)	Kindly provided by Jim Trimmer	N/A	WB 1:100
Antibody	PSD-95 (mouse monoclonal, clone K28/43)	Antibodies Incorporated	Cat# 75–028 RRID: AB_10698024	WB 1:1000
Antibody	Puromycin (mouse monoclonal, clone 12D10)	Millipore	Cat# MABE343; RRID: AB_2566826	WB 1:2000

Continued on next page

Continued

Reagent type (species) or resource	Designation	Source or reference	Identifiers	Additional information
Antibody	Synapsin I (mouse monoclonal, clone 46.1)	Synaptic Systems	Cat# 106 011 RRID: AB_2619772	WB 1:5000
Antibody	Synaptophysin (mouse monoclonal, clone SY38)	Millipore	Cat# MAB5258-20UG; RRID: AB_11214133	WB 1:2000
Antibody	CREB (rabbit monoclonal, clone 48H2)	Cell Signaling Technology	Cat# 9197; RRID: AB_331277	WB 1:1000
Antibody	NR2A (rabbit monoclonal, clone A12W)	Millipore	Cat# 05-901 R; RRID: AB_10805961	WB 1:1000
Antibody	Phospho-CamKinase II alpha (CaMKII α) Thr286 (rabbit monoclonal, clone D21E4)	Cell Signaling Technology	Cat# 12716; RRID: AB_2713889	WB 1:1000
Antibody	Phospho-p70 S6 kinase Thr389 (rabbit monoclonal, clone 108D2)	Cell Signaling Technology	Cat# 9234; RRID: AB_2269803	WB 1:1000
Antibody	Raptor (rabbit monoclonal, clone 24C12)	Cell Signaling Technology	Cat# 2280; RRID: AB_561245	WB 1:1000
Antibody	Rheb (rabbit monoclonal, clone E1G1R)	Cell Signaling Technology	Cat# 13879; RRID: AB_2721022	WB 1:1000
Antibody	Rictor (rabbit monoclonal, clone 53A2)	Cell Signaling Technology	Cat# 2114; RRID: AB_2179963	WB 1:500
Antibody	S6 ribosomal protein (rabbit monoclonal, clone 5G10)	Cell Signaling Technology	Cat# 2217; RRID: AB_331355	WB 1:1000
Antibody	GIT1 (rabbit polyclonal)	Cell Signaling Technology	Cat# 2919; RRID: AB_2109982	IP 1:200, WB 1:1000
Antibody	Egr-1/Zif268 (rabbit polyclonal)	Santa Cruz Biotechnology	Cat# sc-110; RRID: AB_2097174	WB 1:500
Antibody	beta-Pix, SH3 domain (rabbit polyclonal)	Millipore	Cat# 07-1450; RRID: AB_1586904	WB 1:1000
Antibody	c-Fos (rabbit polyclonal)	Santa Cruz Biotechnology	Cat# sc-52; RRID: AB_2106783	WB 1:500
Antibody	CaMKII α (rabbit polyclonal)	Sigma-Aldrich	Cat# C6974; RRID: AB_258984	WB 1:1000
Antibody	mTOR (rabbit polyclonal)	Cell Signaling Technology	Cat# 2972; RRID: AB_330978	IP 1:100, PLA 1:150, WB 1:1000
Antibody	NMDAR2A&B, pan antibody (rabbit polyclonal)	Millipore	Cat# AB1548; RRID: AB_11212156	WB 1:1000
Antibody	NR3A (rabbit polyclonal)	Millipore	Cat# 07-356; RRID: AB_2112620	WB 1:1000
Antibody	p30alpha (rabbit polyclonal)	Santa Cruz Biotechnology	Cat# sc-535; RRID: AB_632138	WB 1:1000
Antibody	p44/42 MAPK (Erk1/2) (rabbit polyclonal)	Cell Signaling Technology	Cat# 9102; RRID: AB_330744	WB 1:1000
Antibody	p70 S6 kinase (rabbit polyclonal)	Cell Signaling Technology	Cat# 9202; RRID: AB_331676	WB 1:1000
Antibody	Phospho-CREB Ser133 (rabbit polyclonal)	Millipore	Cat# 06-519; RRID: AB_310153	WB 1:1000
Antibody	Phospho-mTOR Ser2448 (rabbit polyclonal)	Cell Signaling Technology	Cat# 2971; RRID: AB_330970	WB 1:1000
Antibody	Phospho-p38 MAPK Thr180/Tyr182 (rabbit polyclonal)	Cell Signaling Technology	Cat# 9911; RRID: AB_10695905	WB 1:1000
Antibody	Phospho-p44/42 MAPK (Erk1/2) Thr202/Tyr204 (rabbit polyclonal)	Cell Signaling Technology	Cat# 9101; RRID: AB_331646	WB 1:1000

Continued on next page

Continued

Reagent type (species) or resource	Designation	Source or reference	Identifiers	Additional information
Antibody	Phospho-S6 ribosomal protein Ser240/244 (rabbit polyclonal)	Cell Signaling Technology	Cat# 2215; RRID: AB_331682	WB 1:1000
Cell line (<i>Homo sapiens</i>)	HEK293	ATCC	Cat# CRL-1573; RRID: CVCL_0045	
Chemical compound, drug	(-)-Bicuculline methiodide	Abcam	Cat# Ab120108; CAS: 55950-07-7	
Chemical compound, drug	(D,L)-APV sodium salt	Tocris	Cat# 3693; CAS: 1303993-72-7	
Chemical compound, drug	Anisomycin	Sigma-Aldrich	Cat# A5892; CAS: 22862-76-6	
Chemical compound, drug	B27 supplement	Thermo Fisher Scientific	Cat# 17504044	
Chemical compound, drug	BDNF	PeptoTech	Cat# 450-02; AN: P23560	
Chemical compound, drug	CGP-78608	Tocris	Cat# 1493; CAS: 1135278-54-4	
Chemical compound, drug	cOmplete Protease Inhibitor Cocktail	Sigma-Aldrich	Cat# 04693116001	
Chemical compound, drug	Cycloheximide	Sigma-Aldrich	Cat# C7698; CAS: 66-81-9	
Chemical compound, drug	MK-801	Tocris	Cat# 0924; CAS: 77086-22-7	
Chemical compound, drug	Puromycin dihydrochloride	Sigma-Aldrich	Cat# P8833; CAS: 58-58-2	
Chemical compound, drug	Rapamycin	Alfa Aesar	Cat# J62473; CAS: 53123-88-9	
Chemical compound, drug	Tamoxifen	Sigma-Aldrich	Cat# T5648	
Chemical compound, drug	Tetrodotoxin citrate	Alomone Labs	Cat# T-550; CAS: 18660-81-6	
Commercial assay, kit	Duolink In Situ Red Starter Kit Mouse/Rabbit	Sigma-Aldrich	Cat# DUO92101	
Commercial assay, kit	MasterMix qPCR ROX PyroTaq EvaGreen	cmb	Cat# 87H24	
Commercial assay, kit	Nucleospin RNA	Macherey-Nagel	Cat# 740955.50	
Commercial assay, kit	Pierce BCA Protein Assay kit	Thermo Fisher Scientific	Cat# 23,227	
Commercial assay, kit	SuperScript IV First-Strand cDNA Synthesis System	Invitrogen	Cat# 18-091-050	
Genetic reagent (<i>Mus musculus</i>)	Mouse: B6;129 × 1-Grin3a ^{tm1Nnk/J}	The Jackson Laboratory	Cat# JAX:029974; RRID: IMSR_JAX:029974	
Genetic reagent (<i>Mus musculus</i>)	Mouse: CaMKII α -CreERT2 ^{+/-}	Erdmann et al., 2007		
Genetic reagent (<i>Mus musculus</i>)	Mouse: Grin3a ^{tm1a[EUCOMM]Hmgw/H}	EUCOMM		
Genetic reagent (<i>Mus musculus</i>)	Mouse: Sst-IRES-Cre	The Jackson Laboratory	Stock: 018973	
Genetic reagent (virus)	LV-hSYN-WPRE-hSYN-GFP-WPRE	Gascón et al., 2008		
Genetic reagent (virus)	LV-hSYN-GluN3A-WPRE-hSYN-GFP-WPRE	This paper		See Materials and methods; generated/stored in Perez-Otano's lab.
Genetic reagent (virus)	LV-hSYN-GluN3A1082Δ-WPRE-hSYN-GFP-WPRE	This paper		See Materials and methods; generated/stored in Perez-Otano's lab.

Continued on next page

Continued

Reagent type (species) or resource	Designation	Source or reference	Identifiers	Additional information
Genetic reagent (virus)	pLentiLox3.7-GFP (pLL3.7-GFP)	Kindly provided by Dr. Michael Ehlers	Addgene plasmid #11795; RRID: Addgene_11795	
Genetic reagent (virus)	pLL3.7-shGluN3A1185-GFP (Target sequence: CTACAGCTGAGTTTAGAAA)	Yuan et al., 2013		
Genetic reagent (virus)	pLL3.7-shGIT1-GFP (Target sequence: TGATCACAAGAATGGGCATTA)	This paper		See Materials and methods; generated/ stored in Perez-Otano's lab.
Recombinant DNA reagent (plasmid)	pcDNA1-Amp-GluN1-1A	Perez-Otano et al., 2001		
Recombinant DNA reagent (plasmid)	pcDNA1-Amp-GluN2A	Perez-Otano et al., 2001		
Recombinant DNA reagent (plasmid)	pCIneo-GFPgluN3A	Perez-Otano et al., 2001		
Recombinant DNA reagent (plasmid)	pCIneo-GFPgluN3A1082Δ	This paper		See Materials and methods; generated/ stored in Perez-Otano's lab.
Recombinant DNA reagent (plasmid)	pRK5-GFP	Kindly provided by Dr. Michael Ehlers		
Sequence-based reagent (oligonucleotide)	Arc_fwd (mouse)	This paper		GAGCCTACAGAGCCAGGAGA
Sequence-based reagent (oligonucleotide)	Arc_rv (mouse)	This paper		TGCCTTCAAAGTGCTTGGGA
Sequence-based reagent (oligonucleotide)	c-Fos_fwd (mouse/rat)	Chen et al., 2020		CTGCTCTACTTTGCCCTTCT
Sequence-based reagent (oligonucleotide)	c-Fos_rv (mouse/rat)	Chen et al., 2020;		TTTATCCCCACGGTGACAGC
Sequence-based reagent (oligonucleotide)	GAPDH_fwd (mouse/rat)	This paper		CATGGCCTCCGTGTTCT
Sequence-based reagent (oligonucleotide)	GAPDH_rv (mouse/ rat)	This paper		TGATGTCATCATACTTGGCAGTT
Software, algorithm	ImageJ	Schneider, Rasband and Eliceiri, 2012		https://imagej.nih.gov/ij/
Software, algorithm	ImageQuant software version 5.2	GE Healthcare		
Software, algorithm	Prism software version 7.00	Graphpad		
Software, algorithm	QuantStudio 3 Design and Analysis software v1.5.1	Thermo Fisher Scientific		
Software, algorithm	SMART software for video-tracking	PanLab S.L.		

For RNAseq experiments, we performed bulk mRNA sequencing single end with a length of 50 bp using the RNAseq Illumina Hiseq2500. The preparation of the polyA sequencing library, library's quality control and quantification, sequencing run and base calling data were carried out by the Genomics Core Facility of the Centre for Genomic Regulation (CRG, Barcelona). For the analysis, adapters were trimmed using trim_galore v0.6.4_dev and reads with longer length than 40 bp were selected. Trimmed reads were aligned using star c2.6.1b to the mouse genome (mm10). Reads with mapq >30 were selected using Samtools v1.9. Mapped reads were quantified using R scripts (R version 4.0.3, 2020), Rsubread v2.4.3 and the Mus_musculus.GRCm38.99.gtf annotation data. Differential expression analysis was performed using DESeq2 1.31.1 and limma 3.46.0; genes were annotated using biomaRt v2.46.3 and Volcano plots were performed with EnhancedVolcano 1.6.0. The tracks from the samples were performed with DeepTools v3.5.0, normalized with RPKM and visualization was done in IGV v2.6.3.

Protein extraction and western blotting

Cultured neurons were collected in lysis buffer containing 50 mM Tris-HCl pH 6.8, 10 % glycerol, 2 % SDS, 0.1 M (D,L)-dithiothreitol, 0.04 % bromophenol blue, and supplemented with protease

(cOmplete Protease Inhibitor Cocktail) and phosphatase (PhosSTOP) inhibitors. Lysates were incubated for 10 min at 65 °C, briefly centrifuged at maximum speed and proteins separated by SDS–PAGE. Proteins were transferred onto PVDF membranes (GE Healthcare). After incubation with primary antibodies, membranes were incubated with secondary HRP-conjugated secondary antibodies (1:10,000, GE Healthcare). Signals were visualized with film autoradiography or the Amerham 680 Blot Imager, and nonsaturated immunoreactive bands were quantified using the ImageQuant 5.2 software.

For *in vivo* studies on mouse tissue, hippocampi and somatosensory cortex were dissected on ice, snapped frozen in liquid nitrogen and stored at –80 °C until processing. Tissues were homogenized in 15 (wt/vol) volumes of modified ice-cold RIPA buffer (50 mM Tris–HCl pH 7.5, 150 mM NaCl, 1% NP-40, 0.05 % deoxycholate, 0.01 % SDS) supplemented with protease and phosphatase inhibitors, sonicated and centrifuged for 20 min at 16,200 × *g* at 4 °C. Protein content was estimated using a Pierce BCA Assay kit (Thermo Fisher) before immunoblotting.

Immunoprecipitation

Cultured cortical neurons or mouse hippocampus or somatosensory cortex were solubilized for 30 min in cold lysis buffer containing 0.1 % Triton X-100, 0.1 % SDS, 150 mM NaCl, 10 mM EDTA and 50 mM HEPES or 0.3 % CHAPS 3-[(3-cholamidopropyl)dimethylammonio]-1-propanesulfonic acid, 150 mM NaCl, 1 mM EDTA, and 40 mM HEPES, supplemented with protease and phosphatase inhibitors. Insoluble material was removed by centrifugation at 16,200 × *g* for 15 min and 100–150 µg of the resulting supernatants were incubated overnight at 4 °C with or without (IgG–) the immunoprecipitating antibody. Lysates were then incubated with protein A/G magnetic beads (BioRad) for 2 hr at 4 °C. Beads were precipitated using a magnetic rack, washed thrice in lysis buffer and immunoprecipitated proteins were eluted with SDS sample buffer and analyzed by western blotting.

Proximity ligation assay

Cultured neurons transfected with pRK5-GFP were fixed at DIV17 with 4 % PFA, 4 % sucrose in phosphate buffered Saline (PBS) (RT, 10 min), incubated with blocking solution and permeabilized. Cells were then incubated with rabbit polyclonal anti-mTOR antibody and mouse monoclonal anti-GIT1 antibody overnight at 4 °C, washed with PBS, and incubated for 1 hr with PLA secondary probes (anti-mouse Plus and anti-rabbit Minus, Olink Bioscience) at 37 °C. Cells were washed twice with Duolink II Wash Buffer A (Olink Bioscience) and incubated with the ligase (1:40; Olink Bioscience) in ligase buffer for 30 min at 37 °C. After additional washes with Buffer A, cells were incubated with DNA polymerase (1:80; Olink Bioscience) in amplification buffer for 100 min at 37 °C in the dark. Cells were then washed with Duolink II Wash Buffer B (Olink Bioscience) and incubated with chicken polyclonal anti-GFP for 1 hr at room temperature. After washing with PBS, cells were incubated with secondary goat anti-chicken-Alexa Fluor 488 for 1 hr at room temperature. Finally, cells were washed in PBS and mounted on slides with Fluoroshield mounting medium (Sigma-Aldrich). Fluorescence images were acquired by using Nikon A1 Ti2 system with a sequential acquisition setting at 1024 × 1024 pixels resolution; cells were randomly selected from different coverslips.

Protein synthesis assays

Basal protein synthesis was measured using a SUnSET (surface sensing of translation) assay. Briefly, primary cortical cultures were treated with 10 ng/ml of puromycin for 30 min and lysed as described above. Untreated neurons and neurons preincubated with the protein synthesis inhibitor cycloheximide (15 min before puromycin) were used as controls. Proteins were resolved by SDS–PAGE and analyzed by western blotting using an anti-puromycin antibody. Ponceau S staining was used as protein loading control.

Behavioral analysis

Morris water maze

Mice were trained to find a submerged platform in a circular tank (190 cm diameter) filled with opaque white water in two or four trials per day with 45 min intertrial intervals (ITIs). If mice did not find the platform in 120 s, they were kindly guided to it. The hidden platform was relocated to the opposite quadrant after 7 days of training for the reversal training phase. Sixty-second-long probe tests in which platform was removed were performed at the end of each phase (PT1, after initial hidden

platform learning; PT2, after reversal learning), and time spent in the target quadrant was compared to the average time spent in all other quadrants. Mice were tracked throughout the whole protocol using the video-tracking software SMART (Panlab S.L.).

Y-maze spontaneous alternation

Mice were introduced in a three-armed Y-shaped maze and recorded for 5 min. Correct triad scores were noted when all three arms were sequentially entered. Alternation indices were calculated as correct triads/possible triads. Maze was cleaned between animals with a water-based soap solution.

Conditioned taste aversion

Test was adapted from **Adaikkan and Rosenblum, 2015**. In brief, mice were trained to drink from two bottles of water for 6 days. On conditioning day, water was changed for 0.2 % (regular CTA) or 0.1 % (weak CTA) saccharin for 40 min (regular) or 5 hr (weak) after the exposure, mice were injected LiCl intraperitoneally at 0.15 M (regular) or 0.025 M (weak). Saccharin preference was evaluated 24 hr after injection. For unconditioned taste preference, mice were presented two drinking bottles for 48 hr: one contained water and the other one of the following solutions: sucrose 5 % (sweet), NaCl 75 mM (salty), quinine 300 μ M (bitter), and HCl 0.03 M (sour). Bottle sides were switched after 24 hr to avoid potential side bias. Solution preference was evaluated at 48 hr. For assessing sensitivity to LiCl toxicity, 'lying on belly' behavior was registered after injection of LiCl (0.15 M) or saline. This behavior consists in a totally general suppression of activity, and location of the mouse in the corner of a cage. The activity was measured for 20 min.

Fear conditioning and extinction

FC and FE procedures were carried out with a computerized Fear and Startle system (Panlab-Harvard, Barcelona, Spain). Tones and shocks were delivered and controlled using Freezing v1.3.04 software (Panlab-Harvard, Barcelona, Spain). The fear chambers consisted of a black methacrylate box with a transparent front door (25 × 25 × 25 cm) inside a sound-attenuating cubicle (67 × 53 × 55 cm). Animals were habituated to the chambers for 5 min/day during two consecutive days prior to FC. The chambers were carefully cleaned before and after each mouse.

For contextual FC, mice were placed in the fear chambers and allowed to explore a context (CS) (metal grid floor, no light source) for 2 min. Mice were then presented with a tone (30 s, 2.8 kHz, 85 dB tone) that coterminated with a foot-shock (US) (0.3 mA, 2 s). Sixty seconds later, they were returned to their home cage. Conditioning was assessed at 1 (short-term memory), 24, and 48 hr or 7 days (long-term memory) by reintroducing mice in the conditioning context for 5 min. Freezing behavior, a rodent's natural response to fear defined as the absence of movement except respiration, was scored by a high sensitivity weight transducer system located at the bottom of the experimental chambers which records and analyses the signal generated by the movement of the animal.

For cued FC, mice were placed in the fear chambers for 5 min and then received five trials of a tone (CS) (30 s, 6 kHz, 75 dB) that coterminated with a foot-shock (US) (0.3 mA, 1 s). The ITI was of 3 min, and three additional minutes followed the last trial. The FE sessions were performed four times in consecutive days (FE1, FE2, FE3, and FE4) starting 24 hr after FC. For FE, mice were placed in the fear chambers for 5 min and then exposed to 15 trials of the 30 s CS tone alone (cued-fear) with a 30 s of ITI interval. An additional 30-s interval followed the last trial of FE. Different contexts were used for FC and FE tests. FC context consisted of a yellow light source (~10 lux), a grid floor of 25 bars (3 mm \varnothing and 10 mm between bars), a background noise of 60 dB produced by a ventilation fan and soapy water in a solution of ethanol 70 % was used for cleaning between sessions. FE context consisted of a red-light source (~10 lux), a grey plexiglass floor covering the bars, no background noise and soapy water in a solution of isopropyl alcohol 40 % was used as cleaning agent between sessions. Different routes were used to transport animals from their home cages to testing room in FC and FE days. Freezing levels were scored and averaged in 30-s slots.

Electrophysiology

HEK293 cells were cultured, transfected, and recorded as previously described using GluN1A and GluN2A in pcDNA1/Amp and GFP-tagged GluN3A or GluN3A1082 Δ subcloned in pCI-neo (**Chowdhury et al., 2013**). HEK293 cells were obtained from ATCC, and no mycoplasma contamination was

detected by regular testing. Briefly, cells were transfected with GluN1-1A, GluN2A, and either GFP-GluN3A or GFP-GluN3A1082Δ in a 1:1:3 ratio and maintained in medium with APV (250 μM). GFP was used as a transfection marker in cells where GluN3A constructs were omitted. Whole-cell recordings were made with on GFP-positive cells using a Multiclamp 700 A amplifier (Molecular Devices) 24 hr following transfection. Patch pipettes (2–4 MΩ) contained (in mM): 140 Cs methanesulfonate, 10 HEPES, 5 adenosine triphosphate (Na salt), 5 MgCl₂, 0.2 CaCl₂, and 10 BAPTA (pH 7.4). The extracellular solution contained (in mM) 150 NaCl, 5 KCl, 2 or 10 CaCl₂, 10 HEPES, 10 glucose (pH 7.4), and was adjusted to 330 mOsm with sucrose. Currents were digitized at 2 kHz and filtered at 1 kHz. Series resistance (90–95%) and whole-cell capacitance compensation were employed. Experiments were performed at a holding potential of –80 mV with ramps (300 ms to +50 mV) elicited following a 3 s application of glutamate (1 mM) and glycine (100 μM) at 20 °C. The ΔE_{rev} was calculated by subtracting the E_{rev} obtained in 2 mM Ca²⁺ from the E_{rev} measured in 10 mM Ca²⁺ and corrected for the junction potential between solutions. Initial peak currents were obtained from 1 s agonist applications in 2 mM Ca²⁺ and used to calculate the current density. Experiments on glycine-gated diheteromeric GluN1/GluN3A receptors expressed in HEK293 cells were performed as previously described (**Grand et al., 2018**) using GluN1-1a and GFP-GluN3A or GFP-GluN3A1082Δ subcloned in pCI-neo (see above).

Statistical analysis

Statistical analyses were conducted with GraphPad Prism software. Comparison of quantitative variables between two groups was performed using Student's *t*-test. One- or two-way analysis of variance (ANOVA) followed by a post hoc comparison test were used when more than two groups were compared, as indicated in the corresponding figure legend. Results are presented as mean ± standard error of the mean (SEM). Statistical methods used for behavioral studies are indicated in the corresponding figure legends.

Acknowledgements

We thank Stuart Lipton and Nobuki Nakanishi for providing the *Grin3a* knockout mice, Beverly Davidson for the AAV-caRheb, Jose Esteban for help with behavioral and biochemical experiments, and Noelia Campillo, Rebeca Martínez-Turrillas, and Ana Navarro for expert technical help. Work was funded by the UTE project CIMA; fellowships from the Fundación Tatiana Pérez de Guzmán el Bueno, FEBS, and IBRO (to M.J.C.D.), Generalitat Valenciana (to O.E.-Z.), Juan de la Cierva (to L.G.R.), FPI-MINECO (to E.R.V., to S.N.) and Intertalentum postdoctoral program (to V.B.); ANR (GluBrain3A) and ERC Advanced Grants (#693021) (to P.P.); Ramón y Cajal program RYC2014-15784, RETOS-MINECO SAF2016-76565-R, ERANET-Neuron JTC 2019 ISCIII AC19/00077 FEDER funds (to R.A.); RETOS-MINECO SAF2017-87928-R (to A.B.); an NIH grant (NS76637) and UTHSC College of Medicine funds (to S.J.T.); and NARSAD Independent Investigator Award and grants from the MINECO (CSD2008-00005, SAF2013-48983R, SAF2016-80895-R), Generalitat Valenciana (PROMETEO 2019/020)(to I.P.O.) and Severo-Ochoa Excellence Awards (SEV-2013-0317, SEV-2017-0723).

Additional information

Funding

Funder	Grant reference number	Author
H2020 European Research Council	ERC 693021	Pierre Paoletti
Ministerio de Economía, Industria y Competitividad, Gobierno de España	SAF2016-76565-R	Raül Andero Galí
Ministerio de Economía, Industria y Competitividad, Gobierno de España	SAF2017-87928-R	Angel Barco

Funder	Grant reference number	Author
Generalitat Valenciana	PROMETEO 2019/020	Isabel Perez-Otaño
Ministerio de Economía, Industria y Competitividad, Gobierno de España	CSD2008-00005	Isabel Perez-Otaño
Ministerio de Economía, Industria y Competitividad, Gobierno de España	SAF2013-48983R	Isabel Perez-Otaño
Ministerio de Economía, Industria y Competitividad, Gobierno de España	SAF2016-80895r	Isabel Perez-Otaño
National Institutes of Health	NS76637	Steven J Tavalin
University of Tennessee	UTHSC College of Medicine Funds	Steven J Tavalin
Agence Nationale de la Recherche	GluBrain3A	Pierre Paoletti
Instituto de Salud Carlos III	AC19/00077	Raül Andero Galí
Ministerio de Economía, Industria y Competitividad, Gobierno de España	RYC2014-15784	Raül Andero Galí
Ministerio de Economía, Industria y Competitividad, Gobierno de España	SEV-2013-0317	Isabel Perez-Otaño
Ministerio de Economía, Industria y Competitividad, Gobierno de España	SEV-2017-0723	Isabel Perez-Otaño
Brain and Behavior Research Foundation	NARSAD Independent Investigator Award	Isabel Perez-Otaño
Ministerio de Economía, Industria y Competitividad, Gobierno de España	BFU-2016-80918-R	John F Wesseling
Agencia Estatal de Investigación	PID2019-111112RB-I00	Isabel Perez-Otaño

The funders had no role in study design, data collection and interpretation, or the decision to submit the work for publication.

Author contributions

María J Conde-Dusman, Partha N Dey, Conceptualization, Investigation, Methodology, Writing – original draft, Writing – review and editing; Óscar Elía-Zudaire, Investigation, Methodology, Writing – review and editing; Luis G Rabaneda, Conceptualization, Investigation, Methodology; Carmen García-Lira, Teddy Grand, Victor Briz, Eric R Velasco, Raül Andero, Sergio Niñerola, Angel Barco, Pierre Paoletti, Fabrizio Gardoni, Steven J Tavalin, Investigation; John F Wesseling, Conceptualization, Investigation, Writing – original draft, Writing – review and editing; Isabel Perez-Otaño, Conceptualization, Funding acquisition, Investigation, Methodology, Project administration, Writing – original draft, Writing – review and editing

Author ORCIDs

María J Conde-Dusman  <http://orcid.org/0000-0001-6841-2181>
Óscar Elía-Zudaire  <http://orcid.org/0000-0002-1396-834X>
Victor Briz  <http://orcid.org/0000-0001-6936-0918>
Angel Barco  <http://orcid.org/0000-0002-0653-3751>
Pierre Paoletti  <http://orcid.org/0000-0002-3681-4845>
Fabrizio Gardoni  <http://orcid.org/0000-0003-4598-5563>
Steven J Tavalin  <http://orcid.org/0000-0001-7169-0932>
Isabel Perez-Otaño  <http://orcid.org/0000-0002-7222-8202>

Ethics

All procedures were conducted in accordance with the European and Spanish regulations (2010/63/UE; RD 53/2013) and were approved by the Ethical Committee of the Generalitat Valenciana (2017/VSC/PEA/00196). For the cued-fear conditioning experiments, ethic protocols were approved by the Committee of Ethics of the Universitat Autònoma de Barcelona and the Generalitat de Catalunya.

Decision letter and Author response

Decision letter <https://doi.org/10.7554/eLife.71575.sa1>

Author response <https://doi.org/10.7554/eLife.71575.sa2>

Additional files

Supplementary files

- Transparent reporting form

Data availability

RNAseq data have been deposited at GEO-NCBI under the access code GSE175920.

The following dataset was generated:

Author(s)	Year	Dataset title	Dataset URL	Database and Identifier
Conde-Dusman MJ, Perez-Otaño I	2021	RNAseq data in cultured neurons	https://www.ncbi.nlm.nih.gov/geo/query/acc.cgi?acc=GSE175920	NCBI Gene Expression Omnibus, GSE175920

References

- Abel T**, Martin KC, Bartsch D, Kandel ER. 1998. Memory suppressor genes: inhibitory constraints on the storage of long-term memory. *Science* **279**: 338–341. DOI: <https://doi.org/10.1126/science.279.5349.338>, PMID: [9454331](https://pubmed.ncbi.nlm.nih.gov/9454331/)
- Adaikkan C**, Rosenblum K. 2015. A molecular mechanism underlying gustatory memory trace for an association in the insular cortex. *eLife* **4**: e07582. DOI: <https://doi.org/10.7554/eLife.07582>, PMID: [26452094](https://pubmed.ncbi.nlm.nih.gov/26452094/)
- Andero R**, Ressler KJ. 2012. Fear extinction and BDNF: translating animal models of PTSD to the clinic. *Genes, Brain, and Behavior* **11**: 503–512. DOI: <https://doi.org/10.1111/j.1601-183X.2012.00801.x>, PMID: [22530815](https://pubmed.ncbi.nlm.nih.gov/22530815/)
- Banko JL**, Merhav M, Stern E, Sonenberg N, Rosenblum K, Klann E. 2007. Behavioral alterations in mice lacking the translation repressor 4E-BP2. *Neurobiology of Learning and Memory* **87**: 248–256. DOI: <https://doi.org/10.1016/j.nlm.2006.08.012>, PMID: [17029989](https://pubmed.ncbi.nlm.nih.gov/17029989/)
- Benjamin D**, Hall MN. 2014. mTORC1: turning off is just as important as turning on. *Cell* **156**: 627–628. DOI: <https://doi.org/10.1016/j.cell.2014.01.057>, PMID: [24529368](https://pubmed.ncbi.nlm.nih.gov/24529368/)
- Cammalleri M**, Lütjens R, Berton F, King AR, Simpson C, Francesconi W, Sanna PP. 2003. Time-restricted role for dendritic activation of the mTOR-p70S6K pathway in the induction of late-phase long-term potentiation in the CA1. *PNAS* **100**: 14368–14373. DOI: <https://doi.org/10.1073/pnas.2336098100>, PMID: [14623952](https://pubmed.ncbi.nlm.nih.gov/14623952/)
- Chen LF**, Lyons MR, Liu F, Green MV, Hedrick NG, Williams AB, Narayanan A, Yasuda R, West AE. 2020. The NMDA receptor subunit GluN3A regulates synaptic activity-induced and myocyte enhancer factor 2C (MEF2C)-dependent transcription. *The Journal of Biological Chemistry* **295**: 8613–8627. DOI: <https://doi.org/10.1074/jbc.RA119.010266>, PMID: [32393578](https://pubmed.ncbi.nlm.nih.gov/32393578/)
- Chiang GG**, Abraham RT. 2005. Phosphorylation of mammalian target of rapamycin (mTOR) at Ser-2448 is mediated by p70S6 kinase. *The Journal of Biological Chemistry* **280**: 25485–25490. DOI: <https://doi.org/10.1074/jbc.M501707200>, PMID: [15899889](https://pubmed.ncbi.nlm.nih.gov/15899889/)
- Cho J**, Yu N-K, Choi J-H, Sim S-E, Kang SJ, Kwak C, Lee S-W, Kim J, Choi DI, Kim VN, Kaang B-K. 2015. Multiple repressive mechanisms in the hippocampus during memory formation. *Science* **350**: 82–87. DOI: <https://doi.org/10.1126/science.aac7368>, PMID: [26430118](https://pubmed.ncbi.nlm.nih.gov/26430118/)
- Chowdhury D**, Marco S, Brooks IM, Zandueata A, Rao Y, Haucke V, Wesseling JF, Tavalin SJ, Pérez-Otaño I. 2013. Tyrosine phosphorylation regulates the endocytosis and surface expression of GluN3A-containing NMDA receptors. *The Journal of Neuroscience* **33**: 4151–4164. DOI: <https://doi.org/10.1523/JNEUROSCI.2721-12.2013>, PMID: [23447623](https://pubmed.ncbi.nlm.nih.gov/23447623/)
- Costa-Mattioli M**, Gobert D, Stern E, Gamache K, Colina R, Cuello C, Sossin W, Kaufman R, Pelletier J, Rosenblum K, Krnjević K, Lacaille J-C, Nader K, Sonenberg N. 2007. eIF2alpha phosphorylation bidirectionally regulates the switch from short- to long-term synaptic plasticity and memory. *Cell* **129**: 195–206. DOI: <https://doi.org/10.1016/j.cell.2007.01.050>, PMID: [17418795](https://pubmed.ncbi.nlm.nih.gov/17418795/)

- Costa-Mattioli M**, Monteggia LM. 2013. mTOR complexes in neurodevelopmental and neuropsychiatric disorders. *Nature Neuroscience* **16**: 1537–1543. DOI: <https://doi.org/10.1038/nn.3546>, PMID: 24165680
- De Rubeis S**, Pasciuto E, Li KW, Fernández E, Di Marino D, Buzzi A, Ostroff LE, Klann E, Zwartkruis FJT, Komiyama NH, Grant SGN, Poujol C, Choquet D, Achsel T, Posthuma D, Smit AB, Bagni C. 2013. CYFIP1 coordinates mRNA translation and cytoskeleton remodeling to ensure proper dendritic spine formation. *Neuron* **79**: 1169–1182. DOI: <https://doi.org/10.1016/j.neuron.2013.06.039>, PMID: 24050404
- Erdmann G**, Schütz G, Berger S. 2007. ducible gene inactivation in neurons of the adult mouse forebrain. *BMC Neuroscience* **8**: 63. DOI: <https://doi.org/10.1186/1471-2202-8-63>, PMID: 17683525
- Fiuza M**, González-González I, Pérez-Otaño I. 2013. GluN3A expression restricts spine maturation via inhibition of GIT1/Rac1 signaling. *PNAS* **110**: 20807–20812. DOI: <https://doi.org/10.1073/pnas.1312211110>, PMID: 24297929
- Flavell SW**, Greenberg ME. 2008. Signaling mechanisms linking neuronal activity to gene expression and plasticity of the nervous system. *Annual Review of Neuroscience* **31**: 563–590. DOI: <https://doi.org/10.1146/annurev.neuro.31.060407.125631>, PMID: 18558867
- Fonseca R**, Nägerl UV, Morris RGM, Bonhoeffer T. 2004. Competing for memory: hippocampal LTP under regimes of reduced protein synthesis. *Neuron* **44**: 1011–1020. DOI: <https://doi.org/10.1016/j.neuron.2004.10.033>, PMID: 15603743
- Fulcher BD**, Murray JD, Zerbi V, Wang XJ. 2019. Multimodal gradients across mouse cortex. *PNAS* **116**: 4689–4695. DOI: <https://doi.org/10.1073/pnas.1814144116>, PMID: 30782826
- Gallinat J**, Götz T, Kalus P, Bajbouj M, Sander T, Winterer G. 2007. Genetic variations of the NR3A subunit of the NMDA receptor modulate prefrontal cerebral activity in humans. *Journal of Cognitive Neuroscience* **19**: 59–68. DOI: <https://doi.org/10.1162/jocn.2007.19.1.59>, PMID: 17214563
- Gascón S**, Paez-Gomez JA, Díaz-Guerra M, Scheiffle P, Scholl FG. 2008. Dual-promoter lentiviral vectors for constitutive and regulated gene expression in neurons. *Journal of Neuroscience Methods* **168**: 104–112. DOI: <https://doi.org/10.1016/j.jneumeth.2007.09.023>, PMID: 17983662
- Govindarajan A**, Israely I, Huang SY, Tonegawa S. 2011. The dendritic branch is the preferred integrative unit for protein synthesis-dependent LTP. *Neuron* **69**: 132–146. DOI: <https://doi.org/10.1016/j.neuron.2010.12.008>, PMID: 21220104
- Grand T**, Abi Gerges S, David M, Diana MA, Paoletti P. 2018. Unmasking GluN1/GluN3A excitatory glycine NMDA receptors. *Nature Communications* **9**: 4769. DOI: <https://doi.org/10.1038/s41467-018-07236-4>, PMID: 30425244
- Greenwood TA**, Lazzeroni LC, Maihofer AX, Swerdlow NR, Calkins ME, Freedman R, Green MF, Light GA, Nievergelt CM, Nuechterlein KH, Radant AD, Siever LJ, Silverman JM, Stone WS, Sugar CA, Tsuang DW, Tsuang MT, Turetsky BI, Gur RC, Gur RE, et al. 2019. Genome-wide Association of Endophenotypes for Schizophrenia From the Consortium on the Genetics of Schizophrenia (COGS) Study. *JAMA Psychiatry* **76**: 1274. DOI: <https://doi.org/10.1001/jamapsychiatry.2019.2850>
- Hardingham GE**, Fukunaga Y, Bading H. 2002. Extrasynaptic NMDARs oppose synaptic NMDARs by triggering CREB shut-off and cell death pathways. *Nature Neuroscience* **5**: 405–414. DOI: <https://doi.org/10.1038/nn835>, PMID: 11953750
- Heaton P**, Wallace GL. 2004. Annotation: the savant syndrome. *Journal of Child Psychology and Psychiatry, and Allied Disciplines* **45**: 899–911. DOI: <https://doi.org/10.1111/j.1469-7610.2004.t01-1-00284.x>, PMID: 15225334
- Henson MA**, Larsen RS, Lawson SN, Pérez-Otaño I, Nakanishi N, Lipton SA, Philpot BD. 2012. Genetic deletion of NR3A accelerates glutamatergic synapse maturation. *PLOS ONE* **7**: e42327. DOI: <https://doi.org/10.1371/journal.pone.0042327>, PMID: 22870318
- Hoeffler CA**, Tang W, Wong H, Santillan A, Patterson RJ, Martinez LA, Tejada-Simon MV, Paylor R, Hamilton SL, Klann E. 2008. Removal of FKBP12 enhances mTOR-Raptor interactions, LTP, memory, and perseverative/repetitive behavior. *Neuron* **60**: 832–845. DOI: <https://doi.org/10.1016/j.neuron.2008.09.037>, PMID: 19081378
- Holt CE**, Martin KC, Schuman EM. 2019. Local translation in neurons: visualization and function. *Nature Structural & Molecular Biology* **26**: 557–566. DOI: <https://doi.org/10.1038/s41594-019-0263-5>, PMID: 31270476
- Holtmaat A**, Caroni P. 2016. Functional and structural underpinnings of neuronal assembly formation in learning. *Nature Neuroscience* **19**: 1553–1562. DOI: <https://doi.org/10.1038/nn.4418>, PMID: 27749830
- Hong ST**, Mah W. 2015. A Critical Role of GIT1 in Vertebrate and Invertebrate Brain Development. *Experimental Neurobiology* **24**: 8–16. DOI: <https://doi.org/10.5607/en.2015.24.1.8>, PMID: 25792865
- Hou L**, Klann E. 2004. Activation of the phosphoinositide 3-kinase-Akt-mammalian target of rapamycin signaling pathway is required for metabotropic glutamate receptor-dependent long-term depression. *The Journal of Neuroscience* **24**: 6352–6361. DOI: <https://doi.org/10.1523/JNEUROSCI.0995-04.2004>, PMID: 15254091
- Huang X**, Chen Y-Y, Shen Y, Cao X, Li A, Liu Q, Li Z, Zhang L-B, Dai W, Tan T, Arias-Carrion O, Xue Y-X, Su H, Yuan T-F. 2017. Methamphetamine abuse impairs motor cortical plasticity and function. *Molecular Psychiatry* **22**: 1274–1281. DOI: <https://doi.org/10.1038/mp.2017.143>, PMID: 28831198
- Josselyn SA**, Tonegawa S. 2020. Memory engrams: Recalling the past and imagining the future. *Science* **367**: eaaw4325. DOI: <https://doi.org/10.1126/science.aaw4325>, PMID: 31896692
- Kehoe LA**, Bellone C, De Roo M, Zanduetta A, Dey PN, Pérez-Otaño I, Muller D. 2014. GluN3A promotes dendritic spine pruning and destabilization during postnatal development. *The Journal of Neuroscience* **34**: 9213–9221. DOI: <https://doi.org/10.1523/JNEUROSCI.5183-13.2014>, PMID: 25009255
- Kelleher RJ**, Bear MF. 2008. The autistic neuron: troubled translation? *Cell* **135**: 401–406. DOI: <https://doi.org/10.1016/j.cell.2008.10.017>, PMID: 18984149

- Kim MJ**, Biag J, Fass DM, Lewis MC, Zhang Q, Fleishman M, Gangwar SP, Machius M, Fromer M, Purcell SM, McCarroll SA, Rudenko G, Premont RT, Scolnick EM, Haggarty SJ. 2017. Functional analysis of rare variants found in schizophrenia implicates a critical role for GIT1-PAK3 signaling in neuroplasticity. *Molecular Psychiatry* **22**: 417–429. DOI: <https://doi.org/10.1038/mp.2016.98>, PMID: 27457813
- Klann E**, Dever TE. 2004. Biochemical mechanisms for translational regulation in synaptic plasticity. *Nature Reviews. Neuroscience* **5**: 931–942. DOI: <https://doi.org/10.1038/nrn1557>, PMID: 15550948
- Lipton JO**, Sahin M. 2014. The neurology of mTOR. *Neuron* **84**: 275–291. DOI: <https://doi.org/10.1016/j.neuron.2014.09.034>, PMID: 25374355
- Liu GY**, Sabatini DM. 2020. mTOR at the nexus of nutrition, growth, ageing and disease. *Nature Reviews. Molecular Cell Biology* **21**: 183–203. DOI: <https://doi.org/10.1038/s41580-019-0199-y>, PMID: 31937935
- Lyons MR**, West AE. 2011. Mechanisms of specificity in neuronal activity-regulated gene transcription. *Progress in Neurobiology* **94**: 259–295. DOI: <https://doi.org/10.1016/j.pneurobio.2011.05.003>, PMID: 21620929
- Marco S**, Giralt A, Petrovic MM, Pouladi MA, Martínez-Turrillas R, Martínez-Hernández J, Kaltenbach LS, Torres-Peraza J, Graham RK, Watanabe M, Luján R, Nakanishi N, Lipton SA, Lo DC, Hayden MR, Alberch J, Wesseling JF, Pérez-Otaño I. 2013. Suppressing aberrant GluN3A expression rescues synaptic and behavioral impairments in Huntington's disease models. *Nature Medicine* **19**: 1030–1038. DOI: <https://doi.org/10.1038/nm.3246>, PMID: 23852340
- Marco S**, Murillo A, Pérez-Otaño I. 2018. RNAi-Based GluN3A Silencing Prevents and Reverses Disease Phenotypes Induced by Mutant huntingtin. *Molecular Therapy* **26**: 1965–1972. DOI: <https://doi.org/10.1016/j.ymthe.2018.05.013>, PMID: 29914757
- Martyn AC**, Toth K, Schmalzigaug R, Hedrick NG, Rodriguiz RM, Yasuda R, Wetsel WC, Premont RT. 2018. GIT1 regulates synaptic structural plasticity underlying learning. *PLOS ONE* **13**: e0194350. DOI: <https://doi.org/10.1371/journal.pone.0194350>, PMID: 29554125
- Mueller HT**, Meador-Woodruff JH. 2004. NR3A NMDA receptor subunit mRNA expression in schizophrenia, depression and bipolar disorder. *Schizophrenia Research* **71**: 361–370. DOI: <https://doi.org/10.1016/j.schres.2004.02.016>, PMID: 15474907
- Murillo A**, Navarro AI, Puellas E, Zhang Y, Petros TJ, Pérez-Otaño I. 2021. Temporal Dynamics and Neuronal Specificity of Grin3a Expression in the Mouse Forebrain. *Cerebral Cortex* **31**: 1914–1926. DOI: <https://doi.org/10.1093/cercor/bhaa330>, PMID: 33290502
- Ohi K**, Hashimoto R, Ikeda M, Yamamori H, Yasuda Y, Fujimoto M, Umeda-Yano S, Fukunaga M, Fujino H, Watanabe Y, Iwase M, Kazui H, Iwata N, Weinberger DR, Takeda M. 2015. Glutamate Networks Implicate Cognitive Impairments in Schizophrenia: Genome-Wide Association Studies of 52 Cognitive Phenotypes. *Schizophrenia Bulletin* **41**: 909–918. DOI: <https://doi.org/10.1093/schbul/sbu171>, PMID: 25537281
- Otsu Y**, Darcq E, Pietrajts K, Mátyás F, Schwartz E, Bessaih T, Abi Gerges S, Rousseau CV, Grand T, Dieudonné S, Paoletti P, Acsády L, Agulhon C, Kieffer BL, Diana MA. 2019. Control of aversion by glycine-gated GluN1/GluN3A NMDA receptors in the adult medial habenula. *Science* **366**: 250–254. DOI: <https://doi.org/10.1126/science.aax1522>, PMID: 31601771
- Paoletti P**, Bellone C, Zhou Q. 2013. NMDA receptor subunit diversity: impact on receptor properties, synaptic plasticity and disease. *Nature Reviews. Neuroscience* **14**: 383–400. DOI: <https://doi.org/10.1038/nrn3504>, PMID: 23686171
- Papenberg G**, Li S-C, Nagel IE, Nietfeld W, Schjeide B-M, Schröder J, Bertram L, Heekeren HR, Lindenberger U, Bäckman L. 2014. Dopamine and glutamate receptor genes interactively influence episodic memory in old age. *Neurobiology of Aging* **35**: 1213. DOI: <https://doi.org/10.1016/j.neurobiolaging.2013.11.014>
- Perez-Otano I**, Schulteis CT, Contractor A, Lipton SA, Trimmer JS, Sucher NJ, Heinemann SF. 2001. Assembly with the NR1 subunit is required for surface expression of NR3A-containing NMDA receptors. *The Journal of Neuroscience* **21**: 1228–1237. DOI: <https://doi.org/10.1523/JNEUROSCI.21-04-01228.2001>, PMID: 11160393
- Pérez-Otaño I**, Luján R, Tavalin SJ, Plomann M, Modregger J, Liu X-B, Jones EG, Heinemann SF, Lo DC, Ehlers MD. 2006. Endocytosis and synaptic removal of NR3A-containing NMDA receptors by PACSIN1/syndapin1. *Nature Neuroscience* **9**: 611–621. DOI: <https://doi.org/10.1038/nn1680>, PMID: 16617342
- Pérez-Otaño I**, Larsen RS, Wesseling JF. 2016. Emerging roles of GluN3-containing NMDA receptors in the CNS. *Nature Reviews. Neuroscience* **17**: 623–635. DOI: <https://doi.org/10.1038/nrn.2016.92>, PMID: 27558536
- Poulopoulos A**, Murphy AJ, Ozkan A, Davis P, Hatch J, Kirchner R, Macklis JD. 2019. Subcellular transcriptomes and proteomes of developing axon projections in the cerebral cortex. *Nature* **565**: 356–360. DOI: <https://doi.org/10.1038/s41586-018-0847-y>, PMID: 30626971
- Rao VR**, Pintchovski SA, Chin J, Peebles CL, Mitra S, Finkbeiner S. 2006. AMPA receptors regulate transcription of the plasticity-related immediate-early gene Arc. *Nature Neuroscience* **9**: 887–895. DOI: <https://doi.org/10.1038/nn1708>, PMID: 16732277
- Roberts AC**, Díez-García J, Rodriguiz RM, López IP, Luján R, Martínez-Turrillas R, Picó E, Henson MA, Bernardo DR, Jarrett TM, Clendeninn DJ, López-Mascaraque L, Feng G, Lo DC, Wesseling JF, Wetsel WC, Philpot BD, Pérez-Otaño I. 2009. Downregulation of NR3A-containing NMDARs is required for synapse maturation and memory consolidation. *Neuron* **63**: 342–356. DOI: <https://doi.org/10.1016/j.neuron.2009.06.016>, PMID: 19679074
- Sadat-Shirazi MS**, Ashabi G, Hessari MB, Khalifeh S, Neirizi NM, Matloub M, Safarzadeh M, Vousooghi N, Zarrindast MR. 2019. NMDA receptors of blood lymphocytes anticipate cognitive performance variations in healthy volunteers. *Physiology & Behavior* **201**: 53–58. DOI: <https://doi.org/10.1016/j.physbeh.2018.12.015>

- Sancak Y**, Bar-Peled L, Zoncu R, Markhard AL, Nada S, Sabatini DM. 2010. Regulator-Rag complex targets mTORC1 to the lysosomal surface and is necessary for its activation by amino acids. *Cell* **141**: 290–303. DOI: <https://doi.org/10.1016/j.cell.2010.02.024>, PMID: 20381137
- Santini E**, Huynh TN, MacAskill AF, Carter AG, Pierre P, Ruggiero D, Kaphzan H, Klann E. 2013. Exaggerated translation causes synaptic and behavioural aberrations associated with autism. *Nature* **493**: 411–415. DOI: <https://doi.org/10.1038/nature11782>, PMID: 23263185
- Sarker G**, Sun W, Rosenkranz D, Pelczar P, Opitz L, Efthymiou V, Wolfrum C, Peleg-Raibstein D. 2019. Maternal overnutrition programs hedonic and metabolic phenotypes across generations through sperm tsRNAs. *PNAS* **116**: 10547–10556. DOI: <https://doi.org/10.1073/pnas.1820810116>, PMID: 31061112
- Sharma V**, Sood R, Khlaifia A, Eslamizade MJ, Hung T-Y, Lou D, Asgarihafshejani A, Lalar M, Kiniry SJ, Stokes MP, Cohen N, Nelson AJ, Abell K, Possemato AP, Gal-Ben-Ari S, Truong VT, Wang P, Yiannakas A, Saffarzadeh F, Cuello AC, et al. 2020. eIF2 α controls memory consolidation via excitatory and somatostatin neurons. *Nature* **586**: 412–416. DOI: <https://doi.org/10.1038/s41586-020-2805-8>, PMID: 33029011
- Shrestha P**, Ayata P, Herrero-Vidal P, Longo F, Gastone A, LeDoux JE, Heintz N, Klann E. 2020a. Cell-type-specific drug-inducible protein synthesis inhibition demonstrates that memory consolidation requires rapid neuronal translation. *Nature Neuroscience* **23**: 281–292. DOI: <https://doi.org/10.1038/s41593-019-0568-z>, PMID: 31959934
- Shrestha P**, Shan Z, Mamcarz M, Ruiz KSA, Zerihoun AT, Juan CY, Herrero-Vidal PM, Pelletier J, Heintz N, Klann E. 2020b. Amygdala inhibitory neurons as loci for translation in emotional memories. *Nature* **586**: 407–411. DOI: <https://doi.org/10.1038/s41586-020-2793-8>
- Smithson LJ**, Gutmann DH. 2016. Proteomic analysis reveals GIT1 as a novel mTOR complex component critical for mediating astrocyte survival. *Genes & Development* **30**: 1383–1388. DOI: <https://doi.org/10.1101/gad.279661.116>
- Sossin WS**, Costa-Mattioli M. 2019. Translational Control in the Brain in Health and Disease. *Cold Spring Harbor Perspectives in Biology* **11**: a032912. DOI: <https://doi.org/10.1101/cshperspect.a032912>
- Stern E**, Chinnakkaruppan A, David O, Sonenberg N, Rosenblum K. 2013. Blocking the eIF2 α kinase (PKR) enhances positive and negative forms of cortex-dependent taste memory. *The Journal of Neuroscience* **33**: 2517–2525. DOI: <https://doi.org/10.1523/JNEUROSCI.2322-12.2013>, PMID: 23392680
- Stoica L**, Zhu PJ, Huang W, Zhou H, Kozma SC, Costa-Mattioli M. 2011. Selective pharmacogenetic inhibition of mammalian target of Rapamycin complex I (mTORC1) blocks long-term synaptic plasticity and memory storage. *PNAS* **108**: 3791–3796. DOI: <https://doi.org/10.1073/pnas.1014715108>, PMID: 21307309
- Takata A**, Iwayama Y, Fukuo Y, Ikeda M, Okochi T, Maekawa M, Toyota T, Yamada K, Hattori E, Ohnishi T, Toyoshima M, Ujike H, Inada T, Kunugi H, Ozaki N, Nanko S, Nakamura K, Mori N, Kanba S, Iwata N, et al. 2013. A population-specific uncommon variant in GRIN3A associated with schizophrenia. *Biological Psychiatry* **73**: 532–539. DOI: <https://doi.org/10.1016/j.biopsych.2012.10.024>, PMID: 23237318
- Takei N**, Inamura N, Kawamura M, Namba H, Hara K, Yonezawa K, Nawa H. 2004. Brain-derived neurotrophic factor induces mammalian target of rapamycin-dependent local activation of translation machinery and protein synthesis in neuronal dendrites. *The Journal of Neuroscience* **24**: 9760–9769. DOI: <https://doi.org/10.1523/JNEUROSCI.1427-04.2004>, PMID: 15525761
- Tang SJ**, Reis G, Kang H, Gingras AC, Sonenberg N, Schuman EM. 2002. A rapamycin-sensitive signaling pathway contributes to long-term synaptic plasticity in the hippocampus. *PNAS* **99**: 467–472. DOI: <https://doi.org/10.1073/pnas.012605299>, PMID: 11756682
- Trinh MA**, Kaphzan H, Wek RC, Pierre P, Cavener DR, Klann E. 2012. Brain-specific disruption of the eIF2 α kinase PERK decreases ATF4 expression and impairs behavioral flexibility. *Cell Reports* **1**: 676–688. DOI: <https://doi.org/10.1016/j.celrep.2012.04.010>, PMID: 22813743
- Wang DO**, Martin KC, Zukin RS. 2010. Spatially restricting gene expression by local translation at synapses. *Trends in Neurosciences* **33**: 173–182. DOI: <https://doi.org/10.1016/j.tins.2010.01.005>, PMID: 20303187
- Wang CC**, Held RG, Chang SC, Yang L, Delpire E, Ghosh A, Hall BJ. 2011. A critical role for GluN2B-containing NMDA receptors in cortical development and function. *Neuron* **72**: 789–805. DOI: <https://doi.org/10.1016/j.neuron.2011.09.023>, PMID: 22153375
- Won H**, Mah W, Kim E, Kim J-W, Hahm E-K, Kim M-H, Cho S, Kim J, Jang H, Cho S-C, Kim B-N, Shin M-S, Seo J, Jeong J, Choi S-Y, Kim D, Kang C, Kim E. 2011. GIT1 is associated with ADHD in humans and ADHD-like behaviors in mice. *Nature Medicine* **17**: 566–572. DOI: <https://doi.org/10.1038/nm.2330>, PMID: 21499268
- Yang J**, Wang S, Yang Z, Hodgkinson CA, Iarikova P, Ma JZ, Payne TJ, Goldman D, Li MD. 2015. The contribution of rare and common variants in 30 genes to risk nicotine dependence. *Molecular Psychiatry* **20**: 1467–1478. DOI: <https://doi.org/10.1038/mp.2014.156>, PMID: 25450229
- Yap EL**, Greenberg ME. 2018. Activity-Regulated Transcription: Bridging the Gap between Neural Activity and Behavior. *Neuron* **100**: 330–348. DOI: <https://doi.org/10.1016/j.neuron.2018.10.013>, PMID: 30359600
- Yuan T**, Mameli M, O' EC, Dey PN, Verpelli C, Sala C, Perez-Otano I, Lüscher C, Bellone C. 2013. Expression of cocaine-evoked synaptic plasticity by GluN3A-containing NMDA receptors. *Neuron* **80**: 1025–1038. DOI: <https://doi.org/10.1016/j.neuron.2013.07.050>, PMID: 24183704
- Zhang H**, Webb DJ, Asmussen H, Horwitz AF. 2003. Synapse formation is regulated by the signaling adaptor GIT1. *The Journal of Cell Biology* **161**: 131–142. DOI: <https://doi.org/10.1083/jcb.200211002>, PMID: 12695502
- Zhu PJ**, Chen CJ, Mays J, Stoica L, Costa-Mattioli M. 2018. mTORC2, but not mTORC1, is required for hippocampal mGluR-LTD and associated behaviors. *Nature Neuroscience* **21**: 799–802. DOI: <https://doi.org/10.1038/s41593-018-0156-7>, PMID: 29786082

LETTER**No evidence for cognitive decline or neurodegeneration in strain-matched GluN3A knockout mice**

Letter to the Editor in response to: *Pathogenesis of sporadic Alzheimer's disease by deficiency of the NMDA receptor subunit GluN3A*, Alzheimer's & Dementia: the journal of the Alzheimer's disease association 18 (2022) 222-239.

Zhong et al recently proposed that deficiency of the NMDA receptor subunit GluN3A might be a pathogenic factor in sporadic Alzheimer's disease (AD) because it drove a variety of signs of degenerative excitotoxicity and cognitive decline in adult/aging mice lacking GluN3A¹. The conclusion seemed at odds with previous studies where adult *Grin3a* (gene encoding GluN3A) knockouts performed significantly better in a variety of spatial and associative learning tasks^{2,3}, suggesting that GluN3A functions as a negative regulator of synapse plasticity and memory⁴. It was also intriguing that the cognitive phenotype emerged at early stages but no obvious age-dependent decline, which is the hallmark of AD, was observed within the experimental time-frame of Zhong et al¹.

Because of this uncertainty and the possible importance for understanding AD, we conducted an analysis of a congenic *Grin3a* knockout mouse strain from the latest time-point in Zhong et al (12 months, considered middle-age) to 16-17 months (old mice), using similar techniques. All experiments were conducted and analyzed in a blind fashion. We found no evidence for degenerative excitotoxicity, and cognitive performance was enhanced, rather than diminished, relative to control mice. Specifically: Twelve month-old *Grin3a* knockouts discriminated between two objects in the novel object recognition test and their performance did not differ from controls (Figure 1A). Analysis of older mice revealed a significant enhancement in the retention of associative memories in *Grin3a* knockouts (Figure 1B). No spatial learning deficits were observed during Morris-water maze training (Figure 1C-D, left panels), and a trend towards better learning in probe trials was observed in aged male and female *Grin3a* knockouts (Figure 1C-D, right panels). The new results are in-line with the previous studies in younger animals and suggest that pro-cognitive effects of GluN3A deletion persist into adulthood.

We additionally examined the abundance of synaptic and signaling proteins and looked for signs of neurodegeneration in the hippocampus of wild-type and *Grin3a* knockouts. No differences were detected (Figure 1E, F) arguing against impairments in synaptic integrity or neuronal death. We finally examined GluN3A protein expression in postmortem frontal cortex of control and sporadic AD cases but no changes were found, consistent with the analysis of

1 sporadic AD cases of Zhong et al (Figure 1G). Altogether, our results do not support the
2 conclusion of Zhong et al that loss of GluN3A function plays a pathogenic role in AD.

3
4 We do not know why our results differ from Zhong et al, but one possible confound is genetic
5 background^{5,6,7}. We used a congenic *Grin3a* knockout strain generated by back-crossing F1
6 hybrids⁸ into a C57Bl6/J background for >12 generations to eliminate ambiguities and
7 comparisons in individual experiments were always between knockout and wild-type
8 littermates from heterozygote crosses. In contrast, our understanding is that knockout and
9 control strains in the Zhong et al study were maintained as separate homozygous colonies,
10 making it possible that genetic drift or flanking gene effects not related to GluN3A function
11 caused the disease phenotype.
12
13
14
15
16
17
18

19 ACKNOWLEDGEMENT

20 Work was funded by Juan de la Cierva and Generalitat Valenciana (GVA) fellowships to O.E.Z.
21 and R.V. and grants from the Spanish Ministry of Science (PID2019-111112RB-i00), Prometeo
22 Excellence GVA Program (to I.P.O.), Fondo de Investigaciones Sanitarias (PI22-01329, to
23 J.S.V.). We thank Isidro Ferrer (Hospital Universitario de Bellvitge) for access to human brain
24 samples.
25
26
27
28
29
30

31 CONFLICTS OF INTEREST

32 The authors have declared no conflicts of interest.
33
34
35

36 Remy Verhaeghe¹

37 Oscar Elía-Zudaire¹

38 Sergio Escamilla^{1,2,3}

39 Javier Sáez-Valero^{1,2,3}

40 Isabel Pérez-Otaño¹
41
42
43
44
45
46
47

48 ¹*Instituto de Neurociencias de Alicante, Spanish Research Council and University Miguel*
49 *Hernández (CSIC-UMH), San Juan de Alicante, Spain;* ²*Centro de Investigación Biomédica en*
50 *Red sobre Enfermedades Neurodegenerativas (CIBERNED), Spain;* ³*Instituto de Investigación*
51 *Sanitaria y Biomédica de Alicante (ISABIAL), Alicante, Spain.*
52
53
54
55
56

57 **Correspondence:** Isabel Pérez-Otaño, Instituto de Neurociencias, CSIC-UMH, Spain. Email:
58 otano@umh.es
59
60
61
62
63
64
65

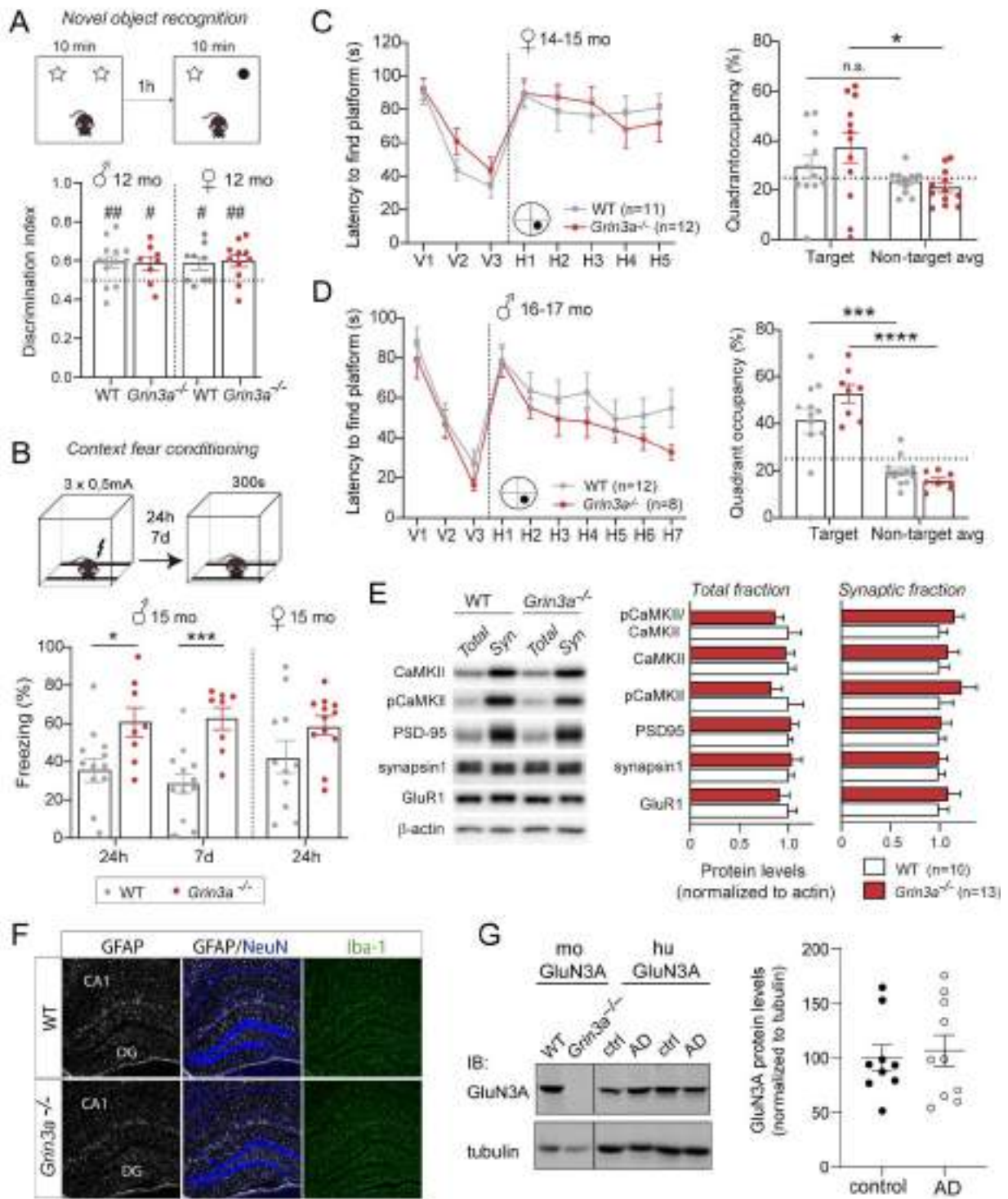
REFERENCES

- 1
2 1. Zhong, W. et al. Pathogenesis of sporadic Alzheimer's disease by deficiency of NMDA
3 receptor subunit GluN3A. *Alzheimer's Dementia*. 18, 222–239 (2022).
- 4
5 2. Mohamad, O., Song, M., Wei, L. & Yu, S. P. Regulatory roles of the NMDA receptor
6 GluN3A subunit in locomotion, Pain perception and cognitive functions in adult mice. *J.*
7
8
9
10
11
12
13
14
15
16
17
18
19
20
21
22
23
24
25
26
27
28
29
30
31
32
33
34
35
36
37
38
39
40
41
42
43
44
45
46
47
48
49
50
51
52
53
54
55
56
57
58
59
60
61
62
63
64
65
Physiol. 591, 149–168 (2013).
3. Conde-Dusman, M. J. et al. Control of protein synthesis and memory by GluN3A-NMDA
receptors through inhibition of GIT1/mTORC1 assembly. *Elife* 10, 71575 (2021).
4. Perez-Otano, I., Larsen, R. S. & Wesseling, J. F. Emerging roles of GluN3-containing
NMDA receptors in the CNS. *Nat. Rev. Neuroscience* 17, 623–635 (2016).
5. Silva, A. J. et al. Mutant mice and neuroscience: Recommendations concerning genetic
background. *Neuron* 19, 755–759 (1997).
6. Gerlai, R. Gene targeting: Technical confounds and potential solutions in behavioral brain
research. *Behavioral Brain Res.* 125, 13–21 (2001).
7. Strobel, M.C., Reinholdt, L.G., Malcolm, R.D., Pritchett-Corning, K. Genetic monitoring of
laboratory mice and rats. In: American College of Laboratory Animal Medicine, *Laboratory
Animals*, 3rd edition. Academic Press, 1403-1416 (2015).
8. Das, S. et al. Increased NMDA current and spine density in mice lacking the NMDA receptor
subunit NR3A. *Nature* **393**, 377–381 (1998).

FIGURE LEGEND**Figure 1. Enhanced learning and no signs of excitotoxicity in aged GluN3A knockout mice**

1
2
3
4
5 A) Male and female wild-type (WT) and *Grin3a*^{-/-} mice display similar novel object preference
6 with an interval of 1 hour between trials. Note that discrimination indexes were above chance
7 level (0.5) in all cases (t-test, #p<0.05, ##p<0.01). B) Enhanced context fear conditioning
8 memory in male *Grin3a*^{-/-} mice after 24h and 7 days (two-tailed unpaired *t*-test, *p < 0.05,
9 ***p<0.001), with a non-significant trend towards enhanced freezing in females. C, D) Left:
10 escape latencies during Morris water maze training (4 trials per day) of female (C) and male
11 (D) of WT and *Grin3a*^{-/-} mice of the indicated ages. Right: probe trial performed 24h after last
12 day of training (two-way ANOVA followed by Tukey post hoc test, *p<0.05, ***p<0.001,
13 ****p<0.0001). E) Western blot analysis of synaptic protein levels in total (H) and synaptic
14 (Syn) fractions from 15-17 month-old WT and *Grin3a*^{-/-} mice hippocampus. F) Representative
15 examples of GFAP, NeuN and IBA-1 immunostaining in the hippocampus of 15-17 month-old
16 WT (n=4) and *Grin3a*^{-/-} (n=4) mice. DG, dentate gyrus. CA1, CA1 hippocampal region. G)
17 Human GluN3A protein expression in membrane fractions of frontal cortex samples from
18 Alzheimer's disease (AD, n=10) patients and control (ctrl, n=9) cases (see Supplementary Table
19 1), as well as the specificity of the GluN3A antibody tested in *Grin3a*^{-/-} mice.
20
21
22
23
24
25
26
27
28
29
30
31
32
33
34
35
36
37
38
39
40
41
42
43
44
45
46
47
48
49
50
51
52
53
54
55
56
57
58
59
60
61
62
63
64
65

FIGURE 1- Verhaeghe et al



SUPPORTING INFORMATION

MATERIAL AND METHODS

Experimental animals

Adult aged (12-17 months old) control and *Grin3a*^{-/-} mice of both sexes were used. *Grin3a*^{-/-} mice in an F1 hybrid background (C57Bl6/Sv129J) were provided by Nobuki Nakanishi and Stuart A. Lipton (Sanford-Burnham Institute) and backcrossed for >12 generations into a C57Bl6/J background to generate a congenic strain and avoid potential confounds of genetic background. The resulting mutant strain was refreshed periodically by backcrossing to C57Bl6/J mice, and WT and *Grin3a*^{-/-} littermates from heterozygote crosses were used for experiments. Animals were housed four to six per cage with ad libitum access to food and water and maintained in a temperature-controlled environment on a 12-hr dark/light cycle. All procedures were conducted in accordance with the European and Spanish regulations (2010/63/UE; RD 53/2013) and were approved by the Ethical Committee of the Generalitat Valenciana (2017/VSC/PEA/00196).

Behavioral analysis

Novel object recognition: Mice were habituated to an open arena (30cm x 20cm) during 10 min. The day after, animals were placed in the arena with two identical objects for ten minutes. After an interval of 1 hour one of the two objects was replaced by a novel different object. The discrimination index was calculated as follows: interaction time with novel object / (interaction time with novel object + interaction time with familiar object).

Contextual fear conditioning: Mice were placed in the fear chambers and allowed to habituate to a context (CS) (metal grid floor, no light source) for 5 min during two days. The third day mice were placed in the fear chambers and received 3 foot shocks (3 x 0.5mA) during 5min. Conditioning was assessed after 24h and 7 days by reintroducing mice in the conditioned context for 5 min. Freezing behavior was scored by a high sensitivity weight transducer system located at the bottom of the chambers which records and analyses the signal generated by the movement of the animal.

Morris water maze: Mice were trained to find a submerged platform in a circular tank (190 cm diameter) filled with opaque white water in four trials per day with 45 min inter-trial intervals. If mice did not find the platform in 120 s, they were kindly guided to it. Sixty-second-long probe tests in which platform was removed were performed one day after the fifth day of

1 learning phase (H5) in females and one day after the seventh day of training (H7) in males.
2 Time spent in the target quadrant was compared to the average time spent in all other quadrants.
3 Mice were tracked throughout the whole protocol using the video-tracking software SMART
4 (Panlab S.L.).
5
6

7 **Western blot analysis**

8
9
10 Mouse hippocampi were microdissected on ice, snapped frozen in liquid nitrogen and stored at
11 -80°C until processing. Tissues were homogenized in 10 (wt/vol) volumes of ice-cold HEPES-
12 sucrose buffer (10mM Hepes pH7.4, 0.32M sucrose, 0.1M PMSF, 1mM NaF) supplemented
13 with protease and phosphatase inhibitors. Synaptosomal fractions were obtained after
14 successive centrifugations. Protein content was estimated using a Pierce BCA Assay kit
15 (Thermo Fisher) before SDS-PAGE and immunoblotting with the following primary
16 antibodies: mouse anti-PSD95 (#MABN68 Merck 1/2000); rabbit anti-CamKII (#C6974 Merck
17 1/1000); rabbit anti-pCaMKII (Thr286) (D21E4, #12716 1/1000); mouse anti-GluR1
18 (#AB1504 Merck 1/1000); mouse anti-synapsin I (#106 011 Synaptic Systems 1/2000); mouse
19 B-actin (#A5441 Sigma-Aldrich 1/10000).
20
21
22
23
24
25
26
27
28

29 **Immunohistochemistry**

30
31 After deep anesthesia with isoflurane, mice were transcardially perfused with 4%
32 paraformaldehyde in phosphate buffered saline (PBS) pH 7.4. Brains were removed and post-
33 fixed overnight at 4°C . Free-floating $40\ \mu\text{m}$ -thick brain sections were permeabilized/blocked
34 for 1-2h in PBST (PBS 0.1% TX100) + 4% Normal serum + 1% BSA and then incubated with
35 primary antibody overnight at 4°C (dilute in PBST + 1% Normal serum + 1% BSA). The
36 primary antibodies used were: goat anti-GFAP (mAB#173002 Synaptic Systems 1/1000);
37 rabbit anti-IBA1 (#019-19741 Wako Chemicals 1/1000). The day after, slices were washed and
38 incubated 2h in fluorochrome-conjugated secondary antibody (dilute in PBST + 1% BSA) and
39 mounted.
40
41
42
43
44
45
46
47

48 **Human postmortem brain tissue**

49
50
51 A collection of postmortem frontal cortex (Brodmann areas 8/9) samples from sporadic AD
52 patients and control cases were obtained from the Brain Bank of the Institute of
53 Neuropathology, Bellvitge University Hospital following the ethical guidelines of the
54 Declaration of Helsinki. Case information can be found in Supplemental Table 1. Cortical tissue
55 (100 mg) was homogenized in 10 (wt/vol) volumes of ice-cold HEPES-sucrose buffer
56 supplemented with protease and phosphatase inhibitors as above. The homogenate was
57
58
59
60
61
62
63
64
65

centrifuged at 1000×g 10 min to discard the pelleted nuclear fraction. The supernatant was then centrifuged at 10,000×g 15 min to obtain the membrane fraction (P2). GluN3A expression was analyzed in P2 fractions by western blotting as above. As in our previous human studies¹, the specificity of the human GluN3A band detected with the anti-GluN3A antibody was assessed by comparison with a mouse GluN3A band that was absent in GluN3A knockout mice, run in parallel in the same blot.

1
2
3
4
5
6
7
8
9
10
11
12
13
14
15
16
17
18
19
20
21
22
23
24
25
26
27
28
29
30
31
32
33
34
35
36
37
38
39
40
41
42
43
44
45
46
47
48
49
50
51
52
53
54
55
56
57
58
59
60
61
62
63
64
65

Supplemental Table 1. Control and Alzheimer's disease (AD) frontal cortex cases. Subjects were categorized according to the Braak stage of neurofibrillary tangle (NFT) pathology^{1,2} and A β stage³. Age (y= years), gender (m=male, f=female), Post-mortem (PM, h=hours). HUSPIR Index >1 ensures that post-mortem cortical samples are optimally preserved for biochemical evaluation of synaptic proteins⁴.

Subject	age (y)	gender	PM (h)	<i>HUSPIR Index</i>
C1 11/2	50	f	14	2.3
C2 11/25	52	m	4	2.2
C3 62	56	m	4	2.3
C4 5/5	58	m	4	6.7
C5 2/98	59	m	4	5.2
C6 3/62	62	m	3	4
C7 8/42	64	f	5	2.7
C8 116	75	f	3	4.3
C9 144	76	m	4	4.6

Subject	age (y)	gender	PM (h)	<i>HUSPIR Index</i>	<i>Braak stage</i>	A β stage
AD1 54	79	m	5	3.2	III	A
AD2 49	71	m	7	4.1	III	0
AD3 115	85	m	14	2.8	IV	B
AD4 97	74	f	9	8.6	V	A
AD5 92	67	f	8	4.7	V	C
AD6 16	81	f	5,5	4.5	V	C
AD7 84	72	m	2	5.1	V	C
AD8 26	87	m	7	3.5	V	C
AD9 121	75	m	12	7.3	VI	B
AD10 51	77	m	16	7.8	VI	C

SUPPLEMENTAL REFERENCES

1. Marco, S. *et al.* Suppressing aberrant GluN3A expression rescues synaptic and behavioral impairments in Huntington's disease models. *Nat. Med.* **19**, 1030–1038 (2013).
2. Braak H, Braak E. Neuropathological staging of Alzheimer-related changes. *Acta Neuropathol* 82:239–59 (1991).
3. Braak H, Alafuzoff I, Arzberger T, Kretschmar H, Del Tredici K. Staging of Alzheimer disease-associated neurofibrillary pathology using paraffin sections and immunocytochemistry. *Acta Neuropathol* 112(4):389-404 (2006).
4. Mirra SS, Heyman A, McKeel D, Sumi SM, Crain BJ, Brownlee LM, et al. The consortium to establish a registry for Alzheimer's disease (CERAD). Part II. Standardization of the neuropathologic assessment of Alzheimer's disease. *Neurology* 41(4):479-86 (1991).
5. Bayés À, Collins MO, Galtrey CM, Simonnet C, Roy M, Croning MD, Gou G, van de Lagemaat LN, Milward D, Whittle IR, Smith C, Choudhary JS, Grant SG. Human post-mortem synapse proteome integrity screening for proteomic studies of postsynaptic complexes. *Mol Brain* 28;7:88 (2014).